Control of Cleavage Furrow Formation During Cytokinesis in Human Cells

Kuan-Chung Su

University College London
and
Cancer Research UK London Research Institute

PhD Supervisor: Mark Petronczki PhD

A thesis submitted for the degree of
Doctor of Philosophy
University College London

September 2012

Declaration

I Kuan-Chung Su confirm that the work presented in this thesis is my own. Where information has been derived from other sources, I confirm that this has been indicated in the thesis.

Abstract

Cytokinesis is the final stage of the cell cycle. It partitions sister genomes and separates the cytoplasm of nascent daughter cells. Cytokinesis is initiated by the formation of a cleavage furrow whose ingression is powered by an actomyosin network known as the contractile ring. Following furrow ingression, the process of cell separation is completed by a membrane scission reaction. For the accurate inheritance of genetic information, it is crucial that furrow formation is initiated at the cell equator between segregating chromosomes and that this occurs after chromatin has cleared the cleavage plane. In animal cells, the mitotic spindle plays a pivotal role in the formation and placement of the cleavage furrow. The coupling of cytokinesis and chromosome segregation to the mitotic spindle ensures that nuclear and cytoplasmic division are tightly coordinated. The spindle midzone, a structure that is formed at anaphase onset between segregating sister genomes, is thought to play an important instructive role during cleavage furrow formation. How the mitotic spindle controls cytokinetic events at the cell envelope is a key challenge in cell division research. Formation of the cytokinetic furrow in animal cells requires activation of the GTPase RhoA by the conserved guanine nucleotide exchange factor Ect2. How Ect2, which is associated with the spindle midzone, controls RhoA activity at the equatorial cell periphery during anaphase is not understood.

Using a genetic complementation system, I have been able to replace the endogenous Ect2 protein with a fluorescently-tagged transgene to study its dynamic localization during cytokinesis. Using live-cell time-lapse microscopy, I found that Ect2 concentrates not only at the spindle midzone but also accumulates at equatorial plasma membrane during cytokinesis. The association of Ect2 with the plasma membrane *in vivo* involves a pleckstrin homology domain and a polybasic cluster that bind to phosphoinositide lipids *in vitro*. I further demonstrated that both guanine nucleotide exchange activity and the membrane targeting domains of Ect2 are essential for RhoA activation, contractile ring formation and cleavage furrow ingression in human cells. Membrane localization of Ect2 is spatially confined to the equator by centralspindlin, Ect2's spindle midzone anchor complex, and is also temporally coordinated with chromosome segregation through the activation state of Cdk1. My results suggest that targeting of Ect2 to the equatorial membrane may represent a key step in the delivery of the cytokinetic signal to the cortex.

Acknowledgements

I would like to thank my supervisor Mark Petronczki, for the continuous encouragement and for always having time for discussions about ideas especially, when troubleshooting is required.

I am also thankful to my thesis committee, Frank Uhlmann and Julian Downward for their valuable advice and guidance through my time at the London Research Institute.

I am very grateful to Tohru Takaki, with whom I was working closely for my project. I also thank him for having taught me almost every single technique I learnt during my time as a PhD student.

Thank you also to all Lab members of the Cell Division and Aneuploidy lab, Sergey Lekomtsev, Lola Vazquez-Novelle, Sriramkumar Sundaramoorthy, Laurent L'Epicier-Sansregret, Kristyna Kotynkova and Murielle Serres for providing such a cheerful and inspiring environment and also for being a great sounding board for all my thoughts about the Clare Hall catering.

Thanks are due to Nicola Brown and Katharina Willmann for sharing the invaluable experience and ups and downs of being students at Clare Hall.

I would like to thank all friends and family who supported me through the years of my studies.

I was a recipient of the DOC-fellowship of the Austrian academy of science for which I am very grateful.

Table of Contents

Table of figures

Abbreviations

AB	Antibody
AcGFP	*Aequora coerulesc*ens GFP
AIM-1	Aurora and Ipl1-like midbody-associated protein
APC/C	Anaphase promoting complex
ATM	Axia telangiectasia mutated
ATR	ATM and Rad3 related
BRCT	Brest cancer gene 1 carboxyl-terminal
Cdc	Cell division cycle
Cdk	Cyclin dependent kinase
Cep55	Centrosomal protein 55
CHMP	Charged multivesicular body proteins
CKI	Cdk inhibitor protein
CPC	Chromosome passenger complex
CR	Conserved region
CS	Central spindle
Dbl	Diffuse B-cell lymphoma
DH	Dbl homology
DNA	Deoxyribonucleic acid
dNTP	Deoxyribonucleotide triphosphate
Ect2	Epithelial cell transforming sequence 2
Ect2CT	Ect2 C-terminal fragment
ESCRT-III	Endosomal sorting complex required for transport-III
Flp1	Cdc fourteen-like-phosphatase
FRAP	Fluorescence recovery after photo bleaching
FRET	Fluorescence resonance energy transfer
FYVE-CENT	FYVE domain-containing centrosomal protein
GAP	GTPase-activating protein
GDP	Guanosine-5'-diphosphate
GEF	Guanine nucleotide exchange factor
GFP	Green fluorescence portein
GST	Glutathione S-transferase
GTP	Guanosine-5'-triphosphate
INCENP	Inner centromere protein
KIF4	Kinesin family member 4
Let-21	Lethal 21

MBP	Maltose binding protein
mDia	Mouse diaphanous homolog
MgcRacGAP	Male germ cell Rac GTPase-activating protein
MT	Microtubule
MYPT1	Myosin phosphatase target subunit 1
MYT1	Membrane-associated tyrosine/threonine 1
NLS	Nuclear localization signal
Noc	Nocodazole
OCRL	Oculocerebrorenal syndrome of Lowe
Par	Partitioning-defective
PBC	Polybasic cluster
Pbl	Pebble
PE	Phosphatidyl ethanolamine
PH	plekstrin homology
PI(4,5)P2	Phosphatidylinositol 4,5-bisphosphate
PI4P	Phosphatidylinositol-4-phosphate
PIP5-K	Phosphatidylinositol-4-phosphate 5-kinase
PLC	Phospholipase C
Plk1	polo-like kinase 1
PP2	Protein phosphatase 2
PPP	Phosphoprotein phosphatases
Prc1	Protein regulator of cytokinesis
Rad21	Radiation sensitive 21
RhoA	Ras homolog family member A
RNA	Ribonucleic acid
RNAi	RNA interference
ROCK	Rho-associated protein kinase
S	Serine
SAC	Spindle assembly checkpoint
Scc1	Sister chromatid cohesion
SCF	Skp, Cullin, F-box containing complex
SDS	Sodium Dodecyl Sulfate
siRNA	Small interfering RNA
T	Threonine
Thy	Thymidine
TTC19	Tetratricopeptide repeat domain 19
WB	Western blot
WT	Wild Type
Y	Tyrosine

Chapter 1. Introduction

All organisms arise from a single cell through division. The birth of every cell occurs when a cell divides into two new daughter cells. In unicellular organisms this is at the same time the beginning of a new life. In multicellular organisms like us, cell division allows the development and growth of a complex organism from a single cell, the fertilized oocyte. Additionally, cell division is necessary in these organisms for the homeostasis of tissues, which replaces shed, damaged or dying cells.

The cell cycle is a repeating sequence of steps that a cell passes through in order to divide. It is therefore an essential characteristic of life. From the very first moment life existed on our planet, it is likely that a form of cell division has been the mechanism for the propagation of life and that cells have been dividing ever since. An unbroken series of cell divisions connects all living organisms on our planet to the universal ancestor. This is a essential part of the cell theory which was popularized by Rudolph Virchow 1858 (Tan and Brown, 2006)

1.1 The Cell cycle

In eukaryotic organisms, the cell cycle is divided into four stages. The duration of each step can vary depending on external and internal signals that are then interpreted by the cell to decide to stop or to progress in the cycle (Figure 1). In G1 (gap-phase 1) cells are growing until they reach a restriction point when they commit themselves to enter the S-phase. During S-phase, DNA is replicated accurately resulting in two identical copies of the genome (Masai et al., 2010). This is then followed by G2 (gap-phase 2), a time of further growth, biosynthesis and preparation, before cells enter M-phase, the actual phase of cell division. During mitosis, the first part of M-phase, the nuclear envelope breaks down and the duplicated DNA is condensed to compacted chromosomes. Each chromosome consists of two genetically identical sister chromatids, which are held together by a multi protein ring complex called cohesion from their synthesis during S-phase (Ocampo-Hafalla and Uhlmann, 2011). After nuclear envelope breakdown, the

mitotic spindle assembles from microtubules that are nucleated by the centrosomes or spindle poles. To ensure the correct segregation of genetic information, kinetochores, protein complexes assembled on centromeric DNA, on each of the two sister chromatids must be attached to microtubules emanating from opposite spindle poles (Musacchio and Salmon, 2007). Once the last chromosome has been attached in such a bipolar fashion, the cohesin complex is proteolytically cleaved and sister chromatids are pulled towards opposite poles inside the cell. During cytokinesis, the second part of the M-phase, the cytoplasm of the dividing cells is split in two (Green et al., 2012). As the two masses of sister chromatids decondense and reform two genetically identical nuclei, a plasma membrane invagination, called the cleavage furrow, divides the cytoplasmic space midway between chromosomes and finally upon membrane fusion splits the mother cell into two daughter cells (Chen et al., 2012).

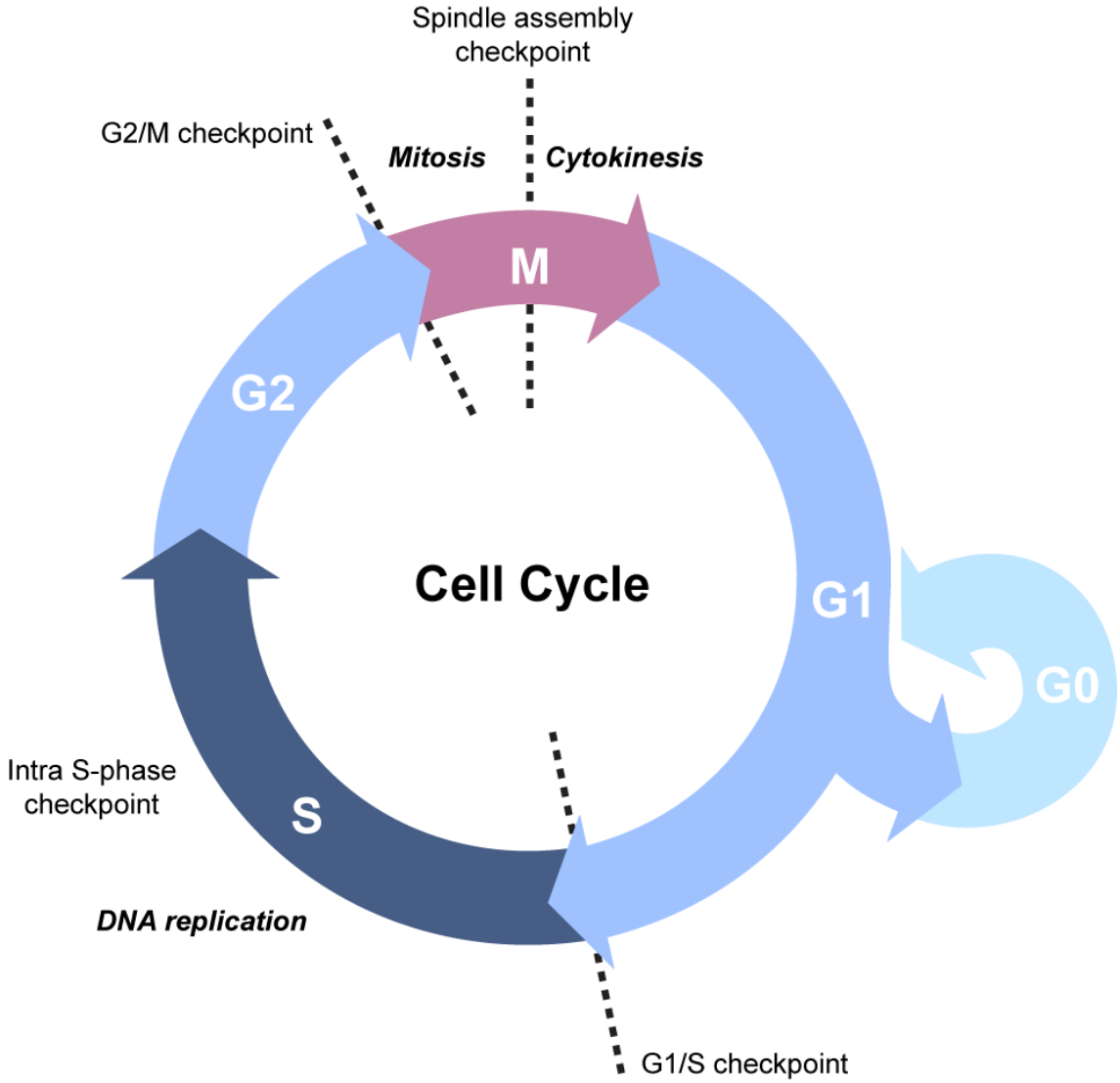

Figure 1 The cell cycle

Illustration of the stages of the eukaryotic cell cycle. In G1-phase cells have just completed division. They can either continue to proliferate and prepare themselves for the next round of DNA synthesis or enter a stationary non-proliferative G0 stage for an indefinite amount of time. DNA damage checkpoints at G1/S or G2/M ensure that no DNA lesion is present before allowing cell cycle to progress into the next stage. In S-phase the DNA is replicated and the intra S-phase checkpoint monitors the completion of DNA replication. In G2 many proteins required for the following cell division stage are synthesized. In M-phase the duplicated DNA is separated during mitosis. Correct chromosome attachment to the mitotic spindle is monitored by spindle assembly checkpoint. Ultimately, cytokinesis, the physical separation of the daughter cells, completes the cell cycle and yields two genetically identical daughter cells. The blue coloured cell cycle stages from G1 to G2 together are also collectively referred to as interphase.

1.2 Regulation of cell cycle progression

A process that is as complex and essential as the cell cycle needs to be tightly regulated. A main challenge in the regulation of cell cycle is to ensure the correct timing and order of the individual events that compose it. Failure to maintain specific temporal control of these events would have catastrophic consequences for genomie stability, cell viability and organismal fitness (Enoch and Nurse, 1990; O'Farrell, 2011; Uhlmann et al., 2011; Malumbres and Barbacid, 2009). Several regulatory mechanisms and feedback mechanisms, called checkpoints, ensure that the events underlying cell proliferation and division happen in a correct and regulated manner through the control of cell cycle.

The detailed set of regulators involved may vary somewhat in different organisms and even cell types or tissues, however there is a high degree of conservation across eukaryotic species. A remarkable example is the fact that the mutant of Cdc2, a key kinase and regulator of mitosis in *Schizosaccharomyces pombe* can be complemented by the human ortholog, Cdk1 (Lee and Nurse, 1987). Studies carried out in multiple model organisms have shown a high degree of similarity in their principles of function. This has lead to our unified view and current understanding we have about how the cell cycle works.

1.2.1 Cyclin-Cdks

Early studies suggested the existence of specific cellular factors that can dictate what stage the cell is in. It was shown that an S-phase cell that is replicating its DNA can induce DNA replication in a G1 cell when both cells are fused. Whereas, a cell in G2-phase that is just about to enter mitosis, can be prevented from doing so by fusion with an S-phase cell (Rao and Johnson, 1970). This suggests that a factor inside the replicating cell can "override" the processes in a cell at another stage of cell cycle and force it to adopt an S-phase state. Studies in *Xenopus* oocytes have shown that injecting cytoplasm from a dividing oocyte can induce meiosis in untreated, non meiotic oocytes (Masui, 1972). This indicated the

existence of maturation stimulating factors in the dividing oocyte that can be transferred.

Tim Hunt and colleagues used sea urchins to study the changes in protein expression pattern as cells progress through the cell cycle, entering and exiting mitosis. They identified a protein whose abundance oscillated depending on the cell cycle stage and called it cyclin due to its cyclic appearance (Evans et al., 1983).

The aforementioned experiments and observations in different eukaryotic model systems led to the identification of cyclins and binding partners Cdks (cyclin dependent kinases) as the agents that define the cell cycle stage. Cdks are present in the cell at all times, but require binding of cyclins to become fully functional. Cyclins do not only determine the activity of the Cdk but also the specificity for their substrates (Ubersax et al., 2003; Loog and Morgan, 2005).

Schizosaccharomyces pombe and *Saccharomyces cerevisiae* express only one Cdk protein. Nevertheless, the kinase can gain specificity for its substrates by binding to different types of cyclin proteins depending on the stage of the cell cycle. At a given stage of the cell cycle different cyclins are present in a yeast cell and are thought to specify Cdk target phosphorylation (Kitagawa and Higashi, 1996; Jeffrey et al., 1995; Nasmyth, 1996). Interestingly, recent work by the Nurse lab in fission yeast (Coudreuse and Nurse, 2010) has shown that a single Cdk-cyclin complex is sufficient to control cell cycle progression merely through different activity levels of the same enzyme (quantitative model). The aforementioned study together with genetic experiments in mice (Malumbres and Barbacid, 2005) challenge the qualitative model of cell cycle control which proposes that the binding of Cdk enzymes to specific cyclin activators defines target specificity and cell cycle progression.

Nevertheless, human cells and other eukaryotic organisms express a broader range of cyclins and Cdk complexes that regulate the cell cycle. They all can be categorized into three general groups depending on when they are active and which processes they promote (Figure 2),

G1 cyclin-Cdk complexes

These complexes phosphorylate proteins that are required to induce the entry into S-phase, for instance, transcription factors that induce expression of dNTP synthesis pathway proteins, DNA polymerases and other proteins involved in DNA replication. G1 cyclins level increases in mid G1 and decreases as cells enter S-phase (Tanaka and Araki, 2010).

S-phase cyclin-Cdk complexes

Synthesized in late G1, they remain inactive because of binding to their inhibitors in mammals of the CIP/KIP family (e.g. p21) and INK4 family (e.g. p19) (Sherr and Roberts, 1999; Nakayama, 1998) or in budding yeast the well characterized protein Sic1 (Schneider et al., 1996). When G1 cyclins reach their highest concentration, the inhibitors are phosphorylated and become targeted for degradation via the SCF (Skp, Cullin, F-box containing complex) ubiquitinylation pathway (Verma, 1997; Kõivomägi et al., 2011). Once uninhibited, S-phase cyclins activate DNA replication complexes that are pre-assembled at DNA replication origins.

Mitotic cyclin-Cdk complexes

M cyclins are synthesized in S and G2, but mitotic Cdk complexes are kept inactive before mitosis. M-phase cyclin-Cdk complexes are inhibited by phosphorylation of Cdk at specific sites and through their binding to CKIs (Cdk inhibitor proteins) (Harper et al., 1993). M cyclin-Cdk complexes activate essential mitotic events, which will be mentioned later. Mitotic cyclins are targeted for proteolysis at the exit of mitosis, via APC/C (Anaphase Promoting Complex/Cyclosome) ubiquitinylation pathway (see 1.3.2).

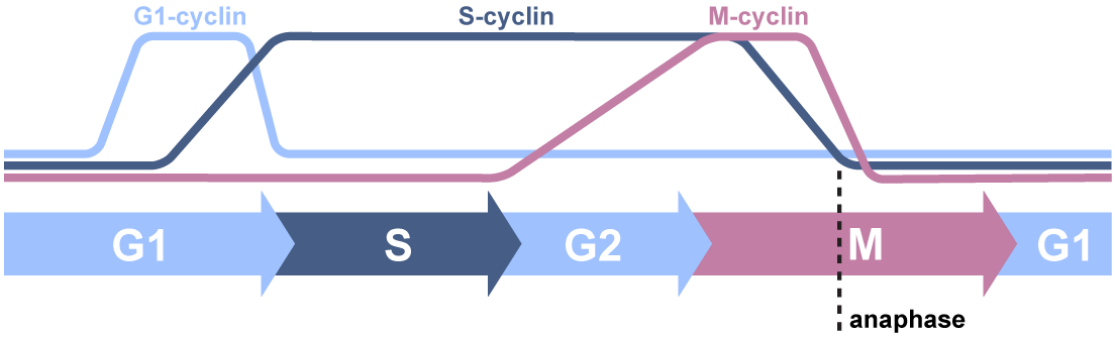

Figure 2 Cyclin-Cdk classes controlling cell cycle progression

Scheme depicts the abundance of different classes of cyclins during cell cycle progression. G1 cyclin levels increase during G1 and decline when S-phase initiates. S-phase cyclins are expressed from G1 onwards and accumulate until degradation in M-phase. Mitotic cyclin levels increase from G2 onwards and drops sharply as cells enter anaphase and cyclins are degraded via APC/C ubiquitination pathway.

1.2.2 Checkpoints

Cell cycle checkpoints play a crucial role in the maintenance of genomic stability of cells. They are able to slow down or halt cell cycle progression at key cell cycle transitions, by e.g. down-regulating the activity of the cyclin-Cdk complexes or preventing the destruction of cyclins. This provides cells with more time to successfully complete all the tasks and previous events before initiating the next cell cycle stage. This 'checkpoint' concept follows the principle of cell cycle feedback control.

By monitoring replication forks the *intra-S-phase checkpoint* ensures that the DNA has been replicated properly before entry into mitosis. It also senses DNA damage and slows down replication if required. There is a high degree of overlap of the key players with the signalling of the DNA damage checkpoint. (Cha and Kleckner, 2002; Gottifredi and Prives, 2005; Jones and Petermann, 2012).

The *DNA-damage checkpoint* acts at the transition between G1/S and G2/M and arrest cells when DNA damage occurs. It allows the cell more time to repair the damage before progression into S-phase or Mitosis, which would lead to mutation of the genome otherwise (Harrison and Haber, 2006).

The *spindle assembly checkpoint* (SAC) ensures the two copies of DNA, generated during S-phase, are properly distributed into the new daughter cells at the end of mitosis. SAC monitors whether the sister chromatids of all chromosomes are correctly attached to microtubules emanating from opposite poles before allowing their segregation. Unattached kinetochores recruit a number of SAC components and generate a diffusible signal that inhibits chromosome segregation and mitotic exit. The mechanism that underlies this feedback control involves the direct inhibition of the activity of the APC/C whose activity normally triggers sister chromatid segregation and mitotic exit (Musacchio and Salmon, 2007).

1.3 Cell division

When DNA synthesis in S-phase is complete, cells prepare themselves for the morphologically most dynamic stage of the cell cycle, M-phase (Figure 3). In mitosis, the first part of M-phase, cells segregate their duplicated DNA by pulling sister chromatids to opposite poles inside the cell. Mitosis is followed by cytokinesis where the cell constricts at the cell equator midway between segregated DNA masses so that sister genomes and cytoplasmic content are physically partitioned into the two nascent daughter cells (see Figure 3).

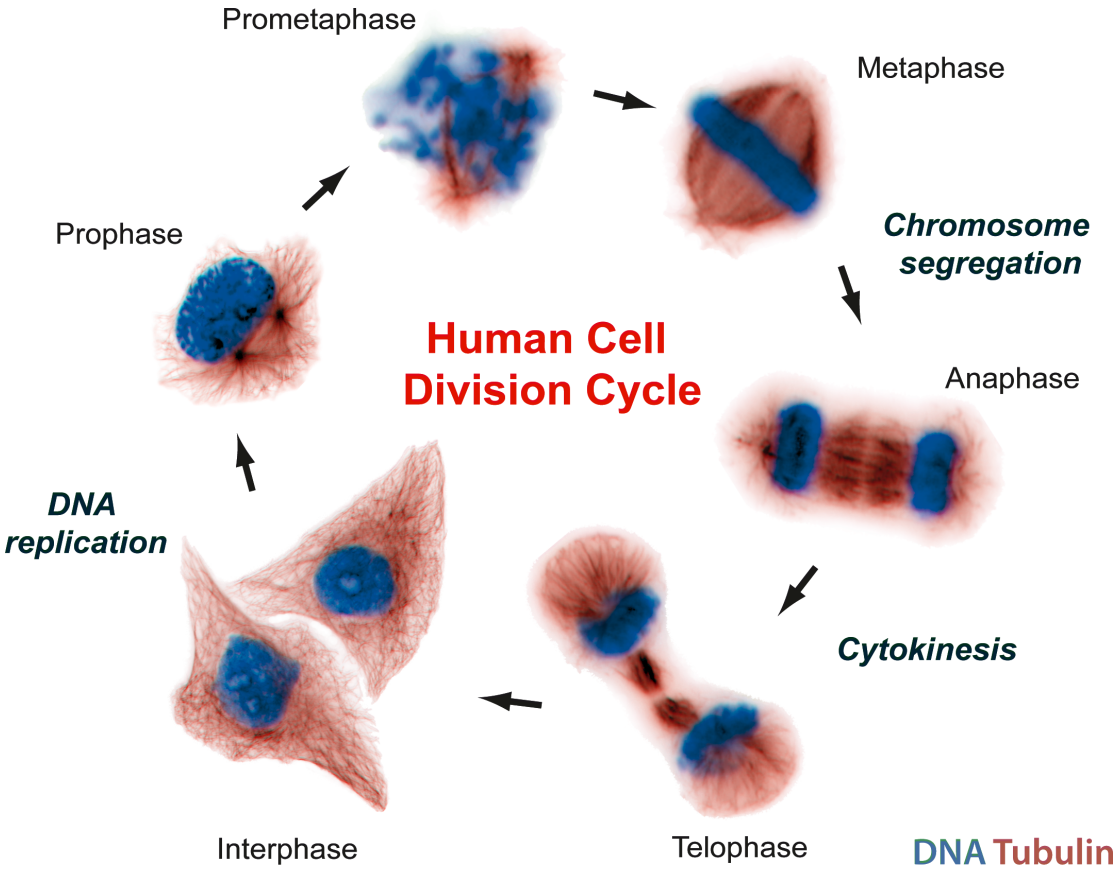

Figure 3 Human cell division cycle

Illustration of the cell division cycle in human cells. In interphase the DNA is replicated. As cells enter mitosis, the nuclear envelope breaks down, the DNA condenses and chromosomes become visible, the centrosomes begin to move apart and to nucleate highly dynamic microtubules. In prometaphase chromosomes begin to attach to microtubules emerging from the centrosomes. In metaphase all chromosomes are bi-orientated and aligned into a chromosomal plate at the centre of the cell. At anaphase onset, sister chromatids cohesion is lost and chromatids are pulled towards opposing poles. Shortly thereafter, chromosomes start to decondense and the nuclear envelope reforms. During cytokinesis and concomitant with the reformation of the nuclear envelope, the invagination of the plasma membrane creates a cleavage furrow that bisects the cytoplasm and compresses microtubules in the middle of the cell. Finally, an abscission event severs the intercellular bridge and separates the daughter cells completely. DNA is displayed in blue and microtubules in red.

1.3.1 Mitosis

The term 'mitosis' was first coined by Walther Flemming in the 19th century to describe the stages of cell division during which chromatin has a threadlike morphological appearance (Flemming, 1882). The different stages of mitosis are still defined based on the appearance of these chromatin threads (Morgan, 2007) (see Figure 3).

In prophase, replicated DNA initiates condensation (Hirano and Mitchison, 1994). The mitotic spindle begin to assemble from the centrosomes and form astral microtubules (Rusan et al., 2001). During prometaphase, the nuclear envelope is broken down and chromosomes are attaching to spindle microtubules via kinetochores (Güttinger et al., 2009; Cheeseman and Desai, 2008). The spindle poles migrate toward opposite poles pushed apart by motor proteins at the microtubules and form a bipolar structure (Tanenbaum and Medema, 2010). The sister chromatids are held together by cohesion (Nasmyth, 2011). The spindle assembly checkpoint ensures that chromosome segregation does not occur until the last chromosome has been correctly attached (Rieder et al., 1994). At metaphase the chromosomes are aligned and bi-oriented at the cell equator to form the metaphase plate between the two centrosomes. At the metaphase-to-anaphase transition, the APC/C initiates the proteasome-dependent destruction of the anaphase inhibitor securin (Funabiki et al., 1996). This liberates the cysteine-protease separase, which cleaves the cohesin subunit Scc1/Rad21 (Uhlmann et al., 1999; Hauf et al., 2001) and triggers the segregation of sister chromatids to opposite poles. Chromatids are pulled by the shortening of kinetochore microtubules during anaphase A. During anaphase B, the spindle elongates by increasing the centrosome-centrosome distance to support chromosome segregation. During anaphase, overlapping polar non-kinetochore microtubules assemble a stable structure called the spindle midzone or central spindle (Glotzer, 2009). The spindle midzone contains tightly bundled microtubules with overlapping plus ends and is formed by the activity of microtubule-binding and cross-linking proteins and microtubule motor proteins. The spindle midzone helps keep segregated chromatids apart and also serves as a signalling platform that recruits a number of important regulators of cytokinesis, such as mitotic kinases and

modulators of Rho GTPase activity. GTPases (guanosine triphosphate hydrolase) are guanine nucleotide binding proteins and can function as molecular switches. They mediate signalling when they are bound to GTP thereby 'switched-on' (Glotzer, 2009). Experiments in nematode embryos, *Drosophila* cells and mammalian cells have shown that the spindle midzone plays an instructive role in positioning of the cleavage furrow (Bringmann and Hyman, 2005; Wolfe and Glotzer, 2009; Rappaport, 1997; Somers and Saint, 2003). In telophase, which marks the end of mitosis, the two masses of DNA have arrived at the spindle poles and begin to decondense while the nuclear envelope reforms around them. Cytokinesis is completed by a process called abscission that severs the intercellular bridge and yields two physically distinct daughter cells.

1.3.2 Regulation of mitosis

Mitosis and cytokinesis are highly dynamic processes that involve the intensive remodelling of cellular architecture and cellular components. Thus, they are largely controlled by post-translational modifications, primary protein phosphorylation, and protein degradation. Phosphorylation of substrates by mitotic kinases (most importantly Cdk1, PLK1, Aurora kinases) allows cells to transit from G2 to M-phase. Dephosphorylation of Cdk1 kinase targets together with inactivation of the kinase itself are required for mitotic exit (Wurzenberger and Gerlich, 2011). Proteasome-mediated proteolysis, as in the case of securin and cyclin B, and site-specific proteolysis, as for cohesin, contributes to the irreversibility of the transition from metaphase to anaphase.

Cdk1 kinase

Phosphorylation of various targets by Cdk1 regulates the entry into mitosis and dictates many steps during mitotic progression, such as cell rounding, nuclear envelope breakdown, chromosome condensation and spindle formation. Both cyclin A and cyclin B contribute to the entry into mitosis, but as cyclin A is degraded soon after mitotic entry, cyclin B-Cdk1 is the crucial key complex that drives cells into metaphase.

The Cdk1-cyclin complexes as such are assembled in G2 before mitosis. However until the cell is ready to enter mitosis, Cdk1 remains inactivated by phosphorylation at T14 and Y15 by Wee1 and MYT1 (Endicott et al., 1994). MYT1 inhibits Cdk1 additionally by binding to cyclin B and preventing it from entering the nucleus (Liu et al., 1999; Wells et al., 1999). Cdk1 becomes active when MYT and Wee1 are both deactivated by hyper phosphorylation (Nakajima et al., 2003; Watanabe et al., 1995). At the same time the inhibitory phosphorylation events on Cdk1 are removed by Cdc25 phosphatases. In mammalian cells all three Cdc25A, B and C, are implicated in the control of mitotic entry through Cyclin B-Cdk1 activation. Cdc25B initiates Cdk1 activation at the centrosomes and subsequently Cyclin B-Cdk1 translocates to the nucleus (Powers et al., 2000; Lammer et al., 1998; De Souza et al., 2000). Cdk1 activation is also reinforced via an auto feedback loop by Cdk1 phosphorylation of Cdc25C and Cdc25A leading to a level of Cdc25 phosphatase activity sufficient to fully activate Cdk1 and the progression of the cell through mitosis (Mailand et al., 2002; Hoffmann et al., 1993; Strausfeld et al., 1994; Izumi et al., 1992). Cdk1 phosphorylates many targets to promote mitotic entry and progression. This induces events such as mitotic cell rounding, chromosome condensation, nuclear envelope break down, mitotic spindle assembly, kinetochore assembly and many others (Güttinger et al., 2009; Kimura, 1998; Nigg et al., 1996). Recent FRET (Fluorescence resonance energy transfer) experiments have measured the activity profile of Cdk1 during mitotic entry (Gavet and Pines, 2010). Although it is clear that Cdk1 activity drives cell into mitosis, the key kinase targets remain less well understood and may be difficult to pinpoint experimentally due to multiple phosphorylation reactions and redundancy.

Recently an important pathway that is required for the entry into mitosis has been identified. In order to maintain the phosphorylated status of Cdk1's mitotic targets, PP2A, the Cdk1 counteracting phosphatase, needs to be inhibited. In mitosis PP2A is kept inactivated by its inhibitor endosulfin which is activated by Greatwall kinase (Gharbi-Ayachi et al., 2010; Mochida et al., 2010).

At anaphase onset Cdk1 has fulfilled most of its functions and it is then deactivated via proteolysis of Cyclin B. Cyclin B contains a destruction box that is recognized

by APC/C for its ubiquitinylation and subsequent degradation (Pines, 2011). For cells to exit mitosis, Cdk1 inactivation is not sufficient. Also its substrates have to be dephosphorylated (Wurzenberger and Gerlich, 2011). This allows reversal of many mitotic entry processes and controls the reassembly of the nuclear envelope or chromosome decondensation (Güttinger et al., 2009; Moser and Swedlow, 2011).

Also the onset of cytokinesis tightly linked to the inactivation of Cdk1 and the dephosphorylation of Cdk1 substrates (Niiya et al., 2005; Potapova et al., 2006) Acute inhibition of Cdk1 using a small molecule compound in mitotic cells for example triggers the rapid onset of cytokinetic activity. This suggests that Cdk1 inhibits cytokinesis prior to anaphase onset and that its inactivation relieves that inhibition. The mechanisms underlying this control have been partially dissected. For example removal of inhibitory Cdk1 phosphorylation of Mklp1 and Prc1 promotes their function as microtubule-bundling and motor proteins at the central spindle, an important structure for the regulation of cytokinesis (Zhu et al., 2006; Mishima et al., 2004). Furthermore, Cdk1 phosphorylation of Prc1 prevents recruitment of Polo-like kinase 1, a kinase required for cleavage furrow formation (Petronczki et al., 2007; Burkard et al., 2009), to the spindle midzone (Neef et al., 2007).

How the dephosphorylation of Cdk1 targets is controlled in animal cells has become a central research focus. However, it is unclear whether the main phosphatase(s) that counteract(s) Cdk1 in mammalian cells has already been identified. In budding yeast, Cdc14 phosphatase is essential to trigger the exit from mitosis (Stegmeier and Amon, 2004). Human Cdc14s can rescue deletion of Flp1/Clp1 (Cdc14 ortholog in fission yeast) demonstrating that the proteins belonging to this family are highly conserved across species (Vázquez-Novelle et al., 2005). Cdc14 phosphatases do not seem to play similarly important role in metazoan organisms (Mocciaro and Schiebel, 2010). RNAi depletion of Cdc14 in C elegans showed no apparent phenotype in mitosis (Saito et al., 2004a). Knock out of Cdc14A or Cdc14B in chicken and human cells only led to increased sensitivity to DNA damage (Mocciaro et al., 2010). Redundancy among Cdc14 phosphatases or with other phosphatases may explain the observed results.

In human cells PP1 and PP2A are believed to contribute to the dephosphorylation of Cdk1 substrates. Phosphoprotein phosphatase PP1 and PP2A phosphatases are PPP family enzymes that in addition to a catalytic subunit can also contain scaffold subunits and a range of different regulatory subunits that are thought to provide a substrate specificity (Virshup and Shenolikar, 2009). Studies of these pathways have been challenging due to the numerical and combinatorial complexity of phosphatase holoenzymes and the high level of redundancy among them. Both protein complexes are also involved in a variety of other processes apart from cell cycle regulation. Experimental evidence suggests that PP2A and its regulatory subunit B55 is responsible for dephosphorylating Cdk1 substrates came from various sources. Firstly, *in vitro* phosphorylated Cdk1 consensus sites (pSer-Pro or pThr-Pro) have been shown to be the preferred target for the PP2A-B55 complex (Agostinis et al., 1992; Ferrigno, 1993). Second, in a genome wide RNAi screen in human tissue culture cells, PP2A and its subunit B55α were both identified as genes whose depletion causes a delay in exit from mitosis. Depletion of B55α causes delay in nuclear envelope reformation, disassembly of the mitotic spindle and chromosome decondensation (Schmitz et al., 2010).

Observations leading to identification of PP1 as the second Cdk1 phosphatase in metazoa came from studies in multiple organisms. In *Drosophila melanogaster,* mutations in PP1 lead to abnormal anaphase configurations and the missegregation of chromosomes (Axton et al., 1990). In mice, increased PP1 activity also reduces Cdk substrate phosphorylation (Manchado et al., 2010). In *Xenopus laevis* egg extracts, the depletion or inhibition of PP1, impairs the dephosphorylation of Cdk1 substrates, such as the APC subunit Cdc27 (Wu et al., 2009). The details of how phosphatases regulate mitotic exit in mammalian organisms are not entirely understood yet and will remain the focus of intense research over the next few years.

Plk1 kinase

Another important kinase regulating different steps during mitosis and also cytokinesis is the polo-like kinase 1 (Plk1) (Petronczki et al., 2008). Kinases of the Polo family are conserved in eukaryotes. Plk1 localizes to centrosomes and kinetochores in early mitosis and to central spindle in anaphase. Plk1 is targeted to

different cellular locations by recognizing a phosphorylated 'primed' protein through its C-terminal polo-box domain. This targets Plk1 to a large number of proteins often phosphorylated primarily by Cdk1 in early mitosis (Elia et al., 2003). In anaphase Plk1 often self primes its targets (Burkard et al., 2009; Neef et al., 2007). During cytokinesis, Plk1 self-priming of Prc1 promotes the recruitment of the kinase to the spindle midzone (Neef et al., 2007). Following recruitment, Plk1 phosphorylates its substrates in close proximity.

Centrosome maturation and microtubule nucleation along with stable attachments of spindle microtubules to kinetochores are the most prominent examples of early mitotic processes that require Plk1 (Petronczki et al., 2008). Loss-of-function mutations in Plk1 orthologs or small molecule inhibition of Plk1 cause monopolar spindles and arrest cells in mitosis (Lénárt et al., 2007; Sunkel and Glover, 1988).

Because Plk1 is essential for early mitotic processes, the crucial role of Plk1 during cytokinetic cleavage furrow formation in mammalian cells was only uncovered once chemical biology or chemical genetic tools became available that allowed the acute and anaphase-specific inactivation of the kinase (Elia et al., 2003; Santamaria et al., 2007; Burkard et al., 2007; Petronczki et al., 2007). Plk1 is targeted for degradation and deactivated when cell exit mitosis (Lindon and Pines, 2004).

Aurora kinases

Aurora kinases form another group of enzymes essential for the regulation of mitosis. Aurora A is required for centrosome maturation and therefore required for the proper assembly of the mitotic spindle (Glover et al., 1995; Marumoto et al., 2005; Barr and Gergely, 2007). Aurora A also promotes the activation of Plk1 by phosphorylating its regulatory T-loop (Macůrek et al., 2008). This is particularly important for the resumption of cell cycle progression and mitotic entry following a DNA damage checkpoint G2/M arrest.

Another key kinase controlling mitosis in eukaryotic cells is Aurora B. Aurora B is the enzymatically active subunit of a protein complex known as the chromosome passenger complex. In addition to Aurora B, the chromosomal passenger complex (CPC) contains the scaffold protein INCENP (Inner Centromere Protein) along with

Survivin and Borealin, (Ruchaud et al., 2007). The CPC localize to chromatin as cells enter mitosis and Aurora B phosphorylates histone H3 at serine 10, thereby generating an iconic mitotic marker. Aurora B and the CPC promotes DNA condensation through regulating the chromatin association of condensin (Macůrek et al., 2008; Lipp et al., 2007; Collette et al., 2011). The CPC and Aurora B activity are also essential for correcting erroneous microtubule kinetochore attachments and maintaining a robust SAC arrest (Tanaka et al., 2002; Hauf et al., 2003; Cheeseman et al., 2002; Musacchio and Salmon, 2007). Aurora B localizes to centromeres in early mitosis and is thought to regulate microtubule-kinetochore attachments by phosphorylating outer kinetochore proteins and decreasing their affinity for microtubules (Cheeseman and Desai, 2008).

At the metaphase-to-anaphase transition, the CPC relocates from the chromosomes and centromeres to the spindle midzone (Ruchaud et al., 2007). This change in localization is dependent on the dephosphorylation of the Cdk1 substrate INCENP (Hümmer and Mayer, 2009) and has given the name to this protein complex (Ruchaud et al., 2007).

In anaphase, the chromosomal passenger complex localizes to the central spindle and acts as an essential regulator of cytokinesis in animal cells (Schumacher et al., 1998; Kaitna et al., 2000; Adams et al., 2000; Hauf et al., 2003). Aurora B generates a phosphorylation gradient at the midzone that is thought to be important for cytokinetic control (Fuller et al., 2008) (see later sections).

APC/C ubiquitin ligase

As mentioned earlier, protein degradation induced by the APC/C is important for cells to exit mitosis (Pines, 2011). APC/C is an E3 ubiquitin ligase that marks proteins for degradation via the 26S proteasome by substrate ubiquitination. APC/C requires its co-activators CDC20 or CDH1 to modify its substrates. CDC20 bound APC/C targets proteins for degradation at the metaphase-to-anaphase transition and thereby regulates mitotic exit (Pines, 2011). APC/C cannot bind to CDC20 unless it is phosphorylated by Cdk1 and Plk1 (Eytan et al., 2006; Shteinberg et al., 1999; Kramer et al., 2000; Kraft et al., 2003; Golan et al., 2002). This ensures that it can only be fully active in mitosis. Furthermore, APC/C activity which triggers the

metaphase-to-anaphase transition is under tight control by the SAC to allow chromosome alignment and bipolar attachment before sister chromatids are split (Musacchio and Salmon, 2007).

The most important mitotic APC/C targets, whose degradation leads to anaphase, are securin and the mitotic cyclins. Degradation of securin releases the protease separase from its inhibitory embrace (Zur and Brandeis, 2001; Leismann et al., 2000; Funabiki et al., 1996; Cohen-Fix et al., 1996; Ciosk et al., 1998) and allows it to cleave the cohesin complex that holds sister chromatids together (Uhlmann et al., 1999, 2000; Hauf et al., 2001). No longer attached to each other, sisters can now move to opposite spindle poles in anaphase. Although APC/C promotes cyclin A degradation early in mitosis (Den Elzen and Pines, 2001; Geley et al., 2001), cyclin B proteolysis does not occur unless spindle assembling checkpoint is satisfied (Clute and Pines, 1999). This guarantees that anaphase does not occur before proper chromosome attachment. Protein degradation mediated by APC/C is thought to ensure that mitotic exit is irreversible and can only occur once per cell cycle. Because securin and cyclin B are degraded at the same time, this also ensures that chromosome segregation and exit from mitosis, including the cytokinetic programme, are temporally coordinated.

1.3.3 Cytokinesis and cytokinesis failure in animal cells

Cytokinesis is the division of the cellular cytoplasm (Fededa and Gerlich, 2012; Green et al., 2012; Barr and Gruneberg, 2007). It consists of a series of steps and in animal cells occurs after the segregation of the sister genomes in mitosis. Ultimately, it leads to the physical separation of one cell into two daughter cells and marks the birth of a new cell (Figure 4). Cytokinesis is initiated by an invagination of the plasma membrane, called the cleavage furrow, after anaphase onset in the equatorial zone of the cell (Green et al., 2012; Fededa and Gerlich, 2012). A network of cortical actomyosin filaments, called the contractile ring, drives ingression of the cleavage furrow. After completion of furrowing, the remaining narrow cytoplasmic bridge that connects nascent daughter cells is severed in a reaction called abscission.

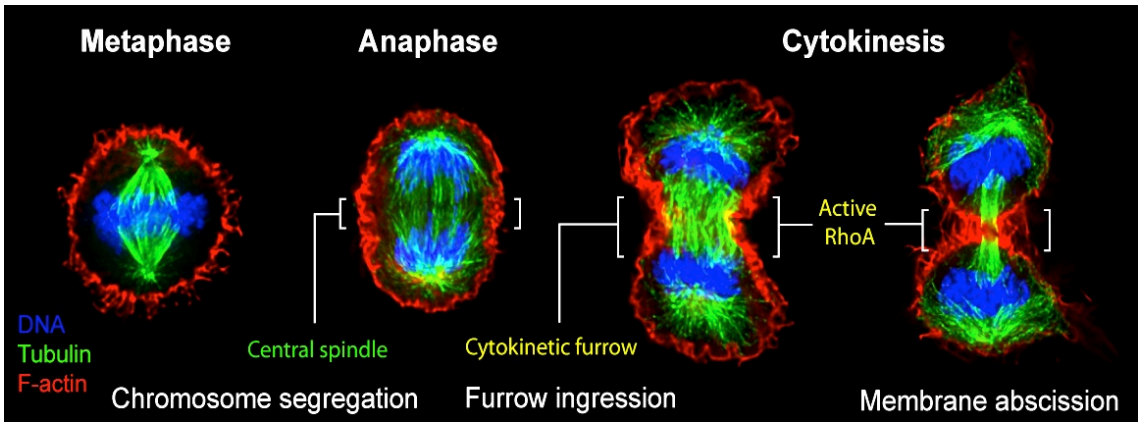

Figure 4 Final steps of cell division

In metaphase, chromosomes, attached to microtubules, align at the centre between opposing centrosomes, forming the metaphase plate. At anaphase sister chromatids separate and move towards spindle poles. Central spindle assembles at the region of antiparallel overlapping microtubules midway between the opposite poles. As cytokinesis begins, stimulated by equatorial active RhoA, the cytokinetic furrow initiates contraction of the cell cortex and compaction of the central spindle. An intercellular bridge remains until the final step, abscission, separates the two daughter cells by fusion of the membrane.

For the accurate inheritance of genetic information, it is crucial that furrow formation is initiated at the cell equator between segregating chromosomes and that this occurs after chromatin has cleared the cleavage plane. In animal cells, the mitotic spindle plays a pivotal role in the formation and placement of the cleavage furrow. The coupling of cytokinesis and chromosome segregation to the mitotic spindle ensures that nuclear and cytoplasmic division are tightly coordinated.

Cytokinesis plays a key role in preventing chromosomal and genomic instability, both hallmarks of human cancers (Ganem et al., 2007). Successful cytokinesis partitions sister genomes and centrosomes into daughter cells. This ensures that both daughter cells inherit a diploid set of chromosomes and only a single centrosome. During the subsequent cell cycle and after centrosome duplication, this allows the formation of a bipolar spindle. Experiments in mice have demonstrated that cytokinesis failure generates unstable tetraploid intermediate cells that undergo further chromosomal instability and promote the formation of malignant tumours (Terada et al., 1998). Subsequent work has shown that the formation of multipolar spindles is largely responsible for the enhanced rate of chromosome non-disjunction (Ganem et al., 2009). Not only cytokinesis failure has dramatic consequences but also collisions between the cleavage furrow and chromatin that has not cleared the cleavage plane. Recent work in human cells has revealed that these collision cause DNA damage and promote the emergence of structural chromosome aberrations such as translocations (Janssen et al., 2011). These studies underscore the importance of undergoing cytokinesis successfully and in a manner that is coordinated with nuclear division. Therefore multi cellular organisms have developed robust and sometimes redundant mechanisms to ensure that cytokinesis occurs accurately.

As discussed above, cytokinesis failure can have detrimental consequences when cells attempt to continue to proliferate. Interestingly, several mammalian cell types, such as hepatocytes and megakaryocytes, are developmentally programmed to undergo cytokinesis failure and hence to become polyploid (Gentric et al., 2012; Lacroix and Maddox, 2012). These cells appear to actively and specifically suppress particular functions of the cytokinetic machinery (Gao et al., 2012; Celton-Morizur et al., 2009) unlike other cell types that undergo endoreduplication without

attempting cell division (Edgar and Orr-Weaver, 2001; Martindill and Riley, 2008). Polyploidization in these cells may confer beneficial physiological properties.
When sister chromatids start to segregate to the opposite poles at the anaphase, the entire mitotic spindle system is rearranged (Von Dassow, 2009; Glotzer, 2009; D'Avino et al., 2005). From this network of microtubules signals for furrow placement and induction are thought to be relayed to the cell periphery and cortex leading to the selective contraction of the equatorial membrane. Some components of the molecular pathways underlying this control have been identified but our understanding of this process is still incomplete. Understanding how the mitotic spindle controls cytokinetic events at the plasma membrane is a key challenge for cell division research.

Studies in different animal cell systems have revealed that the small GTPase RhoA acts as a master regulator of contractile activity during cytokinesis (Melendez et al., 2011; Kamijo et al., 2006; Jantsch-Plunger et al., 2000; Drechsel et al., 1997; Bement et al., 2005; Prokopenko et al., 1999). Activation of RhoA at the equatorial membrane induces the assembly and the contraction of the actomyosin network that drives cleavage furrow ingression. Furrow ingression compacts microtubule bundles of the spindle midzone until they form the core of a dense structure called the midbody. At this stage, the two nascent daughter cells remain connected by an intercellular cytoplasmic bridge until a secondary membrane constriction separates them during abscission (reviewed in (Green et al., 2012)).

1.3.3.1 Assembly of the central spindle (CS)

One characteristic structure that is formed in anaphase cells is the spindle midzone, or central spindle. The spindle midzone plays an important role in regulation of cytokinesis by helping to specify the cleavage plane (see below). As cells enter anaphase Cdk1 activity drops quickly and the microtubule dynamics change dramatically. Chromosomes are being pulled towards the opposite poles of the cell and astral microtubules elongate (Rusan et al., 2001). In the area between segregating masses of chromosomes, an array of antiparallel microtubules that overlap with their plus ends is assembled into the central spindle (see Figure 5)

(Glotzer, 2009). In Ptk1 cells the length of the overlapping region is initially 5 μm in length but shortens as anaphase progresses (Mastronarde et al., 1993). Central spindle MTs are largely derived of interpolar microtubules that are anchored close to the centrosome but some are also formed *de novo* in a manner dependent on the augmin complex (Uehara and Goshima, 2010; Uehara et al., 2009).

The formation of the spindle midzone depends on microtubule-associated and microtubule motor proteins. Prc1, KIF4 are examples of essential MT binding proteins in whose absence no central spindle is formed (Jiang et al., 1998; Kurasawa et al., 2004). Prc1 is a homodimer and cross-links antiparallel microtubules. Cdk1 and Plk1 phosphorylation prevents it from accumulating at MTs and bundling them into a central spindle-like structure prior to anaphase onset (Zhu et al., 2006; Hu et al., 2012). KIF4 is a kinesin and is recruited by Prc1 to modulate the length of the antiparallel MT overlap region. It acts by reducing the growth rate of MTs (Hu et al., 2011). *In vitro* Prc1 and KIF4 have been demonstrated to be sufficient for assembling an overlapping array of MT bundles. Moreover, the length of the overlapping region can be altered by changing concentration of KIF4 (Bieling et al., 2010; Subramanian et al., 2010)

A key structural and signalling scaffold component of the spindle midzone in animal cells is the centralspindlin protein complex (Glotzer, 2009). Loss of centralspindlin function disrupts the formation of the spindle midzone in animal cells (Mishima et al., 2002). Centralspindlin is a heterotetramer consisting of two molecules of the kinesin Mklp1 and two molecules of Rho GTPase activating protein (GAP) MgcRacGAP (Pavicic-Kaltenbrunner, 2007; Mishima et al., 2002). *In vitro*, Mklp1 is a plus-end directed MT motor (Nislow et al., 1992) and centralspindlin can bundle microtubules (Mishima et al., 2002). Recent work has revealed that centralspindlin can form higher order clusters *in vivo* and that the complex migrates along MTs towards the central spindle *in vivo* (Hutterer et al., 2009). Cluster formation is inhibited by binding of Mklp1 to a 14-3-3 protein and this inhibition is alleviated during cytokinesis by Aurora B dependent phosphorylation of Mklp1 (Douglas et al., 2010). Mklp1 is also inhibited before anaphase onset by Cdk1 phosphorylation which reduces its affinity to MT (Mishima et al., 2004).

The CPC and Aurora B are important for the formation of the spindle midzone (Hauf et al., 2003; Kaitna et al., 2000). Although Mklp1 has been identified as an important Aurora B substrate at the midzone (Guse et al., 2005; Douglas et al., 2010), it is likely that the CPC contributes to central spindle formation and stability by targeting additional proteins.

The timing of spindle midzone formation and the position of the structure within the geometry of anaphase cells make it an excellent candidate for controlling the positioning of the cleavage furrow and cleavage plane. Indeed, the spindle midzone can be viewed as a signalling hub that recruits cytokinetic regulators such as mitotic kinases and modulators of RhoGTPase activity. The following section will describe the mechanism how the mitotic apparatus determines the axis of the cell division.

1.3.3.2 Determination of the cell division plane

Ray Rappaport demonstrated first in his studies with echinoderm embryos that a network of microtubules determines where the future cleavage plane will be placed. In his famous 'torus' experiment he inserted a glass rod through a sea urchin embryo to block the access of the spindle apparatus to one side of the cell surface, as the spindles are trapped to one side of the glass rod. As the outcome the furrow initiates at the proximal side of the physical barrier closer to the spindle whereas on the distal side no furrowing occurs. This suggest that access of the microtubules to the cell cortex is required to stimulate contraction at the cortex (Rappaport, 1996). In the subsequent division, a furrow not only forms between segregating chromosomes but also between the asters of adjacent spindles suggesting that asters can be sufficient to position the cleavage furrow in Echinoderm embryos.

Many studies on furrow placement were carried out in various model organisms ever since Rappaport's observation. These studies have confirmed that the mitotic spindle plays a key role in positioning the cleavage plane in animal cells (Alsop and Zhang, 2004, 2003; Pollard, 2004; Wheatley and Wang, 1996; D'Avino et al., 2005;

von Dassow et al., 2009; von Dassow, 2009). This has led to identification of pathways and creation of models how the cytokinetic cue could delivered from the spindle apparatus to a defined region of the cortex (Von Dassow, 2009). The different models of furrow induction can be summarized as followed. Two main signals originate from the mitotic spindle, (1) mediated by astral microtubules and (2) derived from the spindle midzone. Depending on the organism and cell type, one path of signal delivery may dominate over the other or both may act redundantly (Von Dassow, 2009).

In *C. elegans* embryos, microtubule asters and the spindle midzone act sequentially and redundantly to position the cleavage furrow (Bringmann and Hyman, 2005; von Dassow, 2009; Dechant and Glotzer, 2003). Astral microtubules define furrow placement by cortical activation of contractility at the equator (equatorial astral MTs) and inhibition of contractility at the poles (polar astral MTs) (Figure 5) (Motegi et al., 2006; Canman et al., 2003; Werner et al., 2007; Dechant and Glotzer, 2003). Astral MTs also differ different based on their turnover rate. While equatorial MT are rather stable, polar astral MT are going through rapid changes between polymerization and catastrophes (Foe and Von Dassow, 2008). The molecular mechanisms underlying the positive and negative regulation of contractility by astral microtubules have not been fully resolved, MT asters can promote the displacement of myosin filaments from the cell poles (Werner et al., 2007). Furthermore, work in nematode embryos has identified a pathway involving G proteins that are specifically required for aster-mediated cytokinesis (Bringmann et al., 2007). The result of the action of astral MTs is increased contractility at the equator and reduced contractility at the poles (polar relaxation) thereby helping to position the cleavage furrow. Recent work in Drosophila cells has also demonstrated that the selective inactivation of proteins, which are required for cortical stiffness, at the cell poles is likely to contribute to polar relaxation (Kunda et al., 2012).

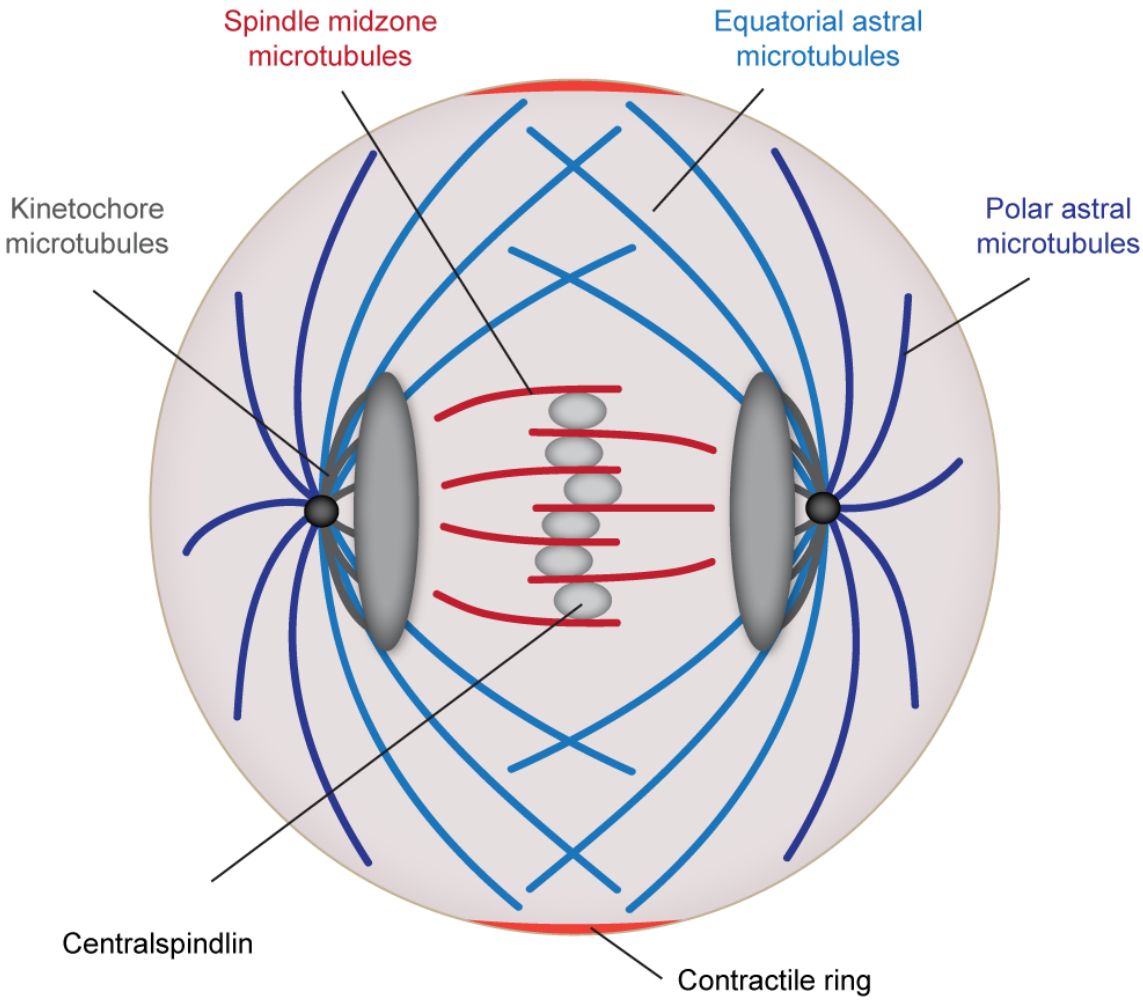

Figure 5 MT arrangement at anaphase

Scheme of the mitotic spindle in an anaphase cell. Kinetochore microtubules (grey) are associated with chromosomes and pull them towards the spindle poles. Spindle midzone microtubules (red) are not interacting with the DNA and forming an overlapping antiparallel array at the centre of the cell that is also called the central spindle. This is the structure where centralspindlin accumulates along with important cytokinetic signalling proteins. Astral microtubules emanate from the centrosomes and reach toward the cell surface. They can be subdivided into two populations: Equatorial astral microtubules (light blue) reach towards the equatorial cortex and site of contraction. Polar astral microtubules (dark blue) are extending towards the poles and surrounding regions. The network of microtubules determines the location of the cytokinetic furrow and the place where contractile ring (orange) forms.

The second pathway, that determines the division plane involves the spindle midzone. While MT aster-stimulated cytokinesis seems to play a dominant role in large embryonic blastomeres, the molecules involved in the spindle midzone-controlled cytokinetic pathway are particularly important for cleavage furrow formation in small somatic animals cells where the midzone is closely juxtaposed to the equatorial cortex. Experiments in mammalian cells have revealed that cleavage furrow ingression requires the constant presence of midzone microtubule bundles. Work in different model organisms has identified the mechanisms of midzone-controlled furrow induction.

As the central spindle is assembled in anaphase, the centralspindlin complex accumulates at the MT overlapping region (see Figure 5). In Drosophila and mammalian cells the centralspindlin subunit MgcRacGAP subsequently recruits the conserved Rho guanine nucleotide exchange factor (RhoGEF) Ect2 to the spindle midzone by direct protein-protein interaction (Yüce et al., 2005; Somers and Saint, 2003). It has been shown that Plk1-mediated phosphorylation of centralspindlin component MgcRacGAP is required for the recruitment of the RhoGEF Ect2 (Petronczki et al., 2007; Wolfe et al., 2009; Burkard et al., 2009, 2007; Brennan et al., 2007). MgcRacGAP, Ect2 and Plk1 activity are essential for cleavage furrow formation and RhoA activation in mammalian cells. Mutations in MgcRacGAP that prevent Ect2 recruitment also block furrow formation. Ect2 binds to MgcRacGAP via its N-terminal BRCT domain repeats. Experiments in human cells suggest that precocious binding of Ect2 to MgcRacGAP is prevented by Cdk1 phosphorylation of Ect2 at T342 (Yüce et al., 2005). These results have led to a model for midzone-stimulated furrow formation. The recruitment of the RhoGEF Ect2 to the spindle midzone promotes the activation of RhoA at the overlaying equatorial cell cortex to trigger cleavage furrow ingression.

How spindle midzone-bound Ect2 activates RhoA and triggers the formation of an equatorial zone has remained largely unexplained. Overexpression experiments have revealed that the C-terminal half of Ect2 can associate with the cell periphery suggesting that this property of Ect2 may be linked to its key role in cleavage furrow formation (Chalamalasetty et al., 2006). Further studies are required to

understand the mechanism and regulation that allows Ect2 to control the formation of a cleavage furrow in animal cells.

Recent work in Drosophila, has identified an interaction between the MgcRacGAP subunit of centralspindlin and the contractile ring component anillin (D'Avino et al., 2008; Gregory et al., 2008). Whether this interaction is conserved in mammalian cells and whether it promotes midzone-controlled contractility remains to be addressed.

Both astral MT-mediated and the spindle midzone-mediated control mechanisms finally converge to define an equatorial activation zone of RhoA (Bement et al., 2005). Subsequently, the activation of RhoA is thought to promote the assembly of the contractile ring and formation of the cytokinetic furrow (Piekny et al., 2005).

1.3.3.3 RhoA activation

RhoA is a member of the Rho subfamily of small GTPases. Rho GTPases, such as Rac, Cdc42 and Rho are involved in many different processes but are best characterized in their role as regulators of the actomyosin system. In various organisms, RhoA has been identified as essential regulator of cleavage furrow formation during cytokinesis (Mabuchi et al., 1993; Kishi et al., 1993; Drechsel et al., 1997; Jantsch-Plunger et al., 2000; Yüce et al., 2005)

RhoA is a very inefficient enzyme and requires guanine nucleotide exchange factors (GEF) and GTPase activating proteins (GAP) to transit between GTP and GDP bound states. Thus, GEF and GAP proteins control the function of RhoA as a switch molecule. In the classical view, GTP bound RhoA ('switch-on') induces cytokinetic ring formation. Once its function is completed a GAP triggers GTP hydrolysis and RhoA becomes inactive (Rossman et al., 2005). When bound to GTP, a conformational switch in the GTPase increases its affinity for downstream effector proteins.

During cytokinesis, the RhoGEF protein Ect2 has emerged as a critical activator of RhoA (Yüce et al., 2005; Somers and Saint, 2003; Kamijo et al., 2006; Zhao and Fang, 2005). The function of a second GEF factor, GEF-H1, possibly also contributes to RhoA function during cytokinesis (Birkenfeld et al., 2007). Counter-intuitively MgcRacGAP, which recruits Ect2 to the midzone, is believed to act as a RhoGAP that can stimulate GTP hydrolysis of RhoA and thereby RhoA inactivation (Jantsch-Plunger et al., 2000). MgcRacGAP's GAP activity has been implicated in cytokinesis in several systems, including *Xenopus* blastomeres, nematode embryos and mammalian cells (Canman et al., 2008; Miller and Bement, 2009; Bastos et al., 2012). However, the GAP activity of MgcRacGAP was found to be dispensable for cytokinesis in chicken lymphocytes (Yamada et al., 2006). Different studies have also come to different conclusions as to what the GTPase target of MgcRacGAP is. Studies in nematodes have suggested that the MgcRacGAP inactivates the GTPase Rac and thereby prevents the formation of branched actin filaments that may interfere with furrow ingression (Canman et al., 2008). In human cells, Rac inactivation by MgcRacGAP has been proposed to prevent precocious attachment of cells to the substratum following cell division (Bastos et al., 2012). In contrast, in *Xenopus* embryos MgcRacGAP's GAP activity limits the width of the contractile zone by targeting RhoA (Miller and Bement, 2009). Future experiments are required to address whether the targets and functions of MgcRacGAP's GAP activity really differ in various organisms and cell types.

Recent studies suggest that instead of activating RhoA at the beginning of cytokinesis and turning it off in the end, a constant flux of RhoA between GTP and GDP bound form may be important for cytokinetic progression (RhoA flux model) (Figure 6). Based on mathematical simulations, the RhoA flux model could help to explain the observed active RhoA-zone during cytokinesis (Bement et al., 2006). Furthermore, many experimental observations suggest that RhoA is indeed constantly shuttling between "on" and "off" states. Using urchin embryos Rappaport was able to repeatedly reinitiate a new site of furrow induction by changing the mitotic spindle localization (Rappaport, 1996). In embryos, the active RhoA zone dynamically changes position if the spindle is displaced, even when contraction has already initiated (Bement et al., 2005). In *Xenopus* embryos, loss of GAP activity leads to a broadened active RhoA zone at the onset of contraction. This suggest

that RhoA is also inactivated throughout the time of furrow contraction and not only after furrow ingression has completed (Miller and Bement, 2009).

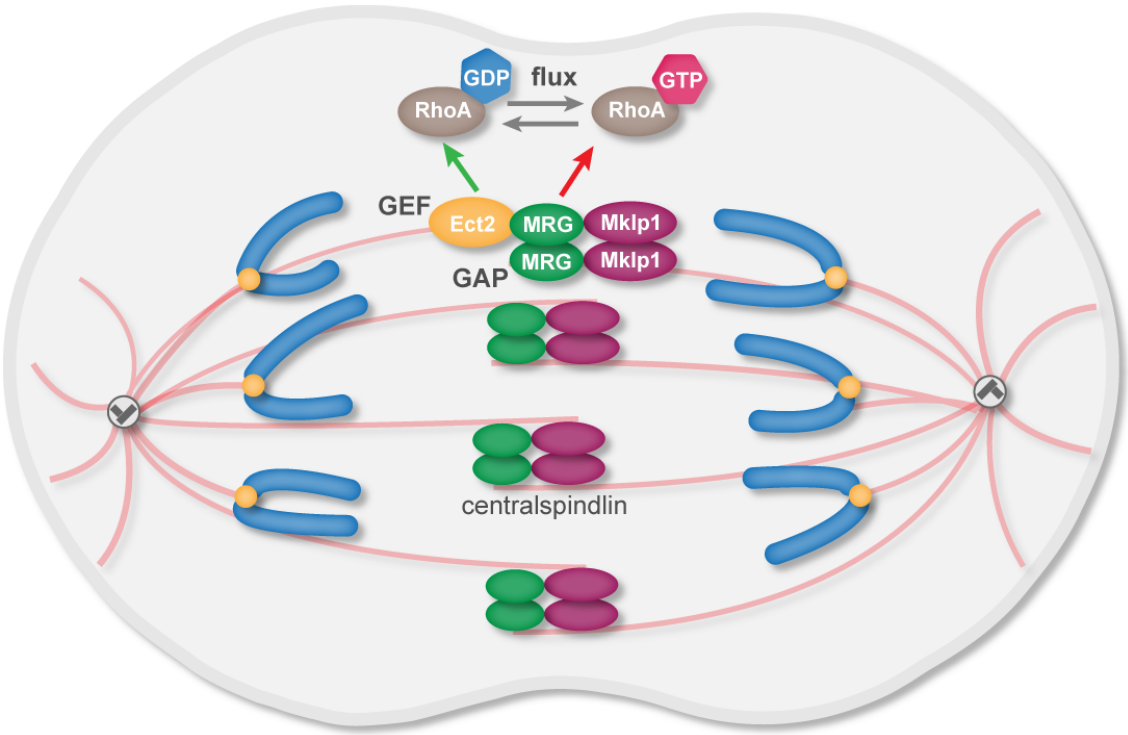

Figure 6 RhoA flux model

Proposed flux model for RhoA activation regulating furrow induction. In anaphase cells, Ect2 is recruited to the spindle midzone via the MgcRacGAP (MRG)/Mklp1-complex. Ect2 activates RhoA by promoting the exchange of GDP to GTP. Activated RhoA induces contractile ring assembly and furrow induction. At the same time MgcRacGAP triggers GTP hydrolysis counteracting Ect2. In this model RhoA is in constant transition between active and inactive states and the level of activated RhoA can be modulated dynamically.

1.3.3.4 Cytokinetic ring and contraction

GTP-bound RhoA at the equatorial membrane activates and recruits a series of proteins that are required for the assembly of the contractile ring. How the cytokinetic ring is formed is not known yet in detail in animal cells and most of our

understanding of the dynamics of contractile ring assembly has emerged from studies in fission yeast (reviewed by (Pollard, 2010)).

Key downstream effectors of activated RhoA during cytokinesis are formins and myosin regulatory kinases (Piekny et al., 2005). Formin family proteins, which catalyse the polymerization of linear actin filaments, are important for cytokinesis in animal cells (Castrillon and Wasserman, 1994; Watanabe et al., 2008; Severson et al., 2002). The formin protein mDia is normally auto-inhibited by an intramolecular interaction. When GTP-RhoA binds to formin this inhibition is alleviated (Alberts, 2001). Formins can then bind to profilin and actin filaments in order to promote the polymerization and nucleation of unbranched actin filaments (Kovar and Pollard, 2004; Pruyne et al., 2002; Pring et al., 2003).

Apart from inducing actin assembly via formin, RhoA also activates members of the ROCK (Rho-associated protein kinase) kinase family (Piekny et al., 2005). Active Rock phosphorylates myosin II regulatory light chain and at the same time also inhibits myosin phosphatase MYPT1 (Amano et al., 1996; Kimura et al., 1996). The Myosin regulatory light chain residues T18 and S19 are the major targets of ROCK kinase. ROCK mediated phosphorylation releases myosin II from auto-inhibition, promotes the formation of myosin II filaments and actomyosin contractility, which is the prerequisite for the activity of the contractile ring (Winter et al., 2001; Uehara et al., 2010). Expression of non-phosphorylatable myosin regulatory light chain version causes cytokinesis defects in Drosophila (Jordan and Karess, 1997).

Another RhoA-activated kinase is the citron kinase which also phosphorylates myosin light chain in *vitro* (Yamashiro et al., 2003). The effect of citron kinase depletion shows however an defect only in later stages of cytokinesis, which suggest that citron kinase may not be essential for contractility (Naim et al., 2004; Shandala et al., 2004). This is in line with the observation that genetic ablation of citron kinase in mice only displays cytokinetic defects in particular tissues (Di Cunto et al., 2000).

Anillin is an essential component of the contractile ring. It functions as a scaffold for the components of the contractile ring. Anillin can bind directly to actin, myosin,

septin proteins, RhoA and MgcRacGAP (Gregory et al., 2008; Piekny and Glotzer, 2008; Piekny and Maddox, 2010). Depletion of anillin leads to oscillations of the cleavage furrow supporting the idea that it acts as a scaffold to stabilize the contractile ring and to promote its anchorage to the plasma membrane (Piekny and Glotzer, 2008; Frenette et al., 2012; Kechad et al., 2012).

Once the actomyosin ring has assembled it initiates the ingression of the cleavage furrow. Ingression of the cleavage furrow proceeds until the formation of an intercellular bridge with the midbody in the centre. Final separation of the daughter cells is achieved by scission of the intercellular bridge in process called abscission (Guizetti and Gerlich, 2010).

The mechanism how the contractile ring generates force is still being debated. The classical model suggests that the contraction is generated like in muscle cells via ATP-powered myosin II-mediated sliding of actin filaments (Carlsson, 2006; Biron et al., 2005). Myosin II is required at the cytokinetic furrow and forms filament structures there (Yumura et al., 2008). Electron microscopy studies have shown alignment of the filaments at the ring support this theory (Maupin and Pollard, 1986; Kamasaki et al., 2007; Tucker, 1971). A Recent study by Ma and colleagues however showed that in COS-7 cells, a mutant of myosin, which can sustain tension but can not translocate actin, is nevertheless able to restore the constriction (Ma et al., 2012). The function of myosin could be primarily to cross-link the filaments rather than to generate the force. An alternative to the classical myosin-sliding model suggests that the energy for contraction could stem from depolymerization of the actin filaments. In cultured cells myosin II has been shown to be required for actin turnover, which could be a source for the contraction force (Murthy and Wadsworth, 2005; Guha et al., 2005).

The behaviour of actin and myosin in the cytokinetic ring is dynamic. This has been demonstrated by photo bleaching experiments (Uehara et al., 2010; Yumura et al., 2008; Murthy and Wadsworth, 2005). However, there is a stable pool of filaments that do not turn over. It is not known yet how these different pools of actin and myosin contribute to force generation in cytokinesis. Further investigations are

required to understand how the action of actomyosin filaments promotes the contraction of the cleavage furrow.

1.3.3.5 Abscission

As the cytokinetic furrow ingresses, MTs of the spindle midzone are compacted into a small structure called the midbody or Flemming body that comes to lie in the centre of the intercellular bridge. Electron microscopy analyses revealed a dense disc in the centre of the midbody containing overlapping antiparallel microtubules (Mullins and Biesele, 1977). The midbody inherits a large number of proteins from the spindle midzone, including centralspindlin and Ect2. The midbody has been proposed to anchor the cleavage furrow after the disassembly of the contractile ring (Mullins and Biesele, 1977). Furthermore, the midbody orchestrates the final abscission reaction by acting as a recruitment platform for abscission proteins (Guizetti and Gerlich, 2010). Proteomic analysis has identified a large number of midbody-associated proteins (Skop et al., 2004). However, the specific function of the majority of these proteins is not yet known.

When furrow ingression is complete and the midbody has formed, an intercellular bridge remains that connects the cytoplasm of the nascent daughter cells. The main challenge for the cell is to maintain the attachment of the membrane and the integrity of the midbody until fission of the membrane has taken place. This can take up to several hours in somatic cells or can take place as quickly as within minutes in dividing blastomeres (Sanger et al., 1985; Carlton et al., 2012; Steigemann et al., 2009). Recent results suggest that anchorage of the midbody to the membrane is mediated by direct interaction of the midbody component and centralspindlin subunit MgcRacGAP with the plasma membrane (Lekomtsev et al., 2012). Mutations within the lipid-interacting C1 domain in MgcRacGAP lead to premature detachment of the membrane and cleavage furrow retraction before abscission can occur. Anillin also contributes to the midbody-membrane anchoring by linking the midbody to membrane-associated septin proteins (D'Avino et al., 2008; Kechad et al., 2012).

To prepare the cell for the abscission, the remaining actin and MT cytoskeletal elements need to be removed as they may occlude the intercellular bridge space. Microtubule severing proteins, such as spastin, and lipid phosphatases, such as OCRL (oculocerebrorenal syndrome of Lowe) that help disassemble actin in the bridge, have been implicated in this process (Connell et al., 2009; Dambournet et al., 2011; Guizetti et al., 2011).

An increasing body of evidence suggests that the final abscission reaction is directed by the ESCRT (endosomal sorting complex required for transport) membrane fission machinery (Guizetti and Gerlich, 2010; Guizetti et al., 2011; Elia et al., 2011; Carlton and Martin-Serrano, 2007). ESCRT proteins mediate membrane fission during retroviral budding and multivesicular body formation (Hurley, 2010). ESCRT proteins are recruited to the midbody through the interaction with the adaptor protein Cep55 (Zhao et al., 2006). Cep55 itself is recruited to the midbody by docking on Mklp1. Recent studies have demonstrated that ESCRT-III filaments composed of the CHMP4B (charged multivesicular body protein 4B) protein form helices or rings adjacent to the midbody (Guizetti et al., 2011; Elia et al., 2011). The ESCRT complexes may provide the force required for the constriction and fusion of the membrane which leads to the final abscission to generate two daughter cells (Guizetti and Gerlich, 2012). In addition to ESCRT centred models of abscission, recycling endosome vesicles have been implicated in abscission (Schiel and Prekeris, 2011). The exact relationship between of ESCRT-III and endosome-driven abscission will require future research in order to be unraveled.

Mitotic kinases also regulate the timing and execution of abscission. As Plk1 activity and protein levels decline when cells exit mitosis, Cep55 is no longer phosphorylated by Plk1 and can then interact with Mklp1 at the central spindle or midbody (Bastos and Barr, 2010). This regulation is thought to be important for timely abscission. In addition to Plk1, Aurora B activity at the midbody is able to delay abscission (Steigemann et al., 2009). This may be particularly important to prevent DNA damage and cytokinesis failure when chromatin is trapped in the cleavage plane. Aurora B phosphorylation of Mklp1 has been proposed to stabilize

the intercellular bridge microtubules (Steigemann et al., 2009). Furthermore, recent work has identified the CHMP4 paralogue CHMP4C as an Aurora B target, whose phosphorylation by the kinase might delay abscission by inhibiting ESCRT-III complex formation (Carlton et al., 2012).

1.3.3.6 Roles of plasma membrane lipids during cytokinesis

While most research on cytokinesis has focused on protein regulators of the process, growing evidence supports the idea that plasma membrane lipids are of great importance for cytokinesis (Atilla-Gokcumen et al., 2010). An accumulation of cholesterol (Ng et al., 2005; Fernández et al., 2004) phosphatidylethanolamine (PE) (Emoto et al., 1996; Emoto and Umeda, 2000), phosphatidylinositol 4,5-bisphosphate (PI(4,5)P2) (Emoto et al., 2005; Field et al., 2005), and ganglioside GM1 (Ng et al., 2005) has been described at the site of cleavage furrow. Interfering with the abundance of these lipids or their availability can cause an increased incidence of cytokinesis failure. However, for the majority of above mentioned membrane lipids the mechanism by which they accumulate at the cytokinetic furrow or their exact functions during cytokinesis are not known.

Phosphoinositides fulfil a variety of signalling and protein docking functions at the membrane, including regulation of actin cytoskeleton (Di Paolo and De Camilli, 2006; McLaughlin and Murray, 2005). With regards to cytokinesis, PI(4,5)P2 is perhaps the best-studied member of this category of phospho-lipids (Echard, 2008). Apart from its role in regulating the actin cytoskeleton and endocytosis (Haucke, 2005; Zhang et al., 2000), PI(4,5)P2 recruit proteins with a pleckstrin homology (PH) domains or with polybasic clusters to the plasma membrane (Logan and Mandato, 2006; Heo et al., 2006)

In mammalian cells, it has been shown that the distribution of PI(4,5)P2 in metaphase is uniform across the cell surface. As cells enter anaphase, PI(4,5)P2 accumulates at the cytokinetic furrow. Injection of antibodies targeting PI(4,5)P2 or overexpression of the PI(4,5)P2-binding PH domain of PLCδ (phospholipase C) domain lead to cytokinesis failure (Field et al., 2005). An explanation for this observation is that this manipulation competes with components of the actomyosin-

based contractile ring for PI(4,5)P2 binding, which could lead to detachment of plasma membrane from the contractile ring (Emoto et al., 2005; Field et al., 2005).

Phosphoinositides have also been implicated in later cytokinetic events. The PI(4,5)P2 5-phosphatase OCRL is transported to the furrow and reduces PI(4,5)P2 levels by hydrolysing it to phosphatidylinositol 4-phosphate (PI4P). This is required for the disassembly of filamentous actin, which facilitates abscission (Dambournet et al., 2011). Phosphatidylinositol 3-phosphate localizes to the midbody and recruits a complex of FYVE-CENT and TTC19 proteins. As result, the CHMP4B subunit of ESCRT-III accumulates at the midbody via interaction with TTC19 controls the abscission step of cytokinesis (Sagona et al., 2010)

Recently, our laboratory demonstrated that MgcRacGAP's C1 domain can link the spindle midzone and midbody to the plasma membrane by binding to the polyanionic inositol lipids PI4P and PI(4,5)P2 (Lekomtsev et al., 2012). This is required to stabilize the intracellular bridge until abscission occurs. The mechanism by which PI(4,5)P2 accumulates at the furrow is only partially known. Phosphatidylinositol 4-phosphate 5-kinase (PIP5-K), which localizes to the cytokinetic furrow, could induce the local accumulation of PI(4,5)P2 by phosphorylating PI4P (Emoto et al., 2005; Zhang et al., 2000). Overexpression of catalytically inactive versions of PIP5-kinase lead to the loss of PI(4,5)P2 at the cleavages furrow and can cause cytokinesis failure (Emoto et al., 2005; Field et al., 2005). Furthermore, the fast recycling endocytic pathway that is controlled by the GTPase RAB35 regulates PI(4,5)P2 levels at the furrow (Kouranti et al., 2006) .

The molecular mechanisms by which phosphoinositides and other lipids contribute to the correct composition and biophysical properties of the membrane during cytokinesis remain an area for future investigations.

1.4 Epithelial cell transforming sequence 2 (Ect2)

1.4.1 Ect2 is required for cytokinesis

Ect2 is an essential and conserved protein in metazoan organisms. Loss-of-function or deletion of the protein has been shown to be lethal in *Drosophila* and mice (Lehner, 1992; Hime and Saint, 1992; Cook et al., 2011). The sequence of Ect2 is highly conserved across species. The Ect2 orthologs in *Caenorhabditis elegans* (Let-21) or *Xenopus* (*XECT2*) along with *Drosophila* (*Pebble/Pbl*) share similarities in amino acid sequence across the different domains of the protein when compared to the human protein (Prokopenko et al., 1999; Dechant and Glotzer, 2003; Tatsumoto et al., 2003).

Activation of RhoA at the cell cortex is thought to be the first step in the formation of the cytokinetic furrow. Ect2 is known to be essential for cytokinesis. *In vitro* it has been shown to act as a guanine nucleotides exchange factor (GEF) for the GTPases RhoA, Rac and Cdc42 (Tatsumoto et al., 1999).

Homozygote lethal *Drosophila pbl* mutants were first isolated in the famous screen by Wieschaus and Nusslein-Vollhard looking for genes affecting embryo cuticular patterning (Nüsslein-Volhard and Wieschaus, 1980). Analysis of the mutants showed that Pbl is required for cytokinesis after the first 13 syncytial mitotic cycles in *Drosophila* embryos. *Pbl* mutants fail to complete cytokinesis from mitotic cycle 14 onwards and become progressively multi-nucleated (Lehner, 1992; Hime and Saint, 1992).

Further detailed analysis in Drosophila revealed that *Pbl* is dynamically expressed during the cell cycle and that it localizes to the cytokinetic ring (Prokopenko et al., 1999). In its absence the contractile ring does not assemble. Genetic studies showed that *Pbl* and RhoA are both components of the same molecular pathway, which induces cytokinesis (Prokopenko et al., 1999). Mutations in either gene result in cytokinesis failure. Based on the fact the Pbl/Ect2 contains a DH-type (Dbl homology) GEF domain (Rossman et al., 2005; Bos et al., 2007), it has been suggested to activate RhoA by supporting exchange from GDP to GTP and

promote the assembly contractile ring assembly and cytokinesis. Consistent with this interpretation, one of the isolated *pbl* alleles harbours a single point mutation in the CR3 helix of the GEF domain (Prokopenko et al., 1999; Rossman et al., 2005). Mutations in this helix are predicted to reduce GEF function. Furthermore, Pbl was shown to interact with RhoA using the yeast two-hybrid system (Prokopenko et al., 1999).

In mammalian cells, Ect2 was first identified in a screen for epithelial genes that are able to transform NIH3T3 cells, hence the name epithelial cell-transforming sequence 2. (Miki et al., 1993). Subsequent studies led to a better understanding of Ect2's role in cytokinesis (see below).

1.4.2 Ect2 domain structure

Human Ect2 encodes a protein of 883 amino acids in length. It contains several annotated and functional domains as illustrated in Figure 7. Whereas the N-terminal region serves as a regulatory region and promotes the localization of the molecule, the C-terminus of Ect2 contains the catalytic DH domain, which mediates the GEF function on Rho GTPases.

When overexpressed, the C-terminal region of Ect2 that contains the guanine nucleotide exchange/Dbl homology domain is able to transform cells (Miki et al., 1993).

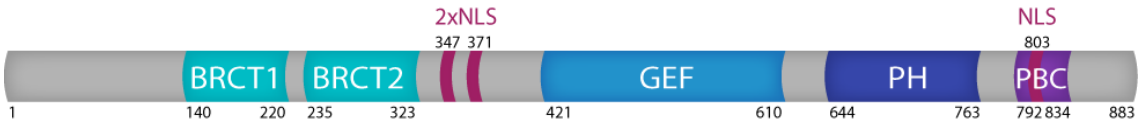

Figure 7 Domain structure of human Ect2

Domain organization of the human Ect2 protein. The two BRCA1 C-terminal repeat domains (BRCT), guanine nucleotide exchange factor domain (GEF), pleckstrin homology domain (PH) and polybasic cluster (PBC). Three nuclear localization signals (NLS) are indicated in red.

Dbl was the first GEF identified to be responsible for cell transformation in B-cell-lymphoma (Srivastava et al., 1986). Like all GEFs, Dbl acts on GTPases by mediating the exchange of GDP for GTP.

GEF proteins usually target one or multiple members of the small GTPases family, which consists of several groups of related molecular switch proteins. Small GTPases change their conformation based their associated guanine nucleotide, GDP (Guanosine-5'-diphosphate) or GTP (Guanosine-5'-triphosphate). When small GTPases are loaded with GTP, they interact with their downstream factors to mediate their signalling function. GTPases regulate a broad range of cellular processes among those cell adhesion, migration, morphology, polarity, growth, survival and others. Loss of GTPase function, as in the case of Ras, can promote tumourigenesis (Rossman et al., 2005).

The DH-type GEF domain is conserved among Ras superfamily GEF proteins: DH-type GEF domains mediate their activity by opening up the nucleotide binding pocket in GTPases. Due to the large excess of GTP over GDP in the cytoplasm of eukaryotic cells, the open GTPases are likely to then acquire a GTP molecule. DH-type GEF proteins contain three conserved regions (CR1-3) consisting of a series of α-helices forming a surface interacting with the GTPase substrates CR1 and CR3 directly interact with the target GTPase (Liu et al., 1998; Worthylake et al., 2000; Zheng, 2001). The aforementioned mutant *pbl* allele in *Drosophila* contains a V531D mutation within the CR3 region and displays a loss-of-Ect2-function phenotype and defective cytokinesis (Prokopenko et al., 1999).

DH-type GEF proteins, like Ect2, contain an obligatory DH/GEF-PH (pleckstrin homology) tandem domain arrangement. The function of Ect2's PH domain has not been resolved thus far. PH domains can serve different purpose ranging from lipid-binding to protein-protein interaction (Scheffzek and Welti, 2012; Lemmon, 2008). PH domains show a low degree of conservation in their protein sequence. There are examples of PH domains in DH-type GEF proteins directly contributing to GEF activity (Rossman et al., 2002, 2003). More often however, PH domains mediates the anchorage of the protein to the plasma membrane via binding to phosphoinositide lipids (Ferguson et al., 1995). Famous examples include the PH

domains of phospholipase C, which specifically binds to $PI(4,5)P_2$, and the PH domain of Grp1, which specifically binds to $PI(3,4,5)P_3$ (He et al., 2008). In cases where PH domains mediate membrane targeting or docking, deletion of the PH domain often leads to a loss of GEF activity *in vivo*. GEF activity can be sometimes be restored by the addition of a membrane targeting sequence, such as a farnesylation signal (Baumeister et al., 2006).

At the N-terminus Ect2 contains two tandem repeats of BRCT (Breast cancer early onset gene 1 carboxyl-terminal) domain. BRCT domains are highly conserved structures often found in proteins regulating the DNA damage response. Tandem BRCT domains act as phospho-peptide binding modules (Yu et al., 2003) and thereby mediate the interaction with phosphorylated proteins (Mohammad and Yaffe, 2009; Leung and Glover, 2011). In the case of Ect2, the BRCT domain has been shown to recognize and bind to the phosphorylated version of the centralspindlin subunit MgcRacGAP at the spindle midzone during anaphase (Yüce et al., 2005). In mammalian cells, this binding requires Plk1-mediated phosphorylation of MgcRacGAP and is responsible for the recruitment of Ect2 to the central spindle (Somers and Saint, 2003; Chalamalasetty et al., 2006; Yüce et al., 2005; Petronczki et al., 2007; Wolfe et al., 2009; Burkard et al., 2009).

At the C-terminal end, Ect2 contains a polybasic cluster (PBC) between amino acid 792 and 834 (this study) (Figure 3). Polybasic clusters are frequently found at the carboxy-termini of small GTPases and target those proteins to the plasma membrane by binding to negatively charged lipids, such as $PI(4,5)P_2$ and $PI(3,4,5)P_3$ (Heo et al., 2006). Deletion of the C-terminal region containing the PBC has been shown to lead to loss of Ect2's transforming activity (Solski et al., 2004). At the same time the PBC harbours a nuclear localization signal and has been proposed to target Ect2 for degradation by APC/C after cells exit mitosis (Liot et al., 2011). The exact function of the PBC of Ect2 during cytokinesis is unknown.

1.4.3 Regulation of Ect2 activity

Ect2's GEF activity is strictly regulated on multiple levels. Two nuclear localization signals (NLS) can be found between the BRCT and DH domains of Ect2 in addition to the third one within the PBC at the C-terminus of the protein. Localization of Ect2 to the nucleus in interphase restricts it from cytoplasm the compartment where Ect2 usually mediates its function. This mechanism may prevent Ect2 from untimely activating GTPases. Indeed, deletion of the NLS leads to elevated levels of Ect2 in the cytoplasm and has shown to increase its transforming capacity (Saito et al., 2004b).

Recent work has demonstrated that Ect2 is exported from the nucleus just prior to the break down of the nuclear envelope (Matthews et al., 2012). This correlates with mitotic cell rounding and is important for Ect2's role in assembling a rigid mitotic cell cortex. Ect2 is hyper-phosphorylated on a series of sites during mitosis (Matthews et al., 2012; Tatsumoto et al., 1999; Niiya et al., 2006). It is possible that these posttranslational modifications promote the export of Ect2 from the nucleus as cells enter mitosis. Although the effects of the individual phosphorylation events on Ect2 remains unknown, in vitro assays demonstrated that dephosphorylated Ect2 displays a reduced GEF activity (Tatsumoto et al., 1999).

The effect of one Cdk1-dependent phosphorylation event on Ect2 has been studied in more detail. Inhibitory phosphorylation of Ect2 at T342 prevents interaction between Ect2 and centralspindlin complex before anaphase onset and may therefore be important in regulating the timely recruitment of Ect2 to the midzone (Yüce et al., 2005). In conflict with proposed inhibitory role of T342 phosphorylation, Hara and colleagues suggest that T342 phosphorylation relieves Ect2 from its auto-inhibition (Hara et al., 2006). The in vivo relevance of T342 phosphorylation clearly merits further investigation.

Binding of Ect2 to centralspindlin has also been proposed to activate its GEF activity (Yüce et al., 2005). The N-terminal region of Ect2 that contains the BRCT domains can acts as an auto-inhibitory moiety by interacting with the C-terminal regions of the protein and possibly inhibiting GEF and PH domain function (Kim et

al., 2005). In pull down assays it has been shown that an N-terminal fragment of Ect2 is able to interact with its C-terminal domain (Saito et al., 2004b). Consistent with this notion, N-terminally truncated versions of Ect2, such as the first isolated sequence, harbour strongly enhanced transforming activity compared to the full-length protein (Miki et al., 1993). Similarly expression of the C-terminal fragment alone but not the full-length protein is able to trigger changes in cell morphology due to ectopic RhoA activation (Matthews et al., 2012).

Finally, recent work has demonstrated that as cell exit mitosis and move into G1, the bulk level of Ect2 decreases due to proteasome-dependent degradation (Liot et al., 2011). Proteolysis is induced through the action of the APC/C bound to its activator CDH1 and involves a targeting sequence within the C-terminal PBC region. Mutation within the destruction sequence of Ect2 leading to stabilization of the protein and increase the transforming activity of Ect2 (Liot et al., 2011).

1.4.4 Ect2 functions beyond cytokinesis

Apart from Ect2's essential contribution to cytokinesis it has been implicated several other cellular functions.

As cells enter mitosis, the cytoskeleton undergoes a large rearrangement to change its shape from flat interphase form to a round mitotic form. This process, known as mitotic cell rounding, is important for proper spindle positioning and assembly and also required for proper chromosome segregation (Kunda and Baum, 2009). Ect2 has been identified to be a critical regulator of the normal speed of mitotic cell rounding (Matthews et al., 2012). It exerts this function by stimulating RhoA activity and cortical contractility. Importantly however, mitotic cell rounding does not require Ect'2 spindle midzone anchor protein MgcRacGAP.

In metaphase, Cdc42 activity regulates the attachment of spindle microtubules to kinetochores (Yasuda et al., 2004). Like many other GEFs Ect2 is able to activate multiple substrates *in vitro* such as Cdc42, Rac1 and RhoA (Tatsumoto et al.,

1999). Ect2 along with MgcRacGAP has been suggested to play a role of Cdc42 modulation during mitosis. Depletion of Ect2 or Cdc42 leads to improper chromosome alignment and segregation (Oceguera-Yanez et al., 2005).

Analogous observations have been made in *Xenopus* extracts *in vitro* (Tatsumoto et al., 2003). Addition of neutralizing antibody against *Xenopus* Ect2 (*XECT2*) leads to the formation of monopolar and multipolar spindles and causes errors in chromosome alignment. This effect could be phenocopied by mutant versions of Cdc42 but not RhoA or Rac1.

In interphase cells, Ect2 is recruited to zonula adherens by α-catenin via centralspindlin and locally activates RhoA (Ratheesh et al., 2012). RhoA is believed to stabilize cell-cell junctional integrity by reshaping the actin myosin cytoskeleton and recruiting downstream effectors including myosin II (Smutny et al., 2010). This shows that the pathway during cytokinetic furrow induction can be utilized in interphase for a different purpose.

Ect2 has also been implicated in establishment of cell polarity (Jenkins et al., 2006; Motegi and Sugimoto, 2006; Liu et al., 2006). In *C. elegans* embryos, Ect2 is localized to the cortex at the anterior side and excluded from the posterior side after fertilization. Depletion of Ect2 leads to loss of embryonic polarity and to mislocalization of the anterior polarity determinant Par-6 (Motegi and Sugimoto, 2006). In epithelial cells, Ect2 has been shown to directly interact with this polarity complex Par6/Par3/aPKC (Liu et al., 2004). Expression of constitutive active or dominant negative alleles of Ect2 disrupts epithelial cell polarity.

1.5 Goal of this research

The mitotic apparatus determines the axis of cell division by controlling RhoA activity and cortical contractility at the equatorial cortex. The mechanism how this cytokinetic signal is delivered is not entirely understood. The RhoGEF Ect2 lies at the heart of RhoA activation and cleavage furrow formation in animal cells. Based on the recruitment of Ect2 to the spindle midzone, it has been proposed that the protein could activate RhoA at the cell equator. How midzone-localized Ect2 promotes the formation of a contractile zone at the cell periphery was unknown. The aim of this study was to investigate how Ect2 controls the formation of the cleavage furrow and how Ect2's function in this process is controlled in space and time. Addressing these questions will further our understanding of the principles that underlie cytokinesis and cell division in animal cells.

Chapter 2. Materials & Methods

2.1 Plasmids, DNA Transfection and Generation of Stable Cell Lines

The cDNA sequence of human Ect2 used in this study (GenBank: AY376439) differs from the published reference sequence (NCBI Gene ID: 1894) by the lack of a single glutamic acid residue after position 44. All amino acid annotations in this study refer to the current reference sequence for Ect2.

To create AcFL-tagged variants of Ect2 for expression in human cells, AcGFP (Aequorea coerulescens GFP) was amplified from pAcGFP-N1 (Clontech) and inserted into pIRESpuro3 (Clontech). During amplification, a Kozak sequence (CGCCACC) and a FLAG epitope (DYKDDDDK) were added to AcGFP before the start codon and after the last amino acid, respectively. Ect2 alleles were inserted into pIRESpuro3-AcFL using EcoRI and AgeI sites. Ect2 deletion and point mutations were created using polymerase chain reactions (Phusion High-Fidelity DNA Polymerase, Finnzymes) and site-directed mutagenesis (QuikChange Lightning Site-Directed Mutagenesis Kit, Stratagene), respectively. All Ect2 variants used in this study are depicted in Figure 14 and Figure 22. To create an siRNA-resistant allele of Ect2, the sequence CACTCACCTTGTAGTT was changed to TACCCACCTGGTAGTA by introducing silent mutations. The 11 N-terminal amino acids of human Lyn kinase (MGCINSKRKDN) were inserted at the N-terminus of FLAG-AcGFP to create MyrPalm-FLAc in pIRESpuro3. pH2B_mCherry_IRES_neo3 (Addgene Plasmid 21044) was kindly provided by Daniel Gerlich (Steigemann et al., 2009).

HeLa ‘Kyoto’ cells were grown at 37% and 5% CO2 in DMEM (Invitrogen) medium with 10% FCS (Sigma). The medium was supplemented with 0.3 µg/ml puromycin (Sigma) to select for and maintain cell lines expressing pIRESpuro3-based AcFL-tagged Ect2 alleles. Cells expressing H2B-mCherry were selected for and grown in medium supplemented with 400 µg/ml G418 (Invitrogen). Plasmids were transfected using FuGENE HD (Roche) for transient expression and FuGENE 6 (Roche) for the generation of stable cell lines. Monoclonal cell lines were isolated after two weeks of antibiotic selection and characterized by immunofluorescence

microscopy and immunoblotting. HeLa “Kyoto” expressing MgcRacGAP-FLAc and H2B-GFP was kindly provided by Sergey Lekomtsev (Lekomtsev et al., 2012)

2.2 siRNA transfection and Drug Treatment

Lipofectamine RNAiMax (Invitrogen) was used for siRNA transfection. The following siRNA duplexes were used at a final concentration of 30 nM: control (Thermo Scientific siGENOME Non-Targeting siRNA #1 D-001210-01), Ect2 (Thermo Scientific siGENOME D-006450-02), Mklp1 (Invitrogen Stealth HSS114138) and MgcRacGAP (Invitrogen Stealth HSS120934).
To disrupt f-actin, cells were incubated in 20 μM dihydrocytochalasin B (Sigma) for 20 min prior to fixation. To acutely inhibit Cdk1, cells were incubated in 165 nM nocodazole (Sigma) for 3 hours before addition of 15 μM flavopiridol (Sigma). To inhibit Plk1 (Figure 30), cells were synchronized by treatment with 2 mM thymidine (Sigma) for 24 hours, released for 6 hours, arrested in mitosis by addition of 165 nM Nocodazole (Sigma) for 4 hours, transferred to medium containing 10 mM MG132 for 2 hours, and then synchronously released and treated with 250 nM BI 2536 20 min after. Lysates for cells in thymidine were collected after 22h incubation in 2 mM thymidine. Nocodazole lysates were taken after 14h incubation in 165 nM nocodazole.

2.3 Preparation of cell lysates

Except for phospho specific AB pT815 (Figure 34 and Figure 35), all lysates were prepared by direct resuspension of PBS washed cells in Laemmli buffer followed by boiling and sonication.
For pT815AB (Figure 34 and Figure 35), cells were resuspended in lysis buffer (20 mM HEPES (pH7.5), 0.1% Triton X-100, 150mM NaCl, 1mM DTT, 5mM MgCl2 and protease inhibitor (Roche)). 20mM NaF and 1μM Microcytin LR (ENZO) were added to inhibit phosphatases.

For the phosphatase treatments (Figure 35), 300µg of lysate protein were incubated with 1600 units of Lambda protein phosphatase (NEB) for 40min at 37°C or 4°C.

2.4 Immunofluorescence microscopy (IF)

Cells on coverslips were fixed for 16 h in -20°C methanol (Figure 9C, Figure 11B, Figure 24B, Figure 26 and Figure 29 anillin), for 10 min at 37°C in 4% formaldehyde (Figure 16B and Figure 17) or for 15 min on ice in 10% tricholoroacetic acid (Figure 29 RhoA. After fixation, samples were permeabilized with 0.5% Trition X-100 in PBS for 15 min and blocked with 3% BSA in PBS containing 0.01%TritonX-100. Samples were incubated for 1 hour each at room temperature with primary and secondary antibodies and mounted with ProLong Gold (Molecular Probes) onto slides. Images for Figure 17, Figure 24B, Figure 26 and Figure 29 were acquired on a Zeiss Axio Imager M1 microscope using a Plan Apochromat 63x/1.4 oil objective lens (Zeiss) equipped with an ORCA-ER camera (Hamamatsu) and controlled by Volocity 5.5.1. software (Improvision). Images in Figure 11B, Figure 17 and Figure 26 were deconvolved using Volocity's iterative restoration function. Images in Figure 16B were acquired with on a Zeiss LSM Upright710 confocal system controlled by Zen 2009 software using a Zeiss Imager.Z2 microscope and a Plan-Apochromat 63x/1.40 Oil DIC M27 lens.

2.5 Antibodies and Dyes

The following primary antibodies were used: mouse monoclonal anti-AcGFP (JL8, Clontech, IF: 1:2000; blot: 1:1000), rabbit anti-AcGFP (Clontech, 1:2000), rabbit anti-anillin (kindly provided by Michael Glotzer, 1:2000) (Piekny and Glotzer, 2008), mouse monoclonal anti-α-tubulin (B512, Sigma, 1:1000), rabbit monoclonal anti-β-tubulin HRP Conjugate (9F3, Cell Signaling Technology, 1:1000), rabbit anti-Ect2 (raised against Ect2 aa 1-421, IF: purified serum 1:100; blot: raw serum 1:2000), rabbit anti-GST (kindly provided by Julian Gannon, 1:600), mouse monoclonal anti-

MBP (kindly provided by Julian Gannon, 1:1000), mouse monoclonal anti-Mklp1 (24, BD Biosciences, IF 1:300), rabbit anti-Mklp1 (N-19, Santa Cruz, blot 1:2000), mouse monoclonal anti-RACGAP1 (1G6, Abnova, 1:2000), mouse monoclonal anti-RhoA (26C4, Santa Cruz 1:75), rabbit anti-phosphospecific T814 (anti-phos-CFSF-1553 animal 20094 02.08.2011) was raised against peptide sequence FSFSK-pT-KRAL following standard provider protocol offered (BioGenes 1:100). Secondary antibodies conjugated to Alexa Fluor 488 or 594 (Molecular Probes) were used for IF detection. DNA was stained with 1 µg/ml DAPI (Molecular Probes). F-actin was labeled with 26.4 nM Alexa Fluor 568 phalloidin (Molecular Probes). HRP-conjugated secondary antibodies were used to detected proteins on immunoblots using chemiluminescence (GE Healthcare). For fluorescence western blott anti rabbit IgG conjugate (Dylight R 680) and anti moudr IgG conjugate (Dylight R 800) (Cell signalling) were used for detection with Odyssey Imaging System (LI-COR Biosciences).

2.6 Live Cell Imaging, FRAP and Image Quantification

Before recording, the medium was changed to phenol-red-free CO2-independent medium supplemented with 20% FCS, 0.2 mM L-glutamine, antibiotics, and 1 mM Na-pyruvate (all Invitrogen). For Figure 11, 31, 30, 33 and Figure 36, frames were acquired at 37°C using a PerkinElmer ERS Spinning disc system equipped with a Nikon TE2000 microscope, a Plan Fluor 40x 1.3 DIC H lens (Nikon) (optovar set to 1.5x), a CSU22 spinning disc scanner (Yokogawa), a IEEE1394 Digital CCD C4742-80-12AG camera (Hamamatsu) and following laser lines: 405 nm (Diode), 440 nm (Diode) 488 and 514 nm (Argon) 568 nm Krypton 640 nm (Diode). Microscope was controlled by Volocity 5.5.1 software (Perkin Elmer). Signal measurement of 16bit image data was carried out using Volocity 5.5.1 software (Perkin Elmer). Excel (Microsoft) was used for further processing of the measured values.

For Figure 12, time-lapse images of the stable cell lines expressing AcFL-Ect2r and H2B-mCherry depleted of endogenous Ect2 were used for image analysis. Mean

AcGFP signal intensities were measured by manually selecting regions of interests for each time point. In the metaphase stage, 3 circular areas, each of 9 pixels diameter were placed spaced 1-2µm apart on the cell membrane near the pole. This was repeated for the other pole of the cell. (2x3 data points). Analogously, 2x3 measurements were taken for the two opposite sides of the equatorial membrane. To measure the central spindle signal intensity, 6 circular regions of 9 pixels each were placed evenly distributed aligned to the metaphase plate within the cell. 4 circular regions of 500-1000 pixels were placed within the cytoplasmic regions to the left and right of the metaphase DNA to obtain the mean cytoplasmic signal. The positions of all regions of interest were adjusted to compensate for movement of the cells when required. As the cell initiated cytokinesis and the midzone compressed, the spacing between individual measurement areas at the equatorial membrane and central spindle were reduced accordingly. Measured mean intensities of all data areas were subtracted by the mean signal intensity outside the cell (manually selected area of >2000 pixels). Signal values of identical cell compartments were averaged for each time point to obtain the data series of one cell. The cytoplasmic signal at t=-2min was used as reference. Signal intensity curves of 5 cells were averaged to obtain the displayed curve including standard deviations.

For Figure 33B and Figure 36B a HeLa cell line stably expressing H2B-mCherry were transiently transfected with AcFL-Ect2CT or AcFL-Ect2CT-T814A constructs and imaged over time. Mean AcGFP intensities were measured for each time point. To obtain membrane signal value, 6 circular regions, each 9 pixels in size, were manually distributed evenly at the cell periphery to measure their mean signal intensities. 2 circular regions of 1000-2000 pixels size were manually defined within the cytoplasmic region and intensities measured to obtain cytoplasmic signal values. Movement of the cell was adjusted when required. Mean signal intensities were subtracted by the mean background signal outside of the cell (manually selected area of >2000 pixels). Values were averaged amongst their categories (membrane or cytoplasm) for every time point. To obtain a membrane to cytoplasm distribution-ratio of a cell over time, the averaged mean membrane signal was divided by averaged mean cytoplasmic signal. First frame of visible separation of chromosomes (Figure 33) or time of CDK inhibitor addition (Figure 36) was set to

t=0. Membrane to cytoplasm distribution curves of 8 individual cells were averaged across time points to obtain the displayed curve including standard deviation.

For the FRAP experiment in Figure 32, untreated monoclonal cell lines stably expressing MgcRacGAP-FLAc or AcFL-Ect2r were used for recording. All lasers were set to maximum intensity and bleaching duration was set to 400ms. Photo bleaching was restricted to a manually selected circular area at the central spindle to a size of 200-400 pixels. Selected area represented <10% of total MgcRacGAP-FLAc signal (Figure 32A) or <3% AcFL-Ect2 before bleaching (Figure 32B). Frames were acquired at 1s intervals. To obtain bleached “Central spindle (bleached)” signal values, mean AcGFP intensities were measured for each time point for a manually selected area (~100 pixels) within the photo-bleached region. This is done to avoid signal from outside of the bleached area moving into the measured area as the central spindle compressed over time. 2 circular regions of 1000-2000 pixels were manually placed in the cytoplasmic area and averaged for measurement of mean cytoplasmic signal. A manually placed area of 500-1000 pixels of unbleached central spindle was also measured over time. All signal values were subtracted of the mean background signal outside of the cell (manually selected area of >2000 pixels). Mean signal values of bleached central spindle or unbleached cytoplasm were divided by the signal of the unbleached central spindle as reference for each time point. The curve was normalized to the averaged “central spindle (bleached)” values before bleaching (t=-4s to t=0). Data from 11 bleaching experiments were averaged to obtain the final displayed curve and standard deviation.

To quantify cytokinetic phenotypes in Figure 28A, phase contrast images of cells were recorded every 5 min in normal medium using an IncuCyte FLR integrated live cell-imaging system (Essen Bioscience). Images in Figure 8C and Figure 28B were acquired at 37°C using a Zeiss Axio Observer Z1 microscope controlled by SimplePCI software (Hamamatsu) and equipped with an Orca 03GO1 camera (Hamamatsu) and a Plan-Apochromat 10x/0.45 and 40x/1.3 DIC H objective.

2.7 Recombinant Protein Purification and Protein Assays

GST-RhoA (NM_001664) was expressed in E. coli (BL21) and purified using Glutathione Sepharose 4 Fast Flow (GE Healthcare). For insect cell expression, Ect2 variants were cloned into pFastBac (Invitrogen) containing a maltose-binding protein moiety (MBP, New England Biolabs). 72 h post infection of Hi-5 cells with MBP fusion protein encoding baculoviruses, proteins were isolated from cleared cell lysates prepared in lysis buffer (50 mM HEPES (pH 7.5), 150 mM NaCl, 1 mM EDTA, 5mM $MgCl_2$, 0.1% NP-40, 1mM DTT, protease inhibitors (Roche)) using amylose resin (NEB). Proteins were released in elution buffer (50 mM HEPES (pH 7.5), 150 mM NaCl, 1 mM EDTA, 0.5 mM $MgCl_2$, 10% glycerol, 1mM DTT) containing 15 mM maltose. Proteins were equilibrated in elution buffer using PD-10 desalting columns (GE Healthcare) and concentrated using a 30kDa cut-off Amicon Ultra unit (Millipore).

Membrane lipid arrays (P-6002, Echelon Biosciences) were incubated with 100 ng/ml MBP fusion proteins or 50 ng/ml GST-GRP1-PH domain (G-3901, Echelon Biosciences) in PBS containing 0.1% Tween-20 and 3% BSA for 1 h at 25 °C. After washing, proteins were detected using anti-GST or anti-MBP antibodies.

For the *in vitro* RhoA exchange assay, 20 pmol of GST-RhoA was incubated with 2 µM [^{3}H]GDP (14 Ci/mmol) in 50 µl binding buffer (50 mM Tris-HCl (pH 7.5), 50 mM NaCl, 1 mM EDTA, and 1 mM DTT) for 20 min at 25 °C. The reaction was terminated by addition of 50 µl chilled stop buffer (50 mM Tris-HCl (pH 7.5), 10 mM $MgCl_2$, and 50 mM NaCl). 4 µg of purified MBP fusion proteins and 50 µl of exchange buffer (75 mM Tris-HCl (pH 7.5), 15 mM $MgCl_2$, 3 mM DTT, 150 mM NaCl, 0.6 mg/ml BSA, 450 µM GTP) were added to the GDP-loaded GST-RhoA, and incubated at 28 °C. At the indicated time points, the reaction was terminated by addition of 200 µl chilled stop buffer and passed through a nitrocellulose filter (HAWP025, Millipore). After washing with chilled stop buffer the remaining radioactivity on the filter was measured using a TRI-CARB 1500 Liquid Scintillation Analyzer (Packard).

Chapter 3. Result 1 - A genetic complementation system to study Ect2 localization in live cells

Soon after the discovery of Ect2/*pebble* in Drosophila, the protein has been defined as an essential activator of RhoA during cytokinesis in animal cells. (Hime and Saint, 1992; Lehner, 1992; Tatsumoto et al., 1999; Prokopenko et al., 1999). Since Ect2 is essential for cell division and viability, early studies of Ect2 relied on chemically-induced mutant alleles or the overexpression of altered versions of the protein in cells that also contained a functional endogenous counterpart (Tatsumoto et al., 1999; Solski et al., 2004; Chalamalasetty et al., 2006) These approaches can be difficult to interpret and do not allow the targeted dissection of Ect2 functions and regulation during cytokinesis.

With the advent of the RNA interference (RNAi) technologies it has become possible to deplete Ect2 acutely and studies were carried out that confirmed the protein's essential role in cytokinesis (Kim et al., 2005; Yüce et al., 2005). Based on RNAi technology, I decided to develop a system in human cells that would allow us to effectively remove the endogenous Ect2 protein and replace its function with an engineered transgene. This system should allow me to introduce targeted mutations in Ect2 and to, for the first time, track the protein's localization during mitotic exit in live cells.

3.1 Ect2 is required for cytokinesis

To test the effect and efficiency of Ect2 depletion, I treated HeLa "Kyoto" cells with an siRNA (short interfering RNA) duplex targeting a specific region of Ect2 (Figure 8). HeLa "Kyoto" cells are derived from a cervix carcinoma background. They are a commonly used model system for the investigation of cell division and are amenable to live cell imaging, DNA and siRNA transfection. 13h after transfection with Ect2 siRNA, cells were recorded using bright field time-lapse microscopy for 24h. In line with observations made in past studies ((Yüce et al., 2005; Chalamalasetty et al., 2006; Nishimura and Yonemura, 2006)), the majority of cells

failed to form a cytokinetic furrow (77.7%) after anaphase onset and exited mitosis as bi-nucleated and poly-nucleated (cells after multiple cycles of cytokinesis failure) cells (n=197). A significant fraction of cells (20.8%) initiated furrowing but displayed subsequent furrow regression and cell division failure. A small fraction of cells (1.5%) divided successfully. For comparison control siRNA treated cells divided successfully (96.5%) with only a minor population of cells (3.5%) failing cytokinesis (n=229). In parallel to imaging, whole cell protein extracts were prepared from cells 48h post transfection and analysed by immunoblotting using an antibody raised against the N-terminal half of human Ect2 (amino acids 1-421). This confirmed the efficient depletion of endogenous Ect2 protein (Figure 8B).

To illustrate the observed cytokinetic phenotype, I have acquired representative time-lapse images of dividing HeLa “Kyoto” cells stably expressing histone H2B-GFP without siRNA treatment or after Ect2 siRNAi transfection (Figure 8C).

3.2 Construction and testing of the genetic complementation system for Ect2 in human cells

To stably express a transgenic version of Ect2 in human cells, I have designed a construct that contains an siRNA-resistant version of human Ect2 cDNA that is N-terminally tagged with *Aequora coerulensces* GFP (AcGFP) and a single FLAG-epitope (AcFL) (AcFL-Ect2r) (Figure 9). Four silent point mutations have been introduced in the coding sequence of the gene to render the construct resistant to siRNA-mediated depletion. The AcFL-Ect2r construct is expressed by a CMV promoter and has been assembled in a bicistronic pIRES vector, which facilitates the selection of stable transgenic cell lines.

Using this siRNA resistant construct, AcFL-Ect2r, I generated a monoclonal stable cell line that co-expressed a marker for chromosomes (H2B-mCherry). The resulting cell line expressed transgenic AcFL-Ect2r in every cell of the population and at a level that is very similar to its endogenous counterpart (Figure 9B and C).

This approach might be suitable to study the localization of Ect2 protein during cytokinesis in live cells and to dissect the protein's function.
To test whether transgenic AcFL-Ect2 can replace the function of the endogenous protein during cell division, I performed siRNA experiments. In the control cell line that only expressed H2B-mCherry, siRNA-mediated depletion of endogenous Ect2 protein converted the entire population into bi-nucleated or multi-nucleated cells. This indicates that all cells have gone through mitosis but have failed to execute cytokinesis successfully. Importantly, this phenotype was completely rescued in the cell line co-expressing siRNA-resistant Ect2 (AcFL-Ect2r) and H2B-mCherry despite the efficient removal of the endogenous Ect2 protein (Figure 9). Thus, transgenic and tagged AcFL-Ect2r is able to entirely replace the cytokinetic function of the endogenous protein.

To determine the minimum protein level of Ect2 required to support cytokinesis in human cells, I generated a series of monoclonal cell lines expressing different levels of AcFL-Ect2r. Subsequently, I have tested the ability of the transgenes to functionally rescue cytokinesis upon depletion of endogenous Ect2 protein after 48h by scoring the fraction of bi-nucleated or multi-nucleated cells (Figure 10). Quantitative immunoblotting using fluorescently labelled secondary antibodies allowed me to measure and compare the expression level of endogenous and transgenic Ect2 proteins in reference to α-tubulin. Remarkably, these experiments revealed that about an AcFL-Ect2r transgene expressed at about one tenth of the reference Ect2 protein level is sufficient to support cytokinesis in HeLa "Kyoto" cells (Figure 10).

Interestingly, I have not been able to isolate cell lines expressing Ect2 at a level higher than the endogenous counterpart (data not shown) suggesting that overexpression of Ect2 beyond a critical threshold may be incompatible with cell viability.

3.3 Ect2 localization during cytokinesis

Using the previously introduced genetic complementation system, I am able now to study Ect2 localization in live cells using time-lapse microscopy. By choosing the correct stable cell line I have ensured that the transgenic AcFL-Ect2 level is similar to the endogenous protein. By depleting the endogenous protein at the same time I ensured that untagged endogenous Ect2 does not compete with the transgenic and AcGFP-tagged copy that will be tracked through cell division. In summary, this system should allow me to monitor the localization of the Ect2 protein that drives cytokinesis in human cells.

Using spinning disc time-lapse microscopy, I observed that AcFL-Ect2r was released from the nucleus around mitotic entry and nuclear envelope breakdown (data not shown) and was distributed throughout the cytoplasm during metaphase. 4 to 6 minutes after anaphase onset, Ect2 accumulated at the central spindle (n=35). In line with observations in fixed samples (Figure 11B) (Tatsumoto et al., 1999; Yüce et al., 2005) , Ect2 remained associated with the spindle midzone during cleavage furrow contraction and thereafter accumulated at the midbody (Figure 11A). Interestingly, 8 minutes after anaphase onset prior to any sign of furrow contraction a fraction of Ect2 associated with the cell periphery and became concentrated at the cell equator. As the furrow ingression progresses, the equatorial membrane bound signal of Ect2 intensified until it converged with the midzone bound signal to form the midbody. Following furrow ingression, Ect2 is imported into the reforming daughter cell nuclei as the nuclear envelope reassembles. These dynamic localization patterns of Ect2 have also been quantified over time and are plotted in Figure 12.

Studies of Ect2 localization during cytokinesis have thus far restricted to fixed cells (Chalamalasetty et al., 2006; Nishimura and Yonemura, 2006; Yüce et al., 2005). Immunofluorescence experiments suggest that the peripheral localization of Ect2 is poorly preserved in fixed samples (Figure 11B) and could not be visualized as clearly as in our live cell observations.

3.4 Conclusions: Result 1 - A genetic complementation system to study Ect2 localization in live cells

I have been able to successfully remove Ect2 in HeLa “Kyoto” cells using siRNA. The majority of cells display an anaphase and mitotic exit without any visible furrow formation as analysed by time-lapse microscopy. The amount of residual Ect2 is not detectable using western blotting (Figure 8B).

By generating stable cell lines expressing AcFL-Ect2r, an siRNA resistant, fluorescence protein tagged Ect2, I have developed a system that successfully replaces endogenous Ect2 with a tagged transgenic copy. This system is able to fully rescue the function of endogenous Ect2 (Figure 9). As little as 13% of the protein level of the endogenous Ect2 is sufficient for an efficient rescue of cytokinesis (Figure 10).

Using fluorescence time-lapse microscopy I have been able to, for the first time, visualize the localization of AcFL-Ect2r through cytokinesis in human cells. Apart from the previously well-documented association of Ect2 with the central spindle after anaphase onset, I could demonstrate the existence of a peripheral pool of Ect2 that accumulates at the cell equator just prior and during the time of furrowing initiation (Figure 11). The temporal and spatial characteristics of this peripheral pool raised the exciting possibility that a membrane-bound or cortex-associated fraction of Ect2 could control the activation of RhoA and the formation of a cleavage furrow during cytokinesis.

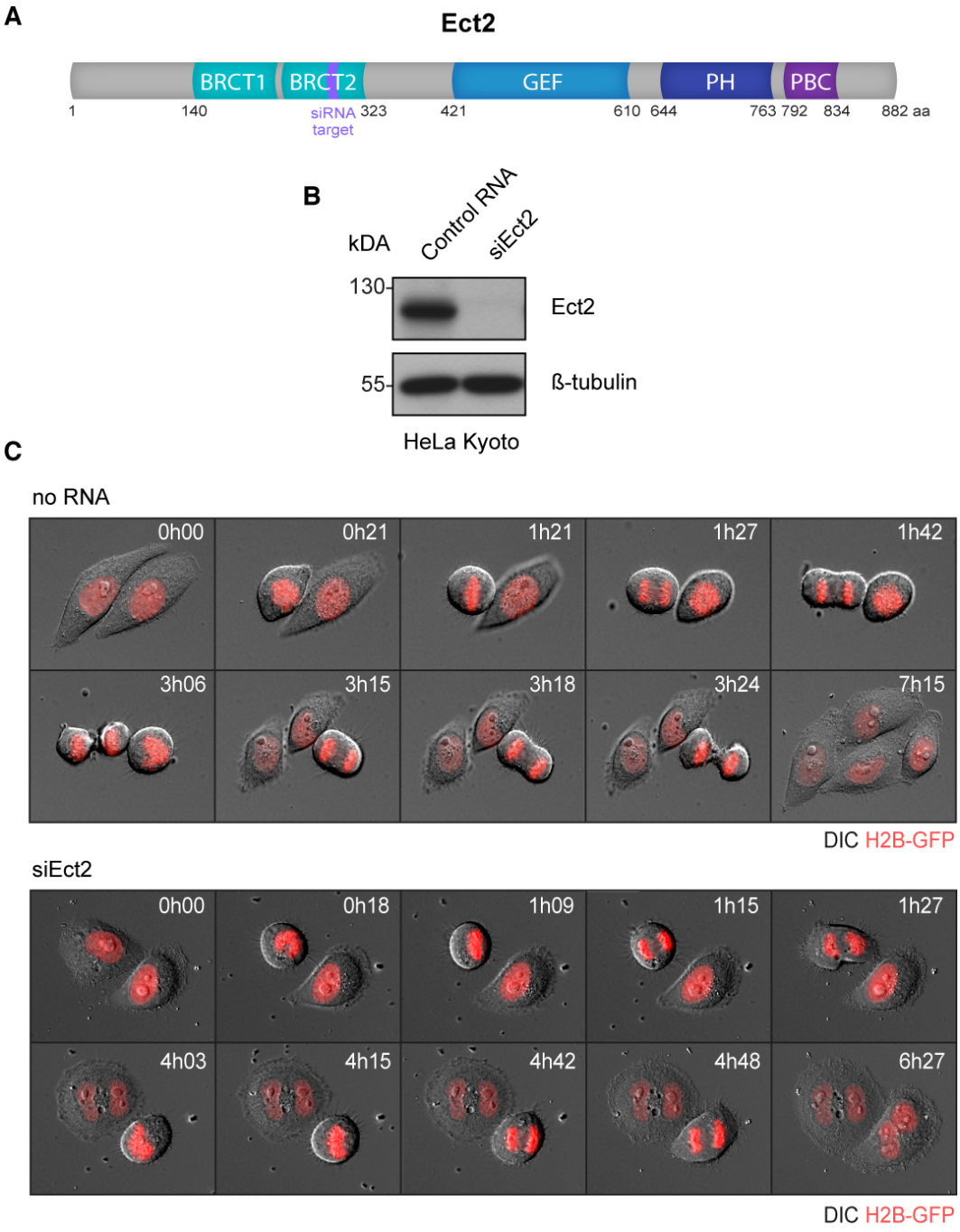

Figure 8 Ect2 is required for cleavage furrow formation during cytokinesis in human cells

A The domain structure of human Ect2. The two BRCA1 C terminal repeat domains (BRCT), guanine nucleotide exchange factor domain (GEF), pleckstrin homology domain (PH) and poly basic cluster (PBC) of Ect2 are highlighted together with the target region of the Ect2 siRNA used in this study.

B Immunoblot of protein extracts prepared from HeLa Kyoto 48 hours after transfection with control siRNA and Ect2 siRNA duplexes. Extracts were probed with antibodies directed against Ect2 and β-tubulin

C Time-lapse microscopy frames of HeLa Kyoto cells stably expressing H2B-GFP cells. Cells were either untreated (upper panel) or transfected with Ect2 siRNA 26h prior to recording (lower panel). DNA is displayed in red, differential interference contrast (DIC) in grey scale. Depletion of Ect2 abrogates cleavage furrow formation in the majority of cells leading to the emergence of bi-nucleate polyploid cells (lower panel).

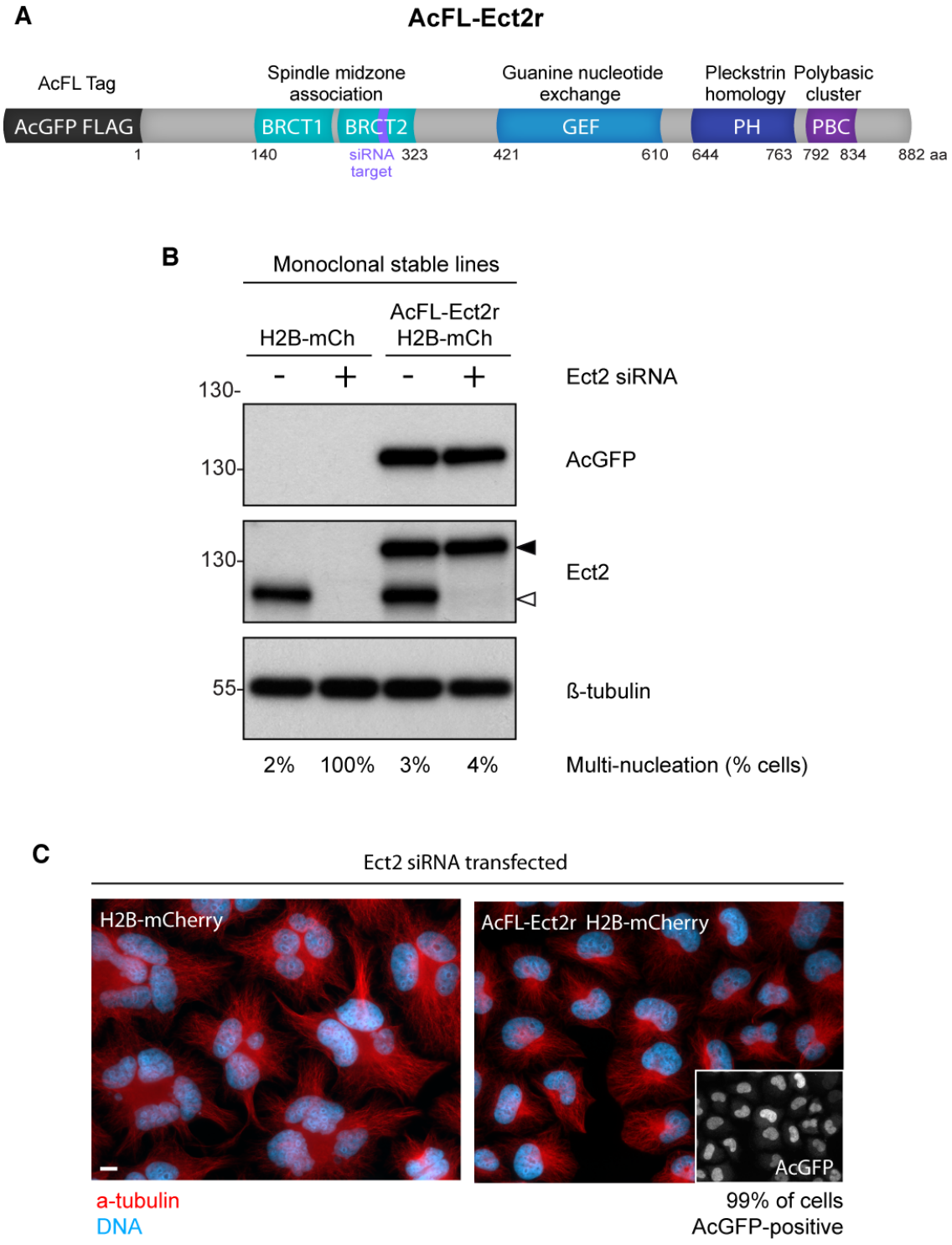

Figure 9 A genetic complementation system for Ect2

Figure 9 A genetic complementation system for Ect2

A Domain organization of AcFL-tagged and siRNA-resistant human Ect2 protein. The two BRCA1 C-terminal repeat domains (BRCT), guanine nucleotide exchange factor domain (GEF), pleckstrin homology domain (PH) and poly basic cluster (PBC) of Ect2 are highlighted together with the target region of the Ect2 siRNA used in this study.
B Immunoblot analysis of protein extracts prepared from a monoclonal stable HeLa Kyoto cell line expressing H2B-mCherry or co-expressing AcFL-Ect2r and H2B-mCherry (top panel). Extracts were prepared 48 hours after transfection with control siRNA (-) or Ect2 siRNA (+) duplexes. Extracts were probed with antibodies directed against AcGFP, Ect2 and β-tubulin. Endogenous Ect2 protein and transgenic AcFL-Ect2r are indicated by open and filled arrowheads, respectively. The percentage of bi-nucleate or multi-nucleate interphase cells (multi-nucleation) 48 hours after siRNA transfection is indicated below the immunoblot lanes (n > 600 cells).
C Immunofluorescence (IF) microscopy analysis of cell lines stably expressing H2B-mCherry or stably co-expressing AcFL-Ect2r and H2B-mCherry 48 hours after transfection with Ect2 siRNA (bottom panel). Scale bar represents 10 μm.

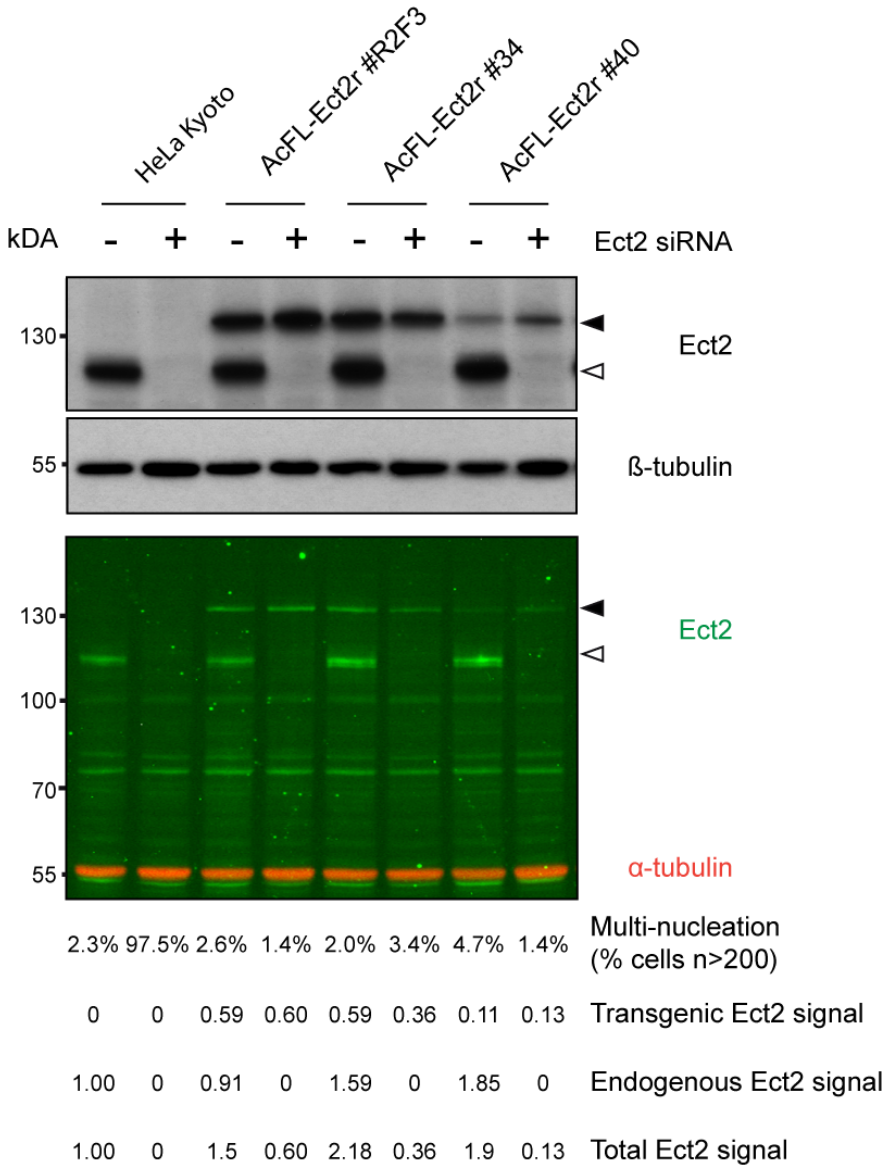

Figure 10 Minimum level of Ect2 required for successful cytokinesis

Quantitative immunoblot analysis of protein extracts prepared from HeLa Kyoto cells and from monoclonal HeLa Kyoto cell lines stably expressing different levels of AcFL-Ect2r. Extracts were prepared 48 hours after transfection with control siRNA (-) or Ect2 siRNA (+) duplexes. Extracts were probed with antibodies directed against AcGFP, Ect2 and tubulin (top and middle panel). Proteins were detected using chemiluminescence (top panel) or fluorescently-labelled secondary antibodies (middle panel). Endogenous Ect2 protein and transgenic AcFL-Ect2r are indicated by open and filled arrowheads, respectively. Endogenous and transgenic Ect2 protein signals (green) are normalized to α-tubulin signals (red) in each lane and expressed in relation to the amount of endogenous Ect2 in non-transgenic HeLa Kyoto cells (bottom panel). The percentages of bi-nucleate or multi-nucleate interphase cells (multi-nucleation) 48 hours after siRNA transfection are indicated below the respective immunoblot lanes (n > 200 cells).

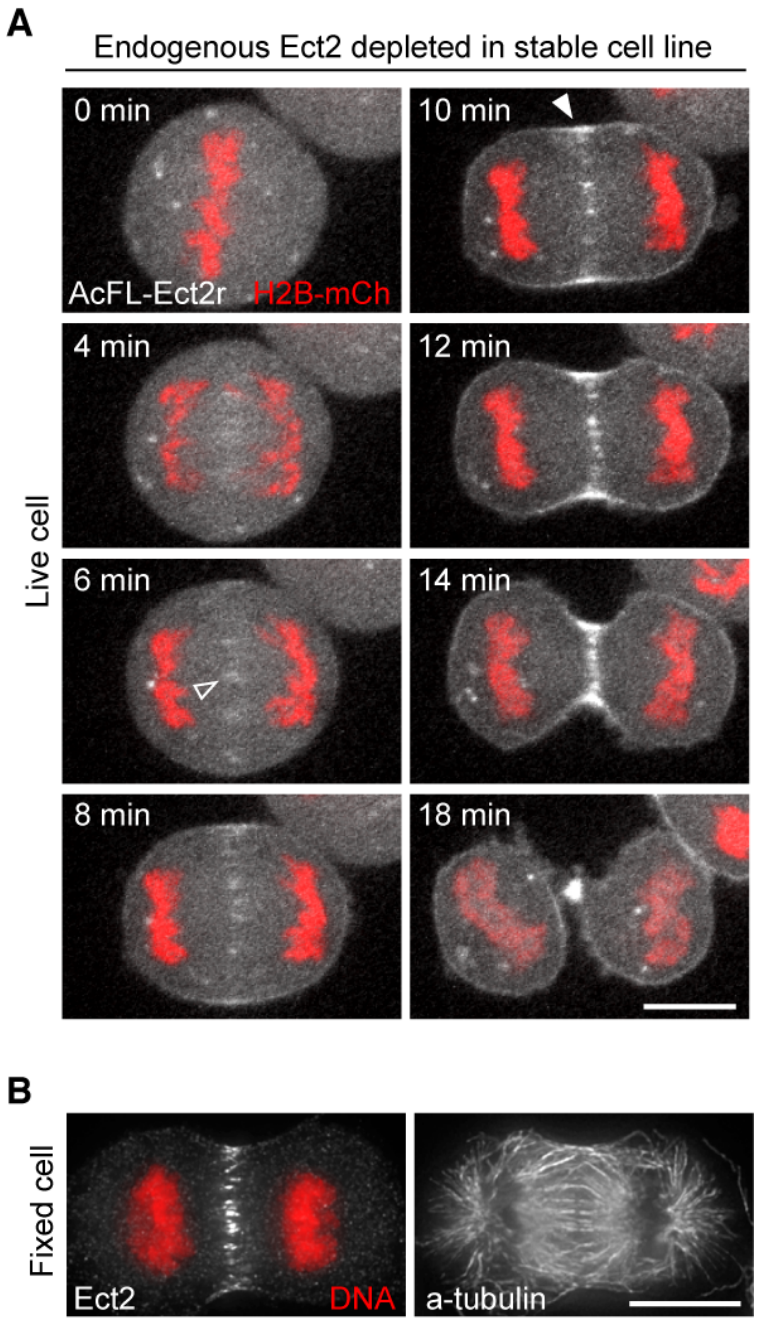

Figure 11 Ect2 localization during cytokinesis

A Spinning disc live-cell imaging of a monoclonal cell line stably expressing AcFL-Ect2r (white) and H2B-mCherry (red). The cell line was characterized in detail in Figure 9.
Recording started 30 hours after transfection with Ect2 siRNA. Time point t = 0 min was set to the metaphase-to-anaphase transition. The open and filled arrowheads indicate Ect2 localization to the spindle midzone and cell cortex, respectively.

B Immunofluorescence (IF) showing Ect2 localization during anaphase. Endogenous Ect2 protein and α-tubulin are detected by antibodies in methanol-fixed HeLa Kyoto cells. No clear membrane bound Ect2 could be detected.

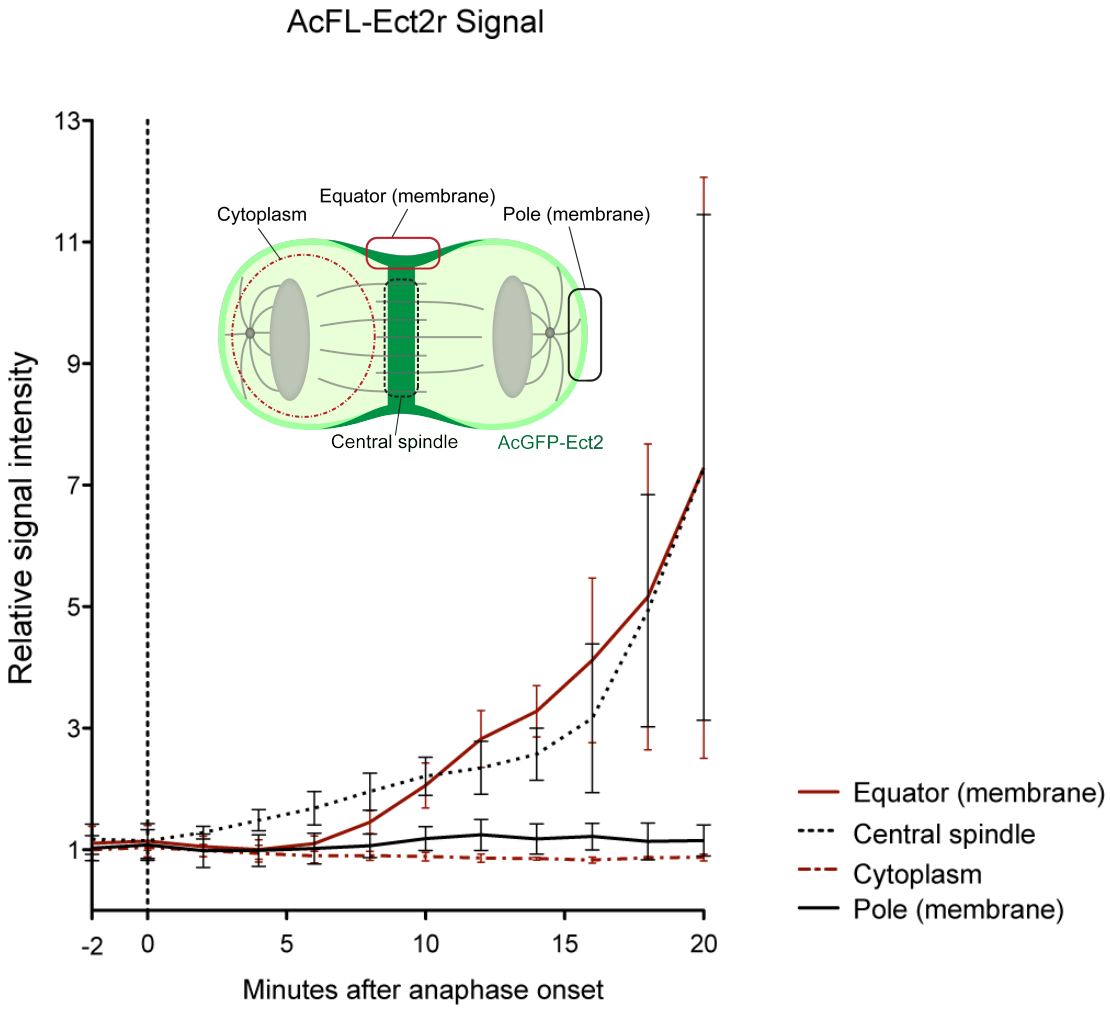

Figure 12 Quantification of dynamic Ect2 localization during cytokinesis

Quantification of AcF-Ect2r signal distribution in different cell compartments based on time-lapse series as shown in Figure 11A (n=5). Time point t = 0 min was set to the metaphase-to-anaphase transition and is indicated by a vertical dashed line. Mean intensity of the cytoplasmic signal (red dashed line) at t = -2 min is used as a reference. Error bars represent the standard deviation of the analysis of five cells.

Chapter 4. Results 2 - Mechanistic basis of Ect2 association with the cell periphery

Using live cell analysis, I have defined a peripheral pool of Ect2 at the cell equator in live cells. I have therefore decided to investigate the molecular mechanism for Ect2 binding to the plasma membrane or cell cortex and to determine the relevance of this localization for cytokinesis. As other DH-type GEF proteins, Ect2 contains a pleckstrin homology domain (PH) that can mediate the binding to membrane lipids (Atilla-Gokcumen et al., 2010) (Figure 8). I analysed Ect2 by sub division in to sections containing one CDK1 consensus site (T/S-P) and identified a conserved polybasic cluster (PBC) in the C-terminal region of Ect2 (Figure 8 and Figure 13). Polybasic clusters are often found at the C-terminus of small GTPase proteins and have been implicated in plasma membrane targeting by associating with the inositol lipids phosphatidylinositol-4,5-biphosphate ($PI(4,5)P_2$) and phosphatidylinositol-3,4,5-biphosphate ($PI(3,4,5,)P_3$ (Heo et al., 2006). Thus, both the PH domain and the PBC are good candidates for being involved in the peripheral localization of Ect2 during cytokinesis. I therefore decided to investigate the protein domain requirements for Ect2's peripheral localization *in vivo* and to test the binding of recombinant Ect2 fragments to lipids *in vitro*. Understanding the nature of Ect2's peripheral accumulation would allow me to test its requirement for Ect2 function during cell division.

4.1 Domain requirements for peripheral Ect2 localization

A previous study has observed that an overexpressed C-terminal fragment of Ect2 can localize to the cell periphery (Chalamalasetty et al., 2006). I have therefore focused our attention on an analogous region (Ect2CT, aa414-883) that spans the GEF domain, the PH domain and the polybasic cluster (Figure 14). Indeed, transiently expressed AcGFP and FLAG-tagged Ect2CT (AcFL-Ect2CT) (Figure 16) associated with the cell periphery in fixed anaphase cells; similar to the lipid-modified plasma membrane marker MyrPalm-FLAc (Figure 16) In contrast, the tag alone, AcFL, remained cytoplasmic. Interestingly, unlike full-length Ect2 (Figure 11),

the Ect2CT fragment was distributed uniformly around the cell cortex in anaphase cells (Figure 16), Furthermore, I observed that expression of Ect2CT caused the rounding of interphase cells (data not shown), presumably due to ectopic RhoA activation and cortex remodelling (Matthews et al., 2012)

Subsequently, I generated a range of deletion and mutant constructs to test the domains and regions of Ect2 that are required for Ect2CT membrane association (Figure 14). Point mutations in basic residues of the PH domain of Ect2 (Ect2CT-PH3E) were designed based on alignment of Ect2's PH domain with the PH domains of other proteins whose structure and lipid binding properties have been determined (Figure 15) (Lietzke et al., 2000; Cronin et al., 2004). Mutations were targeted to basic residues in β-sheet or loop structures based on alignment displayed in Figure 15. To inactivate the exchange factor activity of Ect2, a stretch of four amino acids (PVQR) that is conserved amongst DH-family GEF proteins has been mutated to four alanine residues (Ect2CT-GEF4A) (Figure 19). The GEF mutant allele of Ect2 will be characterized in detail in section 4.4 (page 75).

Following transient transfection of different AcFL-tagged Ect2CT variants into HeLa Kyoto cells, protein extracts were probed for the expression of the transgene (Figure 16A) and immunofluorescence analysis was used to determine protein localization at anaphase (Figure 16B). Deletion of the PH domain and deletion of the PBC-containing tail strongly impaired the association of the transgene with the cell periphery (Figure 16B). A construct only spanning the PH and Tail region was able to weakly associate with the periphery. Neither GEF domain nor the PH domain alone was able to associate with the cortex. The Tail however was able to robustly associate with the cell periphery. Inactivating mutations of the GEF domain had no influence on Ect2CT localization whereas as the PH domain mutations in PH3E abolished the peripheral accumulation (Figure 16B).

These results suggest that the PH domain and the PBC-containing tail region of Ect2CT cooperate to mediate its peripheral localization, while the GEF activity is dispensable for membrane binding. Thus, the peripheral localization of Ect2 is likely to involve multiple regions in the C-terminal half of the protein that in isolation are unable to support full localization.

4.2 Ect2CT associates to cell membrane independently of the actin cortex

Ect2CT's peripheral localization could be mediated by the interaction with the plasma membrane or with the cortical actin cytoskeleton. To address this question, I transfected cells with AcFL-Ect2CT and acutely treated cells with dihydrocytochalasin-B (DCHB). DCHB treatment disrupted the actin cortex in comparison to DMSO-treated control cells, as judged by staining with fluorescently labelled phalloidin (Figure 17). In control anaphase cells Ect2CT co-localized with filamentous actin at the cell periphery. In contrast, DCHB treatment abolished this correlation and the Ect2CT fragment strongly associated with peripheral regions in the absence of cortical actin. This suggests that Ect2CT's peripheral localization is mediated by binding to the inner leaflet of the plasma membrane independently of the actin cortex.

4.3 Recombinant Ect2 protein interacts with polyanionic phosphoinositides *in vitro*

The following experiment was carried out by Tohru Takaki.

Given the actin-independent recruitment of Ect2CT to the plasma membrane *in vivo* (Figure 17), we next investigated whether recombinant Ect2 protein is able to bind to specific lipids *in vitro*. To this end, recombinant maltose binding protein (MBP)-tagged Ect2 full-length protein and several variants thereof were expressed in insect sells using the baculovirus system and purified using amylose resin. The recombinant proteins (Figure 18A) were subsequently incubated with arrays containing different lipids that were immobilized on support matrix. In contrast to MBP, MBP-Ect2 full length and MBP-Ect2CT bound strongly to phosphatidylinositol 4-phosphate (PI4P), phosphatidylinositol 4,5-biphosphate (PI[4,5]P_2) and phosphatidylinositol 3,4,5-phosphate (PI[3,4,5]P_3) (Figure 18B). Weaker binding was observed to the cardiolipin (CL), phosphatidic acid (PA) and sulfatide lipids (Sulf.). Consistent with the localization experiments *in vivo* (Figure 16B), this association was abolished by deletion of Ect2's PH domain and tail region. No

binding was observed to phosphatidylserine, phosphatidylethanolamine, phosphatidylcholine and cholersterol, the 4 most abundant canonical lipid molecules in the plasma membrane. The specificity of the lipid interaction assay has been validated by the selective binding the PH domain of GRP1 to $PI(3,4,5)P_3$. These results demonstrate that Ect2 can bind to negatively charged phospholipids, in particular polyanionic phosphoinositides, *in vitro* and raises the possibility that electrostatic interaction effects may be responsible for the proteins localization to the plasma membrane *in vivo*.

4.4 The PH domain and tail region are not required for GEF activity of Ect2 on RhoA *in vitro*

The following experiment was carried out by Tohru Takaki.

Ect2 has been reported to harbour GEF activity towards RhoA (Tatsumoto et al., 1999). Using purified recombinant proteins, we next tested the ability of different Ect2CT variants to stimulate the exchange of GDP for GTP on RhoA *in vitro.* We generated an Ect2 GEF mutant where 4 residues of the highly conserved DH CR3 helix (565PVQR568 Ect2CT-GEF4A see Figure 19) were mutated to alanine to obtain an allele that has previously been shown to block the transforming activity of Ect2 (Saito et al., 2004b). The assay was intended to test whether the GEF4A mutations abolish GEF activity on RhoA *in vitro*. Furthermore, it could address whether Ect2's GEF activity can be uncoupled from its membrane targeting regions.

We incubated [^{3}H]GDP-loaded GST-RhoA with recombinant MBP or MBP fusions of the indicated Ect2 fragments (Figure 21A) in the presence of unlabelled GTP. GEF activity was inferred by measuring the remaining protein associated radioactivity over time and calculating the fraction of [^{3}H]GDP released (Figure 20). This *in vitro* assay confirmed that Ect2CT can act to catalyse GDP/GTP exchange activity on RhoA. Importantly, the introduction of the GEF4A mutations completely abolished Ect2CT exchange activity (Figure 21B). Importantly, deletion of the PH domain alone or in combination with the tail region did not impair Ect2 GEF activity

(Figure 21B). This suggests that neither the PH domain nor the tail region of Ect2 is required for the protein's *in vitro* GEF activity.

4.5 Conclusions: Results 2 - Mechanistic basis of Ect2 association with the cell periphery

By transiently expressing Ect2CT *in vivo* and determining its subcellular localization, we have established an assay to scrutinize the ability of Ect2 to associate with the cell periphery (Figure 16). Using DHCB to disrupt the actin cortex, we have demonstrated that the peripheral concentration of Ect2CT occurs independently of the actin cytoskeleton (Figure 17). This suggests that Ect2CT may directly associate with the inner leaflet of the plasma membrane. Consistent with this hypothesis, we found that recombinant Ect2 protein is able to bind to phosphoinositides *in vitro* (Figure 18). Using an *in vitro* assay we confirmed that Ect2 has GEF activity towards RhoA. Furthermore, we were able to generate an allele of Ect2 that lacks GEF activity (Figure 21B). While the GEF activity of Ect2 is dispensable for the protein's localization to the membrane (Figure 16 and Figure 21B), deletion of the C-terminal PH domain and polybasic tail region abolished targeting of Ect2CT to the plasma membrane *in vivo* (Figure 16) and prevented the interaction with phospholipids *in vitro* (Figure 18). Conversely, deletion of the membrane interaction regions of Ect2 did not impair the RhoA GEF activity of the protein *in vitro* (Figure 21B). In summary our experiments suggest that, unusual for a DH-type GEF (Rossman et al., 2005; Bos et al., 2007), the PH domain and polybasic tail of Ect2 cooperate to mediate localization of Ect2 to the plasma membrane. Furthermore, they indicate that the GEF activity of the protein can be uncoupled from the membrane targeting regions, at least *in vitro*.

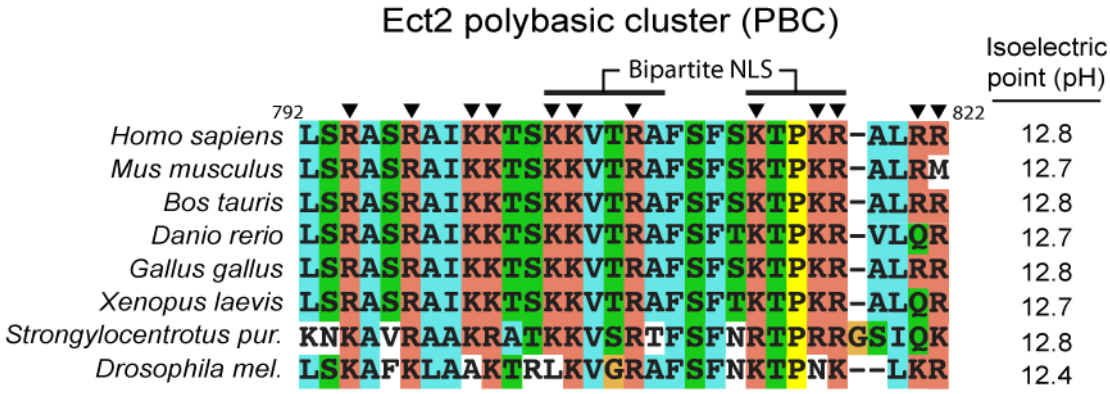

Figure 13 Conservation of Ect2's C-terminal polybasic cluster (PBC)

Sequence alignment of the polybasic cluster region of different Ect2 orthologs. Sequences were aligned to amino acid positions 792 to 822 of human Ect2. Black triangles indicate basic amino acids. A bipartite nuclear localization signal (NLS) is indicated (Liot et al., 2011).

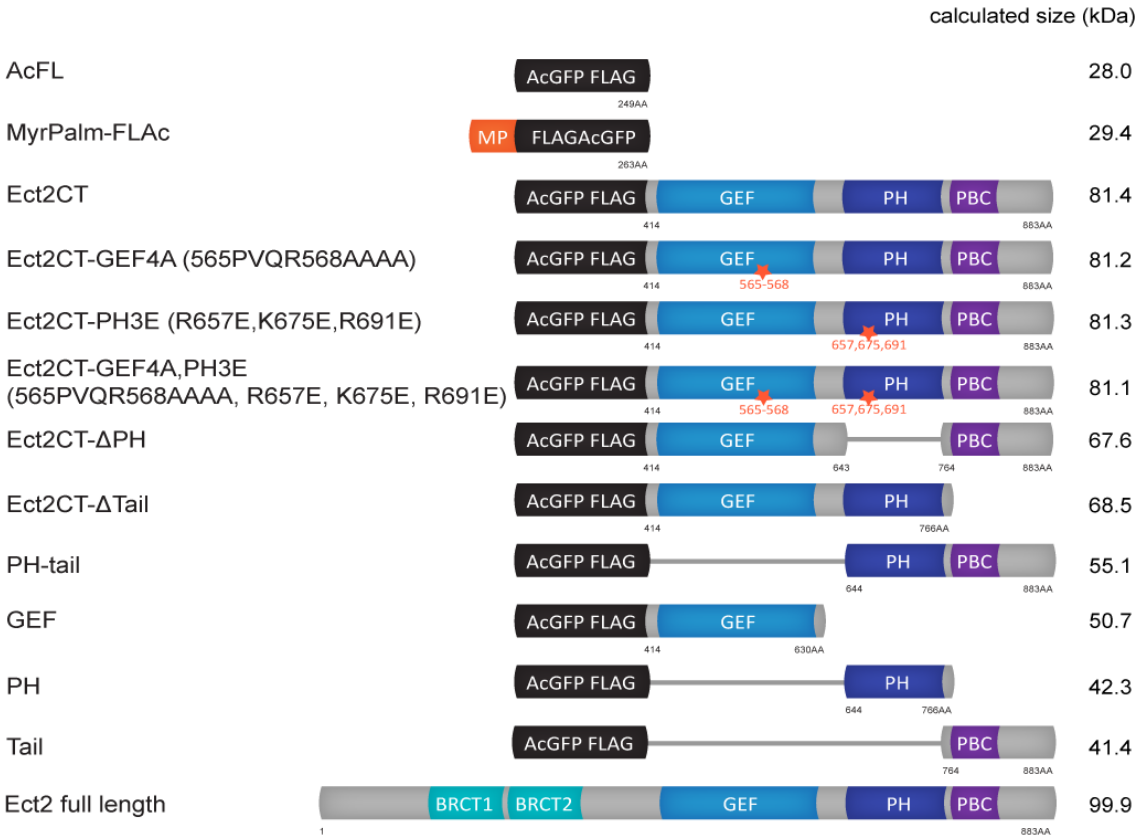

Figure 14 Constructs used for Ect2CT subcellular localization assay

Domain organization of tagged proteins used in transient expression assays to dissect the requirements for membrane targeting of Ect2 (see Figure 16). Amino acid annotations in AcFL-Ect2 fusion proteins correspond to positions in human full-length Ect2 protein.

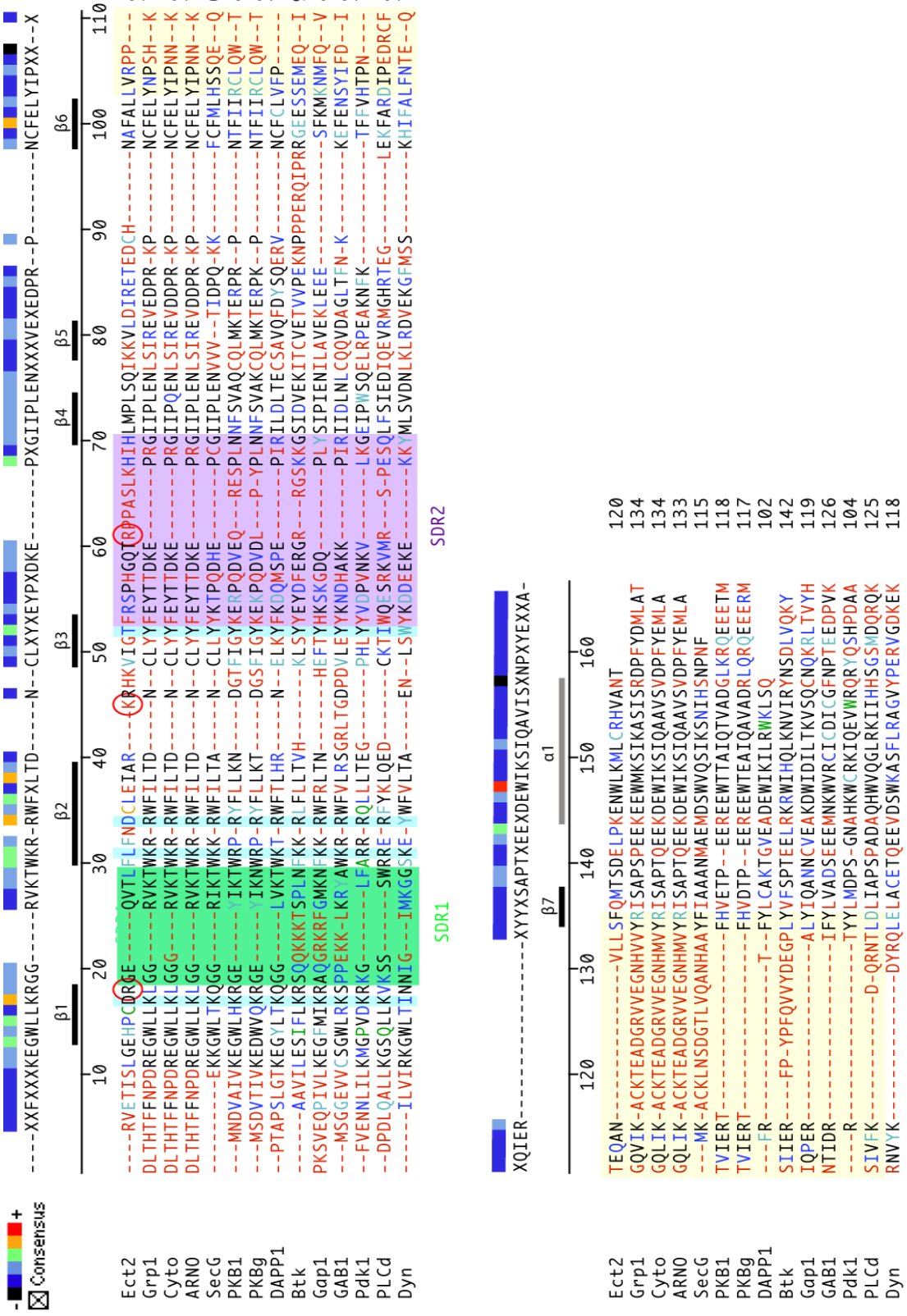

Figure 15 Alignment of PH domains

Figure 15 Alignment of PH

Alignment of Ect2's PH domain (aa 644-763) and PH domains of other proteins to the PH domain of Grp1 whose structure has been determined in a complex with $PI(3,4,5)P_3$ by X-ray crystallography. β1-7 indicate β-sheets, α1 denotes an α-helix structure typically found in in PH domains (Lietzke et al., 2000; Cronin et al., 2004). SDR1-3 (Specificity determining regions) indicate loop regions in PH domains responsible for the specificity of lipid binding. Red circles indicate mutations introduced in the PH3E mutant (R657E, K675E, R691E)

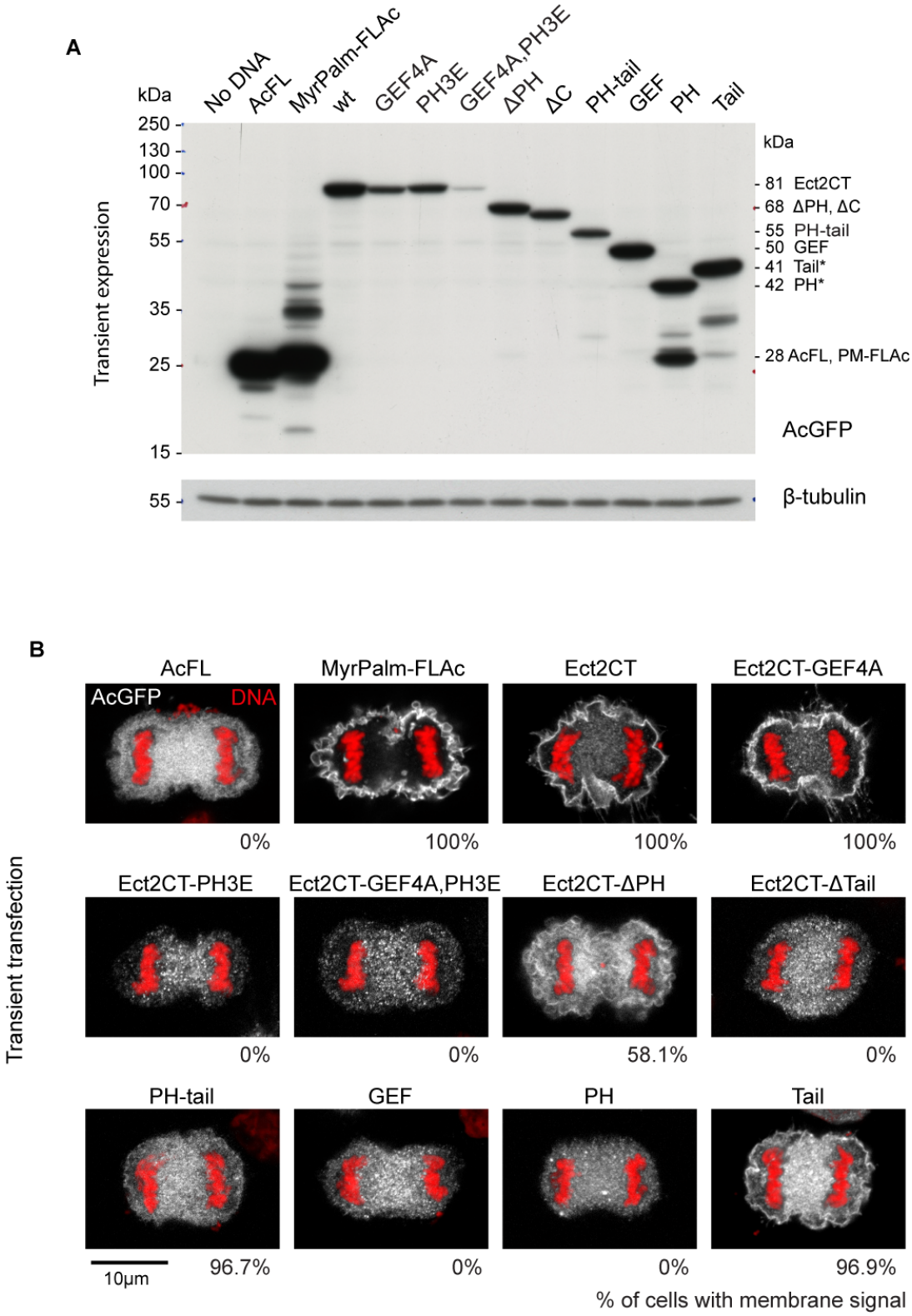

Figure 16 Subcellular localization assay for Ect2CT

A Immunoblot analysis of lysates of HeLa "Kyoto" cells 24 hours after transient transfection with plasmids encoding the indicated proteins. Predicted molecular weights are indicated on the right side. * Migration speed of some Ect2CT

variants does not correlate completely with the predicted molecular weight, possibly due to charge effects.
B IF analysis of indicated control proteins and AcFL-tagged Ect2 fragments in formaldehyde-fixed anaphase cells following transient transfection. Transiently expressed proteins were detected using an antibody directed against the AcGFP moiety of the AcFL and FLAc tags. Percentage of cells displaying membrane association is indicated in the lower right corner (n>30). Displayed images represent the phenotype of majority. Domain organization of all transfected constructs is shown in Figure 14.

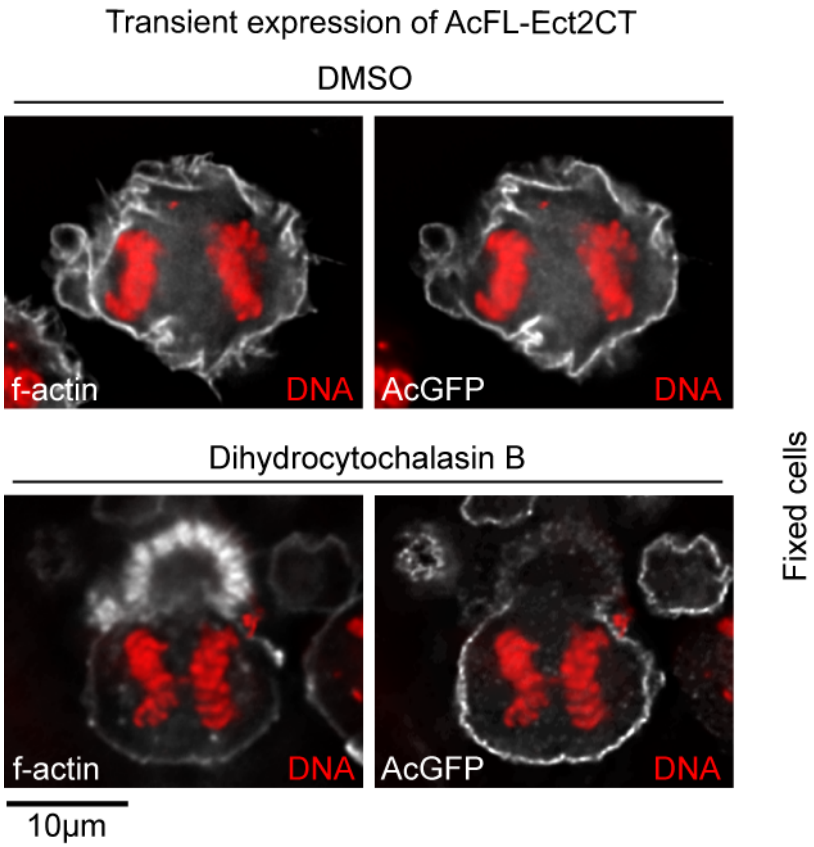

Figure 17 Ect2CT binds independent of actin cortex to cell membrane

IF analysis of transiently expressed AcFL-Ect2CT in formaldehyde-fixed anaphase cells. Cells were treated with dimethyl sulfoxide (DMSO) or 20 µM dihydrocytochalasin B for 20 min prior to fixation. AcFL-Ect2CT and filamentous actin (f-actin) were detected using anti-AcGFP antibodies and fluorophore-conjugated phalloidin, respectively.

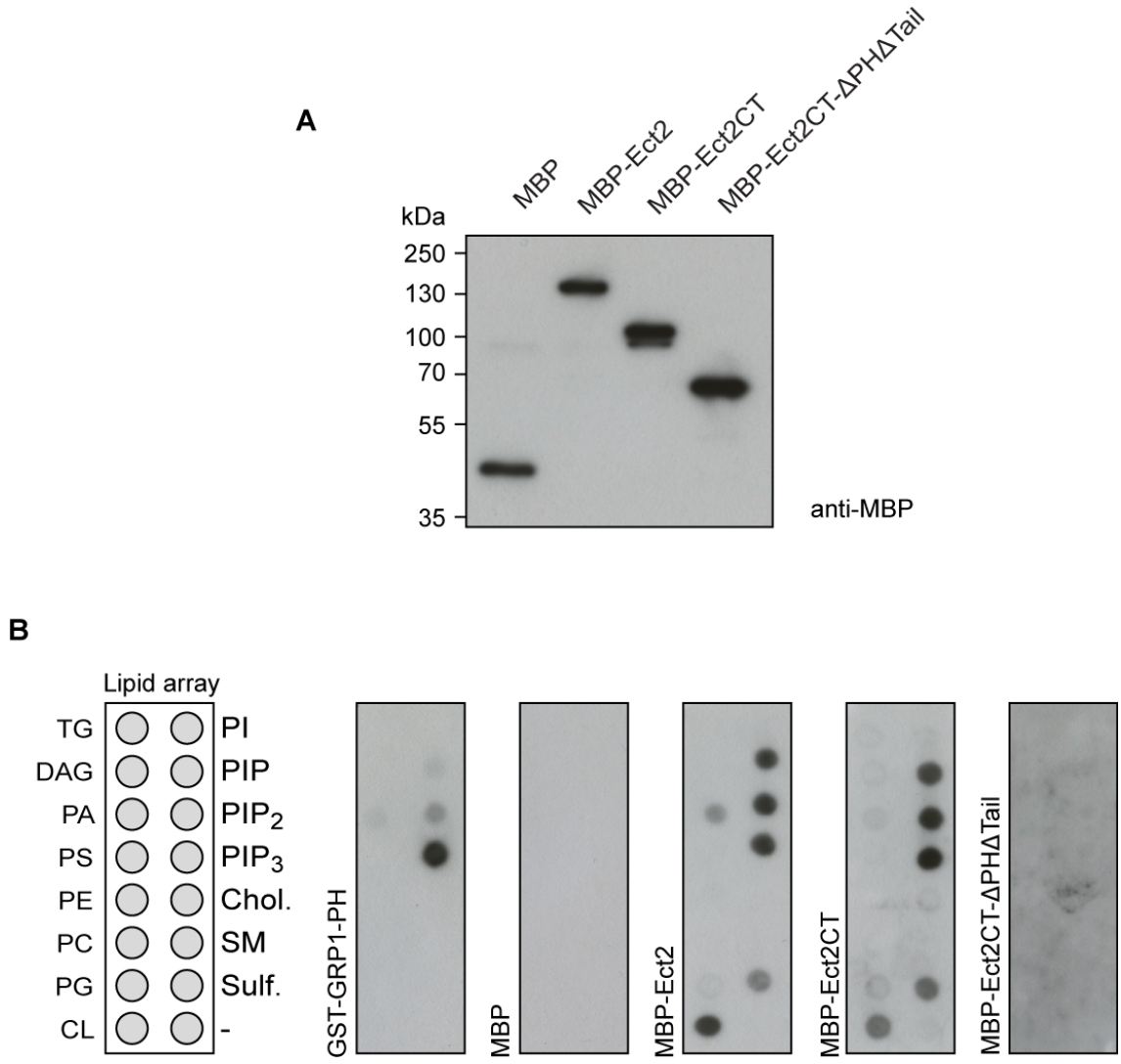

Figure 18 Ect2 binds to anionic phospholipids *in vitro*

A Immunoblot analysis of recombinant maltose-binding protein (MBP) and MBP-Ect2 fusion proteins. MBP fusion proteins were expressed in insect cells using the baculovirus system and purified using amylose resin.

B Lipid arrays were incubated with the indicated recombinant proteins before being probed by anti-GST (for GST-GRP1-PH) or anti-MBP antibodies (right panel). Key for lipid array: triglyceride (TG), diacylglycerol (DAG), phosphatidic acid (PA), phosphatidylserine (PS), phosphatidylethanolamine (PE); phosphatidylcholine (PC), phosphatidylglycerol (PG), cardiolipin (CL), phosphatidylinositol (PI), PtdIns(4)P (PIP), PtdIns(4,5)P2 (PIP2), PtdIns(3,4,5)P3 (PIP3), cholesterol (Chol.), sphingomyelin (SM), sulfatide (Sulf.) See also Figure 14 for schematic representation of constructs and proteins.

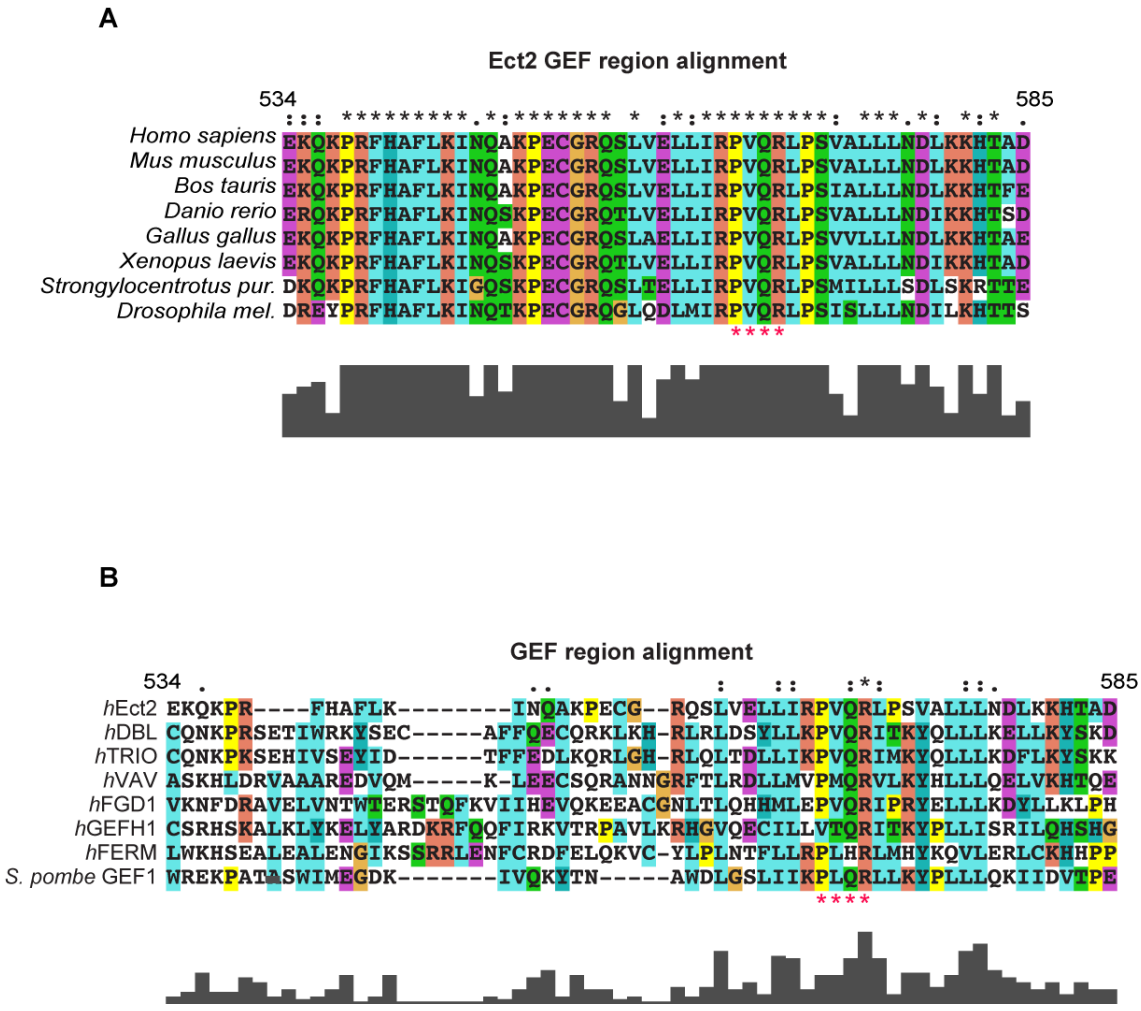

Figure 19 Alignment of Ect2 GEF region

Sequence alignment of a region spanning the CR3 helix of the GEF domain of different Ect2 orthologs (**A**) and other GEF proteins (**B**). Sequences were aligned to amino acid positions 534 to 585 of human Ect2.
* (asterisk) indicate residues 565-568 (PVQR), which were mutated to alanine (AAAA) in GEF4A construct
* (asterisk) indicates fully conserved positions
: (colon) indicates conservation between groups of strongly similar properties
A . (period) indicates conservation between groups of weakly similar properties

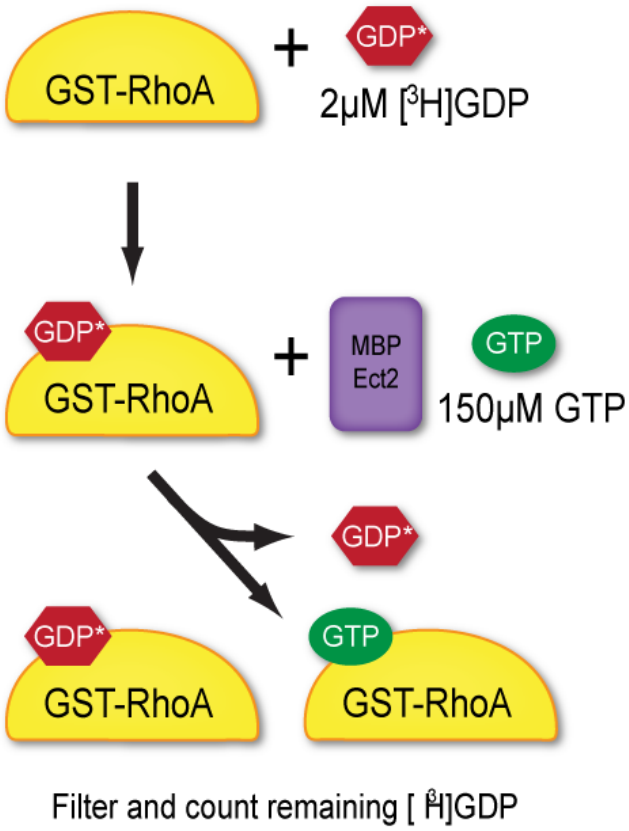

Figure 20 Schematic representation of the *in vitro* RhoA guanine nucleotide exchange assay

[^{3}H]GDP-loaded GST-RhoA is incubated with recombinant MBP or MBP fusions of the indicated Ect2 fragments in the presence of unlabelled GTP. [^{3}H]GDP release was determined by measuring the remaining protein-associated radioactivity.

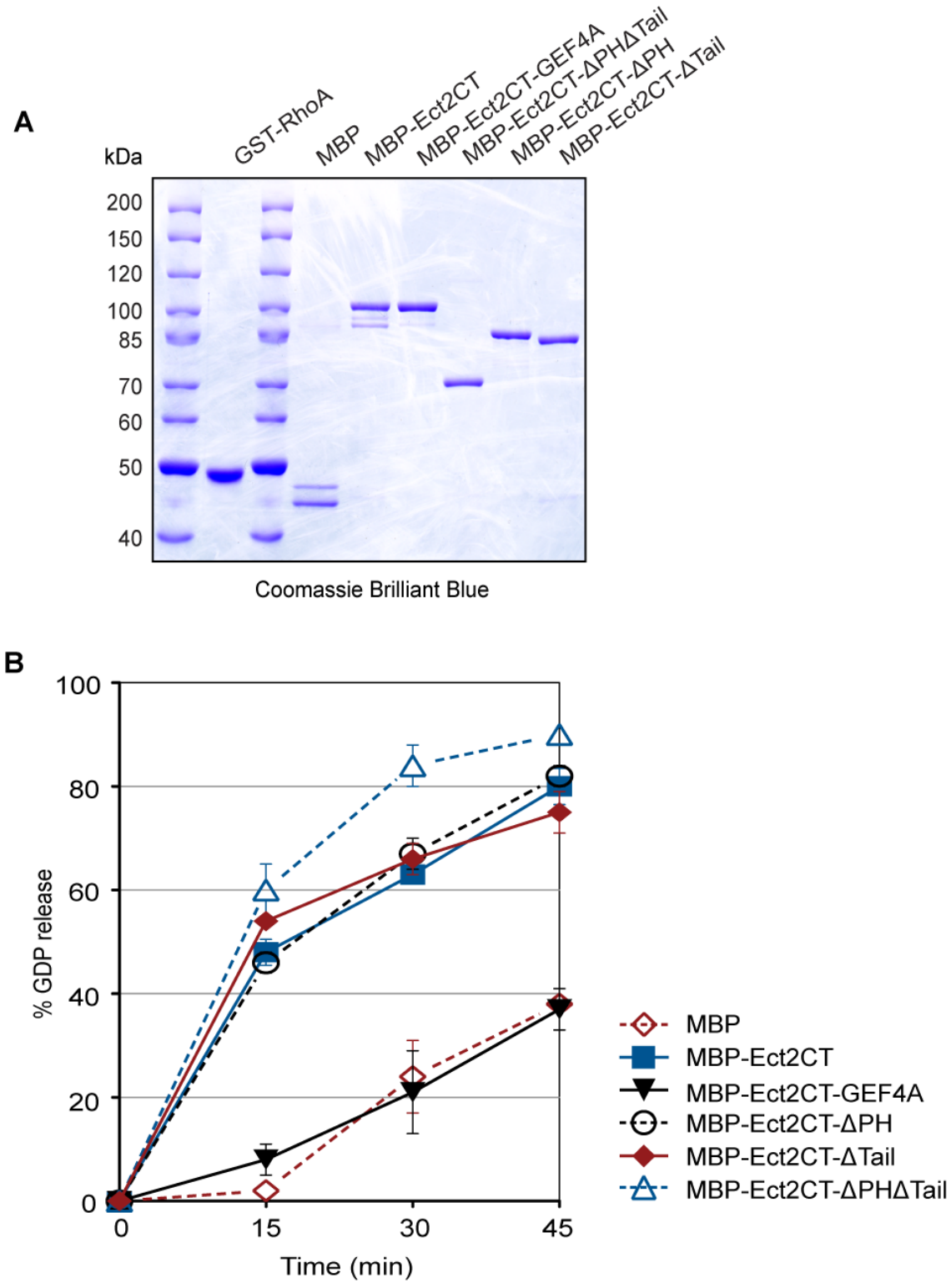

Figure 21 *In vitro* RhoA GDP/GTP exchange assay

A Coomassie brilliant blue-stained gel of GST and MBP fusion proteins expressed in insect cells using the baculovirus system and purified using

glutathione and amylose resin, respectively. The purified proteins were used in the RhoA guanine exchange assay shown in panel B.
B Quantification of the guanine nucleotide exchange assay using [^{3}H]GDP-loaded GST-RhoA and the indicated MBP fusion proteins. [^{3}H]GDP release was determined by measuring the remaining protein-associated radioactivity. Error bars indicate standard deviation of two independent experiments. See also Figure 20.

Chapter 5. Results 3 – Role of Ect2 GEF activity and plasma membrane binding domains during cytokinesis

Using a transient overexpression assay, I could define two C-terminal regions within Ect2, a PH domain and a polybasic cluster, that are required for the association with the plasma membrane. Deletion of both modules abrogates membrane association of the Ect2CT reporter construct. Furthermore, I have generated a mutant allele of Ect2 (GEF4A) that lacks guanine nucleotide exchange factor activity *in vitro*. Our analyses showed that the GEF activity of Ect2 and the protein's ability to associate with the plasma membrane could be experimentally separated. I subsequently decided to employ the efficient genetic complementation system that I have established previously (Figure 9 and Figure 11) to study the role and requirement of Ect2's GEF activity and membrane targeting domains during cytokinesis in the context of the full-length protein.

5.1 The GEF activity and membrane targeting domains of Ect2 are required for cytokinesis

Using HeLa "Kyoto" cells, I generated a range of monoclonal stable cell lines expressing either the tag AcFL alone, an siRNA-sensitive tagged version of Ect2 (AcFL-Ect2s) or variants of tagged siRNA-resistant Ect2 (AcFL-Ect2r) proteins (Figure 22). I selected cell line clones that expressed the AcFL-tagged transgene in more than 96% of cells and at a level very close to the endogenous Ect2 counterpart (Figure 23). Crucially, all cell lines displayed a level of transgene expression level well above the minimum level of Ect2 required for successful execution of cytokinesis (see Figure 10). Therefore, this set of transgenic cell lines should facilitate a structure-function analysis of Ect2.

To assess the requirement for the GEF function of Ect2, the DH domain was deleted (ΔGEF). Alternatively, I used the previously characterized point mutations

within the CR3 helix of the DH domain (GEF4A), which abrogate GDP/GTP exchange activity on Rho in our *in vitro* assay (Figure 21B).

To investigate the requirement of Ect2 membrane targeting for cytokinesis, the PH domain (ΔPH) and the PBC-containing tail region (ΔTail) were deleted separately or in conjunction (ΔPHΔTail). Importantly, we have shown previously that neither individual nor combined removal of the PH and Tail regions reduces Ect2 guanine nucleotide exchange activity on RhoA *in vitro* (Figure 21B).

Transfection of an siRNA targeting Ect2 caused the efficient depletion of endogenous protein in the cell lines (Figure 23). Using immunofluorescence, I scored the rate of multi-nucleation 48 hours post siRNA transfection (Figure 24). AcFL-Ect2s, the siRNA-sensitive Ect2 protein, is efficiently depleted along with the endogenous protein. As a consequence, close to all AcFL-Ect2s cells accumulated as multi-nucleated cells, similar the AcFL tag only cell line. In striking contrast, expression of AcFL-Ect2r, the siRNA resistant allele, was able to fully complement the loss of endogenous Ect2 protein and supported successful cell division (Figure 22).

Deletion and mutation of the DH (ΔGEF, GEF4A) abrogated or strongly impaired cytokinesis (Figure 22). The remaining rescue activity observed in the GEF4A mutant could either be caused by residual GEF activity in the mutant allele or by an additional unknown function of the GEF domain apart to promote the exchange of GDP to GTP. Nevertheless, this result suggests that the guanine nucleotide exchange activity of Ect2 is required for cytokinesis in human cells.

Deletion of the PH domain alone (ΔPH) or in conjunction with the deletion of the C-terminal tail region (ΔPHΔTail) completely abrogated the rescue activity of the AcFL-Ect2r transgene (Figure 22). Deletion of the tail region alone (ΔTail) however displayed an intermediate phenotype with multi-nucleation in about half of the cells in the population. Whether residual membrane-targeting is retained in the ΔTail allele or whether the PH domain of Ect2 has another function besides membrane association is currently unclear. The results of the genetic complementation

analysis were also confirmed in second set of independently isolated monoclonal cell lines (Figure 25).

I have shown here that the guanine nucleotide exchange activity of Ect2 and the proteins' membrane association domains are required for cytokinesis in human cells. This suggests that GEF activity and membrane association may be two separable but essential properties of Ect2.

5.2 Importance of Ect2's GEF activity and membrane targeting domains for cleavage furrow formation and Ect2 protein localization during cytokinesis

I next investigated the effect of Ect2's GEF activity and the proteins membrane interaction domains on Ect2 protein localization and cleavage furrow formation during cytokinesis. By fixing cells after depletion of the endogenous counterpart, I first analysed the accumulation of Ect2 at the spindle midzone in anaphase cells by immunofluorescence microscopy. Spindle midzone localization was assessed by testing colocalization with the centralspindlin subunit Mklp1. Neither deletion of the GEF domain, the GEF activity inactivating GEF4A mutation nor the membrane interacting PH and PBC domains interfered with the accumulation of Ect2 at the spindle midzone during anaphase (Figure 26). This is consistent with previous studies that have revealed that Ect2's midzone association is mediated by the N-terminal tandem BRCT domains (Chalamalasetty et al., 2006; Yüce et al., 2005; Tatsumoto et al., 1999). This result suggests that Ect2's GEF domain and GEF activity as well as the protein's PH and PBC domains regions are dispensable for Ect2 localization to the central spindle.

To study the ability of the engineered Ect2 alleles to associate with the plasma membrane during cytokinesis, I tracked the transgenic proteins through cell division in the absence of the endogenous counterpart using spinning-disc microscopy (n>35 cells for each mutant allele, Figure 27). As shown above (Figure 11), wild-type Ect2 accumulated at the central spindle and the equatorial plasma membrane

during anaphase (Figure 27). Deletion of Ect2'S GEF domain or abrogation of the protein's GEF activity (GEF4A) strongly impaired cleavage furrow formation in anaphase, but did not affect the protein's localization to the equatorial membrane (Figure 27). Interestingly, the GEF4A mutant protein accumulated to higher levels at the equatorial membrane than the wild-type version. Deletion of the PH domain strongly reduced, but did not abolish, membrane localization of Ect2. Accordingly, ΔPH cells were still able to form a cleavage furrow but later underwent furrow retraction (Figure 27). Combined deletion of the PH domain and the PBC-containing tail region (ΔPHΔTail) completely abolished the association of Ect2 with the equatorial plasma membrane while the localization of the ΔPHΔTail allele to the spindle midzone was unaffected (Figure 27)**.** Importantly, loss of both membrane association domains also abolished cleavage furrow formation.

To characterize the cytokinetic phenotype of different Ect2 alleles more quantitatively, I used bright field time-lapse microscopy. This allowed me to analyse a larger number of cells (n≥289) (Figure 28). Similar to our previous observations, depletion of Ect2 in AcFL tag expressing cells resulted in the loss of cytokinetic furrow formation in the majority of anaphase cells (Figure 27). A small fraction of cells however underwent furrowing followed by furrow regression and cytokinesis failure. Although I was able to very efficiently deplete Ect2 by siRNA as judged by immunoblotting (Figure 9 and Figure 10), this fraction of cells presumably displays a hypomorphic Ect2 loss-of-function phenotype. This interpretation is consistent with our previous measurements that revealed that about 13% of the normallevel of cellular Ect2 is sufficient to support cell division (Figure 10). Expression of siRNA-resistant wild-type AcFL-Ect2r was able to fully restore cytokinesis in the absence of the endogenous counterpart. 99% of cells divide reliably into two daughter cells (Figure 28**).** Deletion of Ect2's GEF domain abrogated cleavage furrow formation to a similar extent as the complete absence of an siRNA-resistant allele (AcFL tag only) suggesting that the ΔGEF allele represents an Ect2 null situation (Figure 28). The GEF4A allele, which lacks detectable GEF activity *in vitro* (Figure **19**), displayed strongly impaired cleavage furrow formation, but the penetrance of its phenotype was slightly reduced as compared to the deletion of the entire GEF domain. This is consistent with our previous analysis using bi-nucleation end point assays in fixed cells (Figure 24) and may suggest that the GEF4A allele retains

some exchange activity *in vivo*. The majority of cells expressing a version of Ect2 that lacks the PH domain underwent furrowing but were unable to successfully complete cytokinesis (Figure 28). About half of ΔTail expressing cells underwent cytokinesis failure after cleavage furrow ingression. Combined deletion of both PH domain and the PBC-containing tail resulted in the absence of furrowing in the majority of cells similar to a total loss-of-function situation (Figure 28). These observations are consistent with our previous findings that the PH domain and polybasic cluster within the C-terminus of Ect2 cooperate to mediate membrane association of the protein (Figure 16).

Together with the identification of a GEF domain point mutation in a *pebble* allele in flies (Prokopenko et al., 1999), our analyses provide the strongest evidence yet that the exchange activity of Ect2 is crucial for cleavage furrow formation in animal cells. Importantly, we also found that Ect2's GEF activity is dispensable for the accumulation of the protein at the spindle midzone and equatorial membrane. The loss of Ect2's ability to associate with the plasma membrane correlates with a severe defect in cleavage furrow formation. Based on results obtained using *in vitro* assays, the RhoGEF activity of Ect2 is not affected by the removal of the proteins membrane engagement domains. Although we cannot rule out the PH domain and PBC-containing tail performs additional functions, this suggests that the association of Ect2 with the plasma membrane may be important for the protein's GEF activity to control cleavage furrow formation during cytokinesis *in vivo*. Thus, the ability of Ect2 to stimulate guanine nucleotide exchange on RhoA and the protein's ability to associate with the cell periphery may be two essential but mechanistically distinct functions of Ect2 during cytokinesis.

5.3 RhoA and anillin localization in Ect2 mutant alleles

Consistent with previous observations (Yüce et al., 2005), I found that the formation of the spindle midzone does not require Ect2 and was not altered in different Ect2 alleles as judged by Mklp1 staining in fixed cells (Figure 26). To characterize the defects underlying cytokinesis failure in different Ect2 alleles I focused on the

GTPase RhoA (Eggert et al., 2006; Piekny et al., 2005) and the contractile ring scaffold protein anillin, a downstream effector of RhoA (Piekny and Maddox, 2010). In animal cells, activation of RhoA at the cell equator is thought to stimulate contractile ring assembly, the recruitment of anillin and cleavage furrow ingression. This can be investigated by staining for RhoA in tricholoroacetic acid-fixed cells, which has been shown to preferentially visualize the activated and membrane-associated form of RhoA (Yüce et al., 2005; Nishimura and Yonemura, 2006) at the cell equator (Figure 27).

Consistent with previous reports (Yüce et al., 2005), depletion of Ect2 prevented the accumulation of RhoA and anillin at the cell equator in fixed anaphase cells (data not shown). Expression of wild-type siRNA-resistant Ect2 (AcFL-Ect2r) fully rescued the localization of both contractile zone markers at anaphase (Figure 29). In the mutant alleles abolishing either Ect2's GEF function or its ability to associate with the membrane (ΔPHΔTail), RhoA and anillin fail to accumulate at the equatorial cortex (Figure 29). Deletion of the PH domain only (ΔPH) however, shows a reduced signal for both markers at the equator, consistent with my previous finding that the majority of the cells initiate furrowing but fail to complete cytokinesis in this allele. Overall, the severity of the contractile ring phenotype observed in different allelic Ect2 conditions, correlates well with the penetrance of the furrowing phenotype (Figure 28 and Figure 29).

My analysis suggests Ect2's GEF activity and Ect2's association with the plasma membrane are required for RhoA activation, contractile ring formation and cleavage furrow formation during cytokinesis in human cells. The primary underlying cause for the cytokinesis and furrowing defect observed is likely to be the failure to activate RhoA at anaphase.

5.4 Conclusions: Results 3 – Role of Ect2 GEF activity and plasma membrane binding domains during cytokinesis

We have generated an allelic series of mutations and deletions affecting either the guanine nucleotide exchange activity or membrane targeting of Ect2 in the context of the full-length protein. Using my previously established genetic complementation system I have tested the effects of these changes on the localization of the protein and on the execution of cytokinesis *in vivo*. Our analysis indicates that both GEF activity and membrane association of Ect2 are essential for cytokinesis.

Loss of Ect2 GEF activity leads to an absence of RhoA recruitment and activation at the equatorial cortex and, consequently, also prevents formation of the contractile ring (Figure 29). Despite the absence of furrow formation, Ect2 molecules lacking GEF activity localize to the spindle midzone and equatorial membrane. This suggests that despite the correct localization of the protein, Ect2 is unable to stimulate cortical contractility in GEF mutant alleles thereby placing its GEF activity at the heart of cleavage furrow formation.

Deletion of the membrane association domains prevents the accumulation of Ect2 at the equatorial cell periphery during anaphase and abrogates RhoA activation and anillin recruitment, identical to loss of the GEF activity. Loss of the same membrane association domains does not affect the guanine nucleotide exchange activity of Ect2 on RhoA *in vitro* and *in vivo* does not interfere with the localization of the protein to the midzone. Collectively, these results suggest that cleavage furrow formation in human cells requires the guanine nucleotide exchange activity of Ect2 and depends on the targeting of the molecule to the cell periphery. My analysis raises the exciting possibility that the concentration of Ect2 at the equatorial plasma membrane may play an important role in triggering cleavage furrow formation at the right place and at the right time.

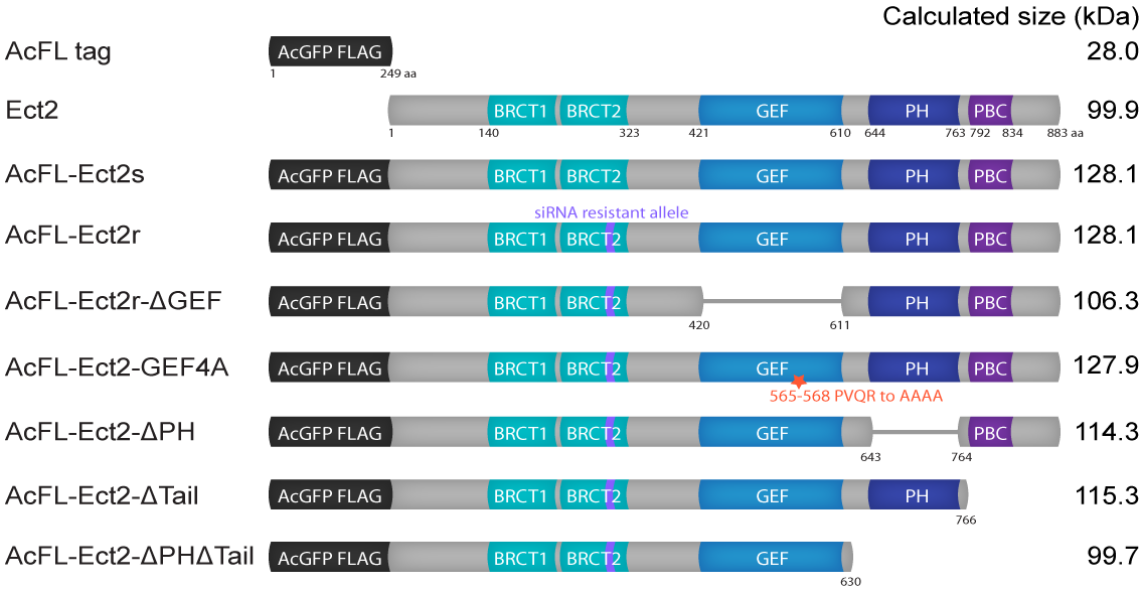

Figure 22 Full-length Ect2 mutant alleles used for the *in vivo* analyses

Schematic illustration of AcFL-tagged constructs used to generate monoclonal cell lines. The cell lines were employed to dissect the function and requirement of different domains of Ect2 during cytokinesis. Amino acid annotations in AcFL-Ect2 fusions correspond to positions in human full-length Ect2 protein.

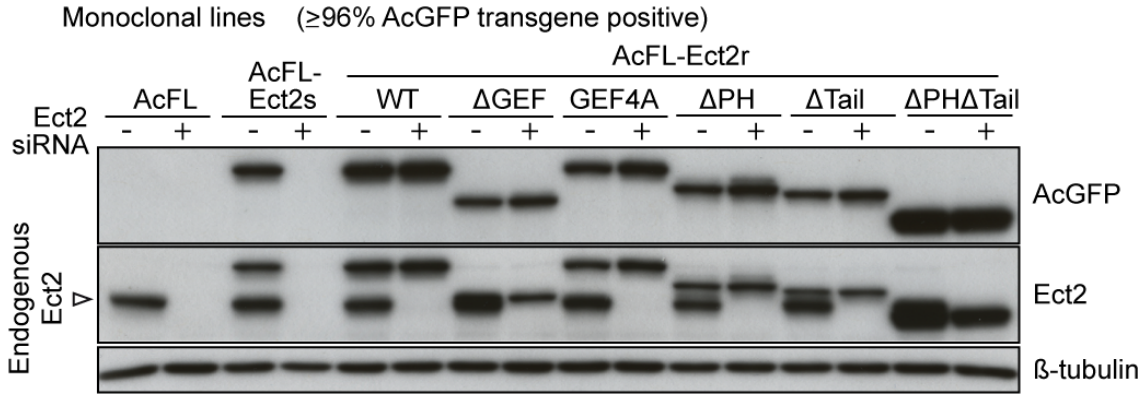

Figure 23 Immunoblotting analysis of monoclonal cell lines expressing AcFL or AcFL-tagged mutant alleles of Ect2

Immunoblot-analysis of protein extracts prepared from monoclonal HeLa 'Kyoto' cell lines expressing the indicated transgenes. Extracts were prepared 48 hours after transfection with control siRNA (-) or Ect2 siRNA (+). Extracts were probed with antibodies directed against AcGFP, Ect2 and ß-tubulin. Domain organization of all constructs used is shown in Figure 22.

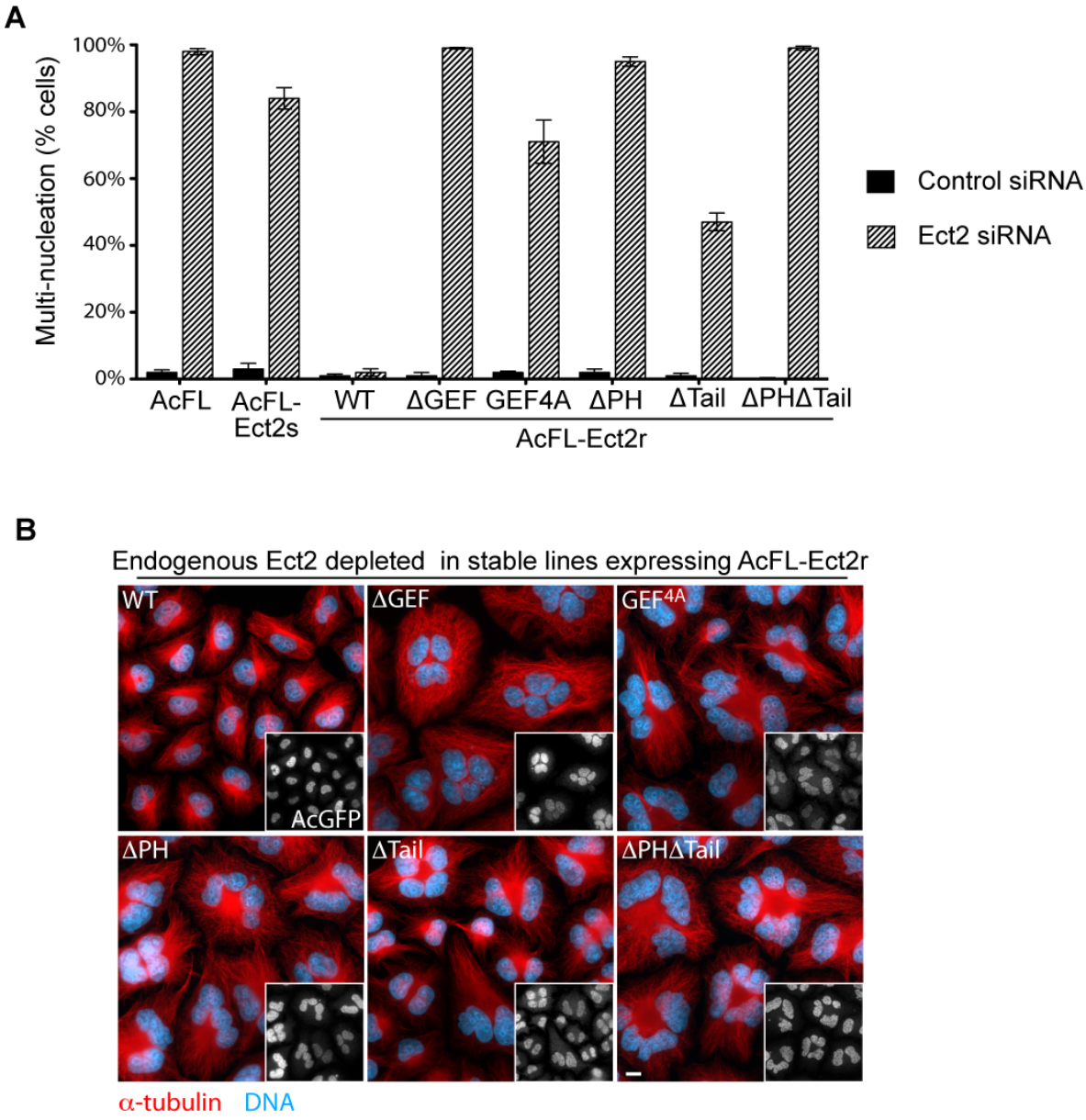

Figure 24 Complementation analysis using Ect2 mutant alleles

A Quantification of the fraction of bi-nucleated and multi-nucleated interphase cells (multi-nucleation) in monoclonal lines expressing the indicated transgenes. Error bars indicate standard deviation of three experiments (n>200 cells each). Cells were analysed by IF 48 hours after transfection with control or Ect2 siRNA. See Figure 25 for the characterization of a second set of independent monoclonal cell lines.
B IF analysis of monoclonal cell lines expressing the indicated transgenes. Cells were analyzed 48 hours after transfection with Ect2 siRNA. Scale bar represents 10 µm.

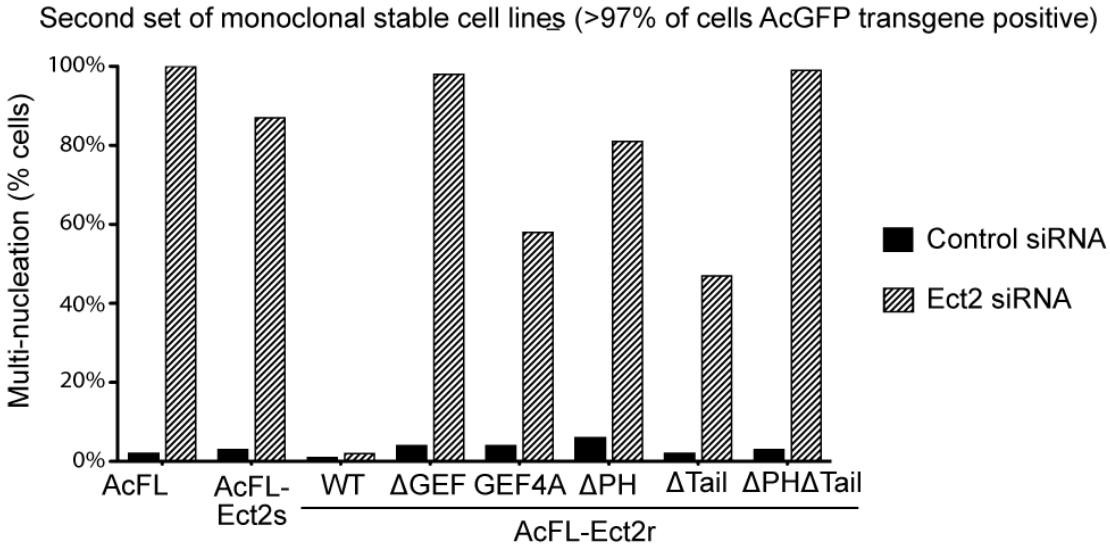

Figure 25 Complementation analysis using second set of monoclonal cell lines expressing Ect2 mutant alleles

Quantification of the fraction of bi-nucleated and multi-nucleated interphase cells in a second set of monoclonal lines expressing the indicated transgenes (n=200). Cells were analysed by IF 48 hours after transfection with control or Ect2 siRNA. This set of cell lines was used to validate the data obtained using independently isolated clones and shown in Figure 24.

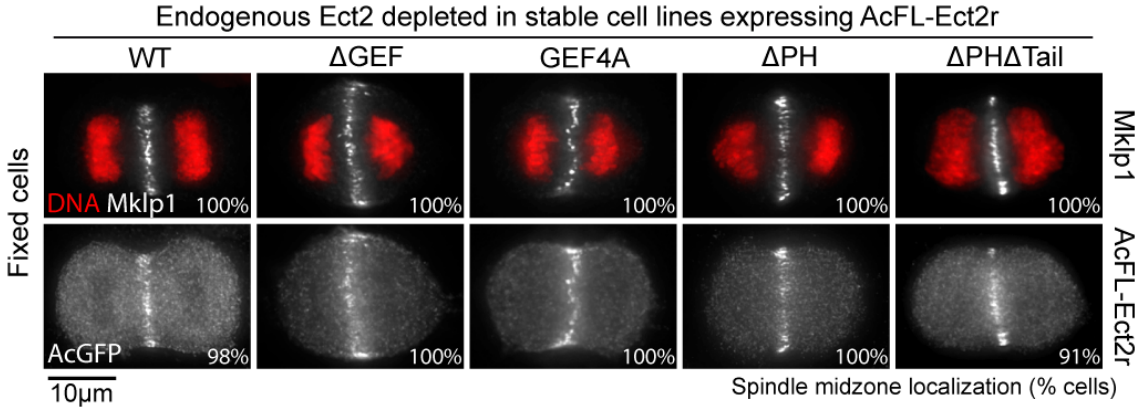

Figure 26 Central spindle localization of mutant Ect2 proteins

IF analysis of cells expressing the indicated transgenes 36 hours after transfection with Ect2 siRNA (n>50 anaphase cells each). Cells were co-stained with anti-Mklp1 and anti-AcGFP antibodies

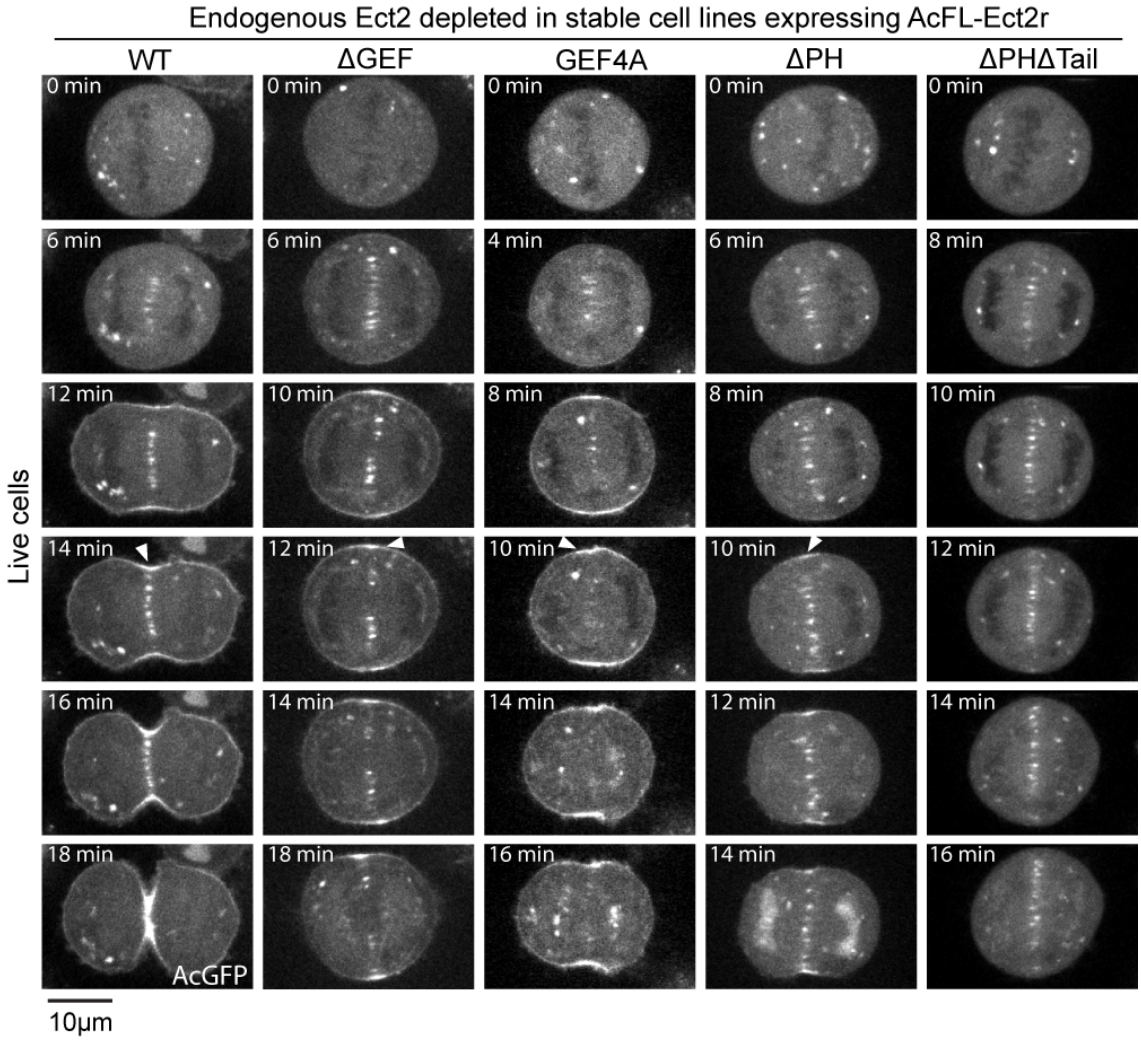

Figure 27 Localization of mutant Ect2 proteins in live cells

Spinning disc live-cell imaging of the indicated AcFL-Ect2r alleles in monoclonal cell lines. Recording started 18 hours after transfection with Ect2 siRNA. Time point t = 0 min was set to the metaphase-to-anaphase transition. The filled arrowheads indicate localization to the cell cortex.

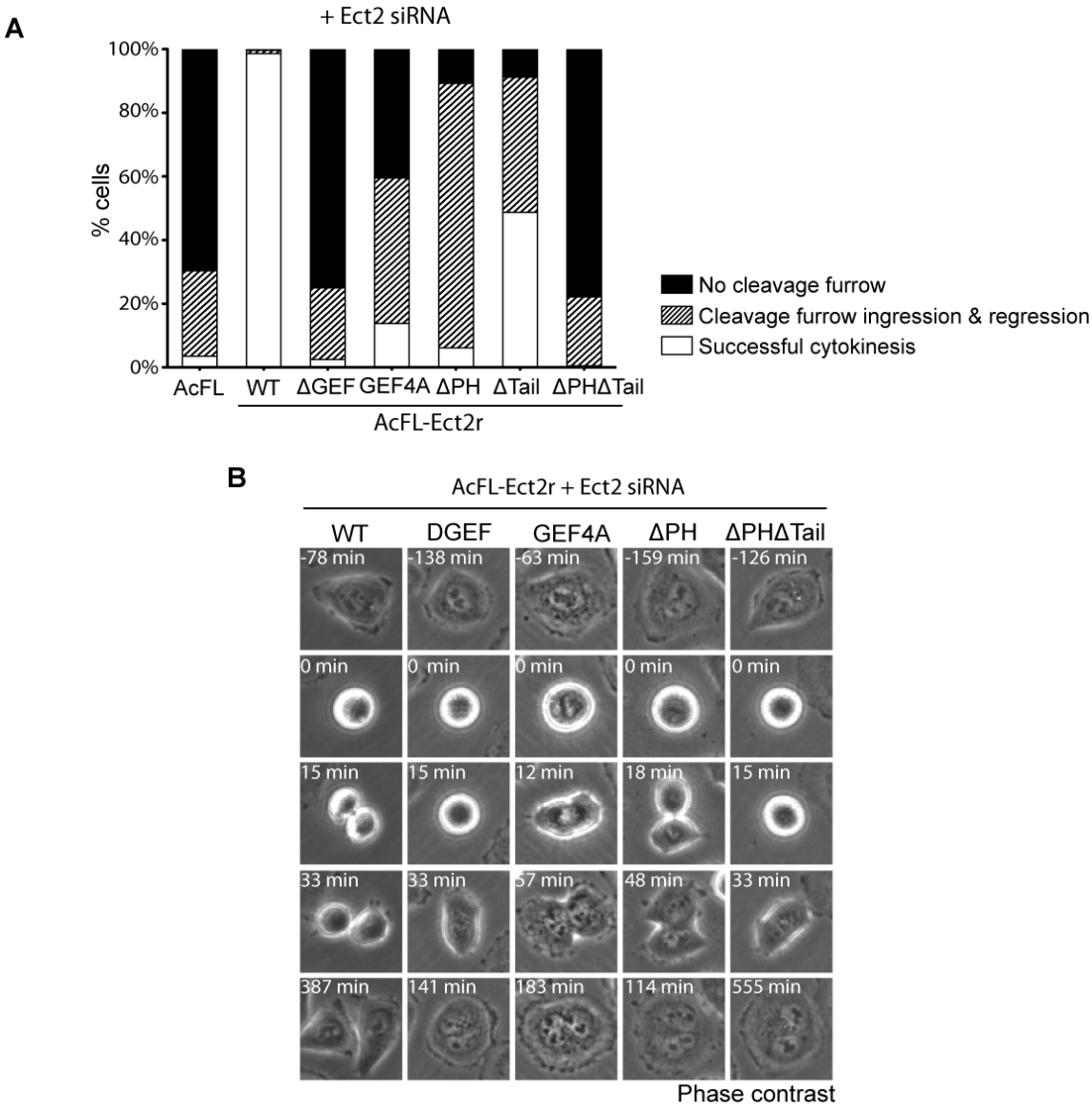

Figure 28 Analysis of cytokinetic phenotypes of mutant Ect2 alleles

A Quantification of cytokinetic phenotypes in monoclonal cell lines expressing the indicated transgenes using time-lapse microscopy after transfection with Ect2 siRNA (n>288 cells each). Mono-nucleate cells entering mitosis were scored from 18 hours to 38 hours post transfection.
B Representative cell division phenotypes of selected cell lines are shown as time-lapse series. Time point t = 0 min was set to the metaphase-to-anaphase transition.

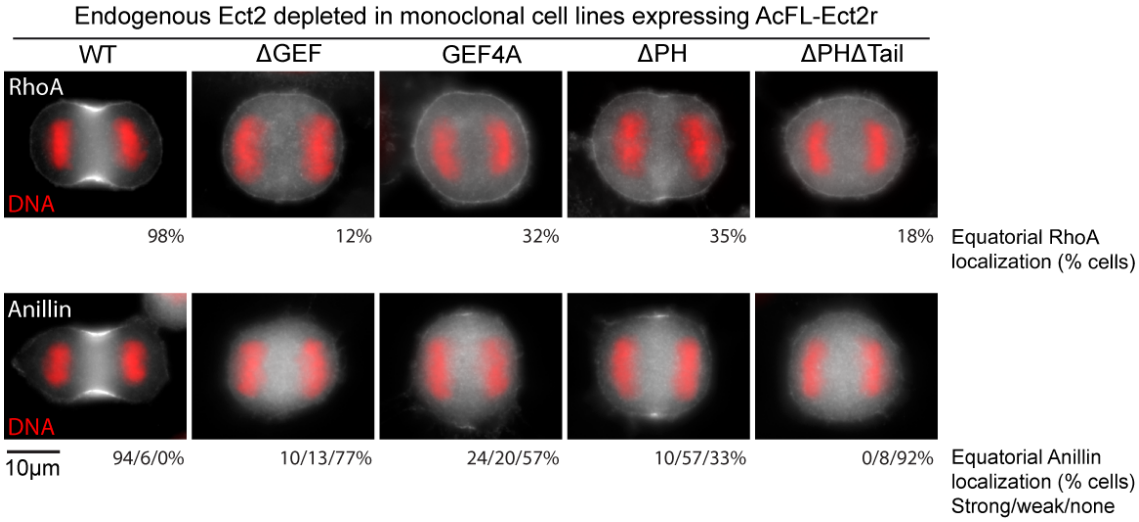

Figure 29 RhoA and anillin localization in mutant Ect2 alleles

IF analysis of anaphase cells expressing the indicated transgenes 32 to 36 hours after transfection with Ect2 siRNA (n > 50 anaphase cells each). Cells were fixed in trichloroacetic acid or methanol and stained with anti-RhoA or anti-anillin antibodies, respectively. Cells were visually categorized based on more intense signal apperance at the equatorial membrane in comparison to signal at the poles. Results are indicated below the images. Displayed images represent majority phenotype.

Chapter 6. Results 4 - Spatial and temporal control of Ect2 localization

Our studies described above have defined a novel localization pattern of Ect2. We found that Ect2 associates with the plasma membrane during cytokinesis. This association is tightly regulated in both space and time (Figure 11). Ect2 translocates to the plasma membrane at anaphase onset and becomes concentrated at the equatorial region. Thus, the spatiotemporal properties of Ect2 membrane association correlate well with cleavage furrow formation. Furthermore, our genetic complementation analysis strongly suggests that the ability of Ect2 to associate with the plasma membrane is essential for RhoA activation and cleavage furrow formation. This raises the possibility that the anaphase-specific localization of Ect2 to the equatorial plasma membrane may contribute to the correct placement and timing of cytokinetic furrowing (Figure 24, Figure 27, Figure 28 and Figure 29). Thus, I decided to investigate the mechanisms that govern the spatiotemporal control of Ect2 plasma membrane localization during cell division.

6.1 Centralspindlin and Plk1 are required for the equatorial concentration of Ect2 at the plasma membrane

Unlike the full-length Ect2 protein that accumulates at the equatorial periphery during anaphase (Figure 11), the Ect2CT fragment lacking the BRCT domains that mediate spindle midzone recruitment is distributed uniformly around the cell periphery at anaphase (Figure 16). This suggests that a polarized distribution of specific lipid species that are recognized by Ect2's membrane targeting domains is not responsible for the accumulation of the protein at the cell equator. We therefore investigated whether the recruitment of Ect2 to the central spindle itself may contribute to the equatorial enrichment of the protein at the plasma membrane.

Ect2's spindle midzone association requires direct binding to centralspindlin (Somers and Saint, 2003; Chalamalasetty et al., 2006; Yüce et al., 2005). To abrogate the association of Ect2 with the spindle midzone, I depleted the

centralspindlin subunits MgcRacGAP and Mklp1 (Figure 30). Furthermore, I acutely treated dividing cells with the Plk1 inhibitor BI 2536. Phosphorylation of MgcRacGAP by Plk1 is required for Ect2 binding and recruitment to the spindle midzone (Burkard et al., 2009; Wolfe et al., 2009). In all cases, Ect2 localization was tracked in a stable cell line co-expressing AcFL-Ect2r and H2B-mCherry.

In control cells, Ect2 first associated with the spindle midzone before appearing at the plasma membrane and becoming concentrated in the equatorial region (n=18 cells) (Figure 30A). In cells depleted for MgcRacGAP and Mklp1, cleavage furrow formation was severely impaired and Ect2 failed to accumulate at the spindle midzone as expected. However as cells progress in anaphase, Ect2 translocated to the plasma membrane on time but without becoming subsequently enriched at the cell equator (n>8 each) (Figure 30A). In the absence of centralspindlin, Ect2's was uniformly distributed at the cell periphery during anaphase. Similar observations (97 of 99 cells) have been made in cells acutely treated with the Plk1 inhibitor BI 2536 (Lénárt et al., 2007). The ΔGEF and GEF4A mutant Ect2 proteins accumulate at the equatorial membrane despite the absence of cleavage furrow and contractile ring formation (Figure 27, Figure 28 and Figure 29). This indicates that the absence of furrow and contractile ring formation cannot account for failure of Ect2 to be concentrated at the equatorial membrane after depletion of centralspindlin subunits or inhibition of Plk1. Thus, the interaction of Ect2 with the spindle midzone is not required not for membrane interaction per se but may be required for the enrichment of the protein at the equatorial membrane. This indicates that two distinct mechanisms govern the spatial and temporal control of Ect2 membrane localization.

6.2 Dynamic properties of centralspindlin and Ect2 at the spindle midzone

The spindle midzone may act as a localized enrichment site for cytoplasmic Ect2. Together with dynamic association of Ect2 with the plasma membrane, this enrichment may promote the accumulation of Ect2 at the equatorial membrane that

is closely juxtaposed to the midzone. Interestingly, we do not observe a significant pool of centralspindlin at the plasma membrane during cytokinesis. This indicates that Ect2 but not the Ect2-centralspindlin complex accumulates at the membrane. Collectively, these considerations predict that Ect2 would have to quickly turn over at the spindle midzone in order for the midzone to play an instructive role in the pattern of Ect2 membrane distribution.

To test this, I measured the dynamic properties of Ect2 and the centralspindlin complex at the spindle midzone in anaphase cells. Using monoclonal cell lines expressing AcFL-Ect2r or MgcRacGAP (Lekomtsev et al., 2012) tagged with FLAG-AcGFP (MgcRacGAP-FLAc), I performed photo-bleaching experiments to determine the rate of recovery at the midzone in anaphase cells after onset of furrow contraction (<40% contracted) (Figure 31 and Figure 32). Analysis of fluorescent intensity of the bleached area revealed a rapid recovery for Ect2 but a slow and incomplete recovery for the centralspindlin subunit MgcRacGAP (n=11) (Figure 31 and Figure 32). In less than 2s after photobleaching, Ect2 recovered 50% of the signal relative to the cytoplasmic signal, whereas MgcRacGAP extended a $t_{1/2}$ recovery time of 52s and never fully recovered by the end of the experiment indicating the presence of an immobile fraction. This suggests that in animal cells the spindle midzone acts as a stable signalling scaffold upon which signalling molecules such as Ect2 rapidly turn over.

6.3 Inactivation of Cdk1 at anaphase onset controls the association of Ect2 with the plasma membrane

Although abolishing Ect2's binding to the spindle midzone also prevented the enrichment of the protein at the equator membrane (Figure 30A), Ect2 was still able to translocate to the plasma membrane from the cytoplasm at the correct time in anaphase. This suggests the existence of a distinct mechanism that regulates the timing of the interaction of Ect2 with the plasma membrane.

To study the control of membrane targeting timing in the absence of the ability of Ect2 to bind to the spindle midzone, I transfected cells stably expressing H2B-mCherry transiently with Ect2CT (Figure 14). In metaphase cells, Ect2CT was largely cytoplasmic and only showed a minor enrichment at the plasma membrane. Quantification of the Ect2CT signal distribution shows a minor accumulation of the transgene at the membrane (1.5 fold) in metaphase. Strikingly, Ect2CT rapidly translocated to the plasma membrane at the metaphase-to-anaphase transition (Figure 33). 3 minutes before anaphase onset indicated by segregation of sister chromatids the ratio of the Ect2CT signals begins to shift toward the membrane and this increases dramatically reaching a maximum of about 6 fold enrichment at the membrane compared to the cytoplasmic signal 10 minutes after anaphase onset. Cells expressing Ect2CT are unable to form a cleavage furrow, presumably due to ectopic and uniform RhoA activation at the cell cortex.

The dephosphorylation of Cdk1 targets at the metaphase-to-anaphase transition is known to induce cytokinesis and mitotic exit (Barr and Gruneberg, 2007; Wurzenberger and Gerlich, 2011). The rapid change of subcellular localization of Ect2CT at this transition suggests that Cdk1 phosphorylation of the PH and PBC regions of Ect2 may prevent its precocious interaction with the membrane in metaphase. Loss of Cdk1 phosphorylation at anaphase onset could then promote the membrane recruitment of Ect2.

In vitro kinase assays have identified multiple phosphorylation sites on Ect2 (Niiya et al., 2006). Among those, T815 has been described as the major Cdk1/cyclin B phosphorylation site within Ect2's C-terminal region. Furthermore, mitosis specific phosphorylation of T815 has been confirmed by global phospho-proteomic experiments *in vivo* (Dephoure et al., 2008) and the site matches an ideal Cdk1 target consensus motif (Figure 13). Interestingly, T815 is localized within Ect2's polybasic cluster. Sequence comparison among orthologs revealed the site of phosphorylation to be highly conserved in evolution (Figure 34A). Thus, T815 emerged as a suitable candidate site for the regulation of Ect2 membrane translocation by Cdk1. We therefore generated a T815A mutant in the Ect2CT fragment and monitored its subcellular distribution around the metaphase-to-anaphase transition (Figure 33A). Strikingly, the mutation T815A caused

precocious localization of the Ect2CT reporter protein to the plasma membrane in metaphase cells (4-fold enrichment over cytoplasm) and prevented the anaphase-specific increase in membrane recruitment (Figure 33B). This observation suggests that, at least in the context of the Ect2CT fragment, T815 represents an important regulatory site for Ect2's ability to associate with the plasma membrane. Furthermore, it raises the possibility that this conserved residue is phosphorylated by Cdk1 to electrostatically prevent the ability of the PBC of Ect2 to associate with the plasma membrane.

To determine whether T815 is phosphorylated *in vivo*, we raised a phospho-specific antibody against the peptide FSFSK-**pT**-PKRAL in rabbits. Immunoblotting analysis revealed that the purified serum (pT815) detected transiently expressed Ect2CT-WT but not Ect2CT-T815A in nocodazole-arrested mitotic cells (Figure 34B). Lysates prepared from cells arrested with thymidine arrested cells expressing Ect2-CT did not display a band because the absence of Cdk1 activity.

Cell synchronization and siRNA transfection experiments showed that the serum recognizes a mitosis-specific modification of endogenous and transgenic full-length Ect2 proteins (Figure 34C). Mutation of T815 to alanine abolished the reactivity with the serum. Phosphatase treatment of lysates before immunoblotting removed all bands detected by pT815 confirming the specificity of the serum for a phosphorylated epitope (Figure 35). These experiments demonstrate that T815 of Ect2 is indeed phosphorylated during mitosis.

To interrogate the regulation of Ect2 membrane association by Cdk1 activity directly, I treated Ect2CT expressing cells that were arrested in mitosis by addition of nocodazole with the Cdk1 inhibitor flavopiridol. Cells were tracked just prior and after flavopiridol treatment using spinning disc time-lapse microscopy. Flavopiridol treatment caused the rapid and quantitative translocation of Ect2CT from the cytoplasm to the plasma membrane (Figure 36). In contrast, the protein remained cytoplasmic in cells kept in nocodazole only (Figure 36A). This result strongly suggests that the ability of Ect2's C-terminal domains to interact with the inner leaflet of the plasma membrane is negatively regulated by Cdk1 activity. The phosphorylation of sites, such as T815, in the PH domain or PBC may prevent the

ability of the protein to interact with polyanionic phosphoinositides in the plasma membrane. Collectively, our analysis supports the notion that the activation state of Cdk1 couples Ect2 membrane translocation to the onset of chromosome segregation.

6.4 Conclusions: Results 4 - Spatial and temporal control of Ect2 localization

I have defined two distinct mechanisms that control the spatial and temporal pattern of Ect2 membrane targeting during cytokinesis. My analysis suggests that the spindle midzone-association of Ect2 could help to direct the protein's accumulation at the equatorial cortex during anaphase. Breaking the isotropic distribution of Ect2 at the cell periphery could be one of the key roles of the spindle midzone during cytokinesis in animal cells. I have also for the first time measured the dynamic behaviour of Ect2 at the spindle midzone and determined that it turns over very quickly on a stable scaffold of centralspindlin molecules (Figure 32). This observation reinforces the view of the spindle midzone as a spatially instructive signalling centre for cytokinesis.

While the anaphase spindle contributes the positioning of Ect2 on microtubules and the cell periphery, our analyses implicates the activation state of Cdk1 in the temporal control of Ect2 membrane translocation. My data are consistent with the interpretation that the rapid inactivation of Cdk1 and the subsequent loss of target phosphorylation by mitotic exit phosphatases directly trigger the membrane binding of Ect2. Thus, the activation state of Cdk1 couples Ect2 membrane translocation to the onset of anaphase. I have also identified one Cdk1 target site in the PBC of Ect2, T815, which, at least in the context of the Ect2CT fragment, is responsible for this regulation. While Cdk1 is known to inhibit multiple spindle-based cytokinetic events prior to anaphase onset (Green et al., 2012; Barr and Gruneberg, 2007), a direct regulation of the membrane binding ability of a key cytokinetic protein by Cdk1 during cytokinesis in animal cells has to my knowledge not been reported previously. It is likely the Cdk1 regulation of microtubule-based cytokinetic

processes and of Ect2 membrane interaction cooperate to avoid the untimely onset of furrowing.

I have characterized mechanistic details that contribute to the spatial and temporal regulation of Ect2 membrane translocation. Experiments in the future have to test the importance of the spatially and temporally restricted action and distribution of Ect2.

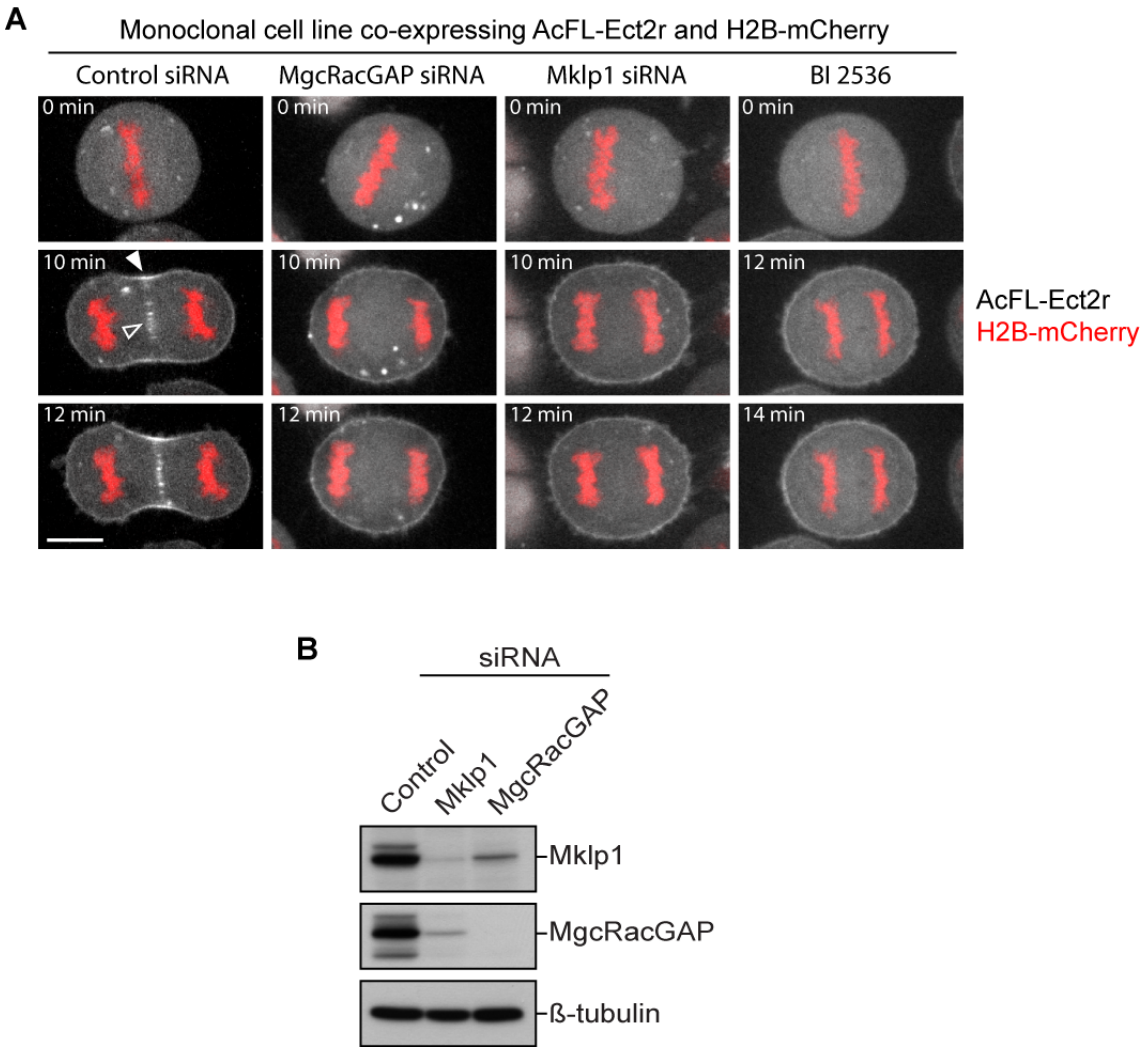

Figure 30 Spatial control of Ect2 membrane translocation

A Confocal live.cell imaging of a monoclonal cell line stably expressing AcFL-Ect2r (white) and H2B-mCherry (red). Cells were recorded 24 hours after transfection with control siRNA, MgcRacGAP siRNA or Mklp1 siRNA. Alternatively, cells were released from a metaphase arrest and treated with 250nM BI 2536 20 minutes after the release prior to recording (right panel). Time point t = 0 min was set to the metaphase-to-anaphase transition. The open and filled arrowheads indicate localization to the spindle midzone and equatorial cell membrane, respectively. Scale bar in this panel represents 10 µm.

B Immunoblot analysis of protein extracts prepared from monoclonal HeLa 'Kyoto' cells stably expressing AcFL-Ect2r and H2B-mCherry. Extracts were prepared 30 hours after transfection with control, Mklp1 and MgcRacGAP siRNA. Depleted cells were analysed by live cell imaging in figure A. Extracts were probed with antibodies directed against Mklp1, MgcRacGAP and ß-tubulin. Please note that depletion of one centralspindlin subunit also reduces the steady state levels of the other subunit.

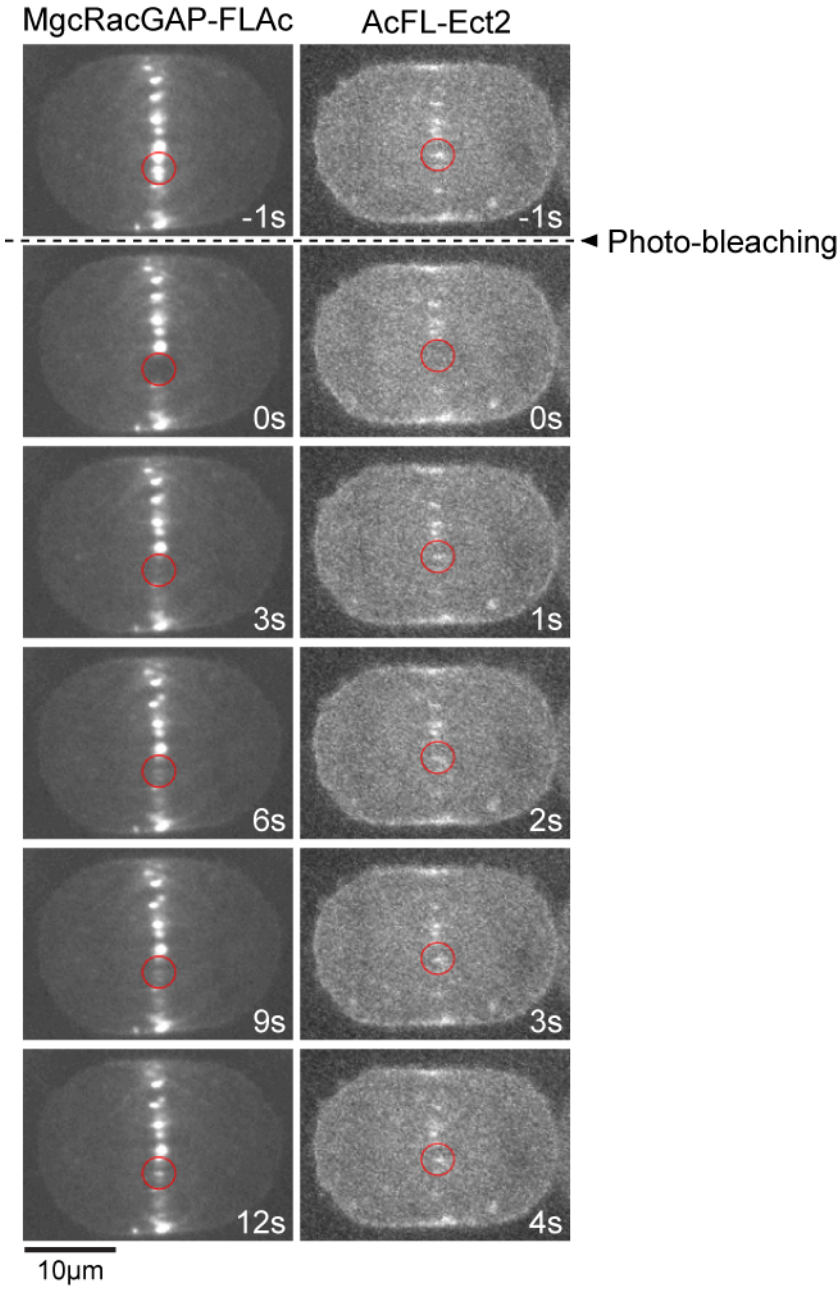

Figure 31 Fluorescence recovery after photobleaching of MgcRacGAP and Ect2 at the spindle midzone

Confocal live cell imaging of a monoclonal cell line stably expressing MgcRacGAP-FLAc (left) or AcFL-Ect2r (right). Red circles indicate the region of photobleaching. Time point t = 0 s was set as the first image acquired after photo bleaching. For the quantification signal recovery please see Figure 32.

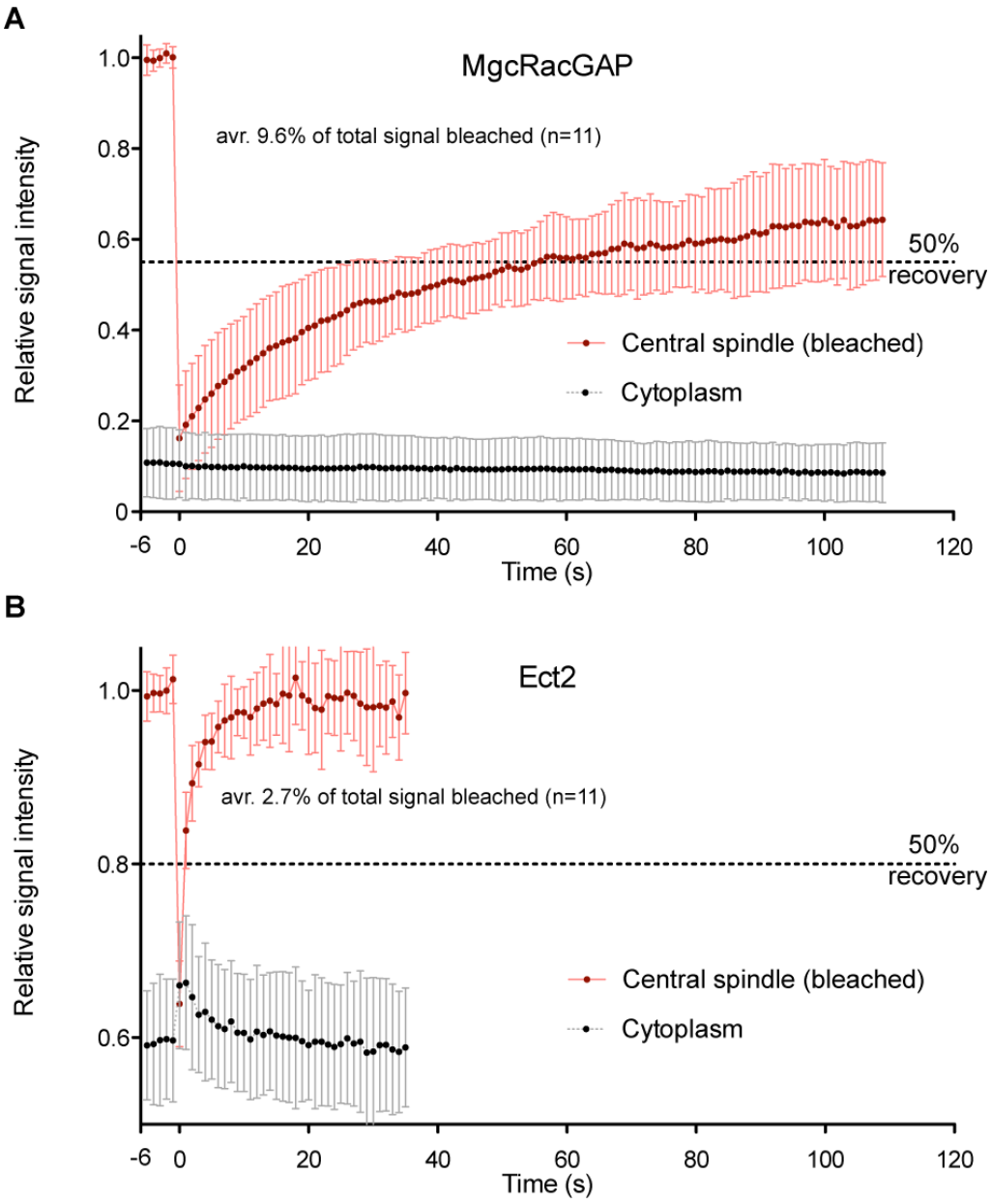

Figure 32 Recovery of MgcRacGAP and Ect2 fluorescence at the spindle midzone

A Quantification of FRAP (fluorescence recovery after photobleaching) in a cell line stably expressing MgcRacGAP-FLAc based on time-lapse series as shown in Figure 31. Graph displays the ratio of mean intensity of a photobleached spindle midzone area (red) and the mean cytoplasmic signal (black) over time referenced to an unbleached central spindle area. All intensities were background-corrected using an area outside of the cell. t=0 was set to first frame after photobleaching.. Error bars represent the standard deviation of the analysis of 11 cells.
B Identical analysis as A using H2BmCherry AcFL-Ect2r cell line. Quantification of AcFL-Ect2r FRAP.

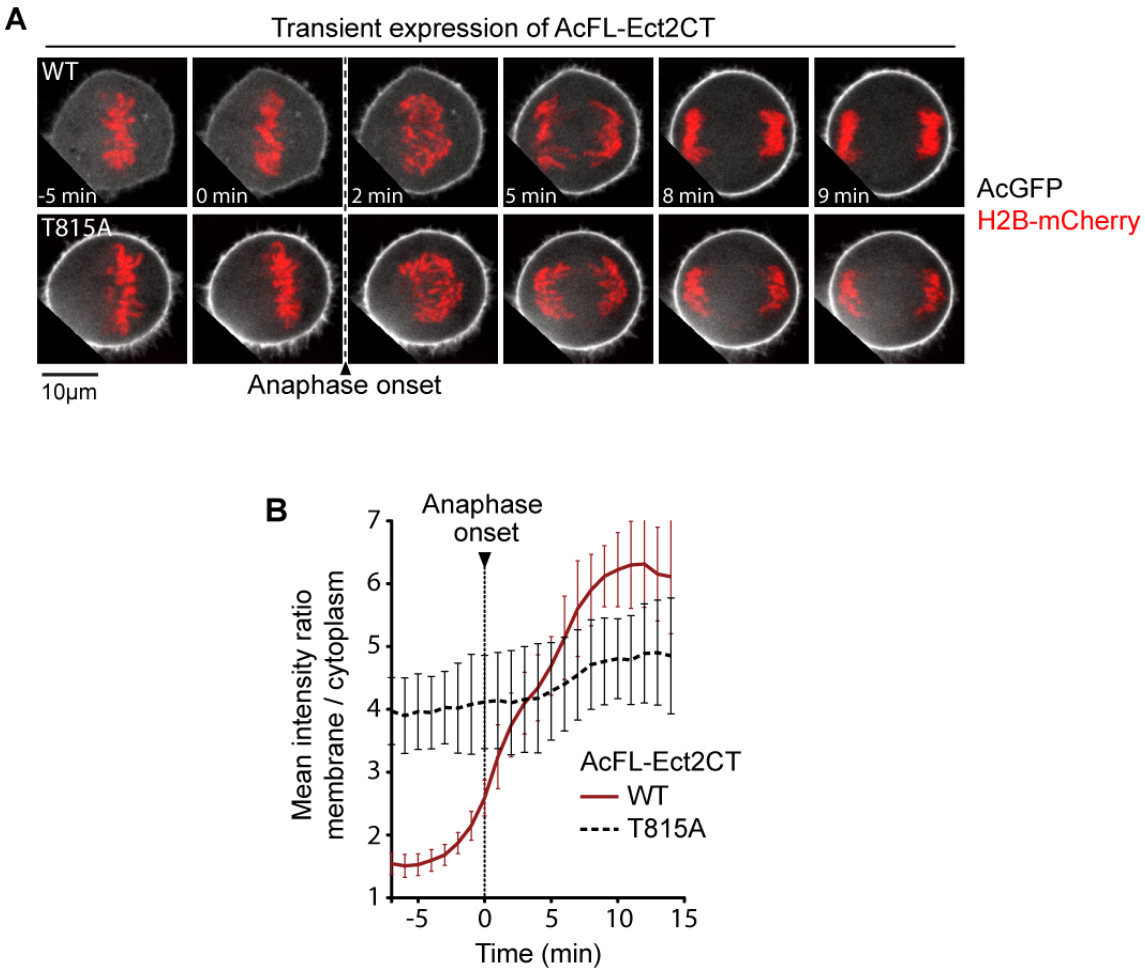

Figure 33 Anaphase-specific membrane translocation of Ect2CT

A Confocal live-cell imaging of HeLa 'Kyoto' cells expressing H2B-mCherry (red) transiently transfected with AcFL-Ect2CT-WT (Figure 14) or AcFL-Ect2CT-T815A. Time point t = 0 min was set to the metaphase-to-anaphase transition and is indicated by the dashed line.

B Quantification of the localization of AcFL-Ect2CT. Anaphase onset is indicated by a dashed line. Quantification of the localization of AcFL-Ect2CT-WT (red line) and AcFL-Ect2CT-T815A (black dashed line) during mitosis based on time-lapse series as shown in **A**. Graph displays the ratio of mean intensity at the plasma membrane to mean intensity in the cytoplasm. Time point t = 0 min was set to the metaphase-to-anaphase transition indicated by a dashed line. Error bars represent the standard deviation of the analysis of 8 cells for each construct.

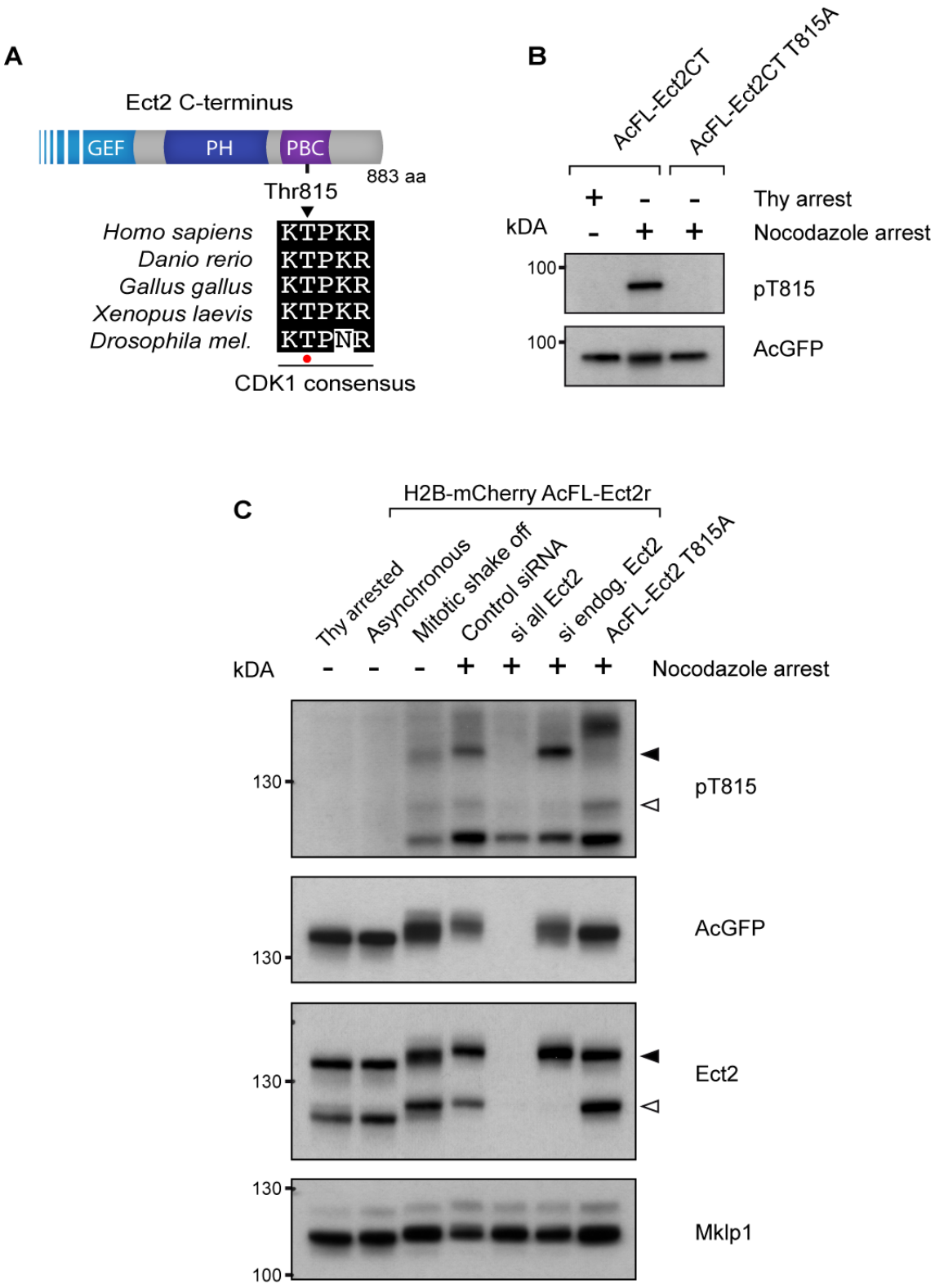

Figure 34 Ect2 T815 phosphorylation

Figure 34 Ect2 T815 phosphorylation

A Sequence alignment of the region surrounding position threonine 815 in human Ect2. Conserved residues are coloured in black. T815 is embedded within the polybasic cluster of Ect2 and is part of a highly conserved bona fide Cdk1 consensus sequence.

B Immunoblot analysis of protein extracts prepared from HeLa 'Kyoto' cells transiently expressing AcFL-Ect2CT-WT or AcFL-Ect2CT T815A. Extracts were prepared 48 hours after transfection from cells that were either arrested using thymidine or nocodazole. Extracts were probed with antibodies directed against pT815 or AcGFP.

C Immunoblot analysis of protein extracts prepared from HeLa 'Kyoto' cells stably expressing H2B-mCherry AcFLEct2r or AcFLEct2r T815A alone. Extracts were prepared from thymidine arrested, asynchronous cells or from cells isolated by mitotic shake off. siRNA treated samples were prepared from nocodazole-arrested cells 48 hours after transfection. Extracts were probed with antibodies directed against pT815 or AcGFP. Endogenous Ect2 protein and transgenic AcFL-Ect2r are indicated by open and filled arrowheads, respectively.

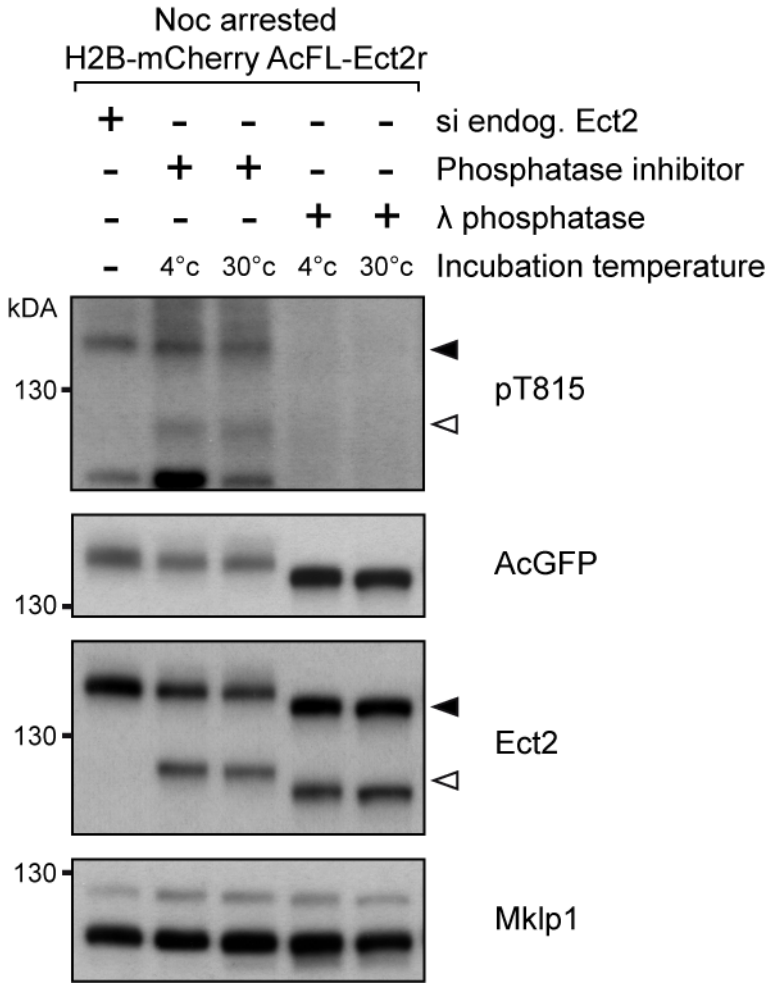

Figure 35 pT815 signal is sensitive to phosphatase treatment

Immunoblot analysis of protein extracts prepared from HeLa 'Kyoto' cells stably expressing H2B-mCherry AcFLEct2r. Extracts were prepared from nocodazole-arrested cells. Extracts were subsequently treated with or without λ phosphatase at indicated temperature for 30 minutes to control loss of phosphorylation in the absence phosphatase. siRNA treated samples were prepared from nocodazole-arrested cells 48 hours after transfection using siRNA targeting endogenous Ect2. Extracts were probed with antibodies directed against pT815, AcGFP, Ect2 and Mklp1. Endogenous Ect2 protein and transgenic AcFL-Ect2r are indicated by open and filled arrowheads, respectively.

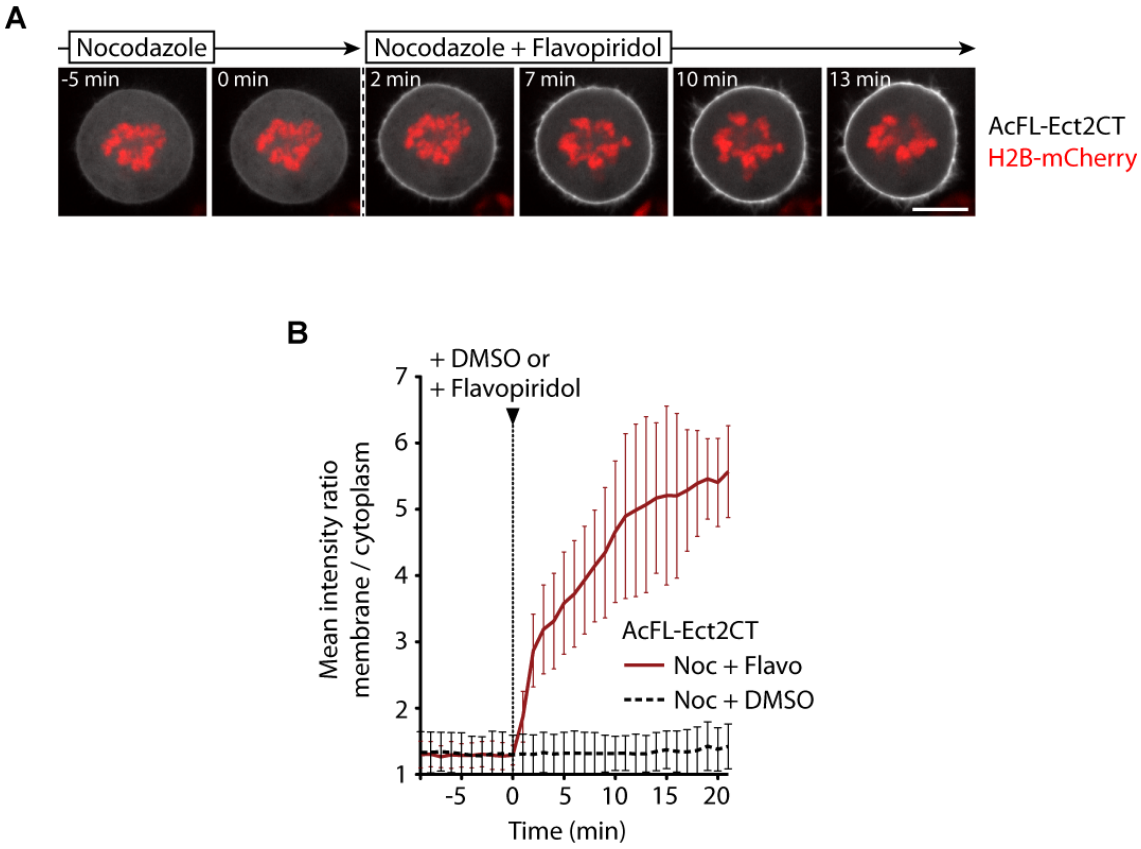

Figure 36 Cdk1 activity regulates Ect2CT localization

A Confocal live-cell imaging of transiently expressed AcFL-Ect2CT (white) in cells stably expressing H2B-mCherry (red). Cells were arrested in mitosis by addition of 165 nM nocodazole and subsequently treated with 15 µM flavopiridol. The time of flavopiridol addition was set to t = 0 min and is also indicated by a dashed line.

B Quantification of the localization of AcFL-Ect2CT in nocodazole-arrested cells treated with either solvent control dimethyl sulfoxide (DMSO) (black dashed line) or 15 µM flavopiridol (red solid line) at t = 0 min. Quantification is based on time-lapse series as shown in A. Graph displays the ratio of mean intensity at the plasma membrane to mean intensity in the cytoplasm. The time-point of DMSO and flavopiridol addition is indicated by a dashed line. Error bars represent the standard deviation of the analysis of 8 cells for each condition.

Chapter 7. Discussion

7.1 Overview

Our understanding about cytokinesis has significantly increased over the last three decades. Early studies using classical micromanipulation experiments in embryos and later studies using genetic and molecular techniques have established that the mitotic spindle plays a crucial role in the formation and positioning of the cleavage furrow in animal cells (D'Avino et al., 2005; von Dassow, 2009). My work in human cells provides new mechanistic insights into how the cytokinetic signal is delivered to the plasma membrane and, importantly, how this process is regulated in space and time. My findings suggest that the targeting of the RhoGEF Ect2 to the plasma membrane at anaphase onset is required for the activation of RhoA. This then leads to the formation of the cleavage furrow and assembly of the contractile ring (Figure 37).

Essential for this study was the establishment of the genetic complementation system that allowed me to scrutinize the mechanism of Ect2 membrane association. I generated a stable cell line expressing siRNA resistant AcGFP-tagged Ect2 with which I was able to monitor the protein localization live during cell division at levels of protein expression similar to those of their endogenous counterpart. By depleting endogenous Ect2 using siRNA, I was also able to study the functionality of the transgenic Ect2 or the mutants we generated, based on the rate of rescued cytokinesis.

It is necessary however to take into consideration that in HeLa cancer cells, the system I used in this study, Ect2 may be present at an elevated level and thus the obtained data may require further validation in other cell-systems. Neoplastic cells have been often shown to overexpress Ect2 (Hirata et al., 2009; Fields and Justilien, 2010). In fact, Ect2 promotes cell transformation when overexpressed (Miki et al., 1993). An increased level of Ect2 may ensure a robust cortical stiffness during cell division, which is of particular importance when cancer cells are

challenged by altered environment such as metastasis (Matthews and Baum, 2012). My analysis further showed that only 13% of the endogenous Ect2 level is sufficient for the execution of cytokinesis. This raises the possibility that the excess of Ect2 may fulfil a function in other cellular processes. One could conclude that mutants that were still able to rescue cytokinesis partially in our assays (e.g. Ect2-ΔTail) may have a more dramatic phenotype when expressed at a lower level in different cellular backgrounds. Similarly, the presence of an excess of Ect2 protein beyond the level required for cytokinesis would not allow us to detect subtle changes in protein activity. For instance a mutation at the conserved Ect2 RhoA interaction surface, V566A displayed non-detectable GEF activity *in vitro* was still able to rescue cytokinesis in the genetic complementation (data not shown).

The control of RhoA by Ect2 represents an integral part of current models that explain how cleavage furrow is induced and formed. By introducing specific mutations and deletions, I have provided strong evidence that the guanine nucleotide exchange activity of Ect2 is indeed essential for cytokinesis and RhoA activation. This confirms early studies in *Drosophila* that proposed but never decisively tested the idea that Ect2's GEF activity controls RhoA activation during cytokinesis (Prokopenko et al., 1999).

I have identified two essential domains that enable Ect2 to interact with the plasma membrane during cytokinesis: the PH domain and a C-terminal cluster of basic amino acids. The presence of a membrane binding cluster of polybasic amino acids is an unusual feature for DH-type GEF proteins (Rossman et al., 2005). Deletion of either of the two domains leads to increased cytokinesis failure. The deletion of the Tail region showed a more dramatic loss of Ect2 membrane signal in comparison to deletion of the PH domain.

The mutants have also allowed me to functionally separate Ect2's GEF activity from its ability to interact with the plasma membrane. Ect2 deletion mutants that lack their membrane association domains but retain their GEF activity were capable of localizing to the spindle midzone. However, in anaphase they failed to induce cleavage furrow formation. This suggests that the localization of Ect2 at the

central spindle is not sufficient for RhoA activation and the induction of cytokinetic events at the cell periphery.

My analysis has led to the finding that both, Ect2's GEF activity and the protein's ability to interact with the plasma membrane are required for RhoA activation at the membrane and the induction of the cytokinetic furrow.

The membrane association of Ect2 in anaphase is independent of the central spindle. However, my results suggest that the concentration of Ect2 at the equatorial membrane requires its interaction with centralspindlin. Thus, the spatial cue provided by the spindle midzone at anaphase might introduce the symmetry-breaking event, which targets the RhoGEF to the equatorial membrane and this may help to determine the cleavage plane of animal cells. Observations made using micromanipulation experiments also support the hypothesis that central spindle formation and centralspindlin accumulation in the midzone is crucial for the positioning and formation of the cleavage furrow (Bement et al., 2005).

MgcRacGAP localizes with Ect2 at the central spindle but does not significantly accumulate at the membrane (Lekomtsev et al., 2012). Thus, it is likely that Ect2 alone and not an Ect2-centralspindlin complex associates with the membrane. The spatial separation of a distinct membrane-associated pool of Ect2 from Ect2 that is bound to MgcRacGAP at the midzone could provide the solution to the question of how a complex containing a RhoGEF and a RhoGAP, two proteins of suggested opposing activities, can control the formation of a RhoA-dependent contractile zone (Miller and Bement, 2009).

My analysis has identified that the association of an Ect2 fragment with the plasma membrane is inhibited by phosphorylation via Cdk1 prior to anaphase onset. As Cdk1 inactivation occurs at the metaphase-to-anaphase transition (reviewed in (Pines, 2011; Wurzenberger and Gerlich, 2011)), this inhibitory mechanism could temporally coordinate chromosome segregation and cytokinesis by blocking Ect2's membrane association (thereby RhoA activation) until anaphase onset.

Over the period of my research for this thesis, I have characterized an important step in the delivery of the cytokinetic signal to the cell membrane (Figure 37). The targeting of Ect2 to the plasma membrane and its regulation in space and time could represent conserved principles that underlie the partitioning of sister genomes and the birth of new daughter cells during cytokinesis in animal cells.

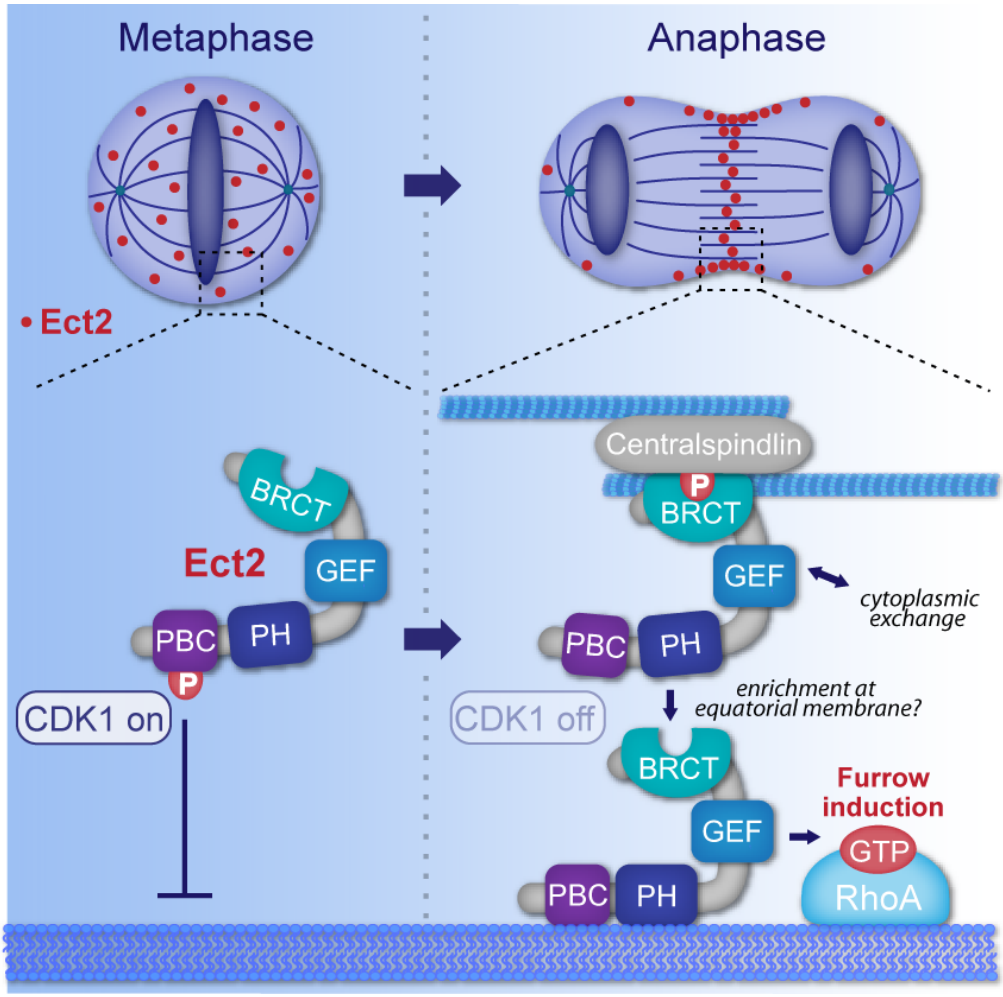

Figure 37 Model of Ect2 regulation during cytokinesis

In metaphase (left), Ect2 (red circles) is maintained in the cytoplasm through Cdk1-dependent phosphorylation of Ect2's PBC. As the cell enters anaphase (right) Ect2 binds to phosphorylated centralspindlin via its BRCT domain and accumulates at the spindle midzone with a rapid turning-over. At the same time Cdk1 activity declines and PBC becomes de-phosphorylated. This allows Ect2 to engage with the plasma membrane by virtue of the interaction of its PH domain and PBC with membrane lipids. At the plasma membrane Ect2's guanine nucleotide exchange factor (GEF) domain activates RhoA and induces the formation of a cleavage furrow. Midzone accumulation of Ect2 is not required for the protein's ability to bind to the plasma membrane but may help to concentrate Ect2 in the equatorial region at the cell periphery.

7.2 Ect2 membrane gradient

Before anaphase, Ect2 localises to the cytoplasm and does not display a particular accumulation at any cellular structure. As the cell initiates anaphase and the central spindle forms, Ect2 can first be detected at the central spindle. 4 to 6 minutes after onset of the sister chromatid segregation, a population of Ect2 can be detected at the plasma membrane with progressive enrichment at the equatorial zone. Our *in vivo* analysis revealed that the formation of an Ect2 gradient at the equatorial membrane requires the membrane binding domains of the protein and the interaction with the Ect2's midzone anchor centralspindlin via its BRCT domains. However, whether the membrane gradient is essential for cytokinesis as such and its influence on the pattern of active RhoA requires further validation (see later section for further discussion).

Various hypotheses could explain how Ect2 forms an equatorial gradient at the plasma membrane:

The rapid exchange of spindle-midzone associated Ect2 with the protein's cytoplasmic pool could create an increased concentration around the spindle midzone. This, combined with the ability of Ect2 to specifically associate with the plasma membrane at later anaphase, could lead to the concentration of Ect2 at the equatorial membrane close to the spindle midzone (Figure 38). Consistent with this model, my fluorescence recovery after photo-bleaching experiments showed that, while centralspindlin is a very stable component at the spindle midzone, Ect2 binds to MgcRacGAP in a transient fashion and is exchanged with a cytoplasmic pool very rapidly. This observation suggests that a possible model where Ect2 is first bound to centralspindlin and then released in a directional movement towards the equatorial membrane is unlikely to be relevant. We have shown that disruption of the Ect2 central spindle interaction via depletion of centralspindlin or prevention of MgcRacGAP phosphorylation by Plk1 lead to loss of the equatorial concentration of Ect2 at the plasma membrane along with cytokinesis failure. Preliminary studies of an Ect2 BRCT domain mutant (T152A K194E) that has lost the ability to bind to phosphor-MgcRacGA, however only showed a delay in Ect2 membrane association and a less steep equatorial gradient with an increased Ect2 signal at

the polar membrane. Interestingly, this mutant retained the capacity to mediate cytokinesis (data not shown). These suggest that it is very likely that additional mechanisms may be involved in enrichment of Ect2 at the equatorial membrane region and that polar inhibition of contractility at the level of RhoA activation or myosin accumulation maybe play a more important role in small human somatic cells as previously assumed

A second mechanism that could explain the enrichment of Ect2 at the membrane could be based on the interaction between centralspindlin component MgcRacGAP and the contractile ring via anillin. This interaction has been observed in *Drosophila* and could help to recruit cortical microtubules to the equatorial membrane (Gregory et al., 2008; D'Avino et al., 2008). Similarly, central spindle-associated MgcRacGAP also has been shown to be able to bind to the membrane directly and could therefore also contribute to Ect2 enrichment in a similar fashion (Lekomtsev et al., 2012).

Recent work has shown that Ect2 can interact with anillin directly via its PH domain (Frenette et al., 2012). Anillin's interaction with Ect2 may be enhanced in the GEF4A mutation and could explain the prolonged retention of the Ect2-GEF4A at the membrane forming foci along with anillin persisting into interphase (Figure 27 and data not shown). The interaction of Ect2 with components of the contractile ring could generally enhance its enrichment at the equatorial membrane.

Contraction of the cytokinetic furrow leads to the compression of the central spindle and therefore to a local increase of the centralspindlin and Ect2 in the equatorial plane. This could provide a positive feedback mechanism leading to increased enrichment of Ect2 at the equatorial membrane and hence further RhoA activation and stimulation of contractility.

Apart from promoting Ect2 accumulation to equatorial region, exclusion from membrane of the poles could also contribute to a polarised localization pattern of Ect2. In *C. elegans* embryos, Ect2 is localized uniformly to the cortex and is actively excluded from the posterior side as cell polarization occurs. Disruption of centrosome function by depletion of SPD-5 (required for centrosome maturation

and spindle assembly) leads to the loss posterior Ect2 exclusion (Motegi and Sugimoto, 2006).

During this study I have identified an anaphase specific localisation pattern of Ect2 forming a concentration gradient at the membrane with a highest accumulation at the equator and decreasing levels towards the cellular poles in mammalian cells. I propose this may be the earliest isotropy-breaking event at the membrane during induction of cytokinesis. Further investigation is required to dissect how various mechanisms may contribute to the induction of an Ect2 gradient at the membrane. This will help us to understand the general principles of isotropy or symmetry breaking as a fundamental process of biology.

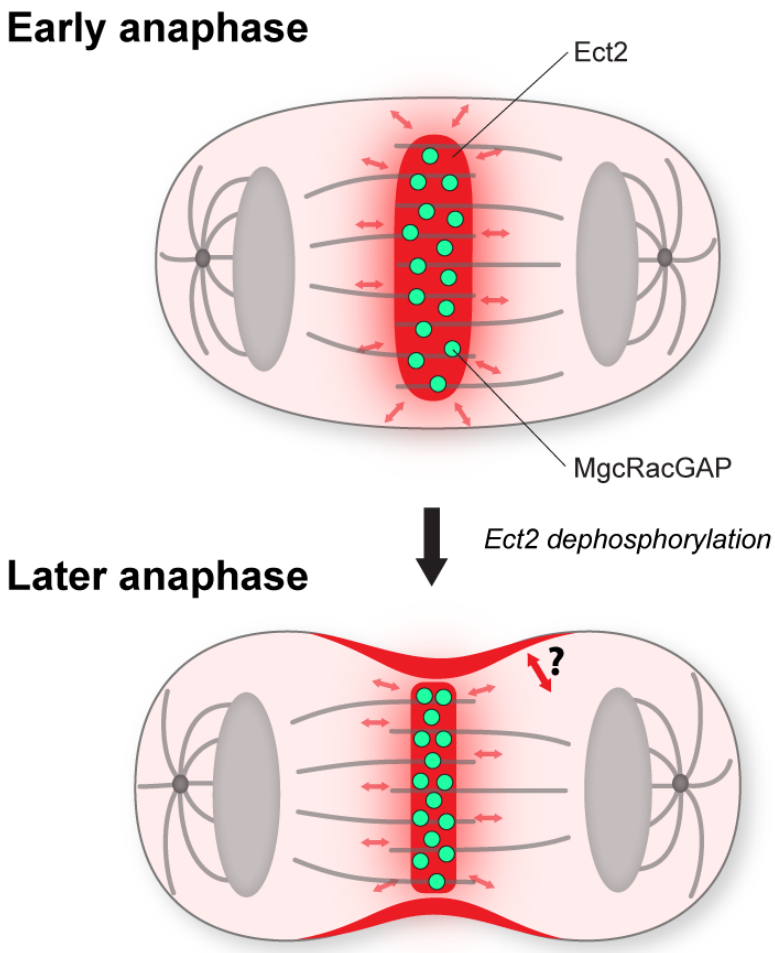

Figure 38 Model for MgcRacGAP interaction based Ect2 membrane gradient formation

Figure 38 Model for MgcRacGAP interaction based Ect2 membrane gradient formation

At the onset of anaphase (upper image), cytoplasmic Ect2 (red) accumulates to the newly assembled central spindle by binding to MgcRacGAP (green). A rapid exchange between central spindle-bound and cytoplasmic Ect2 could lead to an increased Ect2 concentration at the proximity of the central spindle.
In later anaphase upon loss of CDK1 phosphorylation events (lower image) Ect2 gains the ability to bind to the membrane. This could initiate cytokinetic ring assembly through the higher concentration at the equator reflecting the Ect2 gradient induced by the central spindle. As furrow ingression compacts the central spindle, the concentration of Ect2 at the equatorial membrane is further increased potentially leading to more RhoA activation and contractility. The exchange rate between membrane bound and cytoplasmic Ect2 and its significance at the gradient formation requires further investigation by dynamic measurements.

7.3 Ect2 localization in echinoderm embryos

Micromanipulation experiments that alter cell geometry and spindle position in dividing cells would be useful to test whether the position of the spindle midzone contributes to the formation of an equatorial Ect2 gradient. A model system that is large enough to allow micromanipulation are echinoderm embryos where many of the classical cytokinetic studies were carried out (Rappaport, 1996; Miller and Bement, 2009). Additionally, echinoderms could be used as a model system to address whether and how Ect2 travels from the spindle midzone to the cell periphery in conditions where the spindle midzone is separated from the cell cortex by several micrometres. In order to address the above-mentioned questions we initiated a collaboration with William Bement and George von Dassow.

The studies of Ect2 in the echinoderm systems *S. purpuratus*, *D. excentricus, P. miniata described below* were carried out after the first submission of this thesis. I will briefly summarise the observations we have made.

In all echinoderm embryos analysed, Ect2 accumulated at the central spindle during early anaphase. This was followed by the extension of the detectable signal over the plus ends of equatorial astral microtubules towards the equatorial cell cortex. A uniform membrane association of Ect2 accompanied this, when Ect2 was expressed at high level. A moderate expression level Ect2 did not accumulate reproducibly at the furrow. A gradient of Ec2 at the membrane could not be reliably visualized during early divisions (<12h post fertilisation). However in smaller cells (<20µm) ~24h post fertilization, Ect2 formed an equatorial gradient reminiscent of the pattern observed in HeLa cells. This suggests that an equatorial membrane gradient of Ect2 may not be present in early embryonic division but may only occur in smaller embryonic cells.

Overexpression of Ect2 in echinoderm embryos caused cortical hyperactivity in anaphase and the broadening of the zone of active RhoA. Conversely, a mutant of Ect2 that had lost GEF activity (559PVQR562AAAA) had a dominant negative effect and was able to suppress RhoA activity and inhibit cytokinesis completely.

To study furrow induction in the absence of a central spindle, we performed the Rappaport experiment by inserting a glass probe into the centre of a cell and following subsequent divisions. We observed that Ect2 accumulates at the Rappaport furrow where only the astral microtubules from the two centrosomes overlap. This suggests that Ect2 may be involved in cytokinetic constriction induced by astral microtubules alone. The overlapping astral microtubule arrays in Rappaport divisions may also be closely related to the Ect2-positive equatorial astral microtubules observed in normal divisions.

To study the mechanism of how Ect2 could localize to astral microtubules, we tracked GFP-labelled MgcRacGAP, which normally recruits Ect2 to the central spindle. From early anaphase onwards, a pool of MgcRacGAP accumulated at the central spindle. As anaphase progressed however, the spindle apparatus associated fraction of the protein began to migrate towards the plus ends of astral microtubules leading to its enrichment towards the tips of equatorial astral microtubules. This also occurred between spindles in the absence of a classical central spindle in the Rappaport torus experiment. A recent study using fixed

echinoderm embryos showed that MKLP1, the kinesin subunit partner of MgcRacGAP in centralspindlin, localizes to astral microtubules confirming our observations for MgcRacGAP (Argiros et al., 2012).

The fact that MgcRacGAP has been known to direct the localization of Ect2 to the spindle midzone, coupled with centralspindlin's localization described above strongly suggests that centralspindlin could also be responsible for Ect2's localization beyond the central spindle to stretches of equatorial astral microtubules to the cortex in echinoderm blastomeres (Figure 39). This is in accordance with the observation that deletion of the BRCT repeats, the MgcRacGAP interacting domain of Ect2, causes a nonspecific and global cortical RhoA activation in anaphase followed by cytokinesis failure.

Our observations suggest that, like in mammalian cells, Ect2 is important for cytokinesis in echinoderms by regulating RhoA activity. Our study of the localization pattern of the cytokinetic proteins Ect2 and MgcRacGAP leads to novel insights into how the division plane is specified in large embryonic cells, which rely predominantly on astral microtubules to focus and possibly relay the positive cytokinetic signal from the central spindle across a relatively long distance to the cell cortex. Our results also suggest a mechanism that might help create an equatorial cytokinetic signal in the absence of a central spindle.

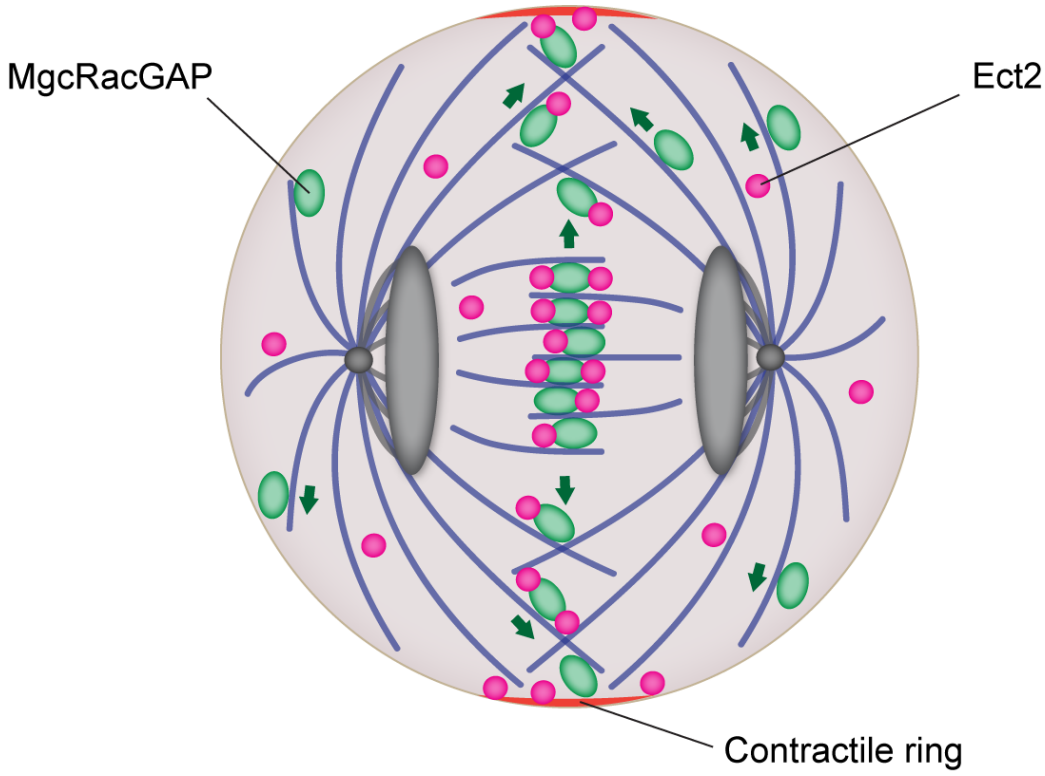

Figure 39 Model for Ect2 distribution in echinoderm blastomeres

In anaphase the majority of MgcRacGAP (green) accumulates to the region of the antiparallel overlapping microtubules as the central spindle assembles. MgcRacGAP serves a binding platform for Ect2. As anaphase progresses the remaining pool of microtubule associated MgcRacGAP migrates towards the plus ends of microtubules and accumulates especially at the ends of equatorial astral microtubules bridging the space between central spindle and the equator membrane. Ect2 colocalises with MgcRacGAP and could then induce the formation of the contractile ring at the membrane.

7.4 Future perspectives and open questions

During my dissertation, I have gained novel insights into the functions of various domains of Ect2. I could show that Ect2 associates with the plasma membrane through the combined action of the protein's PH domain and PBC. The description and functional analysis of this membrane-associated pool of Ect2 and the protein's equatorial gradient is possibly the most striking addition to the well-established localization of Ect2 to the central spindle. Deletion of either of the two membrane association domains leads to a reduction or loss of Ect2 membrane localization. The deletion of the PBC along with the remaining residues (ΔTail) leads to a complete loss of detectable Ect2 at the membrane. In contrast, Ect2 alleles lacking the PH domain (ΔPH) display only a reduced membrane targeting when expressed transiently as Ect2CT fragments (Figure 16) or as a stably expressed full-length protein (Figure 27 and data not shown). My analysis of the functionality of the deletions in full length however revealed that ΔPH was less potent to rescue cytokinesis compared to ΔTail (Figure 24 and 28). An explanation for this discrepancy could be a proposed role for the PH domain in recruitment of anillin (Frenette et al., 2012). Further studies including generation of point mutations affecting only membrane targeting of the PH domain alone are required in order to fully separate the PH domain's role in membrane binding from other additional functions. Rescuing cytokinesis by replacing Ect2 membrane targeting domains with alternative inducible membrane targeting motifs (e.g. phorbol ester inducible C1B domain (Colón-González and Kazanietz, 2006; Lekomtsev et al., 2012) or a light inducible system (Levskaya et al., 2009)) could finally demonstrate that the primary function of the C-terminal region of Ect2 is plasma membrane binding. An Ect2 fusion protein with an inducible membrane binding capacity would additionally allow one to test whether Ect2 membrane targeting is a rate-limiting step that determines the position and formation of the cleavage furrow.

In this study I have presented data that strongly suggest that Ect2's capacity to bind to the plasma membrane is essential for its function in cytokinesis. However, the importance of the formation of an Ect2 concentration gradient at the equator as such requires further investigation. Studies of live GFP-Ect2 localization in various organisms and different cell types lead to different observations. In *C. elegans* 1-

cell embryos, Ect2 initially accumulates uniformly at the cell periphery and is then only displaced from the posterior of the cell. Also sites of cortical contractions do not show a significant local enrichment of Ect2 at membrane in *C. elegans* zyotes (Motegi and Sugimoto, 2006). In *Xenopus* oocytes, Ect2 has been shown to accumulate at the central spindle but not to the membrane during polar body extrusion. Our studies in echinoderm embryos also suggest that during early embryonic divisions, Ect2 may not form a visible gradient at the membrane. One would have to take into consideration however that apart from our analysis of Ect2 localization studies in HeLa cells, all above-mentioned observations were made in systems where Ect2 is overexpressed in the presence of the endogenous protein. Although an explicit Ect2 gradient formation may be less important in large cells and during meiotic division, it may be significant for smaller somatic cells including HeLa cells and echinoderm gastrula cells. Exploring how such a gradient may determine the region of RhoA activation and also the width cytokinetic ring would be essential to understand the regulation of the cytokinetic contraction. For instance, would a broadening of the Ect2 zone at the equator lead to also a broader furrow and how may the absolute Ect2 concentration influence this? Understanding the principles how the Ect2 localisation pattern at the membrane is set up would allow us to modify the system to address these questions. In order to experimentally test my hypotheses and to determine how an Ect2 gradient is formed at the equatorial membrane, one would require tracking of a specific pool of Ect2 during various stages of cytokinesis. This can be achieved by studying the dynamics Ect2 protein by photoactivation. These approaches combined with pharmacological and genetic perturbation methods will be required to test how Ect2's distribution at the plasma membrane is controlled.

Experiments using different model systems have established that the lipid phosphatidylinositol 4,5-bisphosphate localizes to the cleavage furrow (Emoto et al., 2005; Field et al., 2005). Furthermore, the presence and availability of $PI(4,5)P_2$ has been implicated in the successful completion of cytokinesis. Interestingly, our *in vitro* studies suggested that the membrane association domains of Ect2 directly interact with phosphoinositide lipids. These findings raise the exciting possibility that the binding of Ect2 to $PI(4,5)P_2$ to the inner leaflet of the plasma membrane could potentially contribute to the concentration of Ect2 at the equatorial membrane

during cytokinesis. More sophisticated and specific *in vitro* approaches (e.g. lipid vesicle interaction assays) are required to confirm the specificity of Ect2 lipid binding. Following this, pharmacological, chemical and genetic manipulations of candidate lipids could be applied to alter membrane composition *in vivo*. A possible outcome could be a change in Ect2's ability to bind to the membrane or a change in the protein's distribution at the cell periphery, which may have consequences for the formation of a cleavage furrow and the execution of cytokinesis.

The role of central spindle in Ect2 regulation and furrow induction is complex and requires further investigation. I have presented data suggesting that the Ect2-central spindle interaction is required for Ect2 gradient formation by depleting centralspindlin or preventing MgcRacGAP phosphorylation by Plk1 (Figure 30). Consistent with studies of a mutant of MgcRacGAP that cannot be phosphorylated in the Ect2 binding site (Wolfe et al., 2009) and the requirement of Plk1 for cleavage furrow formation, this suggests that Ect2's interaction with centralspindlin and the spindle midzone may be essential for cytokinesis. Under certain conditions where a central spindle is absent, cells are still able to induce furrowing. Cells with monopolar spindles do not possess any apparent special cue from the spindle. Yet those cells are able to bundle microtubules at one end of the cell and induce one ectopic furrow when forced to exit mitosis (Canman et al., 2003; Hu et al., 2008). Ect2 is required for this process and also accumulates at those monopolar furrows along with other proteins of the central spindle (Hu et al., 2011). Ect2 may be recruited to these furrows like in bipolar division by binding to MgcRacGAP. Live-cell protein analysis of tagged proteins would be required to understand the sequence of the protein recruitment during monopolar spindle-driven cytokinetic furrowing. Additionally, the use of a GEF-inactive mutant of Ect2 could answer whether the furrow contraction is actively feeding back to stabilize the monopolar "midzone".

The Ect2 BRCT domain mutant (T152A K194E) protein, which does not accumulate detectably at the spindle midzone, also adds another level of complexity to understanding of the role of Ect2's binding to centralspindlin and the midzone. Despite the fact that in Ect2 BRCT-mutant cells, the membrane recruitment is delayed and displays only a shallow equatorial Ect2 gradient at the

membrane, it appears to be able to rescue cytokinesis (data now shown). More detailed analysis is required to characterize the cytokinetic dynamics in this condition. Activation, timing and the pattern of the recruitment of downstream factors such as RhoA or anillin may be affected in a subtle way that does not impair the successful completion of cell division. It is possible that the inhibitory signal originating from polar astral microtubules rescues cytokinesis in this absence of Ect2's interaction with the central spindle. Disruption of astral microtubules in presence of the BRCT domain mutant Ect2 allele would allow us to address this possibility in the first instance.

Further studies are also required regarding the regulation of full-length Ect2 by Cdk1 *in vivo*. Mutation of the Ect2 Cdk1 site T815A in Ect2CT fragment causes premature membrane association before anaphase (Figure 33) as does full length Ect2 however; this mutant does not show an apparent change in timing of localization and is fully able to rescue cytokinesis (data not shown). The presence of a large number of confirmed mitotic phosphorylation sites may confer robustness and possibly redundancy to this control system.

Inhibitory Ect2 phosphorylation is also likely to cooperate with the well-established inhibition of MT-based cytokinetic events by Cdk1 phosphorylation (reviewed in Glotzer, 2009). Lastly, further work is required to understand how Ect2's functions in cell rounding (Matthews et al., 2012) during early mitosis and during cytokinesis may be differentially controlled by Cdk1.

This thesis has presented novel insights into the temporal and special regulation of Ect2 during the initiation of cytokinesis. Key aspects of Ect2 function during cell division appear fundamentally conserved but subtle differences and adaptations appear to have evolved in order for the different cellular systems to cope with the different parameters such as cell size and requirements such as cell polarity. Future studies of how Ect2 activity and localization is finely regulated will complete our understanding of the signalling processes that initiate cytokinesis in animal cells.

Reference List

Adams, R. R., Wheatley, S. P., Gouldsworthy, A. M., Kandels-Lewis, S. E., Carmena, M., Smythe, C., Gerloff, D. L., and Earnshaw, W. C. (2000). INCENP binds the Aurora-related kinase AIRK2 and is required to target it to chromosomes, the central spindle and cleavage furrow. Current biology *10*, 1075–1078.

Agostinis, P., Derua, R., Sarno, S., Goris, J., and Merlevede, W. (1992). Specificity of the polycation-stimulated (type-2A) and ATP,Mg-dependent (type-1) protein phosphatases toward substrates phosphorylated by P34cdc2 kinase. European journal of biochemistry *205*, 241–248.

Alberts, a S. (2001). Identification of a carboxyl-terminal diaphanous-related formin homology protein autoregulatory domain. Journal of biological chemistry *276*, 2824–2830.

Alsop, G. B., and Zhang, D. (2003). Microtubules are the only structural constituent of the spindle apparatus required for induction of cell cleavage. Journal of cell biology *162*, 383–390.

Alsop, G. B., and Zhang, D. (2004). Microtubules continuously dictate distribution of actin filaments and positioning of cell cleavage in grasshopper spermatocytes. Journal of cell science *117*, 1591–1602.

Amano, M., Ito, M., Kimura, K., Fukata, Y., Chihara, K., Nakano, T., Matsuura, Y., and Kaibuchi, K. (1996). Phosphorylation and activation of myosin by Rho-associated kinase (Rho-kinase). Journal of biological chemistry *271*, 20246–20249.

Argiros, H., Henson, L., Holguin, C., Foe, V., and Shuster, C. B. (2012). Centralspindlin and chromosomal passenger complex behavior during normal and Rappaport furrow specification in echinoderm embryos. Cytoskeleton *69*, 840–853.

Atilla-Gokcumen, G. E., Castoreno, A. B., Sasse, S., and Eggert, U. S. (2010). Making the cut: the chemical biology of cytokinesis. ACS chemical biology *5*, 79–90.

Axton, J. M., Dombrádi, V., Cohen, P. T., and Glover, D. M. (1990). One of the protein phosphatase 1 isoenzymes in Drosophila is essential for mitosis. Cell *63*, 33–46.

Barr, A. R., and Gergely, F. (2007). Aurora-A: the maker and breaker of spindle poles. Journal of cell science *120*, 2987–2996.

Barr, F. A., and Gruneberg, U. (2007). Cytokinesis: placing and making the final cut. Cell *131*, 847–860.

Bastos, R. N., and Barr, F. a (2010). Plk1 negatively regulates Cep55 recruitment to the midbody to ensure orderly abscission. Journal of cell biology *191*, 751–760.

Bastos, R. N., Penate, X., Bates, M., Hammond, D., and Barr, F. a. (2012). CYK4 inhibits Rac1-dependent PAK1 and ARHGEF7 effector pathways during cytokinesis. Journal of cell biology *198*, 865–880.

Baumeister, M. A., Rossman, K. L., Sondek, J., and Lemmon, M. A. (2006). The Dbs PH domain contributes independently to membrane targeting and regulation of guanine nucleotide-exchange activity. Biochemical journal *400*, 563–572.

Bement, W. M., Benink, H. A., and Von Dassow, G. (2005). A microtubule-dependent zone of active RhoA during cleavage plane specification. Journal of cell biology *170*, 91–101.

Bement, W. M., Miller, A. L., and Von Dassow, G. (2006). Rho GTPase activity zones and transient contractile arrays. BioEssays *28*, 983–993.

Bieling, P., Telley, I. a, and Surrey, T. (2010). A minimal midzone protein module controls formation and length of antiparallel microtubule overlaps. Cell *142*, 420–432.

Birkenfeld, J., Nalbant, P., Bohl, B. P., Pertz, O., Hahn, K. M., and Bokoch, G. M. (2007). GEF-H1 modulates localized RhoA activation during cytokinesis under the control of mitotic kinases. Developmental cell *12*, 699–712.

Biron, D., Alvarez-Lacalle, E., Tlusty, T., and Moses, E. (2005). Molecular model of the contractile ring. Physical review letters *95*, 098102.

Bos, J. L., Rehmann, H., and Wittinghofer, A. (2007). GEFs and GAPs: critical elements in the control of small G proteins. Cell *129*, 865–877.

Brennan, I. M., Peters, U., Kapoor, T. M., and Straight, A. F. (2007). Polo-like kinase controls vertebrate spindle elongation and cytokinesis. PLoS one *2*, e409.

Bringmann, H., Cowan, C. R. C., Kong, J., and Hyman, A. A. A. A. (2007). LET-99, GOA-1/GPA-16, and GPR-1/2 are required for aster-positioned cytokinesis. Current biology *17*, 185–191.

Bringmann, H., and Hyman, A. a (2005). A cytokinesis furrow is positioned by two consecutive signals. Nature *436*, 731–734.

Burkard, M. E., Maciejowski, J., Rodriguez-Bravo, V., Repka, M., Lowery, D. M., Clauser, K. R., Zhang, C., Shokat, K. M., Carr, S. A., Yaffe, M. B., et al. (2009). Plk1 self-organization and priming phosphorylation of HsCYK-4 at the spindle midzone regulate the onset of division in human cells. PLoS biology *7*, e1000111.

Burkard, M. E., Randall, C. L., Larochelle, S., Zhang, C., Shokat, K. M., Fisher, R. P., and Jallepalli, P. V (2007). Chemical genetics reveals the requirement for Polo-like kinase 1 activity in positioning RhoA and triggering cytokinesis in human cells. Proceedings of the National Academy of Sciences of the United States of America *104*, 4383–4388.

Canman, J. C., Lewellyn, L., Laband, K., Smerdon, S. J., Desai, A., Bowerman, B., and Oegema, K. (2008). Inhibition of Rac by the GAP activity of centralspindlin is essential for cytokinesis. Science *322*, 1543–1546.

Canman, J., Cameron, L., and Maddox, P. (2003). Determining the position of the cell division plane. Nature *424*, 1074–1078.

Carlsson, A. E. (2006). Contractile stress generation by actomyosin gels. Physical review. E, Statistical, nonlinear, and soft matter physics *74*, 051912.

Carlton, J. G., Caballe, A., Agromayor, M., Kloc, M., and Martin-Serrano, J. (2012). ESCRT-III governs the Aurora B-mediated abscission checkpoint through CHMP4C. Science *336*, 220–225.

Carlton, J. G., and Martin-Serrano, J. (2007). Parallels between cytokinesis and retroviral budding: a role for the ESCRT machinery. Science *316*, 1908–1912.

Castrillon, D. H., and Wasserman, S. A. (1994). Diaphanous is required for cytokinesis in Drosophila and shares domains of similarity with the products of the limb deformity gene. Development *120*, 3367–3377.

Celton-Morizur, S., Merlen, G., Couton, D., Margall-Ducos, G., and Desdouets, C. (2009). The insulin/Akt pathway controls a specific cell division program that leads to generation of binucleated tetraploid liver cells in rodents. Journal of clinical investigation *119*, 1880–1887.

Chalamalasetty, R. B., Hümmer, S., Nigg, E. A., and Silljé, H. H. W. (2006). Influence of human Ect2 depletion and overexpression on cleavage furrow formation and abscission. Journal of cell science *119*, 3008–3019.

Cheeseman, I. M., Anderson, S., Jwa, M., Green, E. M., Kang, J. seog, Yates, J. R., Chan, C. S. M., Drubin, D. G., and Barnes, G. (2002). Phospho-regulation of kinetochore-microtubule attachments by the Aurora kinase Ipl1p. Cell *111*, 163–172.

Cheeseman, I. M., and Desai, A. (2008). Molecular architecture of the kinetochore-microtubule interface. Nature reviews molecular cell biology *9*, 33–46.

Chen, C.-T., Hehnly, H., and Doxsey, S. J. (2012). Orchestrating vesicle transport, ESCRTs and kinase surveillance during abscission. Nature reviews molecular cell biology *13*, 483–488.

Ciosk, R., Zachariae, W., Michaelis, C., Shevchenko, A., Mann, M., and Nasmyth, K. (1998). An ESP1/PDS1 complex regulates loss of sister chromatid cohesion at the metaphase to anaphase transition in yeast. Cell *93*, 1067–1076.

Clute, P., and Pines, J. (1999). Temporal and spatial control of cyclin B1 destruction in metaphase. Nature cell biology *1*, 82–87.

Cohen-Fix, O., Peters, J. M., Kirschner, M. W., and Koshland, D. (1996). Anaphase initiation in Saccharomyces cerevisiae is controlled by the APC-dependent degradation of the anaphase inhibitor Pds1p. Genes & development *10*, 3081–3093.

Collette, K. S., Petty, E. L., Golenberg, N., Bembenek, J. N., and Csankovszki, G. (2011). Different roles for Aurora B in condensin targeting during mitosis and meiosis. Journal of cell science *124*, 3684–3694.

Colón-González, F., and Kazanietz, M. G. (2006). C1 domains exposed: from diacylglycerol binding to protein-protein interactions. Biochimica et biophysica acta *1761*, 827–837.

Connell, J. W., Lindon, C., Luzio, J. P., and Reid, E. (2009). Spastin couples microtubule severing to membrane traffic in completion of cytokinesis and secretion. Traffic *10*, 42–56.

Cook, D. R., Solski, P. a, Bultman, S. J., Kauselmann, G., Schoor, M., Kuehn, R., Friedman, L. S., Cowley, D. O., Van Dyke, T., Yeh, J. J., et al. (2011). The ect2 rho Guanine nucleotide exchange factor is essential for early mouse development and normal cell cytokinesis and migration. Genes & cancer *2*, 932–942.

Coudreuse, D., and Nurse, P. (2010). Driving the cell cycle with a minimal CDK control network. Nature *468*, 1074–1079.

Cronin, T. C., DiNitto, J. P., Czech, M. P., and Lambright, D. G. (2004). Structural determinants of phosphoinositide selectivity in splice variants of Grp1 family PH domains. EMBO journal *23*, 3711–3720.

Di Cunto, F., Imarisio, S., Hirsch, E., Broccoli, V., Bulfone, A., Migheli, A., Atzori, C., Turco, E., Triolo, R., Dotto, G. P., et al. (2000). Defective neurogenesis in citron kinase knockout mice by altered cytokinesis and massive apoptosis. Neuron *28*, 115–127.

Dambournet, D., Machicoane, M., Chesneau, L., Sachse, M., Rocancourt, M., El Marjou, A., Formstecher, E., Salomon, R., Goud, B., and Echard, A. (2011). Rab35 GTPase and OCRL phosphatase remodel lipids and F-actin for successful cytokinesis. Nature cell biology *13*, 981–988.

Von Dassow, G. (2009). Concurrent cues for cytokinetic furrow induction in animal cells. Trends in cell biology *19*, 165–173.

Von Dassow, G., Verbrugghe, K. J. C., Miller, A. L., Sider, J. R., and Bement, W. M. (2009). Action at a distance during cytokinesis. Journal of cell biology *187*, 831–845.

Dechant, R., and Glotzer, M. (2003). Centrosome separation and central spindle assembly act in redundant pathways that regulate microtubule density and trigger cleavage furrow formation. Developmental cell *4*, 333–344.

Dephoure, N., Zhou, C., Villén, J., Beausoleil, S. a, Bakalarski, C. E., Elledge, S. J., and Gygi, S. P. (2008). A quantitative atlas of mitotic phosphorylation. Proceedings of the National Academy of Sciences of the United States of America *105*, 10762–10767.

Douglas, M. E., Davies, T., Joseph, N., and Mishima, M. (2010). Aurora B and 14-3-3 coordinately regulate clustering of centralspindlin during cytokinesis. Current biology *20*, 927–933.

Drechsel, D. N., Hyman, A. A., Hall, A., and Glotzer, M. (1997). A requirement for Rho and Cdc42 during cytokinesis in Xenopus embryos. Current biology *7*, 12–23.

D'Avino, P. P., Savoian, M. S., and Glover, D. M. (2005). Cleavage furrow formation and ingression during animal cytokinesis: a microtubule legacy. Journal of cell science *118*, 1549–1558.

D'Avino, P. P., Takeda, T., Capalbo, L., Zhang, W., Lilley, K. S., Laue, E. D., and Glover, D. M. (2008). Interaction between Anillin and RacGAP50C connects the actomyosin contractile ring with spindle microtubules at the cell division site. Journal of cell science *121*, 1151–1158.

Echard, A. (2008). Membrane traffic and polarization of lipid domains during cytokinesis. Biochemical society transactions *36*, 395–399.

Edgar, B. A., and Orr-Weaver, T. L. (2001). Endoreplication cell cycles: more for less. Cell *105*, 297–306.

Eggert, U. S., Mitchison, T. J., and Field, C. M. (2006). Animal cytokinesis: from parts list to mechanisms. Annual review of biochemistry *75*, 543–566.

Elia, A. E. H., Rellos, P., Haire, L. F., Chao, J. W., Ivins, F. J., Hoepker, K., Mohammad, D., Cantley, L. C., Smerdon, S. J., and Yaffe, M. B. (2003). The molecular basis for phosphodependent substrate targeting and regulation of Plks by the Polo-box domain. Cell *115*, 83–95.

Elia, N., Sougrat, R., Spurlin, T. A., Hurley, J. H., and Lippincott-Schwartz, J. (2011). Dynamics of endosomal sorting complex required for transport (ESCRT) machinery during

cytokinesis and its role in abscission. Proceedings of the National Academy of Sciences of the United States of America *108*, 4846–4851.

Den Elzen, N., and Pines, J. (2001). Cyclin A is destroyed in prometaphase and can delay chromosome alignment and anaphase. Journal of cell biology *153*, 121–136.

Emoto, K., Inadome, H., Kanaho, Y., Narumiya, S., and Umeda, M. (2005). Local change in phospholipid composition at the cleavage furrow is essential for completion of cytokinesis. Journal of biological chemistry *280*, 37901–37907.

Emoto, K., Kobayashi, T., Yamaji, A., Aizawa, H., Yahara, I., Inoue, K., and Umeda, M. (1996). Redistribution of phosphatidylethanolamine at the cleavage furrow of dividing cells during cytokinesis. Proceedings of the National Academy of Sciences of the United States of America *93*, 12867–12872.

Emoto, K., and Umeda, M. (2000). An essential role for a membrane lipid in cytokinesis. Regulation of contractile ring disassembly by redistribution of phosphatidylethanolamine. Journal of cell biology *149*, 1215–1224.

Endicott, J. a, Nurse, P., and Johnson, L. N. (1994). Mutational analysis supports a structural model for the cell cycle protein kinase p34. Protein engineering *7*, 243–253.

Enoch, T., and Nurse, P. (1990). Mutation of fission yeast cell cycle control genes abolishes dependence of mitosis on DNA replication. Cell *60*, 665–673.

Evans, T., Rosenthal, E. T., Youngblom, J., Distel, D., and Hunt, T. (1983). Cyclin: a protein specified by maternal mRNA in sea urchin eggs that is destroyed at each cleavage division. Cell *33*, 389–396.

Eytan, E., Moshe, Y., Braunstein, I., and Hershko, A. (2006). Roles of the anaphase-promoting complex/cyclosome and of its activator Cdc20 in functional substrate binding. Proceedings of the National Academy of Sciences of the United States of America *103*, 2081–2086.

Fededa, J. P., and Gerlich, D. W. (2012). Molecular control of animal cell cytokinesis. Nature cell biology *14*, 440–447.

Ferguson, K. M., Lemmon, M. A., Schlessinger, J., and Sigler, P. B. (1995). Structure of the high affinity complex of inositol trisphosphate with a phospholipase C pleckstrin homology domain. Cell *83*, 1037–1046.

Fernández, C., Lobo Md, M. del V. T., Gómez-Coronado, D., and Lasunción, M. A. (2004). Cholesterol is essential for mitosis progression and its deficiency induces polyploid cell formation. Experimental cell research *300*, 109–120.

Ferrigno, P. (1993). Protein phosphatase 2A1 is the major enzyme in vertebrate cell extracts that dephosphorylates several physiological substrates for cyclin-dependent protein kinases. Molecular biology of the cell *4*, 669–677.

Field, S. J., Madson, N., Kerr, M. L., Galbraith, K. A. A., Kennedy, C. E., Tahiliani, M., Wilkins, A., and Cantley, L. C. (2005). PtdIns(4,5)P2 functions at the cleavage furrow during cytokinesis. Current biology *15*, 1407–1412.

Fields, A. A. P., and Justilien, V. (2010). The guanine nucleotide exchange factor (GEF) Ect2 is an oncogene in human cancer. Advances in enzyme regulation *50*, 190–200.

Flemming, W. (1882). Zellsubstanz, Kern und Zellteilung (Leipzig: Verlag von F. C. W. Vogel).

Foe, V. E., and Von Dassow, G. (2008). Stable and dynamic microtubules coordinately shape the myosin activation zone during cytokinetic furrow formation. Journal of cell biology *183*, 457–470.

Frenette, P., Haines, E., Loloyan, M., Kinal, M., Pakarian, P., and Piekny, A. (2012). An anillin-Ect2 complex stabilizes central spindle microtubules at the cortex during cytokinesis. PLoS one *7*, e34888.

Fuller, B. G., Lampson, M. A., Foley, E. A., Rosasco-Nitcher, S., Le, K. V, Tobelmann, P., Brautigan, D. L., Stukenberg, P. T., and Kapoor, T. M. (2008). Midzone activation of aurora B in anaphase produces an intracellular phosphorylation gradient. Nature *453*, 1132–1136.

Funabiki, H., Yamano, H., Kumada, K., Nagao, K., Hunt, T., and Yanagida, M. (1996). Cut2 proteolysis required for sister-chromatid seperation in fission yeast. Nature *381*, 438–441.

Ganem, N. J., Godinho, S. A., and Pellman, D. (2009). A mechanism linking extra centrosomes to chromosomal instability. Nature *460*, 278–282.

Ganem, N. J., Storchova, Z., and Pellman, D. (2007). Tetraploidy, aneuploidy and cancer. Current opinion in genetics & development *17*, 157–162.

Gao, Y., Smith, E., Ker, E., Campbell, P., Cheng, E., Zou, S., Lin, S., Wang, L., Halene, S., and Krause, D. S. (2012). Role of RhoA-specific guanine exchange factors in regulation of endomitosis in megakaryocytes. Developmental cell *22*, 573–584.

Gavet, O., and Pines, J. (2010). Progressive activation of CyclinB1-Cdk1 coordinates entry to mitosis. Developmental cell *18*, 533–543.

Geley, S., Kramer, E., Gieffers, C., Gannon, J., Peters, J. M., and Hunt, T. (2001). Anaphase-promoting complex/cyclosome-dependent proteolysis of human cyclin A starts at the beginning of mitosis and is not subject to the spindle assembly checkpoint. Journal of cell biology *153*, 137–148.

Gentric, G., Celton-Morizur, S., and Desdouets, C. (2012). Polyploidy and liver proliferation. Clinics and research in hepatology and gastroenterology *36*, 29–34.

Gharbi-Ayachi, A., Labbé, J.-C., Burgess, A., Vigneron, S., Strub, J., Brioudes, E., Van-Dorsselaer, A., Castro, A., and Lorca, T. (2010). The substrate of Greatwall kinase, Arpp19, controls mitosis by inhibiting protein phosphatase 2A. Science *330*, 1673–1677.

Glotzer, M. (2009). The 3Ms of central spindle assembly: microtubules, motors and MAPs. Nature reviews molecular cell biology *10*, 9–20.

Glover, D. M., Leibowitz, M. H., McLean, D. A., and Parry, H. (1995). Mutations in aurora prevent centrosome separation leading to the formation of monopolar spindles. Cell *81*, 95–105.

Golan, A., Yudkovsky, Y., and Hershko, A. (2002). The cyclin-ubiquitin ligase activity of cyclosome/APC is jointly activated by protein kinases Cdk1-cyclin B and Plk. Journal of biological chemistry *277*, 15552–15557.

Green, R. a, Paluch, E., and Oegema, K. (2012). Cytokinesis in Animal Cells. Annual review of cell and developmental biology, 1–30.

Gregory, S. L., Ebrahimi, S., Milverton, J., Jones, W. M., Bejsovec, A., and Saint, R. (2008). Cell division requires a direct link between microtubule-bound RacGAP and Anillin in the contractile ring. Current biology *18*, 25–29.

Guha, M., Zhou, M., and Wang, Y.-L. (2005). Cortical actin turnover during cytokinesis requires myosin II. Current biology *15*, 732–736.

Guizetti, J., and Gerlich, D. W. (2010). Cytokinetic abscission in animal cells. Seminars in cell & developmental biology *21*, 909–916.

Guizetti, J., and Gerlich, D. W. (2012). ESCRT-III polymers in membrane neck constriction. Trends in cell biology *22*, 133–140.

Guizetti, J., Schermelleh, L., Mäntler, J., Maar, S., Poser, I., Leonhardt, H., Müller-Reichert, T., and Gerlich, D. W. (2011). Cortical constriction during abscission involves helices of ESCRT-III-dependent filaments. Science *331*, 1616–1620.

Guse, A., Mishima, M., and Glotzer, M. (2005). Phosphorylation of ZEN-4/MKLP1 by aurora B regulates completion of cytokinesis. Current biology *15*, 778–786.

Güttinger, S., Laurell, E., and Kutay, U. (2009). Orchestrating nuclear envelope disassembly and reassembly during mitosis. Nature reviews molecular cell biology *10*, 178–191.

Hara, T., Abe, M., Inoue, H., Yu, L.-R., Veenstra, T. D., Kang, Y. H., Lee, K. S., and Miki, T. (2006). Cytokinesis regulator ECT2 changes its conformation through phosphorylation at Thr-341 in G2/M phase. Oncogene *25*, 566–578.

Harper, J. W., Adami, G., and Wei, N. (1993). The p21 Cdk-interacting protein Cip1 is a potent inhibitor of G1 cyclin-dependent kinases. Cell *75*, 805–816.

Harrison, J. C., and Haber, J. E. (2006). Surviving the breakup: the DNA damage checkpoint. Annual review of genetics *40*, 209–235.

Haucke, V. (2005). Phosphoinositide regulation of clathrin-mediated endocytosis. Biochemical society transactions *33*, 1285–1289.

Hauf, S., Cole, R. W., LaTerra, S., Zimmer, C., Schnapp, G., Walter, R., Heckel, A., Van Meel, J., Rieder, C. L., and Peters, J.-M. (2003). The small molecule Hesperadin reveals a role for Aurora B in correcting kinetochore-microtubule attachment and in maintaining the spindle assembly checkpoint. Journal of cell biology *161*, 281–294.

Hauf, S., Waizenegger, I. C., and Peters, J. M. (2001). Cohesin cleavage by separase required for anaphase and cytokinesis in human cells. Science *293*, 1320–1323.

He, J., Haney, R. M., Vora, M., Verkhusha, V. V, Stahelin, R. V, and Kutateladze, T. G. (2008). Molecular mechanism of membrane targeting by the GRP1 PH domain. Journal of lipid research *49*, 1807–1815.

Heo, W. Do, Inoue, T., Park, W. S., Kim, M. L., Park, B. O., Wandless, T. J., and Meyer, T. (2006). PI(3,4,5)P3 and PI(4,5)P2 lipids target proteins with polybasic clusters to the plasma membrane. Science *314*, 1458–1461.

Hime, G., and Saint, R. (1992). Zygotic expression of the pebble locus is required for cytokinesis during the postblastoderm mitoses of Drosophila. Development *114*, 165–171.

Hirano, T., and Mitchison, T. J. (1994). A heterodimeric coiled-coil protein required for mitotic chromosome condensation in vitro. Cell *79*, 449–458.

Hirata, D., Yamabuki, T., Miki, D., Ito, T., Tsuchiya, E., Fujita, M., Hosokawa, M., Chayama, K., Nakamura, Y., and Daigo, Y. (2009). Involvement of epithelial cell transforming sequence-2 oncoantigen in lung and esophageal cancer progression. Clinical cancer research *15*, 256–266.

Hoffmann, I., Clarke, P. R., Marcote, M. J., Karsenti, E., and Draetta, G. (1993). Phosphorylation and activation of human cdc25-C by cdc2--cyclin B and its involvement in the self-amplification of MPF at mitosis. EMBO journal *12*, 53–63.

Hu, C.-K., Coughlin, M., Field, C. M., and Mitchison, T. J. (2008). Cell polarization during monopolar cytokinesis. Journal of cell biology *181*, 195–202.

Hu, C.-K., Coughlin, M., Field, C. M., and Mitchison, T. J. (2011). KIF4 regulates midzone length during cytokinesis. Current biology *21*, 815–824.

Hu, C.-K., Ozlü, N., Coughlin, M., Steen, J. J., and Mitchison, T. J. (2012). Plk1 negatively regulates PRC1 to prevent premature midzone formation before cytokinesis. Molecular biology of the cell *23*, 2702–2711.

Hurley, J. H. (2010). The ESCRT complexes. Critical reviews in biochemistry and molecular biology *45*, 463–487.

Hutterer, A., Glotzer, M., and Mishima, M. (2009). Clustering of centralspindlin is essential for its accumulation to the central spindle and the midbody. Current biology *19*, 2043–2049.

Hümmer, S., and Mayer, T. U. (2009). Cdk1 negatively regulates midzone localization of the mitotic kinesin Mklp2 and the chromosomal passenger complex. Current biology *19*, 607–612.

Izumi, T., Walker, D. H., and Maller, J. L. (1992). Periodic changes in phosphorylation of the Xenopus cdc25 phosphatase regulate its activity. Molecular biology of the cell *3*, 927–939.

Janssen, A., Van der Burg, M., Szuhai, K., Kops, G. J. P. L., and Medema, R. H. (2011). Chromosome segregation errors as a cause of DNA damage and structural chromosome aberrations. Science *333*, 1895–1898.

Jantsch-Plunger, V., Gönczy, P., Romano, A., Schnabel, H., Hamill, D., Schnabel, R., Hyman, A. A., and Glotzer, M. (2000). CYK-4: A Rho family gtpase activating protein (GAP) required for central spindle formation and cytokinesis. Journal of cell biology *149*, 1391–1404.

Jeffrey, P. D., Russo, A. A., Polyak, K., Gibbs, E., Hurwitz, J., Massagué, J., and Pavletich, N. P. (1995). Mechanism of CDK activation revealed by the structure of a cyclinA-CDK2 complex. Nature *376*, 313–320.

Jenkins, N., Saam, J. R., and Mango, S. E. (2006). CYK-4/GAP provides a localized cue to initiate anteroposterior polarity upon fertilization. Science *313*, 1298–1301.

Jiang, W., Jimenez, G., Wells, N. J., Hope, T. J., Wahl, G. M., Hunter, T., and Fukunaga, R. (1998). PRC1: a human mitotic spindle-associated CDK substrate protein required for cytokinesis. Molecular cell *2*, 877–885.

Jordan, P., and Karess, R. (1997). Myosin light chain-activating phosphorylation sites are required for oogenesis in Drosophila. Journal of cell biology *139*, 1805–1819.

Kaitna, S., Mendoza, M., Jantsch-Plunger, V., and Glotzer, M. (2000). Incenp and an aurora-like kinase form a complex essential for chromosome segregation and efficient completion of cytokinesis. Current biology *10*, 1172–1181.

Kamasaki, T., Osumi, M., and Mabuchi, I. (2007). Three-dimensional arrangement of F-actin in the contractile ring of fission yeast. Journal of cell biology *178*, 765–771.

Kamijo, K., Ohara, N., Abe, M., Uchimura, T., Hosoya, H., Lee, J.-S., and Miki, T. (2006). Dissecting the role of Rho-mediated signaling in contractile ring formation. Molecular biology of the cell *17*, 43–55.

Kechad, A., Jananji, S., Ruella, Y., and Hickson, G. R. X. (2012). Anillin acts as a bifunctional linker coordinating midbody ring biogenesis during cytokinesis. Current biology *22*, 197–203.

Kim, J.-E., Billadeau, D. D., and Chen, J. (2005). The tandem BRCT domains of Ect2 are required for both negative and positive regulation of Ect2 in cytokinesis. Journal of biological chemistry *280*, 5733–5739.

Kimura, K. (1998). Phosphorylation and Activation of 13S Condensin by Cdc2 in Vitro. Science *282*, 487–490.

Kimura, K., Ito, M., Amano, M., Chihara, K., Fukata, Y., Nakafuku, M., Yamamori, B., Feng, J., Nakano, T., Okawa, K., et al. (1996). Regulation of myosin phosphatase by Rho and Rho-associated kinase (Rho-kinase). Science *273*, 245–248.

Kishi, K., Sasaki, T., Kuroda, S., Itoh, T., and Takai, Y. (1993). Regulation of cytoplasmic division of Xenopus embryo by rho p21 and its inhibitory GDP/GTP exchange protein (rho GDI). Journal of cell biology *120*, 1187–1195.

Kitagawa, M., and Higashi, H. (1996). The consensus motif for phosphorylation by cyclin D1-Cdk4 is different from that for phosphorylation by cyclin A/E-Cdk2. EMBO journal *15*, 7060–7069.

Kouranti, I., Sachse, M., Arouche, N., Goud, B., and Echard, A. (2006). Rab35 regulates an endocytic recycling pathway essential for the terminal steps of cytokinesis. Current biology *16*, 1719–1725.

Kovar, D. R., and Pollard, T. D. (2004). Insertional assembly of actin filament barbed ends in association with formins produces piconewton forces. Proceedings of the National Academy of Sciences of the United States of America *101*, 14725–14730.

Kraft, C., Herzog, F., Gieffers, C., Mechtler, K., Hagting, A., Pines, J., and Peters, J.-M. (2003). Mitotic regulation of the human anaphase-promoting complex by phosphorylation. EMBO journal *22*, 6598–6609.

Kramer, E. R., Scheuringer, N., Podtelejnikov, a V, Mann, M., and Peters, J. M. (2000). Mitotic regulation of the APC activator proteins CDC20 and CDH1. Molecular biology of the cell *11*, 1555–1569.

Kunda, P., and Baum, B. (2009). The actin cytoskeleton in spindle assembly and positioning. Trends in cell biology *19*, 174–179.

Kunda, P., Rodrigues, N. T. L., Moeendarbary, E., Liu, T., Ivetic, A., Charras, G., and Baum, B. (2012). PP1-mediated moesin dephosphorylation couples polar relaxation to mitotic exit. Current biology *22*, 231–236.

Kurasawa, Y., Earnshaw, W. C., Mochizuki, Y., Dohmae, N., and Todokoro, K. (2004). Essential roles of KIF4 and its binding partner PRC1 in organized central spindle midzone formation. EMBO Journal *23*, 3237–3248.

Kõivomägi, M., Valk, E., Venta, R., Iofik, A., Lepiku, M., Balog, E. R. M., Rubin, S. M., Morgan, D. O., and Loog, M. (2011). Cascades of multisite phosphorylation control Sic1 destruction at the onset of S phase. Nature *480*, 128–131.

Lacroix, B., and Maddox, A. S. (2012). Cytokinesis, ploidy and aneuploidy. Journal of pathology *226*, 338–351.

Lammer, C., Wagerer, S., Saffrich, R., Mertens, D., Ansorge, W., and Hoffmann, I. (1998). The cdc25B phosphatase is essential for the G2/M phase transition in human cells. Journal of cell science *111*, 2445–2453.

Lee, M. G., and Nurse, P. (1987). Complementation used to clone a human homologue of the fission yeast cell cycle control gene cdc2. Nature *327*, 31–35.

Lehner, C. F. (1992). The pebble gene is required for cytokinesis in Drosophila. Journal of cell science *103*, 1021–1030.

Leismann, O., Herzig, A., Heidmann, S., and Lehner, C. F. (2000). Degradation of Drosophila PIM regulates sister chromatid separation during mitosis. Genes & development *14*, 2192–2205.

Lekomtsev, S., Su, K.-C., Pye, V. E., Blight, K., Sundaramoorthy, S., Takaki, T., Collinson, L. M., Cherepanov, P., Divecha, N., and Petronczki, M. (2012). Centralspindlin links the mitotic spindle to the plasma membrane during cytokinesis. Nature *492*, 276–279.

Lemmon, M. A. (2008). Membrane recognition by phospholipid-binding domains. Nature reviews molecular cell biology *9*, 99–111.

Leung, C. C. Y., and Glover, J. N. M. (2011). BRCT domains: Easy as one, two, three. Cell cycle *10*, 2461–2470.

Levskaya, A., Weiner, O. D., Lim, W. a, and Voigt, C. a (2009). Spatiotemporal control of cell signalling using a light-switchable protein interaction. Nature *461*, 997–1001.

Lietzke, S. E., Bose, S., Cronin, T., Klarlund, J., Chawla, A., Czech, M. P., and Lambright, D. G. (2000). Structural basis of 3-phosphoinositide recognition by pleckstrin homology domains. Molecular cell *6*, 385–394.

Lindon, C., and Pines, J. (2004). Ordered proteolysis in anaphase inactivates Plk1 to contribute to proper mitotic exit in human cells. Journal of cell biology *164*, 233–241.

Liot, C., Seguin, L., Siret, A., Crouin, C., Schmidt, S., and Bertoglio, J. (2011). APC(cdh1) mediates degradation of the oncogenic Rho-GEF Ect2 after mitosis. PLoS one *6*, e23676.

Lipp, J. J., Hirota, T., Poser, I., and Peters, J.-M. (2007). Aurora B controls the association of condensin I but not condensin II with mitotic chromosomes. Journal of cell science *120*, 1245–1255.

Liu, F., Rothblum-Oviatt, C., Ryan, C. E., and Piwnica-Worms, H. (1999). Overproduction of human Myt1 kinase induces a G2 cell cycle delay by interfering with the intracellular trafficking of Cdc2-cyclin B1 complexes. Molecular and cellular biology *19*, 5113–5123.

Liu, X. F., Ohno, S., and Miki, T. (2006). Nucleotide exchange factor ECT2 regulates epithelial cell polarity. Cellular signalling *18*, 1604–1615.

Liu, X., Wang, H., Eberstadt, M., Schnuchel, A., Olejniczak, E. T., Meadows, R. P., Schkeryantz, J. M., Janowick, D. A., Harlan, J. E., Harris, E. A., et al. (1998). NMR structure and mutagenesis of the N-terminal Dbl homology domain of the nucleotide exchange factor Trio. Cell *95*, 269–277.

Liu, X.-F., Ishida, H., Raziuddin, R., and Miki, T. (2004). Nucleotide exchange factor ECT2 interacts with the polarity protein complex Par6/Par3/protein kinase Czeta (PKCzeta) and regulates PKCzeta activity. Molecular and cellular biology *24*, 6665–6675.

Logan, M. R., and Mandato, C. A. (2006). Regulation of the actin cytoskeleton by PIP2 in cytokinesis. Biology of the cell *98*, 377–388.

Loog, M., and Morgan, D. O. (2005). Cyclin specificity in the phosphorylation of cyclin-dependent kinase substrates. Nature *434*, 104–108.

Lénárt, P., Petronczki, M., Steegmaier, M., Di Fiore, B., Lipp, J. J., Hoffmann, M., Rettig, W. J., Kraut, N., and Peters, J.-M. (2007). The small-molecule inhibitor BI 2536 reveals novel insights into mitotic roles of polo-like kinase 1. Current biology *17*, 304–315.

Ma, X., Kovács, M., Conti, M. A., Wang, A., Zhang, Y., Sellers, J. R., and Adelstein, R. S. (2012). Nonmuscle myosin II exerts tension but does not translocate actin in vertebrate cytokinesis. Proceedings of the National Academy of Sciences of the United States of America *109*, 4509–4514.

Mabuchi, I., Hamaguchi, Y., Fujimoto, H., Morii, N., Mishima, M., and Narumiya, S. (1993). A rho-like protein is involved in the organisation of the contractile ring in dividing sand dollar eggs. Zygote *1*, 325–331.

Macůrek, L., Lindqvist, A., Lim, D., Lampson, M. A., Klompmaker, R., Freire, R., Clouin, C., Taylor, S. S., Yaffe, M. B., and Medema, R. H. (2008). Polo-like kinase-1 is activated by aurora A to promote checkpoint recovery. Nature *455*, 119–123.

Mailand, N., Podtelejnikov, A. V, Groth, A., Mann, M., Bartek, J., and Lukas, J. (2002). Regulation of G(2)/M events by Cdc25A through phosphorylation-dependent modulation of its stability. EMBO journal *21*, 5911–5920.

Malumbres, M., and Barbacid, M. (2009). Cell cycle, CDKs and cancer: a changing paradigm. Nature reviews cancer *9*, 153–166.

Malumbres, M., and Barbacid, M. (2005). Mammalian cyclin-dependent kinases. Trends in biochemical sciences *30*, 630–641.

Manchado, E., Guillamot, M., De Cárcer, G., Eguren, M., Trickey, M., García-Higuera, I., Moreno, S., Yamano, H., Cañamero, M., and Malumbres, M. (2010). Targeting mitotic exit leads to tumor regression in vivo: Modulation by Cdk1, Mastl, and the PP2A/B55α,δ phosphatase. Cancer cell *18*, 641–654.

Martindill, D. M. J., and Riley, P. R. (2008). Cell cycle switch to endocycle: the nucleolus lends a hand. Cell cycle *7*, 17–23.

Marumoto, T., Zhang, D., and Saya, H. (2005). Aurora-A - a guardian of poles. Nature reviews cancer *5*, 42–50.

Masai, H., Matsumoto, S., You, Z., Yoshizawa-Sugata, N., and Oda, M. (2010). Eukaryotic chromosome DNA replication: where, when, and how? Annual review of biochemistry *79*, 89–130.

Mastronarde, D. N., McDonald, K. L., Ding, R., and McIntosh, J. R. (1993). Interpolar spindle microtubules in PTK cells. Journal of cell biology *123*, 1475–1489.

Masui, Y. (1972). Distribution of the cytoplasmic activity inducing germinal vesicle breakdown in frog oocytes. Journal of experimental zoology *179*, 365–377.

Matthews, H. K., and Baum, B. (2012). The metastatic cancer cell cortex: An adaptation to enhance robust cell division in novel environments? BioEssays : news and reviews in molecular, cellular and developmental biology *34*, 1017–1020.

Matthews, H. K., Delabre, U., Rohn, J. L., Guck, J., Kunda, P., and Baum, B. (2012). Changes in Ect2 localization couple actomyosin-dependent cell shape changes to mitotic progression. Developmental cell *23*, 371–383.

Maupin, P., and Pollard, T. D. (1986). Arrangement of actin filaments and myosin-like filaments in the contractile ring and of actin-like filaments in the mitotic spindle of dividing HeLa cells. Journal of ultrastructure and molecular structure research *94*, 92–103.

McLaughlin, S., and Murray, D. (2005). Plasma membrane phosphoinositide organization by protein electrostatics. Nature *438*, 605–611.

Melendez, J., Stengel, K., Zhou, X., Chauhan, B. K., Debidda, M., Andreassen, P., Lang, R. A., and Zheng, Y. (2011). RhoA GTPase is dispensable for actomyosin regulation but is essential for mitosis in primary mouse embryonic fibroblasts. Journal of biological chemistry *286*, 15132–15137.

Miki, T., Smith, C. L., Long, J. E., Eva, A., and Fleming, T. P. (1993). Oncogene ect2 is related to regulators of small GTP-binding proteins. Nature *362*, 462–465.

Miller, A. L., and Bement, W. M. (2009). Regulation of cytokinesis by Rho GTPase flux. Nature cell biology *11*, 71–77.

Mishima, M., Kaitna, S., and Glotzer, M. (2002). Central spindle assembly and cytokinesis require a kinesin-like protein/RhoGAP complex with microtubule bundling activity. Developmental cell *2*, 41–54.

Mishima, M., Pavicic, V., and Grüneberg, U. (2004). Cell cycle regulation of central spindle assembly. Nature *430*, 0–5.

Mocciaro, A., Berdougo, E., Zeng, K., Black, E., Vagnarelli, P., Earnshaw, W., Gillespie, D., Jallepalli, P., and Schiebel, E. (2010). Vertebrate cells genetically deficient for Cdc14A or Cdc14B retain DNA damage checkpoint proficiency but are impaired in DNA repair. Journal of cell biology *189*, 631–639.

Mocciaro, A., and Schiebel, E. (2010). Cdc14: a highly conserved family of phosphatases with non-conserved functions? Journal of cell science *123*, 2867–2876.

Mochida, S., Maslen, S. L., Skehel, M., and Hunt, T. (2010). Greatwall phosphorylates an inhibitor of protein phosphatase 2A that is essential for mitosis. Science *330*, 1670–1673.

Mohammad, D. H., and Yaffe, M. B. (2009). 14-3-3 proteins, FHA domains and BRCT domains in the DNA damage response. DNA repair *8*, 1009–1017.

Morgan, D. O. (2007). The Cell Cycle (New Science Press).

Moser, S. C., and Swedlow, J. R. (2011). How to be a mitotic chromosome. Chromosome research *19*, 307–319.

Motegi, F., and Sugimoto, A. (2006). Sequential functioning of the ECT-2 RhoGEF, RHO-1 and CDC-42 establishes cell polarity in Caenorhabditis elegans embryos. Nature cell biology *8*, 978–985.

Motegi, F., Velarde, N. V, Piano, F., and Sugimoto, A. (2006). Two phases of astral microtubule activity during cytokinesis in C. elegans embryos. Developmental cell *10*, 509–520.

Mullins, J., and Biesele, J. (1977). Terminal phase of cytokinesis in D-98S cells. Journal of cell biology *73*, 672–684.

Murthy, K., and Wadsworth, P. (2005). Myosin-II-dependent localization and dynamics of F-actin during cytokinesis. Current biology *15*, 724–731.

Musacchio, A., and Salmon, E. D. (2007). The spindle-assembly checkpoint in space and time. Nature reviews molecular cell biology *8*, 379–393.

Naim, V., Imarisio, S., Di Cunto, F., Gatti, M., and Bonaccorsi, S. (2004). Drosophila citron kinase is required for the final steps of cytokinesis. Molecular biology of the cell *15*, 5053–5063.

Nakajima, H., Toyoshima-Morimoto, F., Taniguchi, E., and Nishida, E. (2003). Identification of a consensus motif for Plk (Polo-like kinase) phosphorylation reveals Myt1 as a Plk1 substrate. Journal of biological chemistry *278*, 25277–25280.

Nakayama, K. (1998). Cip/Kip cyclin-dependent kinase inhibitors: brakes of the cell cycle engine during development. BioEssays : news and reviews in molecular, cellular and developmental biology *20*, 1020–1029.

Nasmyth, K. (1996). At the heart of the budding yeast cell cycle. Trends in genetics *12*, 405–412.

Nasmyth, K. (2011). Cohesin: a catenase with separate entry and exit gates? Nature cell biology *13*, 1170–1177.

Neef, R., Gruneberg, U., Kopajtich, R., Li, X., Nigg, E. A., Sillje, H., and Barr, F. A. (2007). Choice of Plk1 docking partners during mitosis and cytokinesis is controlled by the activation state of Cdk1. Nature cell biology *9*, 436–444.

Ng, M. M., Chang, F., and Burgess, D. R. (2005). Movement of membrane domains and requirement of membrane signaling molecules for cytokinesis. Developmental cell *9*, 781–790.

Nigg, E. a, Blangy, a, and Lane, H. a (1996). Dynamic changes in nuclear architecture during mitosis: on the role of protein phosphorylation in spindle assembly and chromosome segregation. Experimental cell research *229*, 174–180.

Niiya, F., Tatsumoto, T., Lee, K. S., and Miki, T. (2006). Phosphorylation of the cytokinesis regulator ECT2 at G2/M phase stimulates association of the mitotic kinase Plk1 and accumulation of GTP-bound RhoA. Oncogene *25*, 827–837.

Niiya, F., Xie, X., Lee, K. S., Inoue, H., and Miki, T. (2005). Inhibition of cyclin-dependent kinase 1 induces cytokinesis without chromosome segregation in an ECT2 and MgcRacGAP-dependent manner. Journal of biological chemistry *280*, 36502–36509.

Nishimura, Y., and Yonemura, S. (2006). Centralspindlin regulates ECT2 and RhoA accumulation at the equatorial cortex during cytokinesis. Journal of cell science *119*, 104–114.

Nislow, C., Lombillo, V. A., Kuriyama, R., and McIntosh, J. R. (1992). A plus-end-directed motor enzyme that moves antiparallel microtubules in vitro localizes to the interzone of mitotic spindles. Nature *359*, 543–547.

Nüsslein-Volhard, C., and Wieschaus, E. (1980). Mutations affecting segment number and polarity in Drosophila. Nature *287*, 795–801.

Ocampo-Hafalla, M. T., and Uhlmann, F. (2011). Cohesin loading and sliding. Journal of cell science *124*, 685–691.

Oceguera-Yanez, F., Kimura, K., Yasuda, S., Higashida, C., Kitamura, T., Hiraoka, Y., Haraguchi, T., and Narumiya, S. (2005). Ect2 and MgcRacGAP regulate the activation and function of Cdc42 in mitosis. Journal of cell biology *168*, 221–232.

O'Farrell, P. H. (2011). Quiescence: early evolutionary origins and universality do not imply uniformity. Philosophical transactions of the Royal Society of London. Series B, Biological sciences *366*, 3498–3507.

Di Paolo, G., and De Camilli, P. (2006). Phosphoinositides in cell regulation and membrane dynamics. Nature *443*, 651–657.

Pavicic-Kaltenbrunner, V. (2007). Cooperative assembly of CYK-4/MgcRacGAP and ZEN-4/MKLP1 to form the centralspindlin complex. Molecular biology of the cell *18*, 4992–5003.

Petronczki, M., Glotzer, M., Kraut, N., and Peters, J.-M. (2007). Polo-like kinase 1 triggers the initiation of cytokinesis in human cells by promoting recruitment of the RhoGEF Ect2 to the central spindle. Developmental cell *12*, 713–725.

Petronczki, M., Lénárt, P., and Peters, J.-M. (2008). Polo on the Rise-from Mitotic Entry to Cytokinesis with Plk1. Developmental cell *14*, 646–659.

Piekny, A. J., and Glotzer, M. (2008). Anillin is a scaffold protein that links RhoA, actin, and myosin during cytokinesis. Current biology *18*, 30–36.

Piekny, A. J., and Maddox, A. S. (2010). The myriad roles of Anillin during cytokinesis. Seminars in cell & developmental biology *21*, 881–891.

Piekny, A., Werner, M., and Glotzer, M. (2005). Cytokinesis: welcome to the Rho zone. Trends in cell biology *15*, 651–658.

Pines, J. (2011). Cubism and the cell cycle: the many faces of the APC/C. Nature reviews molecular cell biology *12*, 427–438.

Pollard, T. D. (2010). Mechanics of cytokinesis in eukaryotes. Current opinion in cell biology *22*, 50–56.

Pollard, T. D. (2004). Ray Rappaport chronology: Twenty-five years of seminal papers on cytokinesis in the Journal of Experimental Zoology. Journal of experimental zoology. Part A, Comparative experimental biology *301*, 9–14.

Potapova, T. a, Daum, J. R., Pittman, B. D., Hudson, J. R., Jones, T. N., Satinover, D. L., Stukenberg, P. T., and Gorbsky, G. J. (2006). The reversibility of mitotic exit in vertebrate cells. Nature *440*, 954–958.

Powers, E. A., Thompso, D. P., Garner-Hamrick, P. A., He, W., Yem, A. W., Bannow, C. A., Staples, D. J., Waszak, G. A., Smith, C. W., Deibel, M. R., et al. (2000). Identification of a C-terminal cdc25 sequence required for promotion of germinal vesicle breakdown. Biochemical journal *1*, 653–660.

Pring, M., Evangelista, M., Boone, C., Yang, C., and Zigmond, S. H. (2003). Mechanism of formin-induced nucleation of actin filaments. Biochemistry *42*, 486–496.

Prokopenko, S. N. S. N., Brumby, A., O'Keefe, L., Prior, L., He, Y., Saint, R., and Bellen, H. J. (1999). A putative exchange factor for Rho1 GTPase is required for initiation of cytokinesis in Drosophila. Genes & development *13*, 2301–2314.

Pruyne, D., Evangelista, M., Yang, C., Bi, E., Zigmond, S., Bretscher, A., and Boone, C. (2002). Role of formins in actin assembly: nucleation and barbed-end association. Science *297*, 612–615.

Rao, P. N., and Johnson, R. T. (1970). Mammalian Cell Fusion : Studies on the Regulation of DNA Synthesis and Mitosis. Nature *225*, 159–164.

Rappaport, R. (1997). Cleavage furrow establishment by the moving mitotic apparatus. Development, growth & differentiation *39*, 221–226.

Rappaport, R. (1996). Cytokinesis in Animal cells (Cambridge University Press).

Ratheesh, A., Gomez, G. a, Priya, R., Verma, S., Kovacs, E. M., Jiang, K., Brown, N. H., Akhmanova, A., Stehbens, S. J., and Yap, A. S. (2012). Centralspindlin and α-catenin regulate Rho signalling at the epithelial zonula adherens. Nature cell biology *14*, 818–828.

Rieder, C. L., Schultz, A., Cole, R., and Sluder, G. (1994). Anaphase onset in vertebrate somatic cells is controlled by a checkpoint that monitors sister kinetochore attachment to the spindle. Journal of cell biology *127*, 1301–1310.

Rossman, K. L., Cheng, L., Mahon, G. M., Rojas, R. J., Snyder, J. T., Whitehead, I. P., and Sondek, J. (2003). Multifunctional roles for the PH domain of Dbs in regulating Rho GTPase activation. Journal of biological chemistry *278*, 18393–18400.

Rossman, K. L., Der, C. J., and Sondek, J. (2005). GEF means go: turning on RHO GTPases with guanine nucleotide-exchange factors. Nature reviews molecular cell biology *6*, 167–180.

Rossman, K. L., Worthylake, D. K., Snyder, J. T., Siderovski, D. P., Campbell, S. L., and Sondek, J. (2002). A crystallographic view of interactions between Dbs and Cdc42: PH domain-assisted guanine nucleotide exchange. EMBO journal *21*, 1315–1326.

Ruchaud, S., Carmena, M., and Earnshaw, W. C. (2007). Chromosomal passengers: conducting cell division. Nature reviews molecular cell biology *8*, 798–812.

Rusan, N. M., Fagerstrom, C. J., Yvon, A. M., and Wadsworth, P. (2001). Cell cycle-dependent changes in microtubule dynamics in living cells expressing green fluorescent protein-alpha tubulin. Molecular biology of the cell *12*, 971–980.

Sagona, A. P., Nezis, I. P., Pedersen, N. M., Liestøl, K., Poulton, J., Rusten, T. E., Skotheim, R. I., Raiborg, C., and Stenmark, H. (2010). PtdIns(3)P controls cytokinesis through KIF13A-mediated recruitment of FYVE-CENT to the midbody. Nature cell biology *12*, 362–371.

Saito, R. M., Perreault, A., Peach, B., Satterlee, J. S., and Van den Heuvel, S. (2004a). The CDC-14 phosphatase controls developmental cell-cycle arrest in C. elegans. Nature cell biology *6*, 777–783.

Saito, S., Liu, X.-F., Kamijo, K., Raziuddin, R., Tatsumoto, T., Okamoto, I., Chen, X., Lee, C.-C., Lorenzi, M. V, Ohara, N., et al. (2004b). Deregulation and mislocalization of the cytokinesis regulator ECT2 activate the Rho signaling pathways leading to malignant transformation. Journal of biological chemistry *279*, 7169–7179.

Sanger, J. M., Pochapin, M. B., and Sanger, J. W. (1985). Midbody sealing after cytokinesis in embryos of the sea urchin Arabacia punctulata. Cell and tissue research *240*, 287–292.

Santamaria, A., Neef, R., Eberspächer, U., Eis, K., Husemann, M., Mumberg, D., Prechtl, S., Schulze, V., Siemeister, G., Wortmann, L., et al. (2007). Use of the novel Plk1 inhibitor ZK-thiazolidinone to elucidate functions of Plk1 in early and late stages of mitosis. Molecular biology of the cell *18*, 4024–4036.

Scheffzek, K., and Welti, S. (2012). Pleckstrin homology (PH) like domains - versatile modules in protein-protein interaction platforms. FEBS letters *586*, 2662–2673.

Schiel, J. A., and Prekeris, R. (2011). ESCRT or endosomes?: Tales of the separation of two daughter cells. Communicative & integrative biology *4*, 606–608.

Schmitz, M. H. a, Held, M., Janssens, V., Hutchins, J. R. a, Hudecz, O., Ivanova, E., Goris, J., Trinkle-Mulcahy, L., Lamond, A. I., Poser, I., et al. (2010). Live-cell imaging RNAi screen identifies PP2A-B55alpha and importin-beta1 as key mitotic exit regulators in human cells. Nature cell biology *12*, 886–893.

Schneider, B. L., Yang, Q. H., and Futcher, A. B. (1996). Linkage of replication to start by the Cdk inhibitor Sic1. Science *272*, 560–562.

Schumacher, J. M., Golden, A., and Donovan, P. J. (1998). AIR-2: An Aurora/Ipl1-related protein kinase associated with chromosomes and midbody microtubules is required for polar body extrusion and cytokinesis in Caenorhabditis elegans embryos. Journal of cell biology *143*, 1635–1646.

Severson, A. F., Baillie, D. L., and Bowerman, B. (2002). A Formin Homology protein and a profilin are required for cytokinesis and Arp2/3-independent assembly of cortical microfilaments in C. elegans. Current biology *12*, 2066–2075.

Shandala, T., Gregory, S. L., Dalton, H. E., Smallhorn, M., and Saint, R. (2004). Citron kinase is an essential effector of the Pbl-activated Rho signalling pathway in Drosophila melanogaster. Development *131*, 5053–5063.

Sherr, C. J., and Roberts, J. M. (1999). CDK inhibitors: positive and negative regulators of G1-phase progression. Genes & development *13*, 1501–1512.

Shteinberg, M., Protopopov, Y., Listovsky, T., Brandeis, M., and Hershko, A. (1999). Phosphorylation of the cyclosome is required for its stimulation by Fizzy/cdc20. Biochemical and biophysical research communications *260*, 193–198.

Skop, A. R., Liu, H., Yates, J., Meyer, B. J., and Heald, R. (2004). Dissection of the mammalian midbody proteome reveals conserved cytokinesis mechanisms. Science *305*, 61–66.

Smutny, M., Cox, H. L., Leerberg, J. M., Kovacs, E. M., Conti, M. A., Ferguson, C., Hamilton, N. A., Parton, R. G., Adelstein, R. S., and Yap, A. S. (2010). Myosin II isoforms identify distinct functional modules that support integrity of the epithelial zonula adherens. Nature cell biology *12*, 696–702.

Solski, P. a, Wilder, R. S., Rossman, K. L., Sondek, J., Cox, A. D., Campbell, S. L., and Der, C. J. (2004). Requirement for C-terminal sequences in regulation of Ect2 guanine nucleotide exchange specificity and transformation. Journal of biological chemistry *279*, 25226–25233.

Somers, W. G., and Saint, R. (2003). A RhoGEF and Rho family GTPase-activating protein complex links the contractile ring to cortical microtubules at the onset of cytokinesis. Developmental cell *4*, 29–39.

De Souza, C. P., Ellem, K. A., and Gabrielli, B. G. (2000). Centrosomal and cytoplasmic Cdc2/cyclin B1 activation precedes nuclear mitotic events. Experimental cell research *257*, 11–21.

Srivastava, S. K., Wheelock, R. H., Aaronson, S. A., and Eva, A. (1986). Identification of the protein encoded by the human diffuse B-cell lymphoma (dbl) oncogene. Proceedings of the National Academy of Sciences of the United States of America *83*, 8868–8872.

Stegmeier, F., and Amon, A. (2004). Closing mitosis: the functions of the Cdc14 phosphatase and its regulation. Annual review of genetics *38*, 203–232.

Steigemann, P., Wurzenberger, C., Schmitz, M. H. A., Held, M., Guizetti, J., Maar, S., and Gerlich, D. W. (2009). Aurora B-Mediated Abscission Checkpoint Protects against Tetraploidization. Cell *136*, 473–484.

Strausfeld, U., Fernandez, A., Capony, J. P., Girard, F., Lautredou, N., Derancourt, J., Labbe, J. C., and Lamb, N. J. (1994). Activation of p34cdc2 protein kinase by microinjection of

human cdc25C into mammalian cells. Requirement for prior phosphorylation of cdc25C by p34cdc2 on sites. Journal of biological chemistry *269*, 5989–6000.

Subramanian, R., Wilson-Kubalek, E. M., Arthur, C. P., Bick, M. J., Campbell, E. A., Darst, S. A., Milligan, R. A., and Kapoor, T. M. (2010). Insights into antiparallel microtubule crosslinking by PRC1, a conserved nonmotor microtubule binding protein. Cell *142*, 433–443.

Sunkel, C. E., and Glover, D. M. (1988). polo, a mitotic mutant of Drosophila displaying abnormal spindle poles. Journal of cell science *89*, 25–38.

Tan, S. Y., and Brown, J. (2006). Rudolph Virchow (1821-1902): “pope of pathology”. Singapore medical journal *47*, 567–568.

Tanaka, S., and Araki, H. (2010). Regulation of the initiation step of DNA replication by cyclin-dependent kinases. Chromosoma *119*, 565–574.

Tanaka, T. U., Rachidi, N., Janke, C., Pereira, G., Galova, M., Schiebel, E., Stark, M. J. R., and Nasmyth, K. (2002). Evidence that the Ipl1-Sli15 (Aurora kinase-INCENP) complex promotes chromosome bi-orientation by altering kinetochore-spindle pole connections. Cell *108*, 317–329.

Tanenbaum, M. E., and Medema, R. H. (2010). Mechanisms of centrosome separation and bipolar spindle assembly. Developmental cell *19*, 797–806.

Tatsumoto, T., Sakata, H., Dasso, M., and Miki, T. (2003). Potential roles of the nucleotide exchange factor ECT2 and Cdc42 GTPase in spindle assembly in Xenopus egg cell-free extracts. Journal of cellular biochemistry *90*, 892–900.

Tatsumoto, T., Xie, X., Blumenthal, R., Okamoto, I., and Miki, T. (1999). Human ECT2 is an exchange factor for Rho GTPases, phosphorylated in G2/M phases, and involved in cytokinesis. Journal of cell biology *147*, 921–928.

Terada, Y., Tatsuka, M., Suzuki, F., Yasuda, Y., Fujita, S., and Otsu, M. (1998). AIM-1: a mammalian midbody-associated protein required for cytokinesis. EMBO journal *17*, 667–676.

Tucker, J. B. (1971). Microtubules and a contractile ring of microfilaments associated with a cleavage furrow. Journal of cell science *8*, 557–571.

Ubersax, J. A., Woodbury, E. L., Quang, P. N., Paraz, M., Blethrow, J. D., Shah, K., Shokat, K. M., and Morgan, D. O. (2003). Targets of the cyclin-dependent kinase Cdk1. Nature *425*, 859–864.

Uehara, R., and Goshima, G. (2010). Functional central spindle assembly requires de novo microtubule generation in the interchromosomal region during anaphase. Journal of cell biology *191*, 259–267.

Uehara, R., Goshima, G., Mabuchi, I., Vale, R. D., Spudich, J. A., and Griffis, E. R. (2010). Determinants of myosin II cortical localization during cytokinesis. Current biology *20*, 1080–1085.

Uehara, R., Nozawa, R., Tomioka, A., Petry, S., Vale, R. D., Obuse, C., and Goshima, G. (2009). The augmin complex plays a critical role in spindle microtubule generation for

mitotic progression and cytokinesis in human cells. Proceedings of the National Academy of Sciences of the United States of America *106*, 6998–7003.

Uhlmann, F., Bouchoux, C., and López-Avilés, S. (2011). A quantitative model for cyclin-dependent kinase control of the cell cycle: revisited. Philosophical transactions of the Royal Society of London. Series B, Biological sciences *366*, 3572–3583.

Uhlmann, F., Lottspeich, F., and Nasmyth, K. (1999). Sister-chromatid separation at anaphase onset is promoted by cleavage of the cohesin subunit Scc1. Nature *400*, 37–42.

Uhlmann, F., Wernic, D., Poupart, M. A., Koonin, E. V, and Nasmyth, K. (2000). Cleavage of cohesin by the CD clan protease separin triggers anaphase in yeast. Cell *103*, 375–386.

Verma, R. (1997). Phosphorylation of Sic1p by G1 Cdk Required for Its Degradation and Entry into S Phase. Science *278*, 455–460.

Virshup, D. M., and Shenolikar, S. (2009). From promiscuity to precision: protein phosphatases get a makeover. Molecular cell *33*, 537–545.

Vázquez-Novelle, M. D., Esteban, V., Bueno, A., and Sacristán, M. P. (2005). Functional homology among human and fission yeast Cdc14 phosphatases. Journal of biological chemistry *280*, 29144–29150.

Watanabe, N., Broome, M., and Hunter, T. (1995). Regulation of the human WEE1Hu CDK tyrosine 15-kinase during the cell cycle. EMBO journal *14*, 1878–1891.

Watanabe, S., Ando, Y., Yasuda, S., Hosoya, H., Watanabe, N., Ishizaki, T., and Narumiya, S. (2008). mDia2 induces the actin scaffold for the contractile ring and stabilizes its position during cytokinesis in NIH 3T3 cells. Molecular biology of the cell *19*, 2328–2338.

Wells, N. J., Watanabe, N., Tokusumi, T., Jiang, W., Verdecia, M. A., and Hunter, T. (1999). The C-terminal domain of the Cdc2 inhibitory kinase Myt1 interacts with Cdc2 complexes and is required for inhibition of G(2)/M progression. Journal of cell science *112*, 3361–3371.

Werner, M., Munro, E., and Glotzer, M. (2007). Astral signals spatially bias cortical myosin recruitment to break symmetry and promote cytokinesis. Current biology *17*, 1286–1297.

Wheatley, S. P., and Wang, Y. (1996). Midzone microtubule bundles are continuously required for cytokinesis in cultured epithelial cells. Journal of cell biology *135*, 981–989.

Winter, C. G., Wang, B., Ballew, A., Royou, A., Karess, R., Axelrod, J. D., and Luo, L. (2001). Drosophila Rho-associated kinase (Drok) links Frizzled-mediated planar cell polarity signaling to the actin cytoskeleton. Cell *105*, 81–91.

Wolfe, B. a, and Glotzer, M. (2009). Single cells (put a ring on it). Genes & development *23*, 896–901.

Wolfe, B. a, Takaki, T., Petronczki, M., and Glotzer, M. (2009). Polo-like kinase 1 directs assembly of the HsCyk-4 RhoGAP/Ect2 RhoGEF complex to initiate cleavage furrow formation. PLoS biology *7*, e1000110.

Worthylake, D. K., Rossman, K. L., and Sondek, J. (2000). Crystal structure of Rac1 in complex with the guanine nucleotide exchange region of Tiam1. Nature *408*, 682–688.

Wu, J. Q., Guo, J. Y., Tang, W., Yang, C.-S., Freel, C. D., Chen, C., Nairn, A. C., and Kornbluth, S. (2009). PP1-mediated dephosphorylation of phosphoproteins at mitotic exit is controlled by inhibitor-1 and PP1 phosphorylation. Nature cell biology *11*, 644–651.

Wurzenberger, C., and Gerlich, D. W. (2011). Phosphatases: providing safe passage through mitotic exit. Nature reviews molecular cell biology *12*, 469–482.

Yamada, T., Hikida, M., and Kurosaki, T. (2006). Regulation of cytokinesis by mgcRacGAP in B lymphocytes is independent of GAP activity. Experimental cell research *312*, 3517–3525.

Yamashiro, S., Totsukawa, G., Yamakita, Y., Sasaki, Y., Madaule, P., Ishizaki, T., Narumiya, S., and Matsumura, F. (2003). Citron kinase, a Rho-dependent kinase, induces di-phosphorylation of regulatory light chain of myosin II. Molecular biology of the cell *14*, 1745–1756.

Yasuda, S., Oceguera-Yanez, F., Kato, T., Okamoto, M., Yonemura, S., Terada, Y., Ishizaki, T., and Narumiya, S. (2004). Cdc42 and mDia3 regulate microtubule attachment to kinetochores. Nature *428*, 767–771.

Yu, X., Chini, C. C. S., He, M., Mer, G., and Chen, J. (2003). The BRCT domain is a phospho-protein binding domain. Science *302*, 639–642.

Yumura, S., Ueda, M., Sako, Y., Kitanishi-Yumura, T., and Yanagida, T. (2008). Multiple mechanisms for accumulation of myosin II filaments at the equator during cytokinesis. Traffic *9*, 2089–2099.

Yüce, O., Piekny, A., and Glotzer, M. (2005). An ECT2-centralspindlin complex regulates the localization and function of RhoA. Journal of cell biology *170*, 571–582.

Zhang, Y., Sugiura, R., Lu, Y., Asami, M., Maeda, T., Itoh, T., Takenawa, T., Shuntoh, H., and Kuno, T. (2000). Phosphatidylinositol 4-phosphate 5-kinase Its3 and calcineurin Ppb1 coordinately regulate cytokinesis in fission yeast. Journal of biological chemistry *275*, 35600–35606.

Zhao, W., and Fang, G. (2005). MgcRacGAP controls the assembly of the contractile ring and the initiation of cytokinesis. Proceedings of the National Academy of Sciences of the United States of America *102*, 13158–13163.

Zhao, W., Seki, A., and Fang, G. (2006). Cep55, a microtubule-bundling protein, associates with centralspindlin to control the midbody integrity and cell abscission during cytokinesis. Molecular biology of the cell *17*, 3881–3896.

Zheng, Y. (2001). Dbl family guanine nucleotide exchange factors. Trends in biochemical sciences *26*, 724–732.

Zhu, C., Lau, E., Schwarzenbacher, R., Bossy-Wetzel, E., and Jiang, W. (2006). Spatiotemporal control of spindle midzone formation by PRC1 in human cells. Proceedings of the National Academy of Sciences of the United States of America *103*, 6196–6201.

Zur, A., and Brandeis, M. (2001). Securin degradation is mediated by fzy and fzr, and is required for complete chromatid separation but not for cytokinesis. EMBO journal *20*, 792–801.

Appendix

Targeting of the RhoGEF Ect2 to the equatorial membrane controls cleavage furrow formation during cytokinesis

Developmental Cell
Article

Targeting of the RhoGEF Ect2 to the Equatorial Membrane Controls Cleavage Furrow Formation during Cytokinesis

Kuan-Chung Su,[1,2] Tohru Takaki,[1,2] and Mark Petronczki[1,*]
[1]Cell Division and Aneuploidy Laboratory, Cancer Research UK London Research Institute, Clare Hall Laboratories, Blanche Lane, South Mimms, Hertfordshire EN6 3LD, UK
[2]These authors contributed equally to this work
*Correspondence: mark.petronczki@cancer.org.uk
DOI 10.1016/j.devcel.2011.11.003

SUMMARY

In animal cells, formation of the cytokinetic furrow requires activation of the GTPase RhoA by the guanine nucleotide exchange factor Ect2. How Ect2, which is associated with the spindle midzone, controls RhoA activity at the equatorial cortex during anaphase is not understood. Here, we show that Ect2 concentrates at the equatorial membrane during cytokinesis in live cells. Ect2 membrane association requires a pleckstrin homology domain and a polybasic cluster that bind to phosphoinositide lipids. Both guanine nucleotide exchange function and membrane targeting of Ect2 are essential for RhoA activation and cleavage furrow formation in human cells. Membrane localization of Ect2 is spatially confined to the equator by centralspindlin, Ect2's spindle midzone anchor complex, and is temporally coordinated with chromosome segregation through the activation state of CDK1. We propose that targeting of Ect2 to the equatorial membrane represents a key step in the delivery of the cytokinetic signal to the cortex.

INTRODUCTION

Animal cells divide by segregating sister chromatids to opposite poles before redrawing their boundaries in a process known as cytokinesis (Barr and Gruneberg, 2007; Eggert et al., 2006). During anaphase, the constriction of the plasma membrane leads to the formation of a cleavage furrow that separates the cytoplasm of the two nascent daughter cells. Cleavage furrow ingression is driven by a membrane-associated and actomyosin-based structure, called the contractile ring. Local activation of the small GTPase RhoA at the equatorial cell cortex in anaphase plays a key role in the assembly and constriction of the contractile ring (reviewed in Piekny et al., 2005).

By partitioning segregated sister genomes and centrosomes to daughter cells, cytokinesis prevents chromosomal instability and tumorigenesis (Ganem et al., 2007). Formation of the cleavage furrow has to be tightly coordinated with chromosome segregation so that cytokinesis occurs only after anaphase onset and only at the equator. Temporal control is exerted by cyclin-dependent kinase 1 (CDK1), which inhibits cytokinesis in early mitosis and is inactivated at the metaphase-to-anaphase transition (Barr and Gruneberg, 2007; Wurzenberger and Gerlich, 2011).

Cleavage furrow formation occurs at the plasma membrane. Yet, micromanipulation experiments and functional studies have established that the mitotic spindle positions the cleavage furrow and the zone of active RhoA in animal cells (D'Avino et al., 2005; Rappaport, 1985; von Dassow, 2009). Two components of the anaphase spindle that play a pivotal role in controlling the formation and positioning of the cleavage furrow at the equator are astral microtubules and the spindle midzone, also called the central spindle (Bringmann and Hyman, 2005; Dechant and Glotzer, 2003). The spindle midzone is a stable array of interdigitated microtubules that assembles at anaphase onset midway between segregating chromatids in the equatorial plane (Glotzer, 2009). The ability of microtubule-associated protein complexes to control cytokinetic events at the cell cortex and plasma membrane is a poorly understood but central aspect of cell division.

At the heart of cleavage furrow formation in animal cells lies the conserved Rho guanine nucleotide exchange factor (GEF) Ect2 (epithelial cell transforming sequence 2) (Prokopenko et al., 1999; Tatsumoto et al., 1999). Ect2 and its orthologs, such as Pebble in *Drosophila*, are essential for RhoA activation, contractile ring formation and cytokinesis (reviewed in Barr and Gruneberg, 2007; Piekny et al., 2005). The protein contains two N-terminal tandem BRCT (BRCA1 C-terminal) domains followed by a DH-type RhoGEF domain (Rossman et al., 2005) and a pleckstrin homology (PH) domain at the C terminus (Figure 1A). DH domains in RhoGEF proteins usually occur in conjunction with PH domains, potential phospholipid interaction elements (Lemmon, 2008). In vitro, full-length Ect2 protein and a C-terminal fragment containing the DH-PH region display guanine nucleotide exchange activity on RhoA (Kim et al., 2005; Tatsumoto et al., 1999).

During anaphase Ect2 is recruited to the spindle midzone and equatorial astral microtubules by binding to a conserved protein complex known as centralspindlin, a key structural component of the spindle midzone (Somers and Saint, 2003; Yüce et al., 2005). Centralspindlin is a heterotetramer composed of the mitotic kinesin Mklp1 and the Rho GTPase-activating protein MgcRacGAP (also called HsCyk-4 and RacGAP1) (Glotzer,

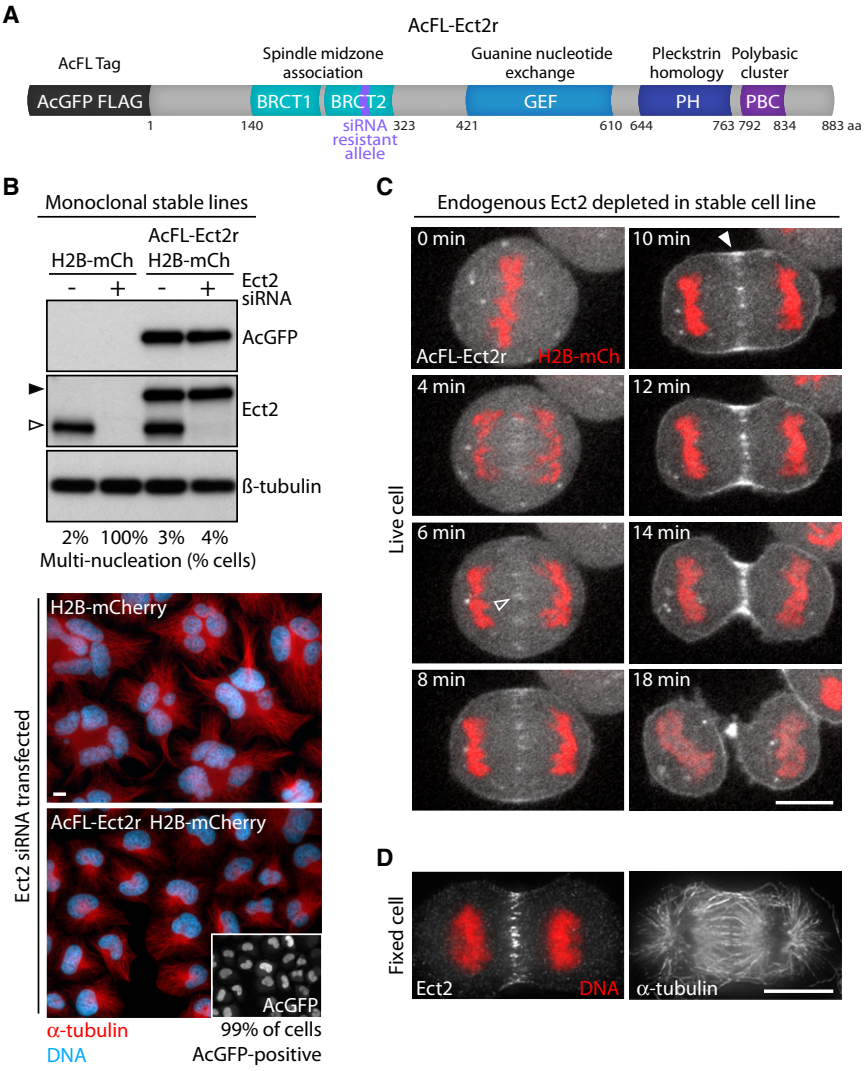

Figure 1. Ect2 Localizes to the Equatorial Membrane during Cytokinesis

(A) Domain organization of AcFL-tagged and RNAi-resistant human Ect2 protein.

(B) Immunoblot analysis of protein extracts prepared from stable HeLa Kyoto cell lines expressing H2B-mCherry or coexpressing AcFL-Ect2r and H2B-mCherry (top panel). Extracts were prepared 48 hr after transfection with control siRNA (–) or Ect2 siRNA (+) duplexes. Extracts were probed with antibodies directed against AcGFP, Ect2 and β-tubulin. Endogenous Ect2 protein and transgenic AcFL-Ect2r are indicated by open and filled arrowheads, respectively. The percentage of binucleated or multinucleated interphase cells (multinucleation) 48 hr after siRNA transfection is indicated below the blot lanes ($n > 600$ cells). Immunofluorescence (IF) microscopy analysis of cell lines stably expressing H2B-mCherry or stably coexpressing AcFL-Ect2r and H2B-mCherry 48 hr after transfection with Ect2 siRNA (bottom panel). Scale bar in this panel and the following panels represents 10 μm.

(C) Confocal live-cell imaging of the monoclonal cell line stably coexpressing AcFL-Ect2r (white) and H2B-mCherry (red). The cell line was characterized in (B). Recording started 30 hr after transfection with Ect2 siRNA. Time point t = 0 min was set to the metaphase-to-anaphase transition. The open and filled arrowheads indicate localization to the spindle midzone and cell cortex, respectively. For full sequence, see Movie S1.

(D) IF analysis of Ect2 localization during anaphase. Endogenous Ect2 protein and α-tubulin were detected by antibodies in methanol-fixed HeLa Kyoto cells.

2009). Complex formation between Ect2 and centralspindlin is directed by the binding of Ect2's N-terminal region and BRCT domains to MgcRacGAP (Somers and Saint, 2003; Yüce et al., 2005). In mammalian cells, this interaction requires the phosphorylation of MgcRacGAP by the mitotic kinase Plk1, which creates a binding site for Ect2's tandem BRCT domains (Burkard et al., 2009; Wolfe et al., 2009). Ect2, MgcRacGAP, and, in mammalian cells, Plk1 are required for the activation of RhoA and cleavage furrow formation (Barr and Gruneberg, 2007). This has lead to the formulation of models proposing that recruitment of the RhoGEF Ect2 to peripheral midzone microtubules or equatorial astral microtubules activates RhoA at the adjacent equatorial membrane, leading to the formation of the contractile ring and the cleavage furrow (D'Avino et al., 2005; Nishimura and Yonemura, 2006; Piekny et al., 2005; Somers and Saint, 2003; Yüce et al., 2005).

Despite our detailed understanding of the mechanism underlying the spindle midzone association of Ect2, the molecular basis for how Ect2 delivers the cytokinetic signal from microtubules to the plasma membrane remains unknown. Transient expression studies in human cells have revealed that a C-terminal region of Ect2 containing the PH domain localizes to the cell periphery (Chalamalasetty et al., 2006). While Ect2 is readily visualized at the spindle midzone, a fraction of the protein has also been detected at the cell cortex in anaphase cells (Chalamalasetty et al., 2006; Nishimura and Yonemura, 2006). These findings raise the possibility that the controlled delivery of Ect2 to the equatorial plasma membrane at anaphase could represent a key but hitherto uncharacterized step in RhoA activation and cleavage furrow formation.

RESULTS

Live-Cell Imaging Reveals Ect2 Localization to the Equatorial Membrane during Cytokinesis

To investigate the function and localization of Ect2 during cytokinesis, we generated a genetic complementation system in human HeLa "Kyoto" cells. We created a stable cell line coexpressing histone H2B-mCherry and an siRNA-resistant allele of Ect2 (Ect2r) that was N-terminally tagged with AcGFP (Aequora coerulescens GFP) and a single FLAG epitope (AcFL) (Figure 1A). The engineered line expressed transgenic AcFL-Ect2r in all cells of the population and at a level indistinguishable from the one

observed for the endogenous counterpart (Figure 1B). siRNA-mediated depletion of endogenous Ect2 protein in a line that only expressed H2B-mCherry converted all cells of the population into bi-nucleated or multinucleated cells, indicative of complete cytokinesis failure (Figure 1B). This phenotype was completely suppressed in the cell line coexpressing H2B-mCherry and siRNA-resistant AcFL-Ect2r despite efficient removal of the endogenous Ect2 protein (Figure 1B). Thus, transgenic and tagged Ect2 is able to entirely replace the cytokinetic function of the endogenous protein.

The established model allowed us to track Ect2 during cytokinesis in live cells at native protein level but in the absence of a competing endogenous counterpart (Movie S1 available online). Time-lapse imaging after depletion of the endogenous protein revealed that AcFL-Ect2r remained in the cytoplasm until the metaphase-to-anaphase transition (Figure 1C). Within 4–6 min after anaphase onset AcFL-Ect2r accumulated at the spindle midzone (Figure 1C, open arrowhead). This spindle midzone localization was maintained throughout cleavage furrow ingression. Eight minutes after anaphase onset the protein also became concentrated at the cell periphery. Shortly before and during cleavage furrow ingression peripheral AcFL-Ect2r became progressively enriched at the equator (Figure 1C, closed arrowhead). After completion of furrow ingression, the protein accumulated around the midbody before being imported into the reforming daughter nuclei during mitotic exit. Our live-cell analysis establishes that Ect2 first localizes to spindle midzone after anaphase onset and then becomes strongly concentrated at the equatorial cortex or membrane during cytokinesis (30/30 cells) (Movies S1 and S2). The localization of Ect2 to the periphery is largely lost during cell fixation (Figure 1D) but can to some extent be preserved using special fixation conditions (Chalamalasetty et al., 2006). Importantly, the peripheral accumulation of Ect2 is tightly correlated in both space and time with the formation of the cleavage furrow at the equator during anaphase (Figure 1C). This raises the possibility that this membrane-proximal pool of the RhoGEF protein Ect2 plays a key role in the activation of RhoA and the initiation of cytokinesis.

Mechanistic Basis for Ect2 Association with the Plasma Membrane

We next sought to determine the mechanism for the association of Ect2 with the cell cortex or plasma membrane. A previous study has demonstrated that the carboxy-terminal half of Ect2 can localize to the cell periphery (Chalamalasetty et al., 2006). We therefore focused our attention on a region of Ect2 (Ect2CT, aa 414–883) (Figure 2A; Figure S1A) that encompasses the GEF domain, PH domain and Tail region but lacks the two BRCT repeats responsible for spindle midzone association of Ect2 (Chalamalasetty et al., 2006; Tatsumoto et al., 1999; Yüce et al., 2005). Similar to a lipid-modified marker protein (Myr-Palm-FLAc), transiently expressed AcFL-Ect2CT was efficiently recruited to the cell periphery in anaphase cells (Figure 2B). The AcFL tag alone remained cytoplasmic (Figure 2B). In contrast to the full-length protein (Figure 1C), transiently expressed Ect2CT was not enriched at the cell equator during anaphase (Figure 2B). Expression of Ect2CT caused severe changes in interphase cell morphology, such as cell rounding, and prevented cleavage furrow ingression during cytokinesis (Figure 6B and data not shown) presumably due to ectopic Rho activation. Although Ect2CT colocalized with cortical actin in solvent treated cells, the protein accumulated in peripheral regions that were largely devoid of cortical actin in dihydrocytochalasin B-treated anaphase cells (Figure 2C) (20/20 cells). This finding together with our observation that Ect2 binds to phospholipids in vitro (Figure 2D, see below) suggests that Ect2 associates directly with the plasma membrane and not with the cortical actin cytoskeleton.

We next investigated which elements within Ect2CT direct membrane targeting of the protein. The localization of Ect2CT to the plasma membrane was not affected by point mutations in the DH domain that abolish the GEF activity of Ect2 on RhoA in vitro (GEF^{4A}) (Figures 2B and 3D). This indicates that the guanine nucleotide exchange activity of Ect2 is dispensable for the recruitment of Ect2 to the membrane. Deletion of the conserved PH domain, a potential lipid interaction module (Lemmon, 2008), severely compromised but, unexpectedly, did not completely abrogate membrane association of Ect2CT (ΔPH) (Figure 2B) suggesting the presence of an additional membrane interaction region. Deletion of the carboxy-terminal Tail region (ΔTail) as well as simultaneous deletion of the PH domain and Tail region abrogated cortical localization of AcFL-Ect2CT (ΔPHΔTail) (Figure 2B). Analysis of the Tail sequence revealed the presence of a polybasic cluster (PBC) between amino acid 792 and 834 of human Ect2 (Figure 2A; Figure S1B). The polybasic nature of this region is strongly conserved in Ect2 orthologs of other animal species (Figure S1B), with *Caenorhabditis elegans* being a notable exception. Interestingly, the C-terminal region containing the PBC has previously been shown to be required for the transforming activity of human Ect2 (Solski et al., 2004) and may contribute to the control of Ect2 protein turnover after mitotic exit (Liot et al., 2011). Polybasic clusters are frequently found at the carboxy-termini of small GTPases and target the proteins to the plasma membrane by binding to negatively charged phosphatidylinositol 4,5-bisphosphate ($PI[4,5]P_2$) and phosphatidylinositol 3,4,5,-triphosphate ($PI[3,4,5]P_3$) lipids (Heo et al., 2006). Expression of the polybasic cluster of Ect2 fused to AcFL revealed that the region alone can be sufficient for plasma membrane targeting (PBC) (Figure 2B). Our transient expression analysis suggests that two conserved regions within the carboxy terminus of Ect2, a PH domain and a polybasic cluster, cooperate to target the protein to the plasma membrane.

To test the ability of Ect2 to directly interact with lipids in vitro, we expressed maltose-binding protein (MBP)-tagged Ect2 protein and variants thereof using the insect cell-baculovirus system (Figure 2D). Purified recombinant proteins were incubated with an array of lipids that were immobilized on a support membrane. MBP fusions of both full-length Ect2 protein and Ect2CT bound to phosphatidylinositol 4-phosphate (PI[4]P), $PI[4,5]P_2$, and $PI[3,4,5]P_3$ (Figure 2D). Consistent with the in vivo membrane targeting experiments described above, simultaneous deletion of the PH domain and the Tail region, which contains the polybasic cluster, abolished the ability of MBP-Ect2CT to interact with phosphoinositides in vitro (Figure 2D). The specificity of the lipid interaction assay was validated by the selective binding the PH domain of GRP1 to $PI(3,4,5)P_3$

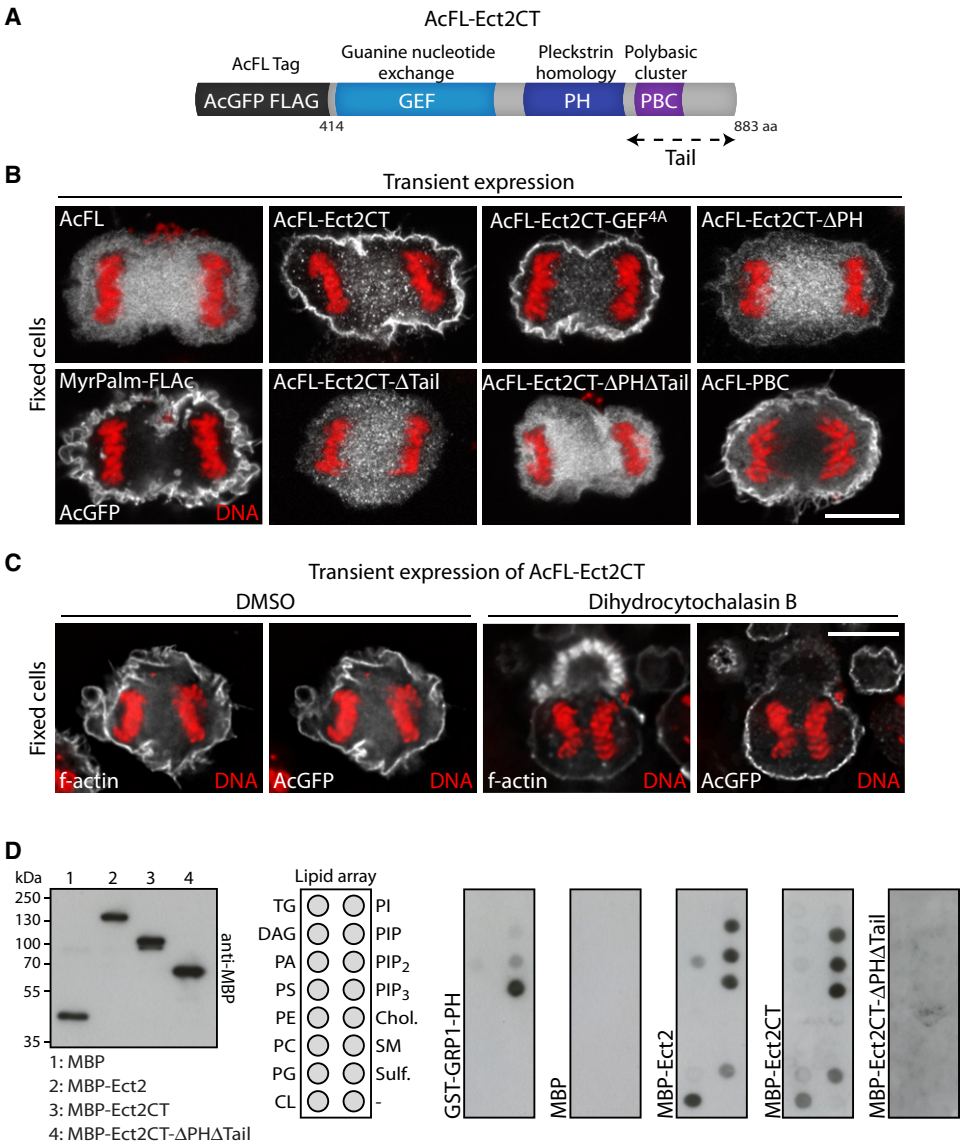

Figure 2. Mechanism of Ect2 Association with the Plasma Membrane

(A) Domain organization of AcFL-Ect2CT spanning aa 414 to 883 of human Ect2.

(B) IF analysis of indicated control proteins and AcFL-tagged Ect2 fragments in formaldehyde-fixed anaphase cells following transient transfection. Transiently expressed proteins were detected using an antibody directed against the AcGFP moiety of the AcFL and FLAc tags. Domain organization of all transfected constructs is shown in Figure S1A. For alignment of polybasic cluster see Figure S1B. Scale bar in this panel and the following panels represents 10 μm.

(C) IF analysis of transiently expressed AcFL-Ect2CT in formaldehyde-fixed anaphase cells. Cells were treated with dimethyl sulfoxide (DMSO) or 20 μM dihydrocytochalasin B for 20 min prior to fixation. AcFL-Ect2CT and filamentous actin (f-actin) were detected using anti-AcGFP antibodies and fluorophore-conjugated phalloidin, respectively.

(D) Immunoblot analysis of recombinant maltose-binding protein (MBP) and MBP-Ect2 fusion proteins (left panel). MBP fusion proteins were expressed in insect cells using the baculovirus system and purified using amylose resin. Lipid arrays were incubated with the indicated recombinant proteins before being probed by anti-GST (for GST-GRP1-PH) or anti-MBP antibodies (right panel). Key for lipid array: triglyceride (TG), diacylglycerol (DAG), phosphatidic acid (PA), phosphatidylserine (PS), phosphatidylethanolamine (PE); phosphatidylcholine (PC), phosphatidylglycerol (PG), cardiolipin (CL), phosphatidylinositol (PI), PtdIns(4)P (PIP), PtdIns(4,5)P_2 (PIP_2), PtdIns(3,4,5)P_3 (PIP_3), cholesterol (Chol.), sphingomyelin (SM), sulfatide (Sulf.).

See also Figure S1.

(Figure 2D) (Klarlund et al., 1997). These results suggest that the targeting of Ect2 to the membrane could be directed by the interaction of the PH domain and polybasic cluster with negatively charged phosphoinositides in the inner leaflet of the plasma membrane.

Cytokinesis Requires Ect2's Guanine Nucleotide Exchange Activity and Its Membrane Association Domains

To scrutinize the function of Ect2's exchange activity and its membrane association domains during cell division, we

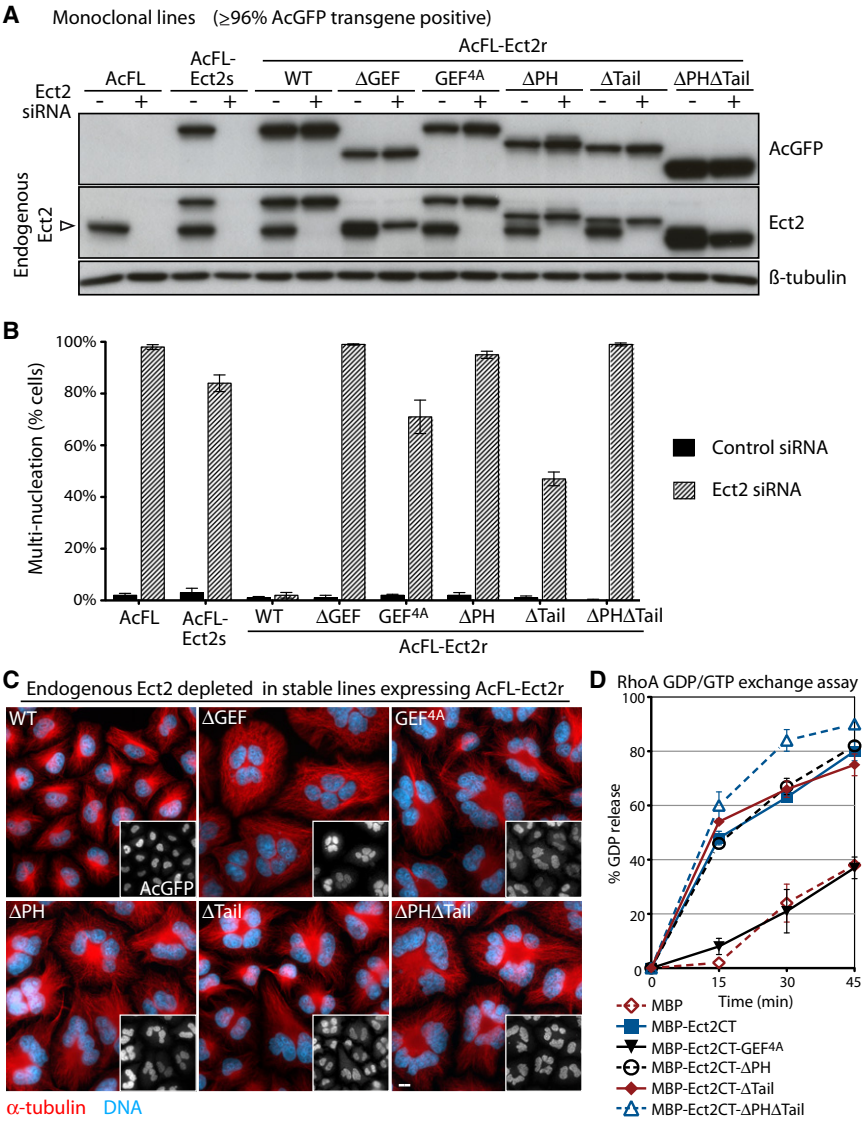

Figure 3. GEF Activity and Membrane Interaction Domains of Ect2 Are Required for Cytokinesis

(A) Immunoblot analysis of protein extracts prepared from monoclonal HeLa Kyoto cell lines expressing the indicated transgenes. Extracts were prepared 48 hr after transfection with control siRNA (–) or Ect2 siRNA (+). Extracts were probed with antibodies directed against AcGFP, Ect2, and β-tubulin. Domain organization of all constructs used is shown in Figure S2A.

(B) Quantification of the fraction of bi-nucleated and multinucleated interphase cells (multinucleation) in monoclonal lines expressing the indicated transgenes. Error bars indicate standard deviation of three experiments (n > 200 cells each). Cells were analyzed by IF 48 hr after transfection with control or Ect2 siRNA. See Figure S2B for the characterization of a second set of independent monoclonal cell lines.

(C) IF analysis of monoclonal cell lines expressing the indicated transgenes. Cells were analyzed 48 hr after transfection with Ect2 siRNA. Scale bar represents 10 μm.

(D) In vitro RhoA GDP/GTP exchange assay. [^{3}H]GDP-loaded GST-RhoA was incubated with recombinant MBP or MBP fusions of the indicated Ect2 fragments in the presence of unlabelled GTP. [^{3}H]GDP release was determined by measuring the remaining protein-associated radioactivity at the indicated time points. Error bars indicate standard deviation of two experiments. A characterization of the recombinant proteins used is shown in Figure S2C.

See also Figure S2.

employed the potent genetic complementation system introduced earlier to generate a series of Ect2 mutant alleles (Figure 3A; Figure S2A). To assess the requirement of the GEF function, the DH domain was deleted (ΔGEF). Alternatively, a stretch of 4 highly conserved residues (565PVQR568) within the CR3 helix of the DH domain was replaced by 4 alanine residues (GEF^{4A}). The CR3 helix is critical for the guanine nucleotide exchange activity of DH domains (Rossman et al., 2005) and mutations therein have previously been shown to block the transforming activity of Ect2 (Saito et al., 2004). Introduction of the GEF^{4A} mutations abolished the GDP/GTP exchange activity of recombinant MBP-Ect2CT on RhoA in vitro (Figure 3D; Figure S2C). To investigate the requirement of Ect2 membrane targeting for cytokinesis, the PH domain (ΔPH) and the PBC containing Tail region (ΔTail) were deleted separately or in conjunction (ΔPHΔTail). Crucially, neither individual nor combined removal of the PH and Tail regions reduced the GDP/GTP exchange activity of recombinant Ect2CT on RhoA in vitro (Figure 3D; Figure S2C). Although we cannot rule out that the PH domain and PBC have functions in addition to membrane targeting, our in vitro experiments suggest that the guanine nucleotide exchange activity of Ect2 can be separated from the ability of the protein to associate with the plasma membrane.

We generated monoclonal HeLa Kyoto lines that express AcFL-tagged RNAi-resistant alleles of Ect2 (AcFL-Ect2r) in at least 96% of cells and at levels close to the one observed for the endogenous protein (Figure 3A; Figure S2A). Test experiments revealed that AcFL-Ect2r expressed at less than 20% of the level of the endogenous counterpart was sufficient to successfully execute cytokinesis in the absence of the endogenous protein (data not shown). To investigate whether specific alleles of Ect2 can support cytokinesis, we depleted the endogenous protein in transgenic monoclonal lines and determined the emergence of bi-nucleated and multinucleated cells, a signature phenotype of defective cytokinesis (Figures 3). Loss of endogenous Ect2 protein abrogated cytokinesis in cells expressing the AcFL tag or an RNAi-sensitive transgenic version of Ect2 (AcFL-Ect2s) (Figure 3B). In contrast, expression of an RNAi-resistant wild-type allele of Ect2 (AcFL-Ect2r-WT) fully rescued the cell division defect caused by depletion of the endogenous protein (Figures 3B and 3C). Deletion of Ect2's GEF domain

(ΔGEF) completely abolished the rescue activity of AcFL-Ect2r (Figures 3B and 3C). Point mutations within the CR3 helix of the GEF domain (GEF^{4A}) severely compromised the ability of AcFL-Ect2r to support cytokinesis in the absence of endogenous protein (Figures 3B and 3C). The difference in phenotypic penetrance between the ΔGEF and GEF^{4A} variants of Ect2 could be caused by either residual exchange activity exhibited by the GEF^{4A} allele in vivo or by an additional function of the GEF domain that is distinct from its exchange activity. Importantly, deletion of the PH domain (ΔPH) and combined deletion of both PH domain and Tail region (ΔPHΔTail) completely abrogated the ability of AcFL-Ect2r to support cytokinesis in the absence of endogenous Ect2 (Figures 3B and 3C). Removal of the Tail region alone (ΔTail) had a weaker effect and blocked cell division in about half of the cell population (Figures 3B and 3C). The results obtained with mutant transgenic alleles of Ect2 were confirmed in a second set of independently isolated monoclonal cell lines (Figure S2B). Our genetic complementation analysis and in vitro assays demonstrate that Ect2's guanine nucleotide exchange activity and its membrane association domains are crucial for the execution of cytokinesis in human cells.

The Pleckstrin Homology Domain and C-Terminal Polybasic Cluster Target Ect2 to the Plasma Membrane during Cytokinesis

To investigate the role of the DH, PH and Tail domains (Figure 4A) in controlling the distribution of Ect2 during cell division, the localization of transgenic Ect2 variants was first determined in fixed cells. Following depletion of the endogenous protein in transgenic monoclonal cell lines, all mutant Ect2 variants associated with the spindle midzone during anaphase (Figure 4B) demonstrating that DH, PH and Tail regions within the carboxy-terminal half of Ect2 are dispensable for spindle midzone association of the protein. This is consistent with the fact that Ect2′s N-terminal BRCT repeats are responsible for the recruitment of the protein to the midzone (Chalamalasetty et al., 2006; Tatsumoto et al., 1999; Yüce et al., 2005).

To scrutinize the localization of Ect2 and its association with the membrane in live cells, we depleted the endogenous protein and used confocal time-lapse microscopy to track the transgenic counterparts (n > 35 cells for each mutant allele). Wild-type Ect2 accumulated at the spindle midzone and the equatorial membrane during anaphase (Figure 4C). Deletion or mutation of the GEF domain (ΔGEF and GEF^{4A}) did not abrogate the localization of the protein to the equatorial membrane (Figure 4C). Ect2-GEF^{4A} showed stronger accumulation at the equatorial membrane than the wild-type counterpart and was partially depleted from the spindle midzone. This indicates that inactivating mutations in the DH domain could lead to the retention of the protein at the equatorial periphery. Despite accumulation at the equatorial membrane, cleavage furrow formation was severely compromised in cells expressing ΔGEF and GEF^{4A} alleles of Ect2 (Figures 4C and 5A). Loss of the PH domain (ΔPH) significantly reduced the association of Ect2 with the membrane (Figure 4C). Crucially, deletion of both PH domains and Tail region (ΔPHΔTail) completely abolished the localization of the protein to the equatorial membrane in anaphase cells, while leaving spindle midzone localization unaltered (Figure 4C). Thus, the localization of Ect2 to the equatorial membrane during cytokinesis requires the protein's PH domain and its PBC containing Tail region. Concomitant with the loss of membrane association, the ΔPHΔTail variant of Ect2 was unable to support cleavage furrow formation (Figures 4C and 5A). While the membrane interaction domains of Ect2 are essential for cell division in vivo (Figures 3B and 3C), they are dispensable for Ect2's exchange activity on RhoA in vitro (Figure 3D). These results suggest that the guanine nucleotide exchange activity and the ability to associate with the plasma membrane are two distinct but key aspects of Ect2 function during cytokinesis.

RhoA Activation and Cleavage Furrow Formation Require the Guanine Nucleotide Exchange Function and Membrane Association of Ect2

To investigate the nature of the cytokinetic defect observed in mutant alleles of Ect2 we used bright-field time-lapse microscopy. This analysis revealed that loss of Ect2 in cells expressing only the AcFL tag prevented cleavage furrow formation in the majority of mitotic cells (Figure 5A). A minor fraction of cells were capable of transiently forming a furrow before ultimately also failing to divide. This suggests that furrow ingression followed by regression represents a hypomorphic Ect2 loss-of-function phenotype. Expression of transgenic wild-type Ect2 (AcFL-Ect2r) completely restored cleavage furrow formation and cytokinesis in the absence of the endogenous counterpart (Figure 5A). In contrast, transgenic alleles of Ect2 lacking either the GEF domain (ΔGEF) or both membrane association domains (ΔPHΔTail) were unable to support cleavage furrow formation (Figure 5A). The phenotype of the two alleles was similar to that of a total loss of Ect2 protein indicating that the deleted regions are indispensible for Ect2's cytokinetic function. Consistent with our terminal phenotype analysis (Figure 3B), inactivating point mutations within the GEF domain (GEF^{4A}) had a slightly weaker impact on furrow formation (Figure 5A). In contrast to the loss of both membrane association domains (ΔPHΔTail), Ect2 variants lacking either the PH domain (ΔPH) or Tail region (ΔTail) were able to transiently support furrowing in the majority of the cells examined (Figure 5A). This hypomorphic phenotype is consistent with our finding that both domains cooperate to direct the association of Ect2 with the membrane (Figure 2B). Our live-cell analysis suggests that formation of a cleavage furrow in human cells requires the guanine nucleotide exchange activity of Ect2 and the interaction of the protein with the plasma membrane.

To address the nature of this requirement, we analyzed the localization of the centralspindlin subunit Mklp1, the GTPase RhoA and the contractile ring component anillin (Eggert et al., 2006) in monoclonal lines expressing different Ect2 alleles after depletion of the endogenous Ect2 protein. Loss of Ect2's GEF function or membrane association domains did not affect the formation of the spindle midzone, as judged by the localization of Mklp1 to the central spindle at anaphase (Figure 4B). In cells complemented by transgenic wild-type Ect2, RhoA and the contractile ring component anillin, localized to the equatorial cell cortex during anaphase (Figure 5B). Loss of either Ect2's GEF function or the protein's ability to associate with the membrane prevented or severely compromised the accumulation of RhoA and anillin at the equator (Figure 5B). Consistent with the observed cleavage furrow phenotypes (Figure 5A),

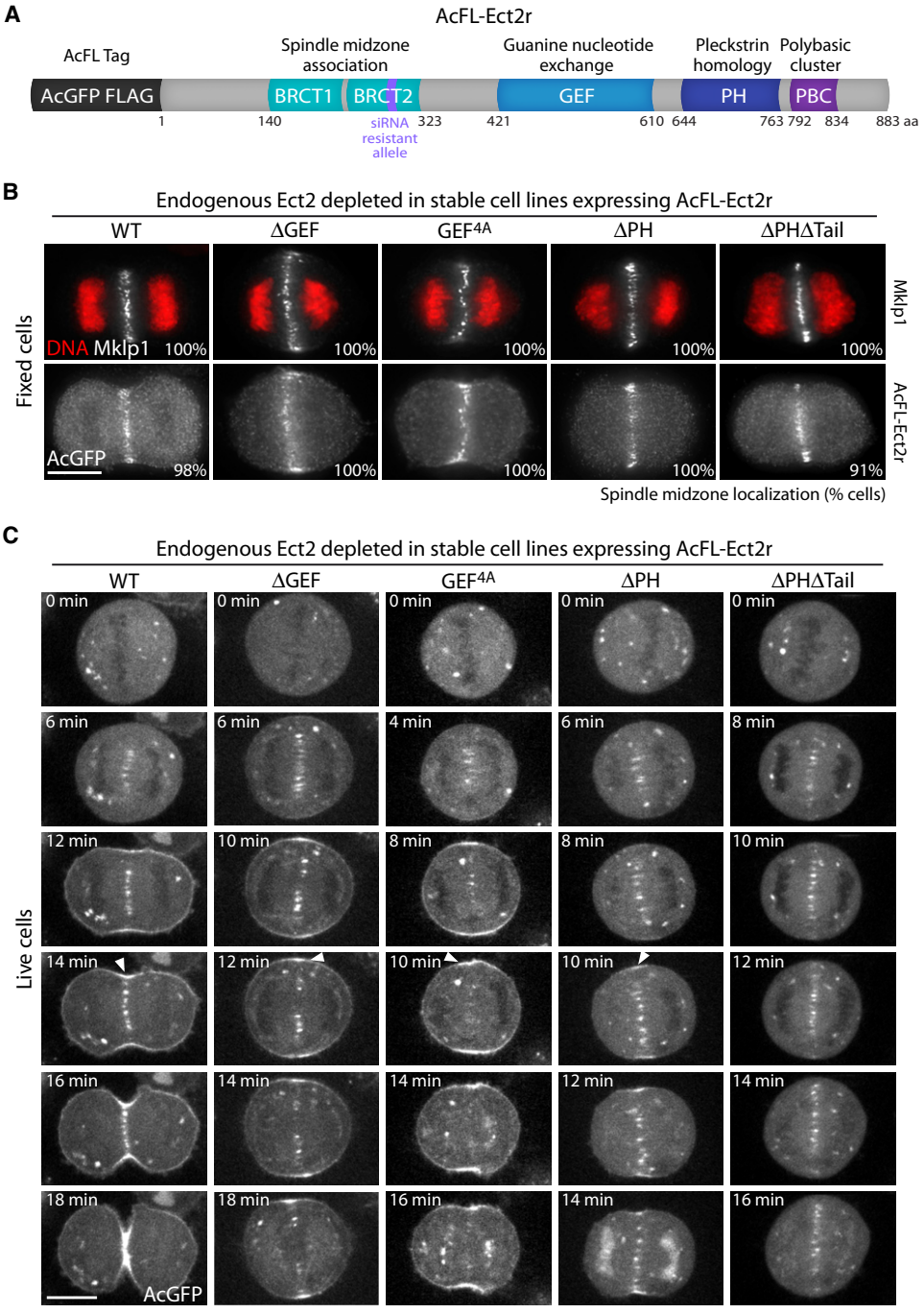

Figure 4. The PH domain and Polybasic Cluster Target Ect2 to the Equatorial Plasma Membrane during Cytokinesis

(A) Domain organization of AcFL-tagged and RNAi-resistant human Ect2 protein.

(B) IF analysis of cells expressing the indicated transgenes 36 hr after transfection with Ect2 siRNA (n > 50 anaphase cells each). Cells were costained with anti-Mklp1 and anti-AcGFP antibodies. Scale bars in this panel and the following one represent 10 μm.

(C) Confocal live-cell imaging of the indicated AcFL-Ect2r variants in the stable cell lines. Recording started 20 hr after transfection with Ect2 siRNA. Time point t = 0 min was set to the metaphase-to-anaphase transition. The filled arrowheads indicate localization to the cell cortex.

deletion of the GEF domain and simultaneous deletion of both membrane association regions had the most severe impact on RhoA and anillin localization (Figure 5B) and closely resembled a complete loss of Ect2 function condition. This analysis provides a mechanistic explanation for the cytokinetic defect caused by mutations in the DH, PH and Tail domains of Ect2. Ect2 variants lacking guanine nucleotide exchange function are unable to activate RhoA despite accumulating at the equatorial membrane. Conversely, Ect2 alleles lacking the ability to interact with the membrane are unable to locally activate RhoA at the

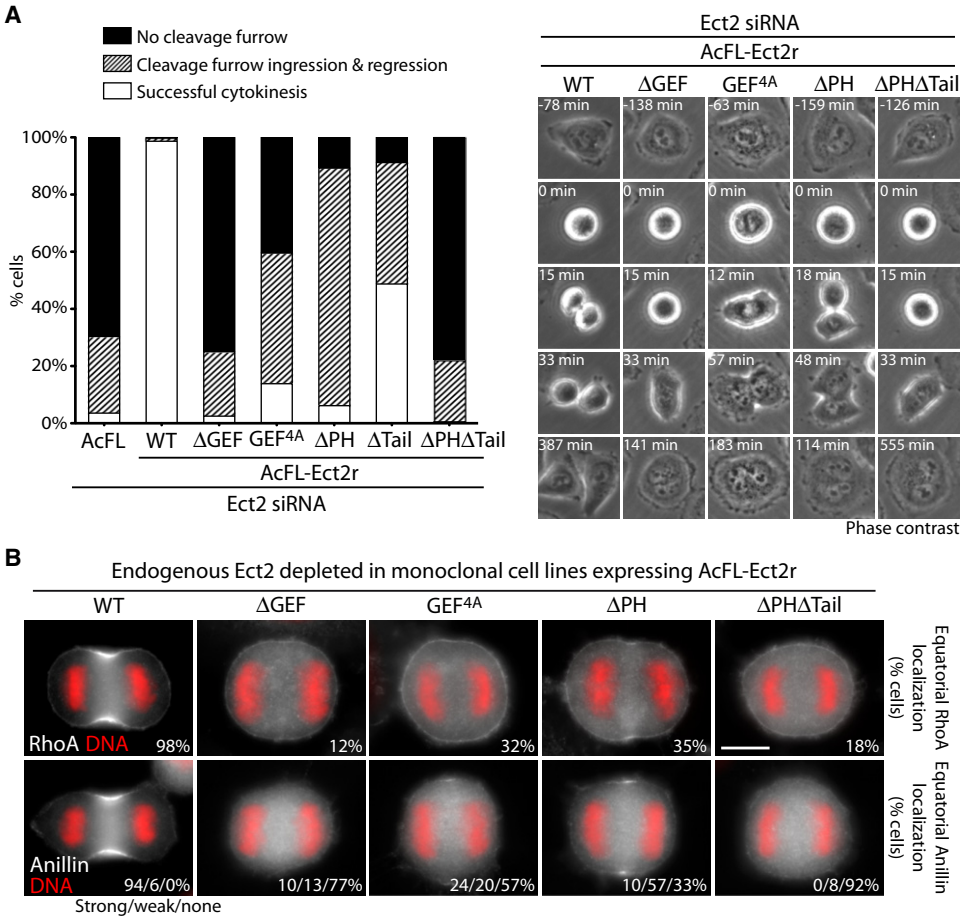

Figure 5. Cleavage Furrow Formation and Equatorial RhoA Concentration Require GEF Activity and Membrane Targeting of Ect2

(A) Quantification of cytokinetic phenotypes in monoclonal cell lines expressing the indicated transgenes using time-lapse microscopy after transfection with Ect2 siRNA (n > 288 cells each) (graph, left panel). Mononucleate cells entering mitosis were scored from 18 to 38 hr posttransfection. Representative cell division phenotypes of selected cell lines are shown as time-lapse series (right panel). Time point t = 0 min was set to the metaphase-to-anaphase transition.

(B) IF analysis of anaphase cells expressing the indicated transgenes 32–36 hr after transfection with Ect2 siRNA (n > 50 anaphase cells each). Cells were fixed in trichloroacetic acid or methanol and stained with anti-RhoA or anti-anillin antibodies, respectively.

equatorial membrane despite retaining exchange activity in vitro. The corollary of these findings is that RhoA activation and contractile ring formation during anaphase requires targeting of Ect2's exchange activity to the equatorial membrane.

Centralspindlin Directs the Concentration of Ect2 at the Equatorial Plasma Membrane

Consistent with its key role in cleavage furrow formation, the association of Ect2 with the plasma membrane is subject to tight spatiotemporal control. Ect2 accumulates at the plasma membrane only after anaphase onset and then becomes concentrated at the cell equator (Figure 6A; Movie S2) (17/18 cells). The transiently expressed Ect2CT fragment that contains both membrane interaction domains but lacks the BRCT repeats required for spindle midzone targeting localizes all around the cell periphery (Figure 2B). This suggests that the primary determinant for the spatial distribution of Ect2 at the membrane is unlikely to be a polarized distribution of membrane lipids. Recruitment of Ect2 to the spindle midzone, which underlies the equatorial cortex, could direct the concentration of the protein at the equatorial membrane. To test this hypothesis, we depleted the MgcRacGAP and Mklp1 subunits of centralspindlin, the protein complex that recruits Ect2 to the spindle midzone, in a monoclonal cell line expressing AcFL-Ect2r and H2B-mCherry (Figure S3). Depletion of MgcRacGAP and Mklp1 abolished the localization of Ect2 to the spindle midzone and prevented cleavage furrow ingression (Figure 6A; Movie S2). Although Ect2 accumulated at the membrane after anaphase onset, the protein was distributed all around the cell periphery and no longer concentrated at the equator (Figure 6A; Movie S2) (n > 8 cells each). Similar results were obtained following acute inactivation of Plk1 by addition of the small molecule inhibitor BI 2536 (Lénárt et al., 2007) (Figure 6A; Movie S2) (97/99 cells). Phosphorylation of MgcRacGAP by Plk1 is required for complex formation between centralspindlin and Ect2 (Burkard et al., 2009; Wolfe et al., 2009). Ect2 proteins lacking the nucleotide exchange function accumulate at the equatorial membrane despite absence of furrowing (Figure 4C). Thus, the failure of Ect2 to accumulate at the equatorial membrane in the absence of Plk1 activity and centralspindlin is unlikely to be an

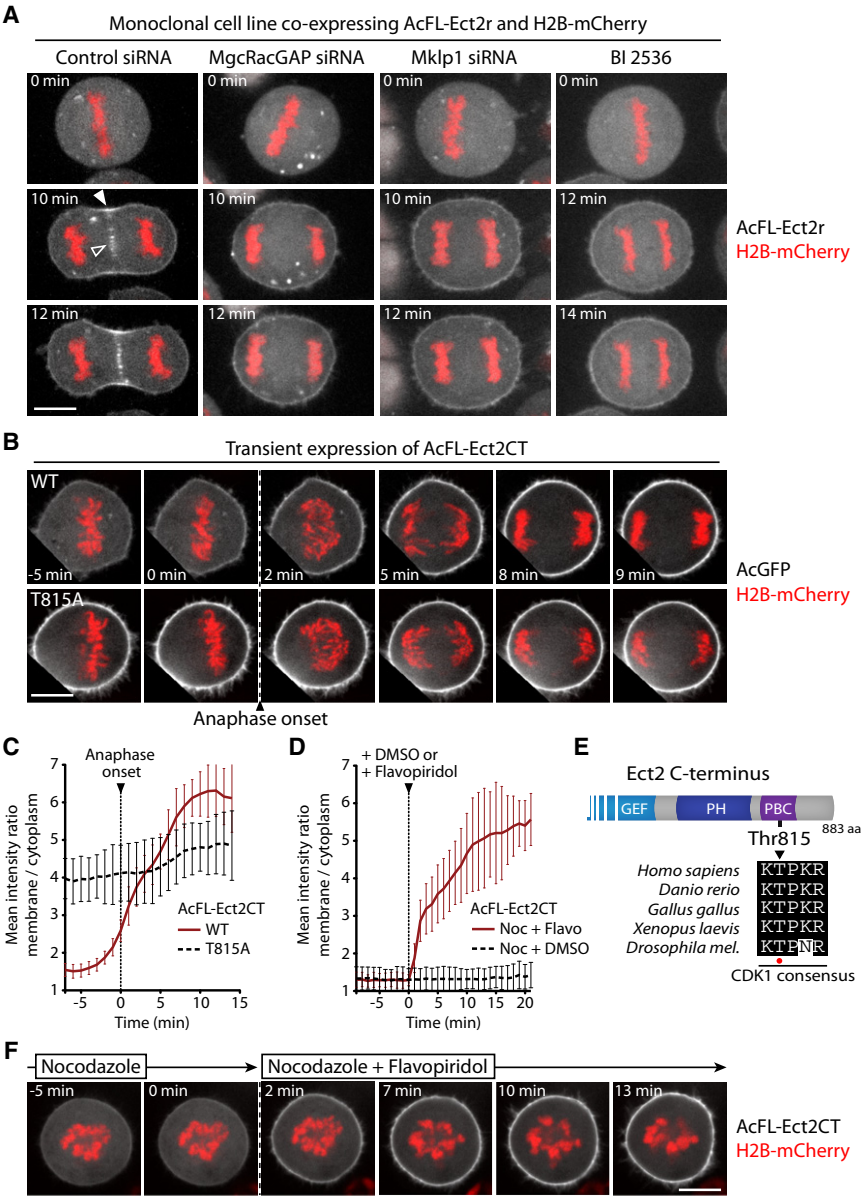

Figure 6. Spatial and Temporal Control of Ect2 Localization to the Equatorial Membrane during Anaphase

(A) Confocal live-cell imaging of a monoclonal cell line stably expressing AcFL-Ect2r (white) and H2B-mCherry (red). Cells were recorded 24 hr after transfection with control siRNA, MgcRacGAP siRNA, or Mklp1 siRNA. Alternatively, cells were released from a metaphase arrest and treated with 250 nM BI 2536 20 min after the release prior to recording (right panel). Time point t = 0 min was set to the metaphase-to-anaphase transition. The open and filled arrowheads indicate localization to the spindle midzone and equatorial cell membrane, respectively. For immunoblot analysis of protein extracts following depletion see Figure S3. Scale bars in this panel and the following panels represent 10 μm. For full sequence, see Movie S2.

(B) Confocal live-cell imaging of transiently expressed AcFL-Ect2CT-WT or AcFL-Ect2CT-T815A (white) (see Figure S1A for constructs) in cells stably expressing H2B-mCherry (red). Time point t = 0 min was set to the metaphase-to-anaphase transition. Anaphase onset is indicated by a dashed line. For full sequence, see Movie S3.

(C) Quantification of the localization of AcFL-Ect2CT-WT (red solid line) and AcFL-Ect2CT-T815A (black dashed line) during mitosis based on time-lapse series as shown in (B). Graph displays the ratio of mean intensity at the plasma membrane to mean intensity in the cytoplasm. Time point t = 0 min was set to the metaphase-to-anaphase transition. Anaphase onset is indicated by a dashed line. Error bars represent the standard deviation of the analysis of eight cells for each construct.

(D) Quantification of the localization of AcFL-Ect2CT in nocodazole-arrested cells treated with either solvent control dimethyl sulfoxide (DMSO) (black dashed line) or 15 μM flavopiridol (red solid line) at t = 0 min. Quantification is based on time-lapse series as shown in (F). Graph displays the ratio of mean intensity at the plasma membrane to mean intensity in the cytoplasm. The time point of DMSO and flavopiridol addition is indicated by a dashed line. Error bars represent the standard deviation of the analysis of 8 cells for each condition.

See also Figure S3.

(E) Sequence alignment of the region surrounding position threonine 815 in human Ect2. Conserved residues are colored in black. Thr815 is embedded within the polybasic cluster of Ect2 and is part of a highly conserved bona fide CDK1 consensus sequence.

(F) Confocal live-cell imaging of transiently expressed AcFL-Ect2CT (white) in cells stably expressing H2B-mCherry (red). Cells were arrested in mitosis by addition of 165 nM nocodazole and subsequently treated with 15 μM flavopiridol. The time of flavopiridol addition was set to t = 0 min and is indicated by a dashed line. For full sequence, see Movie S4.

indirect consequence of the absence of furrow formation. Our experiments suggest that concentration of Ect2 at the equatorial membrane during anaphase requires the interaction of Ect2 with the spindle midzone component centralspindlin.

Inactivation of CDK1 at Anaphase Onset Controls the Association of Ect2 with the Plasma Membrane

Whereas Ect2 remains cytoplasmic until the metaphase-to-anaphase transition, a fraction of Ect2 protein translocates to the plasma membrane and becomes concentrated at the equator upon anaphase onset (Figure 6A; Movie S2). In contrast to the equatorial enrichment, the anaphase-specific surge of Ect2 membrane localization does not require the association of the protein with the spindle midzone (Figure 6A). This suggests that two distinct mechanisms govern the spatial and temporal control of Ect2 membrane targeting.

To investigate the temporal regulation of Ect2 membrane association in the absence of the ability of Ect2 to bind to the midzone, we transiently transfected the carboxy-terminal Ect2CT fragment (Figure 2A) into cells stably expressing H2B-mCherry. Time-lapse imaging revealed that Ect2CT remained largely cytoplasmic with only a weak accumulation at the

membrane (1.5-fold) in early mitosis and prior to anaphase onset (Figure 6B; Movie S3). Strikingly, at the time of sister chromatid segregation the cytoplasmic pool of Ect2CT rapidly and quantitatively translocated to the plasma membrane (Figure 6B; Movie S3). Image analysis revealed that the translocation of Ect2CT to the membrane started 3 min before anaphase onset and was completed 10 min after sister chromatid splitting (Figure 6C). This rapid switch in protein localization at the metaphase-to-anaphase transition raised the possibility that changes in post-translational modification could control the ability of Ect2's PH domain and PBC to interact with the plasma membrane. The loss of CDK1 target phosphorylation at the metaphase-to-anaphase transition triggers the onset of cytokinesis and mitotic exit (reviewed in Barr and Gruneberg, 2007; Wurzenberger and Gerlich, 2011). Thus, phosphorylation by CDK1 represents a candidate mechanism for inhibiting the membrane association of Ect2. Kinase assays have previously identified Thr815 as the major CDK1/cyclin B phosphorylation site within the carboxy-terminal half of Ect2 in vitro (Niiya et al., 2006). Phosphorylation of Thr815 has subsequently been confirmed in vivo by global phosphoproteomic analysis of mitotic cell extracts (Dephoure et al., 2008). Thr815 is embedded in Ect2's polybasic cluster and is the phosphoacceptor residue of a highly conserved CDK1 consensus sequence (Figure 6E). We therefore replaced Thr815 by alanine in Ect2CT and tracked the distribution of the mutant protein through cell division. In stark contrast to the wild-type counterpart, Ect2CT-T815A was strongly enriched at the plasma membrane as soon as cells entered mitosis and no longer displayed the surge in membrane association at anaphase onset (Figures 6B and 6C; Movie S3). To further examine the control of Ect2 membrane localization by CDK1, cells expressing Ect2CT were arrested in mitosis using the spindle poison nocodazole and then treated with the CDK inhibitor flavopiridol. While Ect2CT remained largely cytoplasmic in mitotically arrested cells, acute chemical inhibition of CDK1 by addition of flavopiridol triggered the rapid translocation of the protein to the plasma membrane (Figures 6D and 6F; Movie S4). These data suggest that the activation state of CDK1 acts a switch to temporally control the association of Ect2 with the plasma membrane during mitosis.

DISCUSSION

Over the last three decades, classical micromanipulation experiments and functional studies have established that the mitotic spindle plays a pivotal role in the formation and positioning of the cleavage furrow in animal cells (reviewed in D'Avino et al., 2005; von Dassow, 2009). Our work in human cells has identified the mechanistic basis and spatiotemporal control of an important step in the delivery of the cytokinetic signal to the plasma membrane. We propose that targeting of the RhoGEF Ect2 to the equatorial membrane at anaphase onset activates RhoA and leads to the formation of a cleavage furrow (see Graphical Abstract).

Key to our ability to scrutinize the association of Ect2 with the plasma membrane was the development of a genetic complementation system that allowed us to track the protein at native expression level through cell division in live cells. The interaction of Ect2 with the plasma membrane during cytokinesis requires the protein's PH domain and, unusually for a DH-type GEF (Rossman et al., 2005), a C-terminal polybasic cluster. Ect2's guanine nucleotide exchange activity and its ability to interact with the plasma membrane are mechanistically separable properties that are both required for RhoA activation and cleavage furrow formation. Ect2 variants that lack both membrane association domains but retain exchange activity localize to the spindle midzone, yet are unable to support cleavage furrow formation. This result implies that the recruitment of Ect2 to the spindle midzone might not be sufficient for controlling cortical events during cytokinesis. Although never decisively tested, Ect2's GEF function represents an integral part of current models for cleavage furrow formation. Consistent with the identification of a missense mutation in the DH domain of a *pebble* allele in *Drosophila* (Prokopenko et al., 1999), our in vivo and in vitro experiments provide strong evidence for a key role of Ect2's exchange function in controlling RhoA activity and contractile ring formation.

The local concentration of Ect2 at the equatorial membrane, but not membrane association of the protein per se, requires the interaction of Ect2 with the essential midzone component centralspindlin. Thus, the formation of the spindle midzone at anaphase might break the isotropic distribution of Ect2 at the periphery and target the RhoGEF to the equatorial membrane in the cleavage plane. This hypothesis is supported by micromanipulation experiments (Bement et al., 2005) and could account for the important role of centralspindlin and the spindle midzone in the formation and positioning of the cleavage furrow. In addition to acting as a spatial cue for Ect2 membrane localization, binding to centralspindlin might also contribute to the activation of Ect2's C-terminal domains (Kim et al., 2005; Saito et al., 2004; Yüce et al., 2005).

Although centralspindlin and Ect2 colocalize at the spindle midzone, centralspindlin, unlike Ect2, does not accumulate significantly at the equatorial membrane in human cells (K.-C.S. and M.P., unpublished observation). Consistent with recent observations (von Dassow et al., 2009), a direct transfer of the Ect2-centralspindlin complex from the microtubules to the plasma membrane is therefore unlikely to account for the concentration of Ect2 at the equatorial membrane. Nevertheless, the spatial separation of a membrane-associated pool of Ect2 from MgcRacGAP could provide the solution to the enigmatic question of how a complex containing two proteins of opposing activities, a RhoGEF and a RhoGAP (Miller and Bement, 2009), can control the formation of a Rho-dependent contractile zone.

The requirement for centralspindlin and Plk1 offers an alternative hypothesis for how Ect2 accumulates at the equatorial membrane. The exchange of spindle-midzone associated Ect2 with the protein's cytoplasmic pool could create a concentration gradient around the spindle midzone. Coupled with the ability of Ect2 to dynamically associate with the plasma membrane at anaphase, this local concentration gradient could lead to the accumulation of Ect2 at the equatorial membrane flanking the spindle midzone. Two positive feedback mechanisms might subsequently reinforce the equatorial zone of Ect2. First, the interaction of the centralspindlin subunit MgcRacGAP with the contractile ring component anillin, which was observed in *Drosophila*, could bring cortical microtubules closer to the equatorial membrane (D'Avino et al., 2008; Gregory et al., 2008). Second, the contraction of the cleavage furrow itself will lead to the compression of the spindle midzone and thus to the

increase of the local concentration of Ect2 in the cleavage plane. Testing these hypotheses and deciphering the mechanism underlying the concentration of Ect2 at the equatorial membrane will require the tracking of Ect2 and its dynamic properties at different cellular locations in combination with pharmacological, genetic, and physical perturbation experiments. Future work is also required to test the relative contributions of the spindle midzone and the dominant microtubule asters to the positioning of Ect2 at the membrane in large animal cells, such as embryonic blastomeres.

Although the lipids responsible for Ect2 membrane localization in vivo remain to be determined, the membrane association domains of Ect2 can interact with phosphoinositides in vitro. Experiments in different animal cell systems have established that $PI(4,5)P_2$ localizes to the cleavage furrow and that blocking the access to $PI(4,5)P_2$ prevents cell division (reviewed in Atilla-Gokcumen et al., 2010). These findings raise the exciting possibility that the interaction of Ect2 with $PI(4,5)P_2$ in the inner leaflet of the plasma membrane may contribute to the equatorial concentration of Ect2 during cytokinesis.

Our analysis suggests that the association of Ect2 with the plasma membrane is inhibited by CDK1 phosphorylation prior to anaphase onset. Since CDK1 is inactivated at the metaphase-to-anaphase transition (Wurzenberger and Gerlich, 2011), the CDK1-dependent regulation of Ect2 membrane association allows the temporal coordination of chromosome segregation with cleavage furrow formation. This temporal control mechanism is likely to cooperate with the well-established inhibition of spindle midzone-linked cytokinetic processes by CDK1 (Glotzer, 2009).

This study has characterized an important step in the delivery of the cytokinetic signal to the cell periphery (see Graphical Abstract). The targeting of Ect2 to the plasma membrane and its spatiotemporal control could represent conserved principles that underlie the partitioning of sister genomes and the birth of new daughter cells during cytokinesis in animal cells.

EXPERIMENTAL PROCEDURES

Plasmids, DNA Transfection, and Generation of Stable Cell Lines

For a detailed description please see Supplemental Experimental Procedures. Briefly, AcGFP-FLAG-tagged variants of Ect2 (Figures S1A and S2A) were inserted into pIRESpuro3 (Clontech). The plasmids were transfected into HeLa Kyoto cells that were grown as described in (Petronczki et al., 2007). For the selection of stable cell lines the medium was supplemented with 0.3 μg/ml puromycin (Sigma).

siRNA transfection and Drug Treatment

Lipofectamine RNAiMax (Invitrogen) was used for siRNA transfection. The following siRNA duplexes were used at a final concentration of 30 nM: control (Thermo Scientific siGENOME Non-Targeting siRNA #1 D-001210-01), Ect2 (Thermo Scientific siGENOME D-006450-02), Mklp1 (Invitrogen Stealth HSS114138), and MgcRacGAP (Invitrogen Stealth HSS120934).

To disrupt f-actin, cells were incubated in 20 μM dihydrocytochalasin B (Sigma) for 20 min prior to fixation. To acutely inhibit CDK1, cells were incubated in 165 nM nocodazole (Sigma) for 3 hr before addition of 15 μM flavopiridol (Sigma). To inhibit Plk1 (Figure 6A; Movie S2), cells were synchronized at metaphase as described (Petronczki et al., 2007) and treated with 250 nM BI 2536 (Lénárt et al., 2007) 20 min after release from metaphase.

Immunofluorescence Microscopy

Cells were fixed for 16 hr in −20°C methanol (Figures 1B, 1D, 3C, 4B, and 5B/anillin), for 10 min at 37°C in 4% formaldehyde (Figures 2B and C) or for 15 min on ice in 10% tricholoroacetic acid (Figure 5B/RhoA) before being processed for immunofluorescence (IF) microscopy as described (Lénárt et al., 2007). Images for Figures 1B, 1D, 2C, 3C, 4B, and 5B were acquired on a Zeiss Axio Imager M1 microscope using a Plan Apochromat 63×/1.4 oil objective lens (Zeiss) equipped with an ORCA-ER camera (Hamamatsu) and controlled by Volocity 5.5.1. software (Improvision). Images in Figures 1D, 2C, and 4B were deconvolved using Volocity's iterative restoration function. Images in Figure 2B were acquired with on a Zeiss LSM Upright710 confocal system controlled by Zen 2009 software using a Zeiss Imager.Z2 microscope and a Plan-Apochromat 63×/1.40 Oil DIC M27 lens.

Antibodies and Dyes

For a list of antibodies and dyes used in this study, please refer to Supplemental Experimental Procedures.

Live-Cell Imaging and Image Quantification

Before recording, the medium was changed to phenol-red-free CO_2-independent medium (Lénárt et al., 2007). For Figures 1C, 4C, 6A, 6B, and 6F and Movies S1–S4, frames were acquired at 37°C using a PerkinElmer ERS Spinning disc system equipped with a Nikon TE2000 microscope, a Plan Fluor 40× 1.3 DIC H lens (Nikon) (optovar set to 1.5×), a CSU22 spinning disc scanner (Yokogawa), a IEEE1394 Digital CCD C4742-80-12AG camera (Hamamatsu) and controlled by Volocity 5.5.1 software (Perkin Elmer). Volocity 5.5.1 software was used for quantification of acquired 16 bit images. Mean AcGFP intensities were measured for each time point by averaging six manually placed circular regions of 9 pixels at the cell periphery and two circular regions of 1,000–2,000 pixels size in the cytoplasm followed by subtraction of the mean background signal outside of the cell (Figures 6C and 6D).

To quantify cytokinetic phenotypes in Figure 5A (graph, left panel), phase contrast images of cells were recorded every 5 min in normal medium using an IncuCyte FLR integrated live-cell imaging system (Essen Bioscience). Images in Figure 5A (right panel) were acquired at 37°C using a Zeiss Axio Observer Z1 microscope controlled by SimplePCI software (Hamamatsu) and equipped with an Orca 03GO1 camera (Hamamatsu) and a Plan-Apochromat 10×/0.45 objective.

Purification of Recombinant Proteins and In Vitro Protein Assays

Please refer to Supplemental Experimental Procedures for a description of protein purification procedures, in vitro protein-lipid interaction experiments, and GEF assay.

SUPPLEMENTAL INFORMATION

Supplemental Information includes three figures, Supplemental Experimental Procedures, and four movies and can be found online at doi:10.1016/j.devcel.2011.11.003.

ACKNOWLEDGMENTS

K.-C.S., T.T., and M.P. designed the experiments. K.-C.S. generated the monoclonal cell lines and conducted the cellular analyses. T.T. performed the recombinant protein studies. All authors contributed to the IF analyses. M.P. wrote the manuscript. We would like to thank Julian Gannon, Daniel Gerlich, Michael Glotzer, Alisa Piekny, and María Dolores Vázquez-Novelle for sharing reagents. We are grateful to Daniel Zicha and Peter Jordan for help with microscopy. Kuan-Chung Su is a recipient of a DOC fellowship of the Austrian Academy of Sciences (OEAW). Work in the Petronczki laboratory is supported by Cancer Research UK and the EMBO Young Investigator Programme.

Received: October 10, 2011
Revised: November 9, 2011
Accepted: November 9, 2011
Published online: December 12, 2011

REFERENCES

Atilla-Gokcumen, G.E., Castoreno, A.B., Sasse, S., and Eggert, U.S. (2010). Making the cut: the chemical biology of cytokinesis. ACS Chem. Biol. *5*, 79–90.

Barr, F.A., and Gruneberg, U. (2007). Cytokinesis: placing and making the final cut. Cell *131*, 847–860.

Bement, W.M., Benink, H.A., and von Dassow, G. (2005). A microtubule-dependent zone of active RhoA during cleavage plane specification. J. Cell Biol. *170*, 91–101.

Bringmann, H., and Hyman, A.A. (2005). A cytokinesis furrow is positioned by two consecutive signals. Nature *436*, 731–734.

Burkard, M.E., Maciejowski, J., Rodriguez-Bravo, V., Repka, M., Lowery, D.M., Clauser, K.R., Zhang, C., Shokat, K.M., Carr, S.A., Yaffe, M.B., and Jallepalli, P.V. (2009). Plk1 self-organization and priming phosphorylation of HsCYK-4 at the spindle midzone regulate the onset of division in human cells. PLoS Biol. *7*, e1000111.

Chalamalasetty, R.B., Hümmer, S., Nigg, E.A., and Silljé, H.H. (2006). Influence of human Ect2 depletion and overexpression on cleavage furrow formation and abscission. J. Cell Sci. *119*, 3008–3019.

D'Avino, P.P., Savoian, M.S., and Glover, D.M. (2005). Cleavage furrow formation and ingression during animal cytokinesis: a microtubule legacy. J. Cell Sci. *118*, 1549–1558.

D'Avino, P.P., Takeda, T., Capalbo, L., Zhang, W., Lilley, K.S., Laue, E.D., and Glover, D.M. (2008). Interaction between Anillin and RacGAP50C connects the actomyosin contractile ring with spindle microtubules at the cell division site. J. Cell Sci. *121*, 1151–1158.

Dechant, R., and Glotzer, M. (2003). Centrosome separation and central spindle assembly act in redundant pathways that regulate microtubule density and trigger cleavage furrow formation. Dev. Cell *4*, 333–344.

Dephoure, N., Zhou, C., Villén, J., Beausoleil, S.A., Bakalarski, C.E., Elledge, S.J., and Gygi, S.P. (2008). A quantitative atlas of mitotic phosphorylation. Proc. Natl. Acad. Sci. USA *105*, 10762–10767.

Eggert, U.S., Mitchison, T.J., and Field, C.M. (2006). Animal cytokinesis: from parts list to mechanisms. Annu. Rev. Biochem. *75*, 543–566.

Ganem, N.J., Storchova, Z., and Pellman, D. (2007). Tetraploidy, aneuploidy and cancer. Curr. Opin. Genet. Dev. *17*, 157–162.

Glotzer, M. (2009). The 3Ms of central spindle assembly: microtubules, motors and MAPs. Nat. Rev. Mol. Cell Biol. *10*, 9–20.

Gregory, S.L., Ebrahimi, S., Milverton, J., Jones, W.M., Bejsovec, A., and Saint, R. (2008). Cell division requires a direct link between microtubule-bound RacGAP and Anillin in the contractile ring. Curr. Biol. *18*, 25–29.

Heo, W.D., Inoue, T., Park, W.S., Kim, M.L., Park, B.O., Wandless, T.J., and Meyer, T. (2006). PI(3,4,5)P3 and PI(4,5)P2 lipids target proteins with polybasic clusters to the plasma membrane. Science *314*, 1458–1461.

Kim, J.E., Billadeau, D.D., and Chen, J. (2005). The tandem BRCT domains of Ect2 are required for both negative and positive regulation of Ect2 in cytokinesis. J. Biol. Chem. *280*, 5733–5739.

Klarlund, J.K., Guilherme, A., Holik, J.J., Virbasius, J.V., Chawla, A., and Czech, M.P. (1997). Signaling by phosphoinositide-3,4,5-trisphosphate through proteins containing pleckstrin and Sec7 homology domains. Science *275*, 1927–1930.

Lemmon, M.A. (2008). Membrane recognition by phospholipid-binding domains. Nat. Rev. Mol. Cell Biol. *9*, 99–111.

Lénárt, P., Petronczki, M., Steegmaier, M., Di Fiore, B., Lipp, J.J., Hoffmann, M., Rettig, W.J., Kraut, N., and Peters, J.M. (2007). The small-molecule inhibitor BI 2536 reveals novel insights into mitotic roles of polo-like kinase 1. Curr. Biol. *17*, 304–315.

Liot, C., Seguin, L., Siret, A., Crouin, C., Schmidt, S., and Bertoglio, J. (2011). APC(cdh1) mediates degradation of the oncogenic Rho-GEF Ect2 after mitosis. PLoS ONE *6*, e23676.

Miller, A.L., and Bement, W.M. (2009). Regulation of cytokinesis by Rho GTPase flux. Nat. Cell Biol. *11*, 71–77.

Niiya, F., Tatsumoto, T., Lee, K.S., and Miki, T. (2006). Phosphorylation of the cytokinesis regulator ECT2 at G2/M phase stimulates association of the mitotic kinase Plk1 and accumulation of GTP-bound RhoA. Oncogene *25*, 827–837.

Nishimura, Y., and Yonemura, S. (2006). Centralspindlin regulates ECT2 and RhoA accumulation at the equatorial cortex during cytokinesis. J. Cell Sci. *119*, 104–114.

Petronczki, M., Glotzer, M., Kraut, N., and Peters, J.M. (2007). Polo-like kinase 1 triggers the initiation of cytokinesis in human cells by promoting recruitment of the RhoGEF Ect2 to the central spindle. Dev. Cell *12*, 713–725.

Piekny, A., Werner, M., and Glotzer, M. (2005). Cytokinesis: welcome to the Rho zone. Trends Cell Biol. *15*, 651–658.

Prokopenko, S.N., Brumby, A., O'Keefe, L., Prior, L., He, Y., Saint, R., and Bellen, H.J. (1999). A putative exchange factor for Rho1 GTPase is required for initiation of cytokinesis in Drosophila. Genes Dev. *13*, 2301–2314.

Rappaport, R. (1985). Repeated furrow formation from a single mitotic apparatus in cylindrical sand dollar eggs. J. Exp. Zool. *234*, 167–171.

Rossman, K.L., Der, C.J., and Sondek, J. (2005). GEF means go: turning on RHO GTPases with guanine nucleotide-exchange factors. Nat. Rev. Mol. Cell Biol. *6*, 167–180.

Saito, S., Liu, X.F., Kamijo, K., Raziuddin, R., Tatsumoto, T., Okamoto, I., Chen, X., Lee, C.C., Lorenzi, M.V., Ohara, N., and Miki, T. (2004). Deregulation and mislocalization of the cytokinesis regulator ECT2 activate the Rho signaling pathways leading to malignant transformation. J. Biol. Chem. *279*, 7169–7179.

Solski, P.A., Wilder, R.S., Rossman, K.L., Sondek, J., Cox, A.D., Campbell, S.L., and Der, C.J. (2004). Requirement for C-terminal sequences in regulation of Ect2 guanine nucleotide exchange specificity and transformation. J. Biol. Chem. *279*, 25226–25233.

Somers, W.G., and Saint, R. (2003). A RhoGEF and Rho family GTPase-activating protein complex links the contractile ring to cortical microtubules at the onset of cytokinesis. Dev. Cell *4*, 29–39.

Tatsumoto, T., Xie, X., Blumenthal, R., Okamoto, I., and Miki, T. (1999). Human ECT2 is an exchange factor for Rho GTPases, phosphorylated in G2/M phases, and involved in cytokinesis. J. Cell Biol. *147*, 921–928.

von Dassow, G. (2009). Concurrent cues for cytokinetic furrow induction in animal cells. Trends Cell Biol. *19*, 165–173.

von Dassow, G., Verbrugghe, K.J., Miller, A.L., Sider, J.R., and Bement, W.M. (2009). Action at a distance during cytokinesis. J. Cell Biol. *187*, 831–845.

Wolfe, B.A., Takaki, T., Petronczki, M., and Glotzer, M. (2009). Polo-like kinase 1 directs assembly of the HsCyk-4 RhoGAP/Ect2 RhoGEF complex to initiate cleavage furrow formation. PLoS Biol. *7*, e1000110.

Wurzenberger, C., and Gerlich, D.W. (2011). Phosphatases: providing safe passage through mitotic exit. Nat. Rev. Mol. Cell Biol. *12*, 469–482.

Yüce, O., Piekny, A., and Glotzer, M. (2005). An ECT2-centralspindlin complex regulates the localization and function of RhoA. J. Cell Biol. *170*, 571–582.